

Green Chemistry

Cutting-edge research for a greener sustainable future

www.rsc.org/greenchem

Volume 9 | Number 7 | July 2007 | Pages 705–812



ISSN 1463-9262

RSC Publishing

Gaspar *et al.*
Alternatives for lignocellulosic pulp
delignification

Calò *et al.*
Synthesis of a cardanol-based
benzoxazine monomer

Lourenço *et al.*
Enzymatic resolution of Indinavir
precursor

Kholdeeva *et al.*
Highly efficient production of 2,3,5-
trimethyl-1,4-benzoquinone



1463-9262(2007)9:7;1-5

Green Chemistry Fellow?

Fellowships (x2) • c.€47,000

The Home and Personal Care R&D Laboratories of Unilever at Port Sunlight, has recently been awarded significant support through the EU Marie Curie Transfer of Knowledge Partnerships. This funding will contribute to the development of a significant platform within our research capabilities and scope the future innovation using Green Chemistry approaches. We are seeking experienced scientists from Europe to contribute to our program and foster relationships with key research centres across the EU

It is expected that candidates will have a background in one of the areas indicated below with a relevant degree and PhD. Two Fellowships are available for experienced scientists with post-graduate research experience (including PhD) of Green Chemistry Techniques. The role of each Fellow is to work in close collaboration with other senior Marie Curie research fellows and Home & Personal Care Scientists at Unilever, and carry out the synthetic chemistry programme set out during the first phase of the project.

Organic Chemistry Fellow: Applications are sought from experienced researchers with a background of Green Chemical approaches to Organic Chemistry. Applicants should have an understanding of raw materials from renewable resources, in particular platform molecules from biorefineries, and methods for reacting these raw materials using Green processes. Experience of a wide range of synthetic and characterisation techniques, including: the use of microwaves in chemistry, preparation and analysis of

Port Sunlight, near Liverpool, UK

composite materials, reaction optimisation and catalysis would be of particular interest and applications from chemists with a cross-disciplinary experience (synthesis/materials; chemistry/reaction engineering) would be welcomed. Ref 73921.

Polymer Chemistry Fellow: Applications are sought from researchers with experience of the extraction/modification of macromolecules from biomass and their transformation to form functional polymeric materials. Applicants should have an understanding of a range of bio-materials with special emphasis on polysaccharides, and Green methods for their production and modification. Experience of transformation/modification of biopolymers, extraction techniques, catalysis, enzyme catalysed aqueous reactions, and/or microwave chemistry would be of particular interest. Ref: 73922.

The Fellowships are for 2 years each with the intention to form strong links to EU centres of excellence. A mobility allowance and a yearly travel allowance will be paid in accordance with EU rules.

Candidates, eligible according to the EU Marie Curie scheme guidelines, http://europa.eu.int/comm/research/fp6/mariecurie-actions/indexhtm_en.html should submit a full curriculum vitae and a one-page statement summarising their main research interests, together with the names of two referees, online at www.unilever.co.uk/careers Please quote the appropriate reference on your application.

Please note that the closing date for applications is 30th July 2007 and the earliest start date will be 1st September 2007.

In applying for the above positions, you agree, unless you notify us when responding to this advert, that we may consider you for other vacancies we have and make your details available to other companies in the Unilever Group for the same purpose.

Could it be 
Unilever

LYNX

MARMITE



Dove

PG Tips

Pot Noodle

Persil

BERTOLI

Green Chemistry

Cutting-edge research for a greener sustainable future

www.rsc.org/greenchem

RSC Publishing is a not-for-profit publisher and a division of the Royal Society of Chemistry. Any surplus made is used to support charitable activities aimed at advancing the chemical sciences. Full details are available from www.rsc.org

IN THIS ISSUE

ISSN 1463-9262 CODEN GRCHFJ 9(7) 705–812 (2007)



Cover

Cashew fruits and nuts; a precious renewable bio-resource. Image reproduced with permission from Giuseppe Mele, *Green Chem.*, 9(7), 754.

CHEMICAL TECHNOLOGY

T49

Chemical Technology highlights the latest applications and technological aspects of research across the chemical sciences.

Chemical Technology

July 2007/Volume 4/Issue 7

www.rsc.org/chemicaltechnology

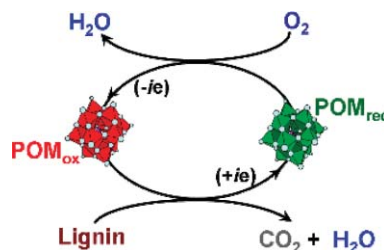
CRITICAL REVIEW

717

Alternatives for lignocellulosic pulp delignification using polyoxometalates and oxygen: a review

Armando R. Gaspar, José A. F. Gamelas,*
Dmitry V. Evtuguin and Carlos Pascoal Neto

The pulp-and-paper industry is facing pressures to replace the conventional chlorine-based chemical bleaching techniques by environmentally friendly technologies. The use of polyoxometalates and oxygen for the delignification may represent a sustainable alternative.



EDITORIAL STAFF

Editor

Sarah Ruthven

Publishing assistant

Emma Hacking

Team leader, serials production

Stephen Wilkes

Technical editor

Edward Morgan

Administration coordinator

Sonya Spring

Editorial secretaries

Donna Fordham, Jill Segev, Julie Thompson

Publisher

Emma Wilson

Green Chemistry (print: ISSN 1463-9262; electronic: ISSN 1463-9270) is published 12 times a year by the Royal Society of Chemistry, Thomas Graham House, Science Park, Milton Road, Cambridge, UK CB4 0WF.

All orders, with cheques made payable to the Royal Society of Chemistry, should be sent to RSC Distribution Services, c/o Portland Customer Services, Commerce Way, Colchester, Essex, UK CO2 8HP. Tel +44 (0) 1206 226050; E-mail sales@rscdistribution.org

2007 Annual (print + electronic) subscription price: £902; US\$1705. 2007 Annual (electronic) subscription price: £812; US\$1534. Customers in Canada will be subject to a surcharge to cover GST. Customers in the EU subscribing to the electronic version only will be charged VAT.

If you take an institutional subscription to any RSC journal you are entitled to free, site-wide web access to that journal. You can arrange access via Internet Protocol (IP) address at www.rsc.org/ip. Customers should make payments by cheque in sterling payable on a UK clearing bank or in US dollars payable on a US clearing bank. Periodicals postage paid at Rahway, NJ, USA and at additional mailing offices. Airfreight and mailing in the USA by Mercury Airfreight International Ltd, 365 Blair Road, Avenel, NJ 07001, USA.

US Postmaster: send address changes to Green Chemistry, c/o Mercury Airfreight International Ltd, 365 Blair Road, Avenel, NJ 07001. All despatches outside the UK by Consolidated Airfreight.

PRINTED IN THE UK

Advertisement sales: Tel +44 (0) 1223 432246; Fax +44 (0) 1223 426017; E-mail advertising@rsc.org

Green Chemistry

Cutting-edge research for a greener sustainable future

www.rsc.org/greenchem

Green Chemistry focuses on cutting-edge research that attempts to reduce the environmental impact of the chemical enterprise by developing a technology base that is inherently non-toxic to living things and the environment.

EDITORIAL BOARD

Chair

Professor Martyn Poliakoff
Nottingham, UK

Scientific Editor

Professor Walter Leitner
RWTH-Aachen, Germany

Associate Editors

Professor C. J. Li
McGill University, Canada
Professor Kyoko Nozaki
Kyoto University, Japan

Members

Professor Paul Anastas
Yale University, USA
Professor Joan Brennecke
University of Notre Dame, USA
Professor Mike Green
Sasol, South Africa
Professor Buxing Han
Chinese Academy of Sciences,
China
Professor Roshan Jachuck
Clarkson University, USA

Dr Alexei Lapkin
Bath University, UK
Dr Janet Scott
Unilever, UK
Professor Tom Welton
Imperial College, UK

INTERNATIONAL ADVISORY EDITORIAL BOARD

James Clark, York, UK
Avelino Corma, Universidad
Politécnica de Valencia, Spain
Mark Harmer, DuPont Central
R&D, USA
Herbert Hugl, Lanxess Fine
Chemicals, Germany
Makato Misono, nite,
Japan
Colin Raston,
University of Western Australia,
Australia

Robin D. Rogers, Centre for Green
Manufacturing, USA
Kenneth Seddon, Queen's
University, Belfast, UK
Roger Sheldon, Delft University of
Technology, The Netherlands
Gary Sheldrake, Queen's
University, Belfast, UK
Pietro Tundo, Università ca
Foscari di Venezia, Italy

INFORMATION FOR AUTHORS

Full details of how to submit material for publication in Green Chemistry are given in the Instructions for Authors (available from <http://www.rsc.org/authors>). Submissions should be sent via ReSource: <http://www.rsc.org/resource>.

Authors may reproduce/republish portions of their published contribution without seeking permission from the RSC, provided that any such republication is accompanied by an acknowledgement in the form: (Original citation) – Reproduced by permission of the Royal Society of Chemistry.

© The Royal Society of Chemistry 2007. Apart from fair dealing for the purposes of research or private study for non-commercial purposes, or criticism or review, as permitted under the Copyright, Designs and Patents Act 1988 and the Copyright and Related Rights Regulations 2003, this publication may only be reproduced, stored or transmitted, in any form or by any means, with the prior permission in writing of the Publishers or in the case of reprographic reproduction in accordance with the terms of licences issued by the Copyright Licensing Agency in the UK. US copyright law is applicable to users in the USA.

The Royal Society of Chemistry takes reasonable care in the preparation of this publication but does not accept liability for the consequences of any errors or omissions.

☞ The paper used in this publication meets the requirements of ANSI/NISO Z39.48-1992 (Permanence of Paper).

Royal Society of Chemistry: Registered Charity No. 207890

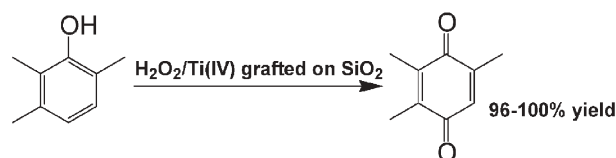
COMMUNICATIONS

731

Highly efficient production of 2,3,5-trimethyl-1,4-benzoquinone using aqueous H₂O₂ and grafted Ti(IV)/SiO₂ catalyst

Oxana A. Kholdeeva,* Irina D. Ivanchikova, Matteo Guidotti and Nicoletta Ravasio

The oxidation of 2,3,6-trimethylphenol with aqueous H₂O₂ over titanium(IV) grafted onto commercial mesoporous silica produces 2,3,5-trimethyl-1,4-benzoquinone, a vitamin E precursor, with nearly quantitative yield.

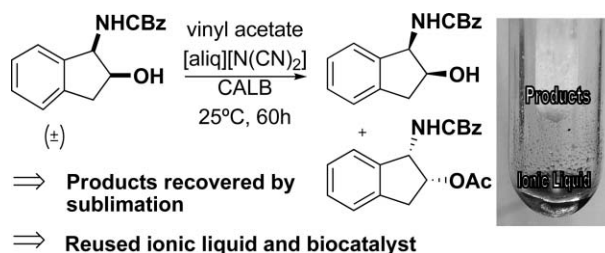


734

Enzymatic resolution of Indinavir precursor in ionic liquids with reuse of biocatalyst and media by product sublimation

Nuno M. T. Lourenço, Susana Barreiros and Carlos A. M. Afonso*

Efficient enzymatic resolution of (±)-*cis*-benzyl *N*-(1-hydroxyindan-2-yl)carbamate in [aliq][N(CN)₂] by acylation using CALB as biocatalyst was achieved, with the possibility of biocatalyst and medium reuse, respectively, by filtration and by sublimation under high vacuum.

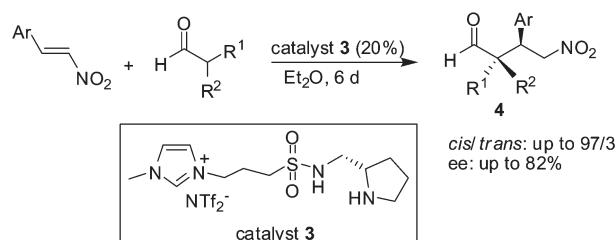


737

Functionalized chiral ionic liquid as recyclable organocatalyst for asymmetric Michael addition to nitrostyrenes

Bukuo Ni, Qianying Zhang and Allan D. Headley*

A new type of pyrrolidine-based chiral ionic liquid has been developed. This chiral ionic liquid was found to catalyze the Michael addition reaction of aldehydes and nitrostyrenes to give moderate yields, good enantioselectivities, high diastereoselectivities, and recyclability.

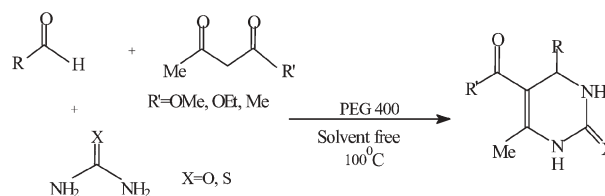


740

PEG-assisted solvent and catalyst free synthesis of 3,4-dihydropyrimidinones under mild reaction conditions

Suman L. Jain, Sweetly Singhal and Bir Sain*

PEG-assisted solvent and catalyst free synthesis of 3,4-dihydropyrimidinones under mild and neutral reaction conditions is described.



COMMUNICATIONS

742



The first Au-nanoparticles catalyzed green synthesis of propargylamines via a three-component coupling reaction of aldehyde, alkyne and amine

Mazaahir Kidwai,* Vikas Bansal, Ajeet Kumar and Subho Mozumdar

Recyclable Au-nanoparticles provide an efficient, economic, novel route for a multi component A³ coupling reaction. This method provides a wide range of substrate applicability.

PAPERS

746

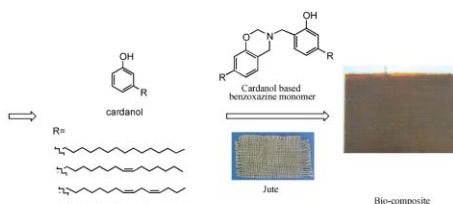


Polyelectrolyte-functionalized ionic liquid for electrochemistry in supporting electrolyte-free aqueous solutions and application in amperometric flow injection analysis

Yanfei Shen, Yuanjian Zhang, Xuepeng Qiu, Haiquan Guo, Li Niu* and Ari Ivaska

A green approach for electrochemistry in aqueous solution without added supporting electrolyte and the application in amperometric flow injection analysis was described based on a simple polyelectrolyte-functionalized ionic liquid-modified electrode.

754



Synthesis of a novel cardanol-based benzoxazine monomer and environmentally sustainable production of polymers and bio-composites

Emanuela Calò, Alfonso Maffezzoli, Giuseppe Mele,* Francesca Martina, Selma E. Mazzetto, Antonella Tarzia and Cristina Stifani

A novel pre-polymer deriving from cardanol—a well known renewable organic resources and harmful by-product of the cashew industry—in combination with cellulose based materials (*i.e.* jute fibres) have been used to produce bio-composites having a high percentage of renewable materials.

760



Effects of different head groups and functionalised side chains on the cytotoxicity of ionic liquids

Stefan Stolte, Jürgen Arning, Ulrike Bottin-Weber, Anja Müller, William-Robert Pitner, Urs Welz-Biermann, Bernd Jastorff and Johannes Ranke*

To enlarge the restricted knowledge about the hazard potentials of ionic liquids to men and the environment we analyse the effect of 100 ionic liquids with different head groups, functionalised side chains and anions on cytotoxicity and confirm its correlation with cation lipophilicity.

PAPERS

768

A novel approach to the synthesis of SiO₂-PVAc nanocomposites using a one-pot synthesis in supercritical CO₂

Paul A. Charpentier,* William Z. Xu and Xinsheng Li

A novel one-step synthesis route has been developed for making the polymer nanocomposites silica-poly(vinyl acetate) (SiO₂-PVAc) in supercritical CO₂ (scCO₂); this green process has potentially many advantages in producing new and unique materials, along with waste-reduction and energy-saving properties.

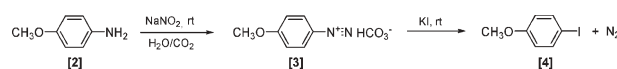


777

Formation and reaction of diazonium salts in a CO₂/H₂O system

Pietro Tundo,* Alessandro Loris and Maurizio Selva

The formation of diazonium salts from the corresponding primary aromatic amines and their reaction with potassium iodide to give the corresponding aryl iodide have been performed in a CO₂/H₂O solvent system.

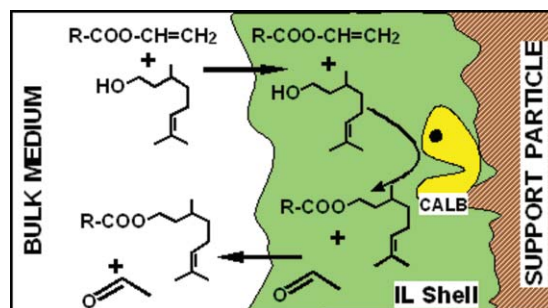


780

Ionic liquids improve citronellyl ester synthesis catalyzed by immobilized *Candida antarctica* lipase B in solvent-free media

Pedro Lozano, Rungtiwa Piamtongkam, Kevin Kohns, Teresa De Diego, Michel Vaultier and José L. Iborra*

Several citronellyl esters (acetate, propionate, butyrate, caprate and laurate) were synthesized by Novozym coated with ionic liquids in high yields (>99%) using equimolar mixtures of substrates in solvent-free medium.

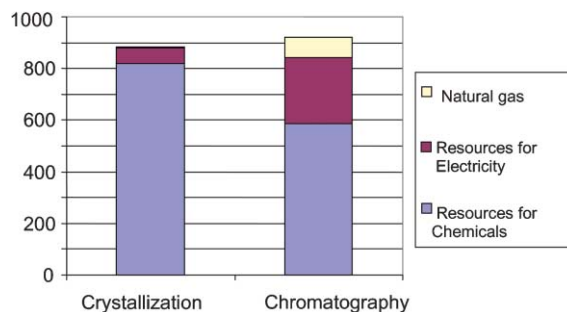


785

Integral resource management by exergy analysis for the selection of a separation process in the pharmaceutical industry

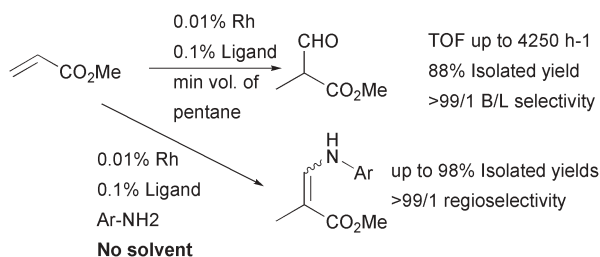
J. Dewulf,* G. Van der Vorst, W. Aelterman, B. De Witte, H. Vanbaelen and H. Van Langenhove

Overall natural resource intake (MJ_{exergy} mol⁻¹) for (2*R*,3*R*)-3-(3-methoxyphenyl)-*N,N*-2-trimethylpentanamine—an intermediate in Tapentadol production—manufacturing and isolation through crystallisation or chromatography has been quantified.



PAPERS

792

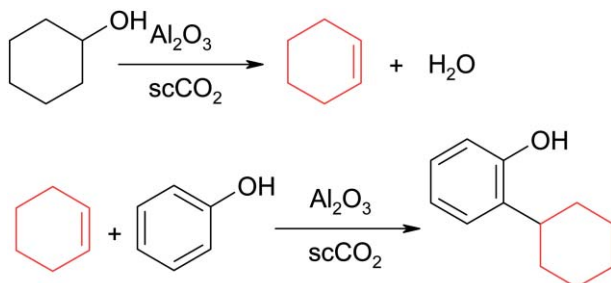


A highly efficient procedure for hydroformylation and hydroamino-vinylation of methyl acrylate

Matthew L. Clarke* and Geoffrey J. Roff

Methyl acrylate can be hydroformylated exclusively to the branched aldehyde with overall turnover frequencies of up to 4250 h⁻¹. Performing these reactions without solvent in the presence of aromatic amines gives excellent yields of enamines in a highly efficient hydroaminovinylation reaction.

797

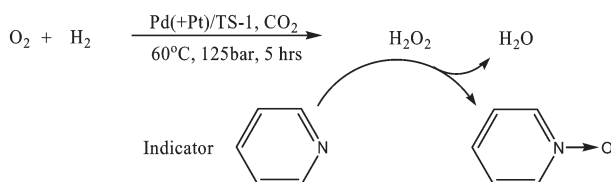


The synthesis of *o*-cyclohexylphenol in supercritical carbon dioxide: towards a continuous two-step reaction

Rodrigo Amandi, Katherine Scovell, Peter Licence, Tobias J. Lotz and Martyn Poliakoff*

Supercritical carbon dioxide is used as a solvent for the continuous alkylation of phenol using a solid acid catalyst, $\gamma\text{-Al}_2\text{O}_3$, with either cyclohexene or cyclohexanol as alkylating agents.

802



Direct synthesis of H_2O_2 from O_2 and H_2 over precious metal loaded TS-1 in CO_2

Qunlai Chen and Eric J. Beckman*

An indicator was used to determine the amount of directly synthesized H_2O_2 in compressed CO_2 . Experimental results proved that H_2O_2 could be effectively synthesized from O_2 and H_2 in CO_2 over precious metal loaded TS-1.

ADDITIONS AND CORRECTIONS

809

Anthony K. Burrell, Rico E. Del Sesto, Sheila N. Baker, T. Mark McClesky and Gary A. Baker

The large scale synthesis of pure imidazolium and pyrrolidinium ionic liquids

AUTHOR INDEX

Aelterman, W., 785
 Afonso, Carlos A. M., 734
 Amandi, Rodrigo, 797
 Arning, Jürgen, 760
 Bansal, Vikas, 742
 Barreiros, Susana, 734
 Beckman, Eric J., 802
 Bottin-Weber, Ulrike, 760
 Calò, Emanuela, 754
 Charpentier, Paul A., 768
 Chen, Qunlai, 802
 Clarke, Matthew L., 792
 De Diego, Teresa, 780
 De Witte, B., 785
 Dewulf, J., 785
 Evtuguin, Dmitry V., 717
 Gamelas, José A. F., 717
 Gaspar, Armindo R., 717

Guidotti, Matteo, 731
 Guo, Haiquan, 746
 Headley, Allan D., 737
 Iborra, José L., 780
 Ivanchikova, Irina D., 731
 Ivaska, Ari, 746
 Jain, Suman L., 740
 Jastorff, Bernd, 760
 Kholdeeva, Oxana A., 731
 Kidwai, Mazaahir, 742
 Kohns, Kevin, 780
 Kumar, Ajeet, 742
 Li, Xincheng, 768
 Licence, Peter, 797
 Loris, Alessandro, 777
 Lotz, Tobias J., 797
 Lourenço, Nuno M. T., 734
 Lozano, Pedro, 780

Maffezzoli, Alfonso, 754
 Martina, Francesca, 754
 Mazzetto, Selma E., 754
 Mele, Giuseppe, 754
 Mozumdar, Subho, 742
 Müller, Anja, 760
 Neto, Carlos Pascoal, 717
 Ni, Bukuo, 737
 Niu, Li, 746
 Piamtongkam, Rungtiwa, 780
 Pitner, William-Robert, 760
 Poliakov, Martyn, 797
 Qiu, Xuepeng, 746
 Ranke, Johannes, 760
 Ravasio, Nicoletta, 731
 Roff, Geoffrey J., 792
 Sain, Bir, 740
 Scovell, Katherine, 797

Selva, Maurizio, 777
 Shen, Yanfei, 746
 Singhal, Sweetie, 740
 Stifani, Cristina, 754
 Stolte, Stefan, 760
 Tarzia, Antonella, 754
 Tundo, Pietro, 777
 Vanbaelen, H., 785
 Van der Vorst, G., 785
 Van Langenhove, H., 785
 Vaultier, Michel, 780
 Welz-Biermann, Urs, 760
 Xu, William Z., 768
 Zhang, Qianying, 737
 Zhang, Yuanjian, 746

FREE E-MAIL ALERTS AND RSS FEEDS

Contents lists in advance of publication are available on the web via www.rsc.org/greenchem - or take advantage of our free e-mail alerting service (www.rsc.org/ej_alert) to receive notification each time a new list becomes available.



Try our RSS feeds for up-to-the-minute news of the latest research. By setting up RSS feeds, preferably using feed reader software, you can be alerted to the latest Advance Articles published on the RSC web site. Visit www.rsc.org/publishing/technology/rss.asp for details.

ADVANCE ARTICLES AND ELECTRONIC JOURNAL

Free site-wide access to Advance Articles and the electronic form of this journal is provided with a full-rate institutional subscription. See www.rsc.org/ejs for more information.

* Indicates the author for correspondence: see article for details.



Electronic supplementary information (ESI) is available via the online article (see <http://www.rsc.org/esi> for general information about ESI).

Image reproduced by permission of the Central Science Laboratory, UK

**Better, faster
communication**

Look no further than the *Journal of Environmental Monitoring* for urgent publication of your cutting-edge research.

Journal of Environmental Monitoring communications report high impact, preliminary results of current and immediate interest. Communications are fast-tracked through the publication process, given a high profile in the journal and widely promoted.

Featured on the cover is a recent communication on the rapid detection of contaminants in potable water.

Adrian J. Charlton *et al.*, *J. Environ. Monit.*, 2006, 8, 1106

Submit your communication today!



16040724

RSCPublishing

www.rsc.org/jem/communications

Registered Charity Number 207890

Future Energy: Chemical Solutions

12 - 14 September 2007
University of Nottingham, UK

This unique three-day conference recognises the importance of the chemical sciences in the field of sustainable energy, a priority of the RSC.

The scientific programme is representative of the key energy areas, including sessions on energy materials, energy innovation and policy, fuel cells, nuclear waste management, carbon capture and storage, bio-energy and catalysts for energy.

Call for poster abstracts deadline - 13 July

Early booking deadline – 13 July

Invited speakers include:

- Steve Koonin (*BP plc*)
- Sir Richard Friend FRS (*Cambridge*)
- Peter Edwards FRS (*Oxford*)
- John Griffiths (*Leeds*)
- Keith Shine (*Reading*)
- Bernard Boullis (*CEA, France*)
- David Carslaw (*Leeds*)
- David Vincent (*Carbon Trust*)

Register now – see the website for full programme and registration information



Chemical Technology

Toxic and radioactive caesium isotope removal studied by molecular dynamics

Making sense of solvent extraction

Computational chemists in France are closer to understanding a process that enhances the extraction of nuclear waste.

Caesium-137 is a toxic and radioactive waste product from nuclear power generation. It can be removed from the waste by an extraction method that uses a type of compound called a calixarene. This forms a complex with the caesium ion (Cs^+), which can then dissolve in an organic solvent and be removed.

In nuclear waste, however, the counter ion for Cs^+ is often a nitrate ion, which does not dissolve well in organic solvents and so Cs^+ is poorly extracted. The extraction can be improved by adding a co-solvent, known as a 'solvent modifier'. Georges Wipff and Nicolas Sieffert at the University Louis Pasteur in Strasbourg wanted to find out how these modifiers work. 'This is important for basic science, as well as for technological applications,' Wipff explained.

Wipff and Sieffert used a



type of computer simulation called molecular dynamics to model systems with a calixarene complex of Cs^+ and nitrate in chloroform, which was modified by a fluorinated alcohol. They

Calixarenes trap the waste, making it easier to remove

looked at systems that contained water as well, as it would be present in the extraction process. They concluded that the modifier worked by improving how well the nitrate ion interacted with the organic phase and by acting as a surfactant, making it easier for the ions to cross the interface between the organic solvent and water.

Jean-Claude Bünzli, an expert in lanthanide supramolecular chemistry from the Swiss Federal Institute of Technology at Lausanne, believes that the research will help chemists to design extraction processes 'in a rational and predictive way'. 'The synergy between theoretical chemistry and experiments therefore leads to a new era in solvent extraction, which will help solve the difficult problem of nuclear waste reprocessing and disposal,' he said.

Rachel Warfield

Reference

N Sieffert and G Wipff, *Phys. Chem. Chem. Phys.*, 2007, DOI: 10.1039/b704395c

In this issue

Molecular sensor for harmful organics

Supramolecular cavitand aids detection of airborne benzene

Chiral quantum dots

Right- and left-handed nanoparticles give off polarised fluorescence

Interview: Water, water everywhere...

Deborah Swackhamer talks to Kathryn Lees and Neil Withers about water pollution and her dream to sing jazz in piano bars

Instant insight: Polymers in nanobionics

Gordon Wallace and Geoffrey Spinks take a close look at the interface between electronics and biology



The latest applications and technological aspects of research across the chemical sciences

Application highlights

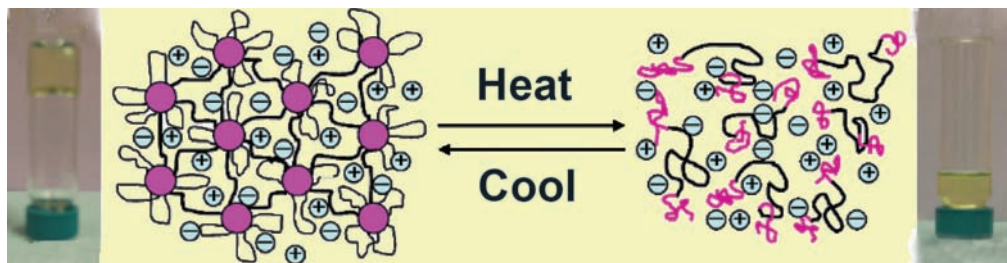
Ionic conductivity improved with less polymer required

Ion gels offer strength and conduction

Reversible liquid–soft solid polymer gels can combine with ionic liquids to provide an alternative to traditional liquid electrolytes. Timothy Lodge and Yiyong He, from the University of Minnesota, US, made ‘ion gels’, networks of a three-part polymer molecule swollen with a large amount of ionic liquid.

‘Compared to other approaches, our gels require significantly less polymer (4% by weight) and offer improved ionic conductivity,’ said Lodge. ‘In addition, they avoid the leakage and flammability issues of organic solvent-based electrolytes.’

The thermoreversible nature of the ion gels, the ability to reverse polymer cross-linking with a change in temperature, enables the material to be processed in the liquid state, but used in the solid state. Lodge said that the ability to



The gels change from solid to liquid with temperature

fine-tune the physical properties of the polymer was ‘achieved through judicious selection of polymer and ionic liquid’.

The ionic conductivity of Lodge’s system was only a few percent below that of the pure ionic liquid but it possessed good mechanical strength, even under heavy strain, and offered the advantage of solvent-free processing.

Lodge expects the ion gels to find diverse applications,

including sensors, transistors, electromechanical systems, light-emitting cells and gas separation. Pradip Bhowmik of the University of Nevada agreed: ‘These ion gels will definitely find applications in many new technologies and the design of smart materials in the near future.’

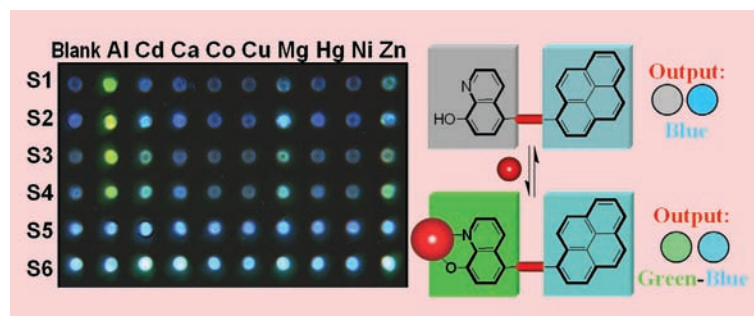
Michael Spencelayh

Reference

Y He and T P Lodge, *Chem. Commun.*, 2007 DOI: 10.1039/b704490a

Heavy metal ions recognised by changes in emission

Sensor arrays for cations



The colour of the emission depends on the metal ion

A series of hydroxyquinolines show promise as elements in sensor arrays for detecting metal ions in water.

Some heavy metals such as mercury have no known vital or beneficial effect on organisms and their accumulation over time in the body can cause serious illness. Because they cannot be degraded or destroyed, they have significant potential to impact human health and the whole environment. Thus, sensing of heavy metal ions in water is important for maintaining

the well-being of humans and protecting the environment, said Pavel Anzenbacher of Bowling Green State University, US.

A sensor array is made up of several sensor elements. These elements are not highly selective toward specific analytes, but the specificity of the device comes from recognition of response patterns such as fluorescence. This pattern originates from interactions of the analyte with each of the sensors in the array. This response pattern is unique to the analyte, like a

fingerprint.

Anzenbacher’s team designed sensors comprising an 8-hydroxyquinoline ligand and blue emitting residues. The quinoline forms luminescent chelates with a number of metal ions. It also shows a handy turn-on signal, because it is non-fluorescent in water but emits a blue–green colour when it binds to a metal. The colour depends on the 8-hydroxyquinoline substituents and, crucially, the metal ion.

By extending the length of these conjugated chromophores (the colour-emitting groups) they were able to vary the ratio of the blue to green emissions from the metal chelates. Changes in the blue and green emissions of the metal complexes are then used to distinguish between the cations.

‘The novelty of our approach is the use of one receptor (ligand) type and varying the chromophore to generate variable signal output,’ said Anzenbacher.

Sarah Corcoran

Reference

M A Palacios *et al*, *Chem. Comm.*, 2007, DOI: 10.1039/b705392d

Cavitand trap detects low concentrations of airborne benzene

Molecular sensor for harmful organics

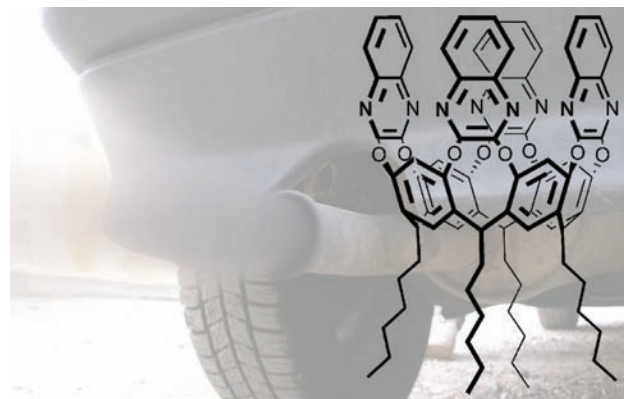
Monitoring levels of organic contaminants in roadside air is now possible thanks to a supramolecular approach developed by Italian scientists. They used molecular cavities to detect aromatic compounds at concentrations lower than parts per billion (ppb).

Measuring sub-ppb amounts of airborne organic contaminants is difficult as readings can be swamped by other compounds present in high concentrations. Current metal oxide gas sensors are not selective enough to detect organic molecules.

By trapping and concentrating the aromatic organic compounds in a supramolecular cavity, Enrico Dalcanele, Stefano Zampolli and colleagues at the University of Parma and the National Research Council, Bologna, have designed a sensor capable of detecting low levels of aromatic compounds.

'The main drive is to provide low-cost, stand-alone sensor systems for outdoor pollution monitoring, in particular benzene,' said Dalcanele.

The sensor is palm-sized and connected to a detector composed of a micromachined gas chromatographic column and metal oxide sensor array. The result of the combination of supramolecular



sensor and detector is increased selectivity and sensitivity.

'The system automatically performs sampling, injection, separation and cleaning steps and the sampling phase has a typical duration of 10–60 minutes,' said Dalcanele. 'So it measures volatile organic compounds, stand-alone and in real-time, as an average value over the sampling period.'

The supramolecular trap, a quinoxaline-bridged cavitand, is bowl-like with a cavity about eight Ångströms deep and wide. The cavitand has two roles – it separates the aromatic compounds from other pollutants and interferents in the air and it concentrates the aromatic organic compounds to a

The cavity could be tailored to trap different compounds

Reference
S Zampolli *et al*, *Chem. Commun.*, 2007, DOI: 10.1039/b703747c

level sufficient to be detected by the metal oxide sensor.

As the cavitand only traps aromatic compounds, it is insensitive to aliphatic carbons, water and other polluting gases. However, the same system could be adapted for other applications by tailoring the supramolecular receptor to the desired analyte.

'The selectivity of the new approach is a real breakthrough: single aromatic compounds are chromatographically separated and quantified,' said Dalcanele. 'The proposed sensor system is very small, easy to use and shows exceptional performance in the sub-ppb range.'

Franz Dickert, an analytical chemist at the University of Vienna, praised the strategy and thought it could be used in workplace monitoring. 'A pre-concentration step will improve the sensitivity and selectivity of the sensor, in contrast to chromatography in sensors where there is only one separation step,' said Dickert.

Dalcanele and co-workers are actively collaborating with local environmental protection agencies and the system is currently being validated in the field.

Alison Stoddart

Right- and left-handed nanoparticles give off polarised fluorescence

Chiral quantum dots

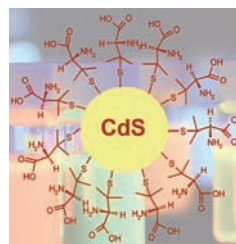
Fluorescent semiconductor nanoparticles that exhibit chiral luminescence have been made by scientists from Ireland.

Chirality is an important factor in molecular recognition, so a nanosized probe with chiral luminescence would be useful in chemistry and biology. By stabilizing cadmium sulfide nanoparticles, or quantum dots (QDs), with penicillamine Yuriy Gun'ko's team at Trinity College, Dublin, believe they have done just that.

Gun'ko's team prepared the chiral QDs by heating naked ones with

either left- or right-handed forms (enantiomers) of penicillamine. These gave off a green–white light when excited with UV light. When a fifty–fifty (racemic) mixture of the two enantiomers was used, the QDs gave off a blue–white light instead.

Circular dichroism studies (used to distinguish between left- and right-handed circular polarised light) found that while the racemic QDs displayed only a weak signal, the right- and left-handed QDs rotated light in opposite directions, producing almost symmetric signals. This would allow the QDs to be used



Reference
M P Moloney, Y K Gun'ko and J M Kelly, *Chem. Commun.*, 2007, DOI: 10.1039/b704636g

as fluorescent chirality sensors and in molecular recognition.

Paul O'Brien of the University of Manchester, UK, was enthusiastic about Gun'ko's work, and said 'producing a chiral emission from a quantum dot is an exciting development that could lead to new applications in chiral probes and even electronics'.

Gun'ko agreed, saying 'chiral QDs could find important applications in the pharmaceutical industry, asymmetric catalysis, and in vitro medical diagnostics.'

Vikki Chapman

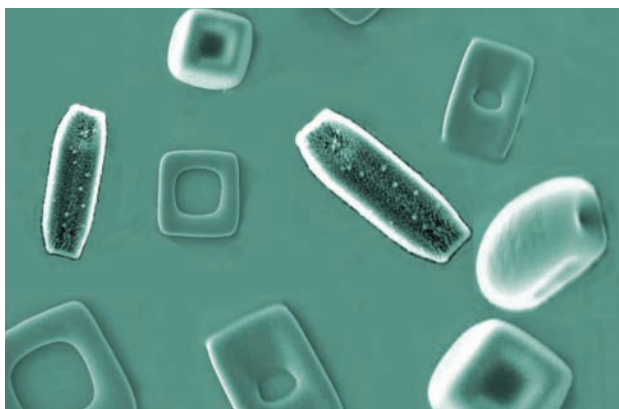
Higher throughput and better particle resolution available

The shape of things to come

A microfluidic device technique called stop-flow lithography, for making custom designed polymeric particles with complex geometric shapes, has been developed by US researchers.

Patrick Doyle and colleagues from MIT are working on methods for synthesising particles with complex geometric shapes. While spherical particles are widely used in applications like optical devices, drug delivery and diagnostics, more complicated particles could enable new technologies in these areas, but they are difficult to make. Building on his team's previous work to face this challenge, with a method combining microfluidics with projection-photolithography called continuous flow lithography (CFL), Doyle devised a technique called stop-flow lithography (SFL).

SFL gives a higher particle throughput and better particle



resolution than CFL. A unique feature of the new method is that the particles formed are not just spherical – it can make a wide range of shapes. SFL also allows the formation of particles in biocompatible and easily functionalised materials that are not typically amenable to

A wide range of complex shapes can be made

Reference

D Dendukuri *et al*, *Lab Chip*, 2007, DOI: 10.1039/b703457a

photolithographic methods.

Doyle hopes to expand the range of particle morphologies and materials accessible to SFL. 'We are also looking at several potentially interesting applications for these particles in diagnostics as well as in conducting fundamental studies on colloidal assembly and rheology,' he said.

A challenge for the future is the scale-up of particle throughput to match current industrial processes. 'This is not so much of a concern for niche applications enabled by complex particles where no alternative technology exists and only small volumes of particles are desired. However, it is important when particles made using microfluidic techniques are sought to be used in more routine applications such as paints or coatings,' said Doyle.

Elinor Richards

Road run-off systems could improve collection of heavy metals

Modelling metallic emissions



Researchers in Switzerland have developed a method of modelling heavy metal emissions from road traffic.

Many heavy metal pollutants such as cadmium and lead are toxic at fairly low concentrations and

can poison biological organisms if they are accumulated. A variety of heavy metal contaminants can enter the environment from road traffic emissions. Once released into the environment, these pollutants can enter groundwater and contaminate

Pollutants can enter groundwater or soil

the soil.

Now Michele Steiner and co-workers at the Swiss Federal Institute of Aquatic Science and Technology and Swiss Federal Institute of Technology have developed a model describing heavy metal emissions from road traffic. This model describes metal fluxes into the roadside environment as a function of the distance from the road. The model distinguishes between three different pollutant transport mechanisms (road run-off, spray and drift), and was applied to a case study of Burgdorf, Switzerland.

The team found that up to 50% of the heavy metal emissions from road traffic could be collected and treated with the design and implementation of appropriate road run-off treatment systems.

Russell Johnson

Reference

M Steiner *et al*, *J. Environ. Monit.*, 2007, DOI: 10.1039/b703509h

Interview

Water, water everywhere...

Deborah Swackhamer talks to Kathryn Lees and Neil Withers about water pollution and her dream to sing jazz in piano bars



Deborah Swackhamer

Deborah Swackhamer is professor of environmental chemistry at the University of Minnesota, US, and chair of the editorial board of the *Journal of Environmental Monitoring*. Her work focuses on water pollution, in particular, on the chemical and biological processes that control the fate of toxic organic contaminants in the Great Lakes of North America.

What inspired you to become a scientist?

As a child, I spent my summers in Canada. Our family had a summer cottage on a lake and it was so pristine and beautiful – I thought everyone had lakes like that! At college, I studied math but took a writing tutorial on water chemistry. This grabbed my interest and I switched majors to focus on environmental chemistry.

What is the focus of your research?

When I was a graduate student I saw the Great Lakes for the first time – I was stunned by their size and beauty. As a result, I spent my graduate work understanding the chemical behaviour of the Great Lakes and, ever since, I've focussed on water chemistry programmes of the Great Lakes basin. Because the Great Lakes act like fresh water oceans, you can understand global processes by studying them. They're also easily accessible and urbanised – 42 million people live in the basin so they're reasonably polluted.

What are the main pollutants in the Great Lakes?

There are still 'legacy pollutants' such as polychlorinated biphenyls (PCBs) and DDT coming from atmospheric deposition as well as phosphorus and nitrogen from agriculture and sewage. However, the new problem is with endocrine disrupters. We know little about where they're coming from but we know they're causing oestrogenic effects. At present, they are impacting fish and birdlife but we are not sure if they are affecting people who are drinking the water.

What is the greatest threat to the Great Lakes?

In addition to the chemicals, biologically, there are close to 200 invasive species and a new one is added every eight months. The impact on food webs and ecology could be enormous. However, a dominant factor is the physical threat of global climate change. It affects how chemicals behave in the environment and it drives change in an ecosystem too. Everything is interrelated.

What influences where a particular pollutant will end up?

Luckily, it's pretty easy to predict that sort of thing from chemical structure. You can predict a chemical's behaviour by knowing two things: its aqueous solubility and its vapour pressure. Its solubility tells you whether it will be in fish or our food supply and its vapour pressure and Henry's

law constant tells you whether it will end up in soil, water or air. Finally, you can use the structure of the chemical to see if it will break down or not. We know quite a bit about which bonds are easy to break or metabolise in animal systems.

You often appear on news programmes. How important is it for scientists to have a voice in the media?

It is absolutely critical. We often say the media doesn't ask good questions, but if that's the case it's because we're not communicating well enough with them. It's our responsibility to make sure that what we do is translated appropriately to the media and the general public. Otherwise, others will do it for us and will do it poorly. It's very important that scientists who deal with real world issues inform the decision makers too.

Do you have any involvement with politicians?

We often get asked our opinions on things, but there's a fine line between advocating for a policy and informing for a policy. Many scientists say 'No, I shouldn't even talk to a decision-maker!', but others advocate very strongly. I think it is our role to speak out when people are misusing science to set policy. I'm not sure it's my role as a scientist advocate for a policy – but it's certainly my role to advocate for the truth.

Some pollutants are of great use to many people – how can we find a balance?

Part of the problem is that our regulatory systems for evaluating chemicals are not rigorous enough. If you add something to a soap powder to make it an improved detergent, there are many things you could use. Typically, the least expensive product is added but these additives may be oestrogenic in the environment. The US Toxic Substances Control Act (TSCA) was meant to regulate toxic compounds, but they have allowed many harmful chemicals through their regulatory 'filter'. The EU is moving towards a more stringent filtering process with REACH. We need better modelling tools for predicting toxicity and environmental behaviour so that we can design chemicals that will benefit society and not hurt the environment.

If you weren't a scientist what would you do?

My second love is singing. If I could wave a magic wand, I would sing jazz in a piano bar. I'd have to find someone who could play the piano though!



IST Sample Preparation • Bioanalysis • Clinical • Environmental • Forensic • Agrochemical • Food • Doping Control

EVOLUTE™ ABN—easy and reliable

Minimize matrix effects, reduce ion suppression and concentrate analytes of interest for better quantitation

EVOLUTE™ ABN (Acid, Base, Neutral) is a water-wettable polymeric sorbent optimized for fast generic reversed phase SPE. The smaller (40Å) pore diameter prevents the retention of large molecular weight interferences providing cleaner extracts and higher analyte recoveries. Available in 96-well plate and column formats. Visit www.biotage.com to request a FREE sample.


Biotage
www.biotage.com

Instant insight

Polymers in nanobionics

Gordon Wallace and Geoffrey Spinks of the University of Wollongong, Australia, take a close look at the interface between electronics and biology

Effectively bridging the interface between electronics and biology is critically dependent on advances in new electronically conducting materials. The discovery of inherently conducting polymers (ICPs) in the late 1970s revolutionised this field and organic electronic conductors are now at our disposal. The soft character of ICPs provides an extra dimension in designing interfaces between the hard, digital electronics world and the soft, amorphous world of biological systems. ICPs are unique with their potential to impact on bionic devices from the molecular, through the cellular, to the skeletal level.

For any implanted bionic material it is the initial interactions at the (bio)molecular level that will determine longer term performance. Initially, the ability to incorporate biomolecules during the growth of conducting polymers and to expel these molecules by electrical stimulation was seen as a means to develop controlled release systems for active ingredients such as anticancer drugs or anti-inflammatories.

This ability to control biomolecular interactions on conducting polymer surfaces provides a pathway for controllable interactions with whole cells. ICP platforms have been used to promote neuronal cell growth and the application of an electrical stimulus to the cell culture on the PPy film significantly increased the expression of neurites in the cells. These new materials might well eventually find use in medical implants that require electrical connection to nerve cells (for example, as bionic ears or eyes).

The popular concept of bionic devices is at the whole organ or the skeletal level. The ability to monitor and manipulate human movement and senses such as hearing and sight is physically demonstrable



Truly bionic limbs are still a long way from reality

with devices such as the Cochlear Implant (the 'bionic ear'). Manipulating human movement is the most mammoth of tasks. It is amazing to admit that in this highly technological world we live in, we still do not have adequate light weight, low power consumption technologies that can be strapped on to assist in human movement.

ICPs are promising materials for building artificial muscles. Their development for this can be traced to Baughman's paper in 1990.¹ Numerous applications have been proposed or demonstrated including robotics, an electronic Braille screen and in bionic applications like a 'rehabilitation glove'.

While significant improvement in artificial muscle performance based on conducting polymers has occurred in recent years, there is still some way to go before we can match natural muscle in terms of speed, efficiency and control. The amount of movement that can be generated has increased dramatically in recent years to around 40% (comparable to natural muscle), although with conducting polymers this takes several minutes to occur. The speed of response has been increased by tuning the electronic control system and the conductivity of the structure

used. The fastest response from an ICP actuator (15%/s) is still considerably slower than natural skeletal muscle (~80%/s). Next to large movements, speed is critically important in generating useful motion. The large, fast movements possible through musculo-skeletal systems in animals is the basis of running, flying, swimming – attributes that would be highly desirable in nimble, dexterous and possibly miniaturised robots.

Recent material developments move us closer to these possibilities. Like natural muscle, the formation of ICPs into fibres provides a better geometry for actuator performance. For example, polyaniline fibres are now readily available in high strength and conductivity. Furthermore, we have shown that the addition of small quantities of carbon nanotubes to polyaniline, followed by wet-spinning and drawing, produces superior actuation response under an external load. In fact, we measured an actuation response at more than 100 MPa applied stress, three times higher than previously reported for conducting polymer actuators.

This is just one example wherein advances in nanomaterials and nanofabrication have already impacted on the performance of organic conducting polymers as bionic devices. Nanostructuring provides dramatic improvements in the electronic properties of conducting polymers.

As material scientists delve into the nanodomain, the boundaries between electronics and biology become fuzzy. This is exactly what we want – a seamless transition between the hard world of electronics and the soft world of biology!

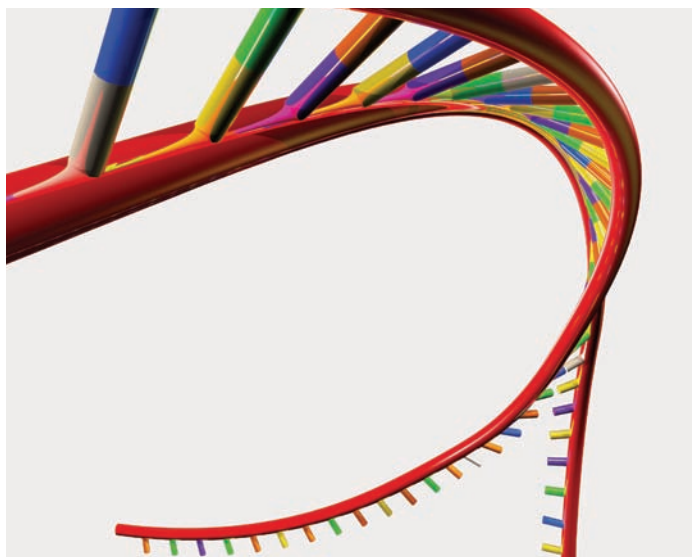
Read the full Opinion article 'Conducting polymers – bridging the bionic interface' in June's issue of Soft Matter.²

References

- 1 R Baughman *et al*, in *Conjugated polymeric materials: opportunities in electronics, optoelectronics and molecular electronics*, ed. J Bredas and R Chance, Kluwer, Dordrecht, 1990, 559.
- 2 G Wallace and G Spinks, *Soft Matter*, 2007, **3**, 665 (DOI: 10.1039/b618204f)

Essential elements

Molecular BioSystems unzips...



From January 2008 *Molecular BioSystems* will form its very own strand of science as a solo monthly journal, made available to readers and subscribers independently of its host journal. 'We're proud of the progress

Molecular BioSystems has made since its launch in 2005,' said Robert Parker, managing director at RSC Publishing. 'The journal has grown, the quality of science is excellent and feedback from readers has been

overwhelmingly positive. Now is an appropriate time for this success to be translated into a solo publication.'

Since the publication of the first issue, *Molecular BioSystems* has been paired with *Chemical Communications*. This interaction with the host has resulted in an excellent communication channel for the published content, which has reached a wide and interdisciplinary audience. Online pairing with four other complementary publications (*Organic & Biomolecular Chemistry*, *Lab on a Chip*, *The Analyst* and *Analytical Abstracts*) ensured optimum visibility.

'Now is the perfect time to unzip *Molecular BioSystems* from its hosts,' commented Michael Smith, commissioning editor. 'We believe the journal has a great deal to offer to the chemical biology community.'

Read more at www.molecularbiosystems.org/unzip

Pioneers in Miniaturisation Prize

Leading the way in miniaturisation, *Lab on a Chip* has teamed up with Corning Incorporated to again host the Pioneers in Miniaturisation Prize. Spanning a variety of disciplines, this prize recognises outstanding achievements and significant contributions by a younger scientist to the understanding and advancement of micro- and nanoscale science.

As a leading-edge science and technology organisation, Corning Incorporated is keen to reward, recognise and encourage the development of miniaturisation in the chemical and biological sciences and promotes interdisciplinary research required for the most significant innovations in this area.

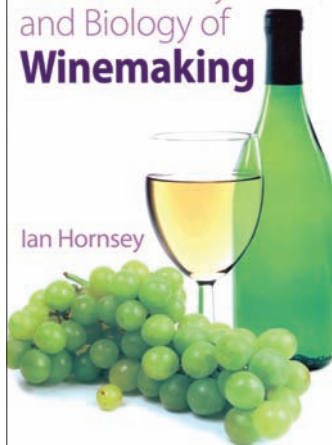
The recipient of the award

will receive a \$5000 bursary to support their continued contribution to the field. A deadline for applications has been set for 31st August 2007. Following the final decision, which will be made by committee, a winner will be announced at μ TAS 2007 conference, in Paris, France.

For further information visit www.rsc.org/loc/pioneerprize

And finally...

The Chemistry and Biology of Winemaking

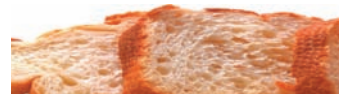


In the past twelve months the RSC book *Kitchen Chemistry* has become an international bestseller! It is an exceptional learning resource and offers a fascinating insight into the science in our kitchens.

RSC Publishing also has an extensive food science book list that caters for scientists at all levels, from schools through to industry.

Newly published books include *The Science of Bakery Products* and *The Chemistry and Biology of Winemaking*, which now join other bestselling titles such as *The Science of Chocolate* and *Gums and Stabilisers for the Food Industry*.

For more information visit www.rsc.org/books



Chemical Technology (ISSN: 1744-1560) is published monthly by the Royal Society of Chemistry, Thomas Graham House, Science Park, Milton Road, Cambridge UK CB4 0WF. It is distributed free with *Chemical Communications*, *Journal of Materials Chemistry*, *The Analyst*, *Lab on a Chip*, *Journal of Environmental Monitoring*, *Green Chemistry*, *CrystEngComm*, *Physical Chemistry Chemical Physics* and *Analytical Abstracts*. *Chemical Technology* can also be purchased separately. 2007 annual subscription rate: £199; US \$376. All orders accompanied by payment should be sent to Sales and Customer Services, RSC (address above). Tel +44 (0) 1223 432360, Fax +44 (0) 1223 426017 Email: sales@rsc.org

Editor: Neil Withers

Associate editors: Nicola Nugent, Celia Clarke

Interviews editor: Alison Stoddart

Essential Elements: Valerie Simpson, Caroline Wain, Ricky Warren

Publishing assistant: Jackie Cockrill

Publisher: Graham McCann

Apart from fair dealing for the purposes of research or private study for non-commercial purposes, or criticism or review, as permitted under the Copyright, Designs and Patents Act 1988 and the copyright and Related Rights Regulations 2003, this publication may only be reproduced, stored or transmitted, in any form or by any means, with the prior permission of the Publisher or in the case of reprographic reproduction in accordance with the terms of licences issued by the Copyright Licensing Agency in the UK. US copyright law is applicable to users in the USA.

The Royal Society of Chemistry takes reasonable care in the preparation of this publication but does not accept liability for the consequences of any errors or omissions.

Royal Society of Chemistry: Registered Charity No. 207890.

RSC Publishing

©The Royal Society of Chemistry 2007

NEW
& IMPROVED

Analytical Abstracts...



Analytical Abstracts covers all areas of analytical and bioanalytical science, including the latest applications and cutting edge techniques. The database is updated weekly and spans 25 years of research sourced from over 100 international journals.

...the first stop for analytical scientists

New and improved features include:

Improved search features with a basic search and optional advanced searches by index term and bibliographic data. You can also browse by subject area.

Results can be sorted and displayed in different formats and have additional information embedded in the text accessed via pop up boxes.

Results can be exported to reference management software and to email.

RSC Publishing

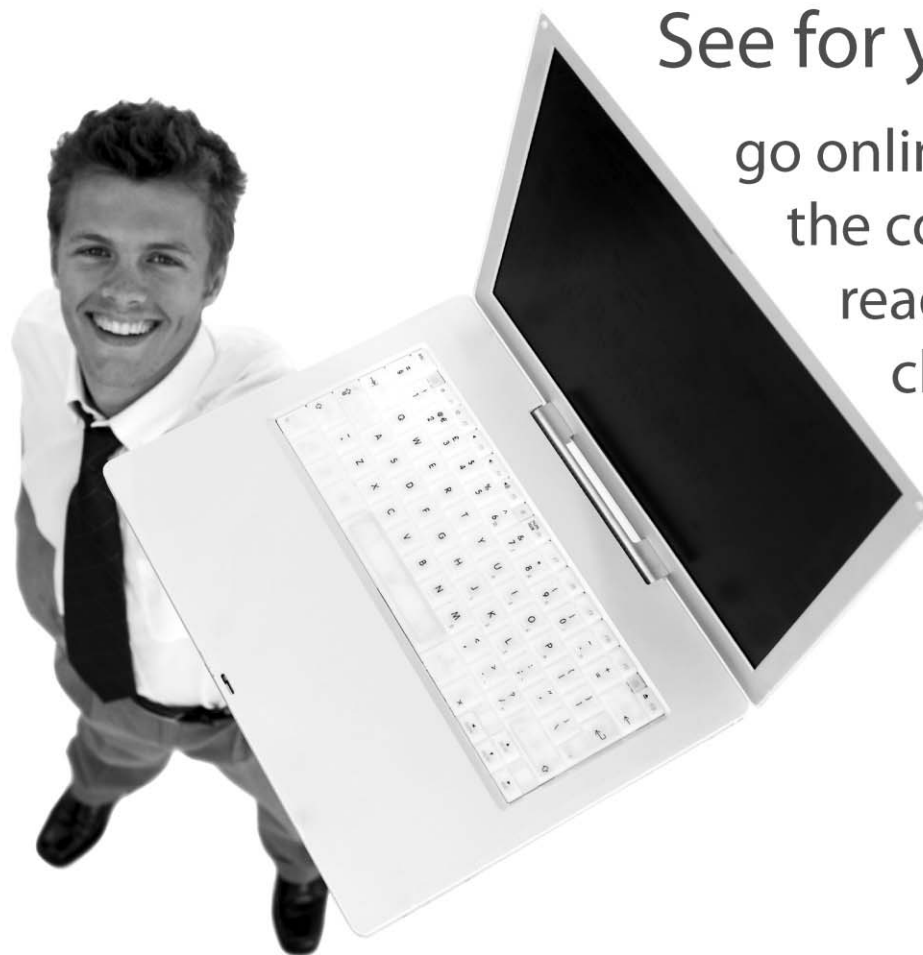
www.rsc.org/aa
Registered Charity Number 207890

RSC eBook Collection

Access and download existing and new books from the RSC

- **Comprehensive:** covering all areas of the chemical sciences
- **Fully searchable:** advance search and filter options
- **Wide ranging:** from research level monograph to popular science book

See for yourself –
go online to search
the collection and
read selected
chapters
for free!



Registered Charity Number 207890

20100654

RSC Publishing

www.rsc.org/ebooks

Alternatives for lignocellulosic pulp delignification using polyoxometalates and oxygen: a review

Armindo R. Gaspar,^a José A. F. Gamelas,^{*b} Dmitry V. Evtuguin^b and Carlos Pascoal Neto^b

Received 1st June 2006, Accepted 30th January 2007

First published as an Advance Article on the web 26th February 2007

DOI: 10.1039/b607824a

A review on the use of polyoxometalates (POMs) and oxygen, for the delignification of lignocellulosic pulps is presented. Two main processes using POMs for the delignification of pulp have been investigated: an anaerobic process in which the POMs have been used, in aqueous solutions, as stoichiometric reagents for the oxidative degradation of residual lignin, with their re-oxidation by oxygen occurring in a subsequently separate stage; and an aerobic process in which the POMs were designed to perform as catalysts in the oxygen delignification. In the aerobic approach, the lignin oxidation and the reactivation of the POM take place in the same stage of the process. The feasibility of the catalytic system was shown by pilot plant experiments. Following the green chemistry goals, these processes are environmentally friendly approaches and may allow a significant decrease of chlorine-based chemical consumption by the pulp-and-paper industry. The use of the POMs together with laccase for the oxygen delignification of lignocellulosic pulps will also be considered. Final comments regarding the practical application of the POMs are pointed out.

1. Introduction

The pulp-and-paper industry represents one of the biggest industries worldwide. The main goal is the production of a fibrous material from wood that possesses physical and mechanical properties appropriate for the manufacture of paper. Typically, this is performed through two main processes: pulping and bleaching. In the pulping process, most of the lignin is removed from the wood leading to an unbleached chemical pulp, composed mainly of cellulose (80–90%), hemicelluloses (5–15%) and still a small amount of

lignin (2–5%).¹ It is followed by bleaching processes in which the residual lignin is removed (delignification), originating the so-called bleached pulp.² The major part of the bleaching technologies still employ chlorine dioxide, which has proved to be very selective oxidant, oxidising the residual polymeric lignin with minimal degradation of the polymeric chain of polysaccharides.¹ However, the impact of the chlorine reagents on the environment is high. The chlorinated organic by-products released in the bleach plant effluent may accumulate and progressively destroy the life of ecosystems near the paper manufacture factories. The use of ‘alternative’ oxidants for the delignification of pulp, such as oxygen, ozone, or hydrogen peroxide, is recommended. In particular, oxygen (and water) are the ideal oxidant (and solvent) respectively, in terms of green chemistry.

^aDepartment of Wood and Paper Science, North Carolina State University, Raleigh, NC 27695-8005, USA

^bCICECO and Department of Chemistry, University of Aveiro, 3810-193 Aveiro, Portugal. E-mail: jgamelas@dq.ua.pt



Armindo Ribeiro Gaspar

Armindo Ribeiro Gaspar, born in 1969, studied analytical chemistry at the University of Aveiro (Portugal). He received his MSc (1996) in materials engineering and his PhD (2002) in chemistry by the University of Aveiro. His PhD and followed post-doctoral studies were completed with the supervision of Professor Evtuguin and Professor Pascoal Neto. Subsequently, industrial experience was accomplished in RAIZ, Portugal. Since 2004, he joined the Professor Argyropoulos's group at the North Carolina State University. One of his research interests is the catalytic processes applied to the pulp and paper industry.

Armindo Ribeiro Gaspar, born in 1969, studied analytical chemistry at the University of Aveiro (Portugal). He received his MSc (1996) in materials engineering and his PhD (2002) in chemistry by the University of Aveiro. His PhD and followed post-doctoral studies were completed with the supervision of Professor Evtuguin and Professor Pascoal Neto. Subsequently, industrial experience was accomplished in RAIZ, Portugal. Since 2004, he joined



José António Ferreira Gamelas

José António Ferreira Gamelas, born in 1970, studied analytical chemistry at the University of Aveiro (UA), Portugal. In 2001 he received his PhD degree at the same University, with a thesis on the ‘Synthesis and characterization of novel polyoxometalate compounds’. He taught chemistry at the UA from 2000 to 2003. Since, then, he has been working as a post-doctoral fellow in the area of chemistry and technology of lignocellulosic materials. He is the author/co-author of several papers in prestigious journals of inorganic chemistry, catalysis and electrochemistry.

José António Ferreira Gamelas, born in 1970, studied analytical chemistry at the University of Aveiro (UA), Portugal. In 2001 he received his PhD degree at the same University, with a thesis on the ‘Synthesis and characterization of novel polyoxometalate compounds’. He taught chemistry at the UA from 2000 to 2003. Since, then, he has been working as a post-doctoral fellow in the area of chemistry and technology of lignocellulosic materials. He is the author/co-author of several papers in prestigious journals of inorganic chemistry, catalysis and electrochemistry.

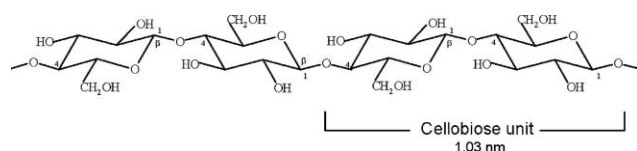


Fig. 1 Simplified representation of cellulose structure.

Since the middle of the 1990s, considerable efforts have been made to introduce a new class of compounds – the polyoxometalates – together with oxygen for lignocellulosic pulp delignification. Polyoxometalates are metal–oxygen clusters,^{3–7} widely studied as oxidation catalysts,^{8–11} and which have also been found to be effective for oxidative pulp delignification. Anaerobic systems in which they act as potential renewable oxidants, or aerobic systems where they are used simultaneously with oxygen have been tested. In this paper we review the state of the art on the use of polyoxometalates (mainly in aqueous solutions) as oxidants or catalysts for the delignification of pulp as an alternative in reducing the use of hazardous chlorine-based reagents, such as ClO_2 . The use of polyoxometalates coupled with enzymes will be considered as well. Environmentally friendly alternatives are presented, regarding the efficiency and selectivity of the various systems and the practical aspects of their potential application. Some background on the chemistry of wood and polyoxometalates is initially given.

2. Wood, pulping and oxidative pulp delignification

Wood is the biological feedstock for the manufacture of paper and is composed mainly of polymeric substances such as cellulose, hemicelluloses and lignin. The relative amounts of wood components vary with wood species, within the tree, with cell wall type and within the cell wall.^{2,12,13}

Cellulose, which constitutes the main component of wood, is a linear homopolysaccharide composed of β -D-glucopyranose units (about 5000–6000), which are linked by (1 \rightarrow 4)-glycosidic bonds (Fig. 1). Along the chain direction, the repeating

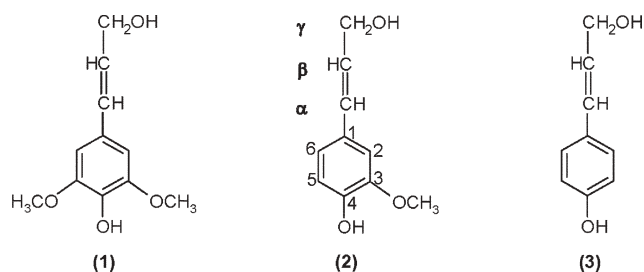


Fig. 2 Structures of lignin precursors (1–3).

stereo-regular unit is a cellobiose residue (1.03 nm) and every glucose residue is accordingly displaced 180° with respect to its neighbours. As a consequence of its fibrous structure and due to the strong tendency to form intramolecular and intermolecular hydrogen bonds, cellulose has a high tensile strength, which is responsible for wood rigidity. Besides the crystalline regions, cellulose also presents amorphous regions, which are more vulnerable to degradation. By contrast, hemicelluloses are predominantly branched hetero-/homopolysaccharides of non-cellulose type, which have a degree of polymerization between 100 and 200. Like cellulose, most hemicelluloses function as a supporting material in the cell wall.^{2,12,13} The major hemicellulose of hardwoods is glucuronoxylan, which suffers partial demethoxylation during the kraft pulping, thus originating a small proportion of hexenuronic groups (HexA). These unsaturated residues may consume some bleaching chemicals (such as ozone, chlorine dioxide, and peroxyacids).^{1,2}

Lignin is a tri-dimensional heteropolymer built up of hydroxylated and methoxylated phenylpropane units (C_9). The α,β -unsaturated C_6C_3 precursors of lignin are the sinapyl alcohol (1), coniferyl alcohol (2) and *p*-coumaryl alcohol (3) (Fig. 2; see also the common designation of each carbon in the phenylpropane unit) which gives rise in the lignin structure to the syringyl (S), guaiacyl (G) and *p*-hydroxyphenyl (H) units, respectively.^{2,12,13} Lignin is the component of wood that should be degraded selectively to obtain high quality cellulose



Dmitry V. Evtuguin

Dmitry V. Evtuguin was born in Petrozavodsk (Republic of Karelia, USSR) on 5 April 1963. Graduated in Chemical Engineering and Technology, specialty of Chemical Processing of Wood, by the Leningrad Forest Technical Academy (LFTA), USSR (1985). Candidate of Chemical Science (PhD) in Wood Chemistry by LFTA, USSR (1988). Associate Professor at the Department of Chemistry of the University of Aveiro since 1995. He is the author/co-author of 98 articles and book chapters, 147 conference communications and four patents.



Carlos Pascoal Neto

Carlos Pascoal Neto, born in Ponte de Vagos (Vagos, Portugal) in 1965, studied Chemistry at the University of Aveiro (UA), Portugal. In 1992 he has got a PhD degree at the Institut National Polytechnique de Grenoble (EFGG-INPG, France) in Pulp and Paper Processing. In the same year, he became a staff member of the Department of Chemistry of UA, firstly as Assistant Professor then, in 2000, as Associate Professor and, from 2005 till now, as Full Professor in Chemistry and Technology of Lignocellulosic Materials. He is the author/co-author of six book chapters, 105 papers in international journals, two patents and about 140 papers in conference proceedings.

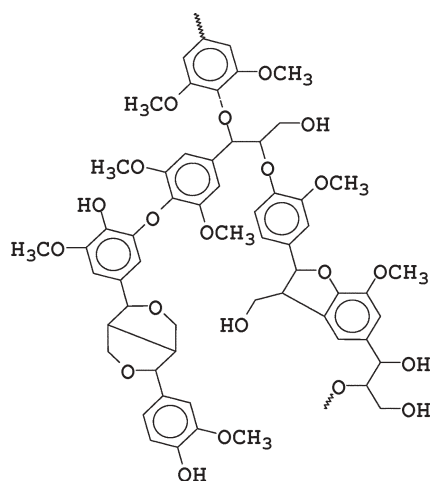


Fig. 3 Schematic representation of the chemical structure of hardwood lignin. The lignin biosynthesis is also accompanied by the formation of lignin–carbohydrate links in cell walls.

fibres. Lignins of softwoods, hardwoods and grasses are different with regard to their structural elements. So-called ‘guaiacyl lignin’ (G-type lignin) which occurs in almost all softwoods is largely a polymerization product of coniferyl alcohol. The ‘guaiacyl-syringyl lignin’ (GS-type lignin) typical of hardwoods is a copolymer of coniferyl and sinapyl alcohols, with the S/G ratio varying from 4 : 1 to 1 : 2. It is noteworthy that in all kinds of lignins there exist the three types of units in different concentrations. In wood lignin, more than two thirds of the phenylpropane units are linked by ether bonds and the rest mainly by carbon-to-carbon bonds (Fig. 3).^{2,12,13}

Wood pulping processes range from purely physical fibre separation procedures to full chemical methods of degrading and removing lignin, the inter-fibre bonding material. The sulfate or kraft process is the dominant chemical pulping process.^{2,12,13} Wood chips are impregnated with the pulping liquor (pH > 13–14) at liquor-to-wood ratios of about 4. The soaked chips are heated up to 150–180 °C, for 1–2 h, in batch or continuous systems. None of the commercial pulping processes can completely delignify wood without adversely affecting the strength properties of the fibres. In the kraft process, the delignification takes place mainly through the cleavage of the aryl ether bonds. Traditionally, about 2–3% of lignin is left in unbleached hardwood pulps and about 3–5% in softwood pulps. The unbleached kraft pulps have a characteristic brown colour, mainly due to the lignin chromophore groups.

Bleaching^{1,14,15} is a chemical process applied to ligno-cellulosic materials in order to remove the residual lignin (delignification) present in the pulp and achieve an adequate brightness (a measure of how much light is reflected from a handsheet of paper) by elimination of the chromophore groups. The bleaching reactions that occur are highly complex due to the heterogeneity of lignin and the wide variety of reactive bleaching species present. The chemicals commonly used for pulp bleaching include oxidants such as chlorine (C), chlorine dioxide (D), oxygen (O), ozone (Z) and hydrogen peroxide (P), and NaOH, used in the alkaline extraction stage (E). Bleaching chemicals are frequently applied sequentially

with intermediate washing between treatments (stages), because it is not possible to achieve sufficient removal of lignin or decolourisation by the action of any chemical in a single treatment or stage without significant cellulose damage. Multi-stage sequences take advantage of the different action of each chemical and provide synergy in bleaching or delignification. Typically, there are two main process variables usually determined to evaluate the degree of delignification and the degradation of the polysaccharides: kappa number and intrinsic viscosity. The kappa number is a parameter that estimates the amount of potassium permanganate oxidisable moieties in the pulp, mainly residual lignin. The intrinsic viscosity is an index related to the degree of polymerization of the polysaccharides. In the delignification process the kappa number of the pulp must be reduced with the minimal decrease of intrinsic viscosity. Both analyses allow determining the selectivity of the process.

There has been a rapid evolution of processes for the production of bleached pulp. Much of this technological activity has been environmentally driven. First, by trying to substitute elemental chlorine by chlorine dioxide, as, for instance, in the bleaching sequence D(EO)DED, an elemental chlorine-free (ECF) sequence; another important improvement was the incorporation of an oxygen delignification pre-bleaching stage, such as in the ODED bleaching sequence. Later, all chlorine-based compounds substituted by others less toxic, such as oxygen, ozone and hydrogen peroxide as the bleaching chemicals [totally chlorine-free (TCF) sequences].¹

The preferable oxidant by excellence is oxygen, especially if we speak in terms of green technologies. Oxygen delignification can be defined as the process involving molecular oxygen (dioxygen) for the oxidative degradation of lignin in ligno-cellulosic materials. However, the autooxidation of residual lignin in pulp with oxygen requires relatively high temperatures and it is impossible to reach a delignification degree of unbleached pulp higher than 40–45% without notable oxidative degradation of the polysaccharides and a decrease of pulp quality.¹⁶

The oxygen delignification may be improved by the use of metal–oxygen cluster anions (polyoxometalates) as reagents or catalysts for selective lignin oxidation, overcoming the previously indicated drawbacks – the topic of this review.

3. Polyoxometalates (general properties)

Polyoxometalates (POM) of general formulae $M_xO_y^{m-}$ or $X_zM_xO_y^{n-}$ ($M = Mo, W, V$; $X = P, Si, B, Ge$, among others) are metal–oxygen cluster anions with relevant structural and electronic properties and a wide range of potential applications.^{3–11} From the structural point of view they may be viewed as clusters formed by the condensation of metal–oxygen polyhedra, namely octahedral (the most frequent), pentagonal bipyramids or square pyramids. These polyhedra are linked by sharing corners and edges, and, more rarely, faces. Two sub-classes of polyoxometalates are usually considered: isopolyanions and heteropolyanions. Isopolyanions, having the general formula $M_xO_y^{m-}$, are composed of two types of elements: oxygen and a d^0 metallic element ($M = Mo, W$ or less frequently V, Nb or Ta). Heteropolyanions present

in their constitution other elements, named the heteroatoms X (more than 70 heteroelements have yet been observed). For these heteroatoms, distinction is made between the primary heteroatom, which may be viewed as a basic element for the structure of the heteropolyanion, and the secondary heteroatom, which may be released and substituted with no degradation of the remaining structure.^{3,4} For instance, in the $[\text{SiW}_{11}\text{Mn}^{\text{III}}(\text{H}_2\text{O})\text{O}_{39}]^{5-}$ heteropolyanion, Si (at the centre of the structure) is the primary heteroatom, while Mn(III) is the secondary heteroatom and may be substituted by other transition metal ions.

Polyoxometalate compounds have distinct properties. One important characteristic is their robustness to oxidative degradation and their action as potential electron reservoirs. This property accounts for the fact that the metal M (Mo or W) is usually in its highest oxidation state for most of the POMs.^{3,4,17} Second, the solubility of heteropolyanion salts is determined mainly by the counter-cation type, as their lattice energy and the solvation energy of the anions are considered to be low.¹⁷ Thus, potassium, sodium, and ammonium salts are soluble in water; tetrabutylammonium salts are soluble in some polar organic solvents, and surfactant-cation-based salts are soluble in non-polar solvents. This is of particular importance for the design of liquid-phase catalysis experiments. Third, the redox properties of POMs may be altered by varying the structure of the polyoxometalate or the type and number of the substituting metals. This is of special interest for oxidative catalysis experiments such as those of the delignification of pulps that will be discussed here.

The most common structures of polyoxometalates include the Keggin, Dawson, and the sandwich-type anions. The Keggin anion (Fig. 4a) of general formula $\alpha\text{-}[\text{XM}_{12}\text{O}_{40}]^{m-}$ (XM_{12}) has tetrahedral symmetry and approximately spherical shape with 1 nm size. In this POM, the central group XO_4 is

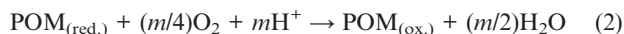
surrounded by 12 MO_6 octahedra in groups of three edge-sharing octahedra.³ From the Keggin anion, the lacunar $\alpha\text{-}[\text{XM}_{11}\text{O}_{39}]^{(m+4)-}$ is obtained by the release of one MO_4^{4+} group. The latter anion is a ligand for transition metal ions M' , originating the Keggin-type transition metal-substituted polyoxometalates, $\alpha\text{-}[\text{XM}_{11}\text{M}'(\text{H}_2\text{O})\text{O}_{39}]^{n-}$ (Fig. 4b). Similarly, the trilacunar $\alpha\text{-}[\text{XM}_9\text{O}_{34}]^{p-}$ is obtained by the removal of one $\text{M}_3\text{O}_6^{6+}$ fragment from the Keggin anion, and in this case two types of structures are possible: $\alpha\text{-A}$ and $\alpha\text{-B}$ from the removal of three corner-sharing octahedra and three edge-sharing octahedra, respectively. Trilacunar-related polyoxometalates include the sandwich-type anions $[(\text{XW}_9\text{O}_{34})_2\text{M}'_4(\text{H}_2\text{O})_2]^{p-}$ whereas two fragments of the Keggin anion $\alpha\text{-B-}[\text{XW}_9\text{O}_{34}]^{p-}$ are linked to each other by a belt of four metal ions (Fig. 4c), and the Dawson anion $[\text{X}_2\text{W}_{18}\text{O}_{62}]^{p-}$ whose structure may be visualized as the condensation of two $\alpha\text{-A-}[\text{XW}_9\text{O}_{34}]^{p-}$ subunits (Fig. 4d).³ Polyoxometalates may be up to 3–4 nm in size such as the giant rings and spheres characterized by Müller group,^{18,19} which is out of the scope of this paper. Of particular interest for the delignification of pulp are the mixed-addenda anions $[\text{PMo}_x\text{V}_{(12-x)}\text{O}_{40}]^{m-}$ and the transition metal-substituted polyoxotungstates $\alpha\text{-}[\text{XW}_{11}\text{M}'(\text{H}_2\text{O})\text{O}_{39}]^{n-}$ (several combinations of X and M'), with the Keggin-type structure. Manganese(III) sandwich anions have also been used for delignification of the pulp.

Several reviews concerning the use of polyoxometalates in oxidative and acid catalysis are presented in the literature.^{8–11} Their use for the delignification of wood pulp is strictly related to their performance as oxidative catalysts or oxidative reagents.

4. Oxidative delignification with polyoxometalates and oxygen

Polyoxometalates can be used for oxidative delignification processes with oxygen. The main goal is the selective oxidation of residual lignin. This achievement is possible, due to the lower redox potential of lignin (easier oxidative degradation) in comparison with that of polysaccharides²⁰ and, also, due to the suppression of radical-chain oxygen reactions (which contribute to the polysaccharide degradation) by using polyoxometalates.²¹

The scheme for the lignin oxidative degradation with oxygen and POMs may be summarized by reactions (1) and (2):



where $\text{POM}_{(\text{ox.})}$ and $\text{POM}_{(\text{red.})}$ are the oxidised and reduced polyoxometalate form, respectively, and $\text{lignin}_{(\text{ox.})}$ represents the products of lignin oxidative degradation (polymeric or low molecular weight products).

Two main systems are considered. An anaerobic system in which these two reactions occur at separate stages, with the first stage under anaerobic conditions [reaction (1)] and the second stage under vigorous conditions of oxygen pressure and temperature [reaction (2)], where the POM acts as a regenerable oxidant. And an aerobic system in which both reactions

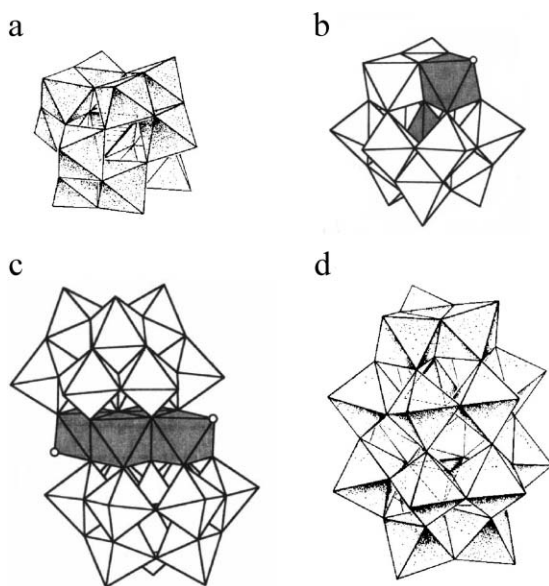


Fig. 4 Structures of typical polyoxoanions: (a) Keggin anion $\alpha\text{-}[\text{XM}_{12}\text{O}_{40}]^{m-}$; (b) Keggin-type transition metal-substituted anion $\alpha\text{-}[\text{XM}_{11}\text{M}'(\text{H}_2\text{O})\text{O}_{39}]^{n-}$; (c) sandwich-type anion $[(\text{XW}_9\text{O}_{34})_2\text{M}'_4(\text{H}_2\text{O})_2]^{p-}$; and (d) Dawson anion $[\text{X}_2\text{W}_{18}\text{O}_{62}]^{p-}$.

take place at the same stage, in the presence of oxygen, where the POM acts as an oxidative catalyst.

The thermodynamic conditions required for lignin oxidation [reaction (1)] and re-oxidation of the POM [reaction (2)] are as follows:

$$E(\text{lignin}) < E(\text{POM}) < E(\text{O}_2) = 1.22 - 0.059 \text{ pH} \quad (3)$$

Therefore, POMs should have a higher redox potential than the lignin structures, so that they can oxidise the lignin, and potentials lower than oxygen, allowing their possible re-oxidation by oxygen. Taking into account the oxidation peak potential of different lignin structure units, their oxidative degradation can take place at potentials between 0.6 and 0.8 V for phenolic units and at around 1.0 V for non-phenolic units (vs. NHE at pH 2).²² The $\text{O}_2/\text{H}_2\text{O}$ redox potential is 1.22 V (vs. NHE) at pH 0.²³ Thus, POMs with $M^{(n+1)/n}$ redox potentials between about 0.6 and 1.2 V are potential oxygen delignification catalysts.

It is noteworthy that other factors, such as kinetic factors, may limit the practical re-oxidation by oxygen of several POMs and, thus, their use as real catalysts in the aerobic system.

5. Delignification of pulp with polyoxometalates under anaerobic conditions

Polyoxometalates have proved to be effective oxidants of residual lignin in unbleached pulps. Weinstock *et al.* have developed an interesting approach.^{24–26} The wood pulp is heated under anaerobic conditions with an aqueous solution of an appropriate POM (Scheme 1; unit operation A). Then, the aqueous solution of the reduced POM, after careful separation from the partially delignified fibres, is sent to a second reactor (Scheme 1; unit operation D) to be heated under oxygen pressure, where re-oxidation of the POM and the oxidation of dissolved organic materials to carbon dioxide and water take place (wet oxidation). The aqueous solution of re-oxidised POM could then be used in further delignification, by recycling it to unit operation A. The typical temperature and POM concentration used in laboratory experiments for the anaerobic delignification were in the range 100–125 °C and 0.05–0.5 mol L⁻¹ (ca. 130–1300 g L⁻¹), respectively. For the aerobic re-oxidation of the POM, temperatures of 150–200 °C and O_2 pressure of 0.6–0.8 MPa were used. The overall

effluent-free delignification process also comprised a unit operation B (pulp washing), in which the reduced form of the POM and the partially oxidised dissolved lignin fragments are removed from the bleached pulp after filtration and washing, and a unit operation C, where the wash water is concentrated and undesirable inorganic salts are removed by cationic exchange or crystallization (Scheme 1).

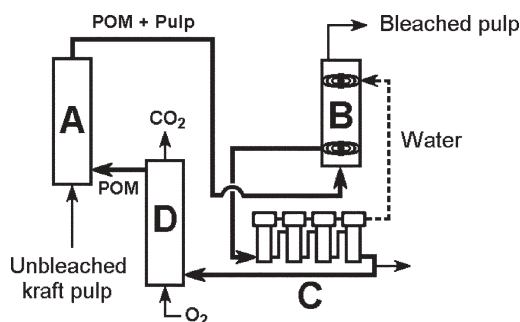
Typically, the POM solution used in the delignification process under anaerobic conditions includes a buffering component to avoid a decrease of pH during the delignification and re-oxidation reactions. Below a pH value of 2, extensive degradation of the polysaccharides may occur. The POMs were selected taking into consideration several factors: the POM should have a reduction potential high enough to oxidise lignin; it should be re-oxidised by oxygen under the conditions of the aerobic step; it should be stable under the applied conditions of pH and temperature, and the aqueous phase including POM and buffer should be readily separated from the pulp after the delignification treatment.²⁷

5.1. First generation of polyoxometalates ($\text{PMo}_{10}\text{V}_2$, XW_{11}V and SiW_{11}Mn)

POMs such as $[\text{PMo}_{10}\text{V}_2\text{O}_{40}]^{5-}$ ($\text{PMo}_{10}\text{V}_2$), $[\text{PW}_{11}\text{VO}_{40}]^{4-}$ (PW_{11}V), $[\text{SiW}_{11}\text{VO}_{40}]^{5-}$, $[\text{BW}_{11}\text{VO}_{40}]^{6-}$ and $[\text{SiW}_{11}\text{Mn}(\text{H}_2\text{O})\text{O}_{39}]^{5-}$ (SiW_{11}Mn) (all α isomers) have been used for delignification processes of pine kraft pulp under anaerobic conditions.^{24–31} All studied POMs were able to delignify the pulp (compared with the results of control experiments with no POM), the best results being obtained with SiW_{11}V and SiW_{11}Mn (Table 1).²⁶ Considerable cellulose degradation occurred with $[\text{PW}_{11}\text{VO}_{40}]^{4-}$, due to the lower pH used (on account of the stability of this POM at pH < 2) which promoted cellulose acid hydrolysis. The delignification effectiveness of different POMs is related to their redox potentials. POMs with lower redox potentials ($\text{PMo}_{10}\text{V}_2$ and BW_{11}V) presented a lower degree of delignification whereas those of SiW_{11}V and SiW_{11}Mn , with a higher redox potential, were the most effective for the delignification of pulps.²⁶ Polyoxometalate re-oxidation was demonstrated for $\text{PMo}_{10}\text{V}_2$ at 150 °C, since its reduced form was rapidly re-oxidised by oxygen, despite its low effectiveness for anaerobic delignification.^{25,26,30} In contrast, for the SiW_{11}V and SiW_{11}Mn anions the re-oxidation of the reduced anions by oxygen was slow, even at conditions of elevated temperature and oxygen pressure, limiting the useful application of this system.^{26,27,31}

5.2. Further generations of polyoxometalates ($\text{SiW}_{10}\text{V}_2$, AlW_{11}V and others)

A second generation of POMs emerged as suitable for both delignification and wet oxidation, which are also stable above pH 7 so that hydrolysis of the cellulose can be significantly reduced. These include $[\text{SiW}_{10}\text{V}_2\text{O}_{40}]^{6-}$ ($\text{SiW}_{10}\text{V}_2$), $[\text{AlW}_{11}\text{VO}_{40}]^{6-}$ (AlW_{11}V), and $[\text{SiW}_{10.1}\text{Mo}_{1.0}\text{V}_{0.9}\text{O}_{40}]^{32–34}$. Another important advance associated with this new generation of POMs was the development of a new synthetic procedure (using hydrothermal methods) that results in an equilibrium composition which is inherently stable and, therefore, can be recycled repeatedly in a closed system.



Scheme 1 Simplified schematic of an effluent-free POM delignification process.²⁵

Table 1 Results of delignification trials with POMs under anaerobic conditions^{a,26}

POM	<i>E</i> (V) vs. NHE at pH 5	Trial/sequence	pH of POM stage	Kappa number	Viscosity/mPa s
[PMo ₁₀ V ₂ O ₄₀] ⁵⁻	0.5	Initial kraft pulp		33.6	34.2
		ME	3.0	22.3	16.9
		ME	4.0	25.6	25.5
		Control	4.0	28.6	23.7
[PW ₁₁ VO ₄₀] ⁴⁻	0.80	ME	1.5	7.6	Low
		Control	1.5	18.5	Low
		EM ₁ M ₂ M ₃ E	7.0	5.0	23
[SiW ₁₁ VO ₄₀] ⁵⁻	0.65	Control	7.0	30.0	25
		M ₁ M ₂ M ₃ E ^b	7.0	4.7	23
		Control ^b	7.0	19.5	22
		M ₁ M ₂ M ₃ E	9.5	19.7	—
[BW ₁₁ VO ₄₀] ⁶⁻	0.40 ^c	M ₁ M ₂ M ₃ E	5.0	6.5	27
[SiW ₁₁ Mn(H ₂ O)O ₃₉] ⁵⁻	0.65	Control	5.0	27.0	24.5

^a Experimental conditions: 3% consistency ($w_{\text{(of pulp)}}/w_{\text{(of suspension)}}$); [POM] = 0.05 mol L⁻¹; stage M at 100 °C for 4 h, stage M₁ at 125 °C for 1 h, stage M₂ at 125 °C for 1.5–2 h, and stage M₃ at 125 °C for 2 h. ^b Initial kraft pulp with kappa number 24.1 and viscosity 27.8 mPa s.

^c At pH 6.

The POM that has been studied most extensively is SiW₁₀V₂, which has been routinely used to reduce the kappa number from about 33 to below 10. The effectiveness of this POM was shown by the results obtained from a cyclic experiment using the same POM solution on different pulps (20 cycles). The delignification step was carried out at a consistency of 3%, for 3 h at 150 °C, wherein the same 0.5 mol L⁻¹ solution of SiW₁₀V₂ was used. Repeatedly, the pulp fibres were first delignified, and then the POM liquor submitted to the wet oxidation with the removal of the organics and re-oxidation of the POM prior to its re-use. The kappa number decreased from 33 to an average value of 8 and the average drop in viscosity was from 30.4 to 19.4 mPa s (a decrease of 36%). Self-buffering of the medium at a pH of *ca.* 9.5 was observed during both the delignification and re-oxidation steps.³² In addition to the extensive use of SiW₁₀V₂ in tests with pulps at kappa levels of 30, this POM has also been used to test the feasibility of applying POM technology to higher kappa pulps. The results of some trials, with a southern pine linerboard pulp with a kappa of 65, could enhance the effectiveness to the point where the properties of the pulps match those of commercial elemental chlorine-free (ECF) pulps.³²

Thermodynamically-controlled self-assembly of an equilibrated ensemble of polyoxometalates, with the heteropolytungstate anion AlW₁₁V as its main component, imparts both stability in water and self-buffering of the medium.³³ An equilibrium mixture containing mainly [AlW₁₁VO₄₀]⁶⁻ (α and β isomers) but, also, in minor amounts, other species such as [AlW₁₁AlO₃₉]⁶⁻, [V₂W₄O₁₉]⁴⁻ and [W₇O₂₄]⁶⁻ is previously prepared. The [AlW₁₁VO₄₀]⁶⁻ is the lignin oxidant, capable of undergoing repeated cycles of reduction and re-oxidation. This and the other POM species participate in the reactions that self-buffer the medium at a pH near 7.³³ Designed to operate at near-neutral pH, this system facilitates a two-step, O₂-based process for the selective delignification of the pulp.

The use of 'SiW_{10.1}Mo_{1.0}V_{0.9}O₄₀' polyoxoanions as readily synthesized and as an inherently self-buffering system was also considered. An equilibrium mixture containing [SiW₁₀MoVO₄₀]⁵⁻ and [SiW₁₁VO₄₀]⁵⁻, as the dominant species, is prepared and used in the delignification (these POM species are the lignin oxidants). A self-buffering of the

medium at a pH near 5.5 is also achieved.³³ In the context of traditional delignification, this ensemble of polyoxometalates showed the capacity to decrease the kappa number levels of softwood kraft pulps from 30 to less than 5, while retaining an intrinsic viscosity higher than 20 mPa s. The ensemble 'SiW_{10.1}Mo_{1.0}V_{0.9}O₄₀' could effectively delignify kraft pulps at much higher kappa number levels in the 100–110 range, and soda anthraquinone pulps at kappa number levels of around 120.³⁴

Recent reviews have been published describing the ultimate progress of the anaerobic POM-based delignification process.^{35,36} They summarize progress along the multiple fronts that have been investigated, including the possibilities of using POMs as a complement to high-yield pulping and electrochemical delignification using POMs as mediators. The latest concern was on searching for more efficient POMs in the uptake of electrons from the pulp substrates. Also studied were the determinants of rates of electron transfer from the substrates to the POMs. All of these must be optimized in order to achieve the full economic potential of POM-based delignification.

5.3. Catalytic oxidative mechanism

Reactions of lignin model compounds with PMo₁₀V₂ were performed. Phenolic compounds, such as 2-methoxyl-4-methoxyl phenol and 4-hydroxy-3-methoxybenzyl alcohol (vanillyl alcohol) were oxidised by PMo₁₀V₂ within 10 min at 60 °C. Veratryl alcohol, a non-phenolic lignin model compound, was oxidised to veratryl aldehyde with PMo₁₀V₂ during 30 min at 100 °C. These results indicate the higher difficulty of oxidising the non-phenolic lignin structures in comparison with the phenolic ones with PMo₁₀V₂. At 100 °C under anaerobic conditions almost no reaction was detected between cotton cellulose and the above-mentioned POM in aqueous solution.²⁰

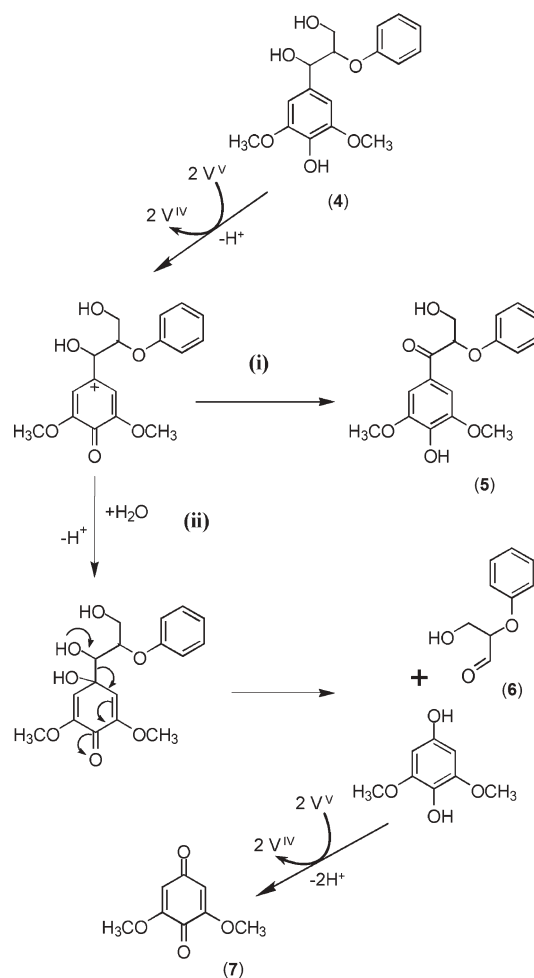
Structural changes occurring in the residual lignin of pine kraft pulp during the reaction with PMo₁₀V₂ under anaerobic conditions were investigated by FT-Raman spectroscopy.³⁷ A complete analysis suggests that, during the POM stage on the residual lignin, quinone and α -carbonyl structures are generated from phenolic and α -hydroxylated moieties, respectively.

Kinetic studies were performed on the SiW₁₁V-based delignification process under anaerobic conditions, where three subsequent SiW₁₁V POM stages (M₁M₂M₃) were used to delignify pine kraft pulp.^{26,31} The POM in the oxidised form was consumed as delignification progressed. The kinetic model consisted of two independent reactions: a fast reaction, first order in both oxidised POM concentration and lignin concentration (second-order reaction overall) for the first two delignification stages (M₁M₂) and a slow, zero-order reaction for the third delignification stage (M₃) in which the rate of reaction was unaffected by either POM or lignin concentration. The activation energies for the whole data set were $15.5 \pm 0.4 \text{ kJ mol}^{-1}$ for the second-order reaction and $113.4 \pm 0.2 \text{ kJ mol}^{-1}$ for the zero-order reaction. The activation energy of the second-order reaction (15.5 kJ mol^{-1}) was lower than that typically observed for oxidation reactions suggesting that the rate of reaction is likely to be controlled by a mass transport resistance. The activation energy of the other reaction, $113.4 \text{ kJ mol}^{-1}$, was approximately that expected in a chemical-reaction-controlled process. It was pointed out that full understanding of the reactions of POMs within pulp fibres must include consideration of a number of issues arising from the effects of heterogeneity and surface phenomena.²⁶

The reaction of SiW₁₁V with non-phenolic 1-(3,4,5-trimethoxyphenyl)-2-(phenoxy)propane-1,3-diol did not take place under delignification conditions (3 h at 125 °C), whereas with the phenolic 1-(3,5-dimethoxy-4-hydroxyphenyl)-2-(phenoxy)propane-1,3-diol (**4**) lignin model, a fast reaction rate led to dimer cleavage.^{25,26} These results clearly indicate that only hydroxylated phenyl substructures react with SiW₁₁V. Taking into account that the POM SiW₁₁V is an one-electron oxidant, it was proposed that 2 equiv. of V(V) oxidise the phenolic moiety to a cyclohexadienyl cation that either: (i) isomerises to give an α -ketone (**5**) or (ii) is hydrolytically cleaved to give 2-phenoxy-3-hydroxypropane aldehyde (**6**) and a hydroquinone which is oxidised to the 2,6-dimethoxy-*p*-benzoquinone (**7**) by an additional 2 equiv. of V(V) (Scheme 2).²⁸

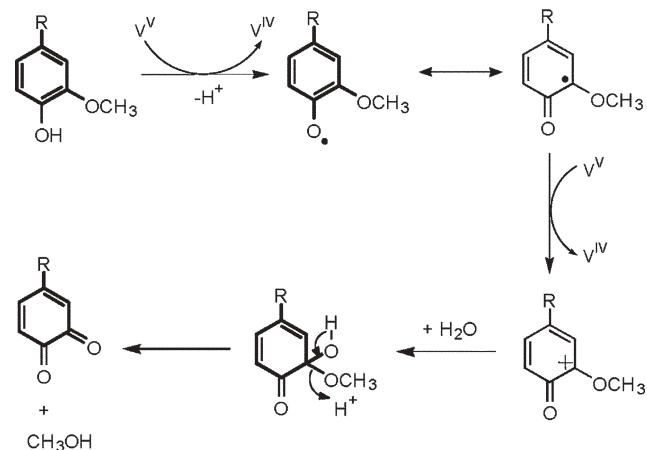
Other studies have been conducted in order to evaluate the reactivity of phenolic and non-phenolic lignin structures with POM. These studies included the oxidation of four lignin model compounds (phenolic and non-phenolic, with or without an α -carbonyl group): vanillin, creosol, veratryl alcohol and veratrol with SiW₁₁V.³⁸ It was found that the reactivity of non-phenolic lignin structures towards POMs at 25 °C is negligible, whereas the reaction with phenolic lignin structures takes place readily. A reaction mechanism between SiW₁₁V and the lignin model compounds was proposed (Scheme 3). It consists of a one-electron transfer from the phenol structure to SiW₁₁V, leading to the formation of a phenoxyl radical and further one-electron oxidation of the formed phenoxyl radical with the formation of an aromatic cation structure.³⁸ Hydrolysis of the aromatic cation structure yields quinone structures, which have been previously detected.^{39,40}

The oxidative degradation of non-phenolic lignin model compounds, 1-(3,4,5-trimethoxyphenyl)ethanol and 1-(3,4-dimethoxyphenyl)ethanol by the equilibrated ensemble 'SiW_{10.1}Mo_{1.0}V_{0.9}O₄₀' in an inert atmosphere was studied.^{41,42} Unlike the phenolic lignin model compounds which reacted immediately at room temperature, the non-phenolic lignin



Scheme 2 Proposed mechanism of 1-(3,5-dimethoxy-4-hydroxyphenyl)-2-(phenoxy)propane-1,3-diol (**4**) oxidation with [SiW₁₁VO₄₀]⁵⁻.²⁸

model compounds required stronger reaction conditions. Reaction temperatures of 180 °C were needed to obtain more than 90% degradation of 1-(3,4,5-trimethoxyphenyl)ethanol after 6 h of reaction. It was proposed that the oxidation of the latter proceeds *via* successive oxidations of the benzylic carbon atom.



Scheme 3 Reaction mechanism for the lignin model compound oxidation with [SiW₁₁VO₄₀]⁵⁻.³⁸

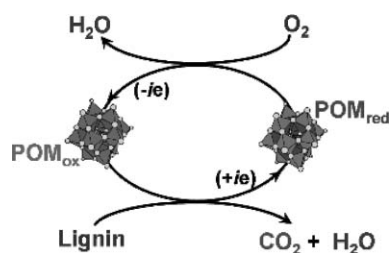
The kinetics of redox reactions between residual lignin and POM anions $[\text{AlW}_{11}\text{Mn}^{\text{III}}(\text{H}_2\text{O})\text{O}_{39}]^{6-}$ and $[\text{SiW}_{11}\text{Mn}^{\text{III}}(\text{H}_2\text{O})\text{O}_{39}]^{5-}$ in a suspension of unbleached softwood kraft pulp were studied, taking into account the effect of cation concentration (mainly potassium), pH, ionic strength and temperature.^{43,44} According to the results, cation concentration and pH had a remarkable effect on the reactivity of the POMs toward the phenolic lignin structures. At cation concentrations lower than 0.10 mol L^{-1} , no reaction was observed during the first hour and 20 min; at a concentration of 0.30 mol L^{-1} , the reactions were significantly more rapid, and the rate correlated strongly with increasing pH for both POMs. The kinetics of re-oxidation of $[\text{AlW}_{11}\text{Mn}^{\text{II}}(\text{H}_2\text{O})\text{O}_{39}]^{7-}$ by oxygen at various conditions of pH (3–7), temperature (55–75 °C) and oxygen pressure (0.3 and 0.5 MPa) were determined. Oxidation was observed only at pH 3 and 5. The conversion of the POM always remained lower than 20% for 2 h of reaction.^{43,45}

6. Delignification of pulp with polyoxometalates under aerobic conditions

The ideal polyoxometalate, acting as a catalyst for oxygen delignification should be strong enough to oxidise the residual lignin of pulp without degrading the polysaccharides, and, simultaneously, be re-oxidised by oxygen at the same stage of the process. Lignin is oxidised by POMs in the oxidised form, yielding CO_2 and H_2O as the main final products of lignin oxidative degradation (Scheme 4). The generated reduced POM is subsequently re-oxidised by oxygen producing water as a by-product and the POM in the oxidised form (Scheme 4). This cycle is continuously repeated. To achieve this purpose, several polyoxometalates were considered.

6.1. HPA-5/ O_2 system

6.1.1. HPA-5 as a catalyst. The heteropolyanion $[\text{PMo}_7\text{V}_5\text{O}_{40}]^{8-}$ in solution (HPA-5 for short) has shown catalytic activity under O_2 for the delignification of eucalyptus sawdust and for the delignification of kraft pulp, in water or ethanol–water medium under appropriate conditions.^{46–50} Delignification of kraft pulp at temperatures of 90 °C and at an optimized pH of 1.8–2.0 and an oxygen pressure of 0.6 MPa originated pulps with significantly lower kappa numbers than those of the experiments performed with no POM after 2 h of reaction (Table 2).^{46,47} However, owing to the low pH used,



Scheme 4 General scheme of oxygen delignification catalysed by POM (presented as Keggin compounds in polyhedral-filling representation; terminal oxygen atoms are depicted as unfilled balls).

Table 2 Results on kraft pulp bleaching with HPA-5^{a,46,47}

Bleaching conditions	Kappa number	Brightness (%)	Viscosity/ $\text{cm}^3 \text{ g}^{-1}$
Initial kraft pulp	16.9	33	1270
EtOH– H_2O (50 : 50, v/v); 90 °C; 120 min	6.6	62	975
[HPA-5] = 2 mmol L^{-1} ; pH = 1.9			
EtOH– H_2O (50 : 50, v/v); 90 °C; 120 min	11.6	44	1020
[H_2SO_4] = 0.01 mol L^{-1}			
H_2O ; 90 °C; 120 min	5.2	68	620
[HPA-5] = 2 mmol L^{-1} ; pH = 1.9			
H_2O ; 80 °C; 120 min	9.6	51	890
[HPA-5] = 2 mmol L^{-1} ; pH = 1.9			
H_2O ; 90 °C; 120 min	10.4	43	1100
NaOH (2% on pulp)			
H_2O ; 106 °C; 80 min	6.3	61	755
NaOH (2% on pulp)			

^a Consistency = 3%; $p(\text{O}_2)$ = 0.6 MPa.

polysaccharide destruction also occurred. This was assumed to be mainly related to the hydrolysis reactions by acid catalysis, as similar intrinsic viscosities were obtained for the experiment carried out with no POM.^{46,47} Notwithstanding, the delignification process catalysed by the HPA-5/ O_2 system was more selective than the conventional oxygen delignification in alkaline medium, when the oxidative degradation was carried out to a kappa number of around 6–7 (Table 2).^{46,47}

It was demonstrated that the HPA-5/ O_2 system could be used in multiple delignification cycles without losing its activity for the delignification of the pulp. These results showed that no catalyst deactivation occurred.⁵⁰ The chemical oxygen demand index, after the second cycle, indicated that the oxidised organic materials accumulation and their dissolution in the multiple delignification liquors was roughly the same. This fact indicates that the HPA-5/ O_2 system yields the total oxidation of lignin to carbon dioxide and water. These results are extremely important for a possible application of HPA-5 as a catalyst for an oxygen delignification stage in a totally effluent-free (TEF) bleaching plant. Since the delignification liquor may be continuously re-used it could be carried out in a closed system. In this way, POM delignification opens new perspectives for the implementation of the closed-mill concept and for the reduction of the environmental impact of the bleached kraft pulp mill.

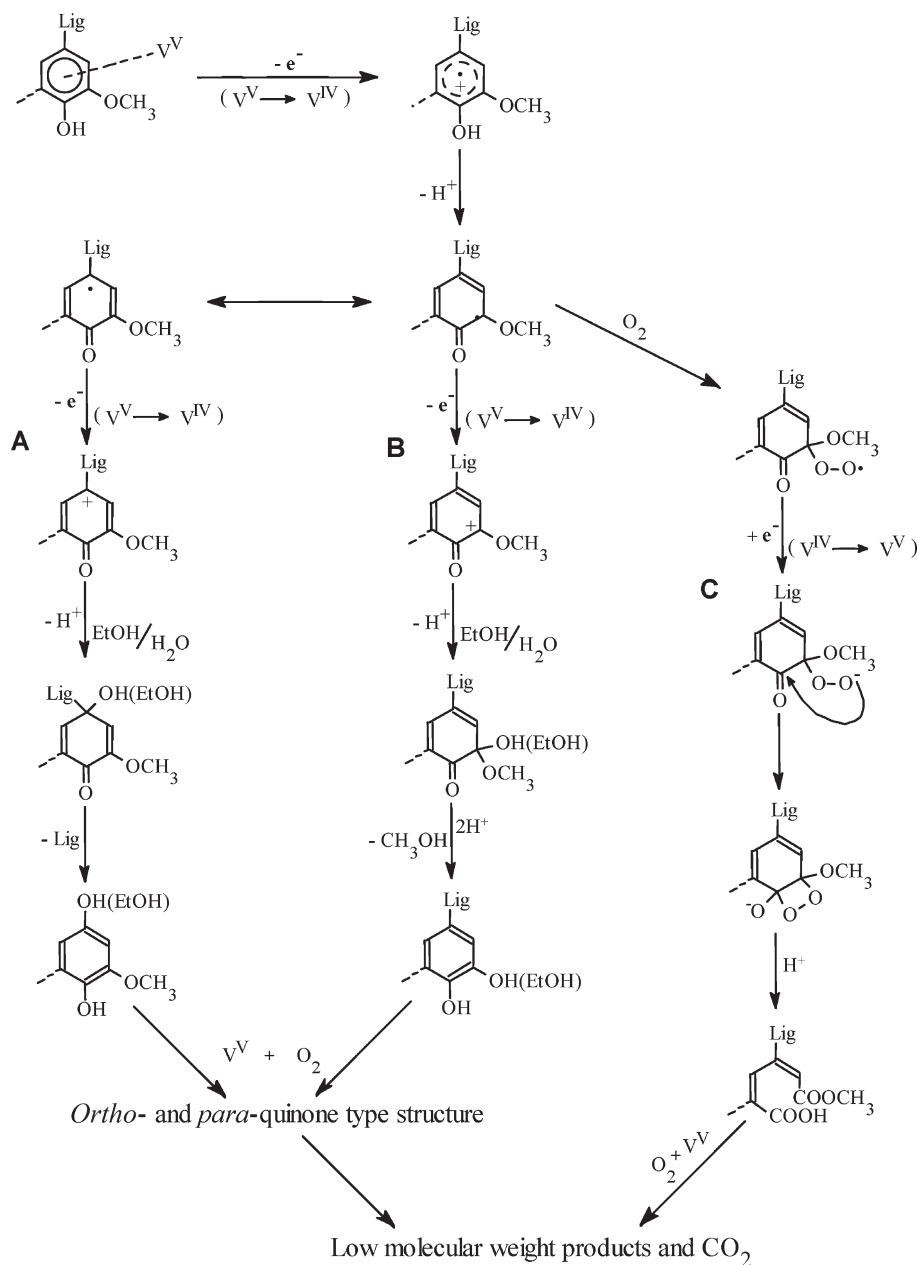
6.1.2. Catalytic oxidative mechanisms. It was clearly demonstrated by cyclic voltammetry and ^{51}V NMR that VO_2^+ are released from the anion $[\text{PMo}_7\text{V}_5\text{O}_{40}]^{5-}$ under the working conditions of the pH applied.^{22,47} In fact, the predominant POM species detected by ^{51}V NMR were $[\text{PMo}_{(12-n)}\text{V}_n\text{O}_{40}]^{(3+n)-}$ with $n = 1–3$,⁴⁷ and an oxidation peak due to $\text{VO}^{2+} \rightarrow \text{VO}_2^+$ was observed in the cyclic voltammogram after the cathodic scan.²² The latter species was proposed as principally responsible for the cellulose depolymerization, leading to a remarkable decrease of pulp viscosity. Owing to their high redox potential (around +1.1 V vs. NHE), VO_2^+ ions released from the partial dissociation of $[\text{PMo}_7\text{V}_5\text{O}_{40}]^{5-}$ under acidic conditions oxidise the glucopyranosic units of cellulose on the C-6 and C-1 positions. This

is followed by solvolysis of the oxidised cellulose chains and further formation of low molecular weight oxidation products.

Studies on the oxidation of non-phenolic model compounds such as veratryl alcohol and acetovanillone showed the activity of the HPA-5/O₂ system.²² The oxidation potentials of these compounds were found to be too high (>+1.0 V) to be oxidised by [PMo_(12-n)V_nO₄₀]⁽³⁺ⁿ⁾⁻ (0.7–0.8 V vs. NHE). Thus, once more it was assumed that VO₂⁺ released from the POM sphere was the active oxidant of those non-phenolic compounds. In the oxidation of phenolic compounds such as vanillyl alcohol, besides VO₂⁺, [PMo_(12-n)V_nO₄₀]⁽³⁺ⁿ⁾⁻ should play an important role as the oxidant.²²

Based on the analyses of the residual lignin from eucalyptus wood by ¹³C NMR after delignification with oxygen in the

presence of HPA-5, as well as by GC–MS analysis of the liquor of the delignification process after the reaction, a mechanism for lignin oxidation in the HPA-5/O₂ reaction system was proposed (Scheme 5).⁵¹ The pathway C consists of homolytic stages that lead to the aromatic ring cleavage. The pathways A and B show the oxidation of the lignin aromatic group with V(v) (in the composition of free VO₂⁺ ions or in HPA), yielding structures of cyclohexadienyl cations, which subsequently undergo hydrolytic cleavage. The interaction between the lignin and the VO₂⁺ ions or HPA is possible due to the formation of an electronic transition complex between the VO₂⁺ ions or HPA and the lignin aromatic π -electron system. One-electron-oxidised lignin structural units can also form coupling products.⁵¹



Scheme 5 Scheme proposed for the lignin oxidative degradation in the HPA-5/O₂ system. V(v) and V(IV) are found in the composition of VO₂⁺ or VO₂²⁺ as well as in the HPA-oxidised or -reduced forms, respectively.⁵¹

6.1.3. HPA-5 stages incorporated in bleaching sequences. The possibilities of integrating the procedure of oxygen delignification catalysed by HPA-5 as a pre-bleaching stage in different ECF and TCF sequences were investigated.^{50,52} The HPA-5-catalysed delignification in ethanol–water (50 : 50, v/v) solution (stage designated as O_{POM}) with 60% delignification allowed the same pulp brightness to be obtained in the O_{POM}E_pD sequence as in the DE_pD sequence (E_p refers to alkaline extraction stage using small amounts of hydrogen peroxide), but with a three-fold lower ClO₂ consumption. The pulp viscosity at the end of the O_{POM}E_pD sequence was nearly 10% lower than at the end of a classical DE_pD procedure. The main physical properties of pulps bleached by a sequence incorporating the O_{POM} stage were slightly lower than those bleached by the DE_pD process.

The use of aqueous solutions instead of an aqueous organic medium for the delignification is preferred, since the presence of organic solvents may pose problems in the technological implementation of a POM-based delignification process and reduce its economical feasibility. One way to improve the delignification results in aqueous media is by increasing the ionic strength of the solution, for example, by the addition of Na₂SO₄.⁵³ The O_{POM}E_pDD bleaching sequence was selected as an alternative to the nowadays exploited DE_pDE_pD process. For nearly 40% of delignification in the O_{POM} stage, a reduction in ClO₂ consumption of about 40% is achieved (90% brightness). A further increase of the degree of delignification in the O_{POM} stage allowed the same brightness to be reached in O_{POM}E_pDD process with proportionally lower ClO₂ demand, but led to decreasing viscosity of the bleached pulp. However, this drop in viscosity had no dramatic influence on the strength properties of the bleached pulps. Compared with a pulp bleached by a standard DE_pDE_pD process, that bleached using an ECF sequence including an O_{POM} stage had slightly lower strength properties (nearly 10–15%) but better optical properties (e.g. opacity).

6.2. HPA-5-Mn^{II}/O₂ system

6.2.1. Mn^{II}-assisted HPA-5 as a catalyst. In spite of the good delignification extent obtained during oxygen delignification catalysed by HPA-5, the selectivity of residual lignin oxidation was restricted by two main factors: (i) the low pH of the best delignification medium (*ca.* pH 2), which promotes acid-catalysed hydrolysis of polysaccharides; and (ii) the undesirable and not easily controllable degradation of polysaccharides with VO₂⁺ ions dissociated from parent structure of HPA-5. To overcome these drawbacks, new development was carried out on the preparation and structure of the catalyst.

Manganese(II) ions in the form of manganese diacetate were added in the last stage of the synthesis of HPA-5 under acidic conditions with the purpose of preparing Mn-substituted HPA-5 structures (HPA-5-Mn^{II} for short) as suggested by electrochemical experiments.⁵⁴ This experiment accounted for the partial dissociation of HPA-5 at pH ≤ 3, leading to the formation of the so-called lacunary derivatives of the parent Keggin polyoxoanions. Moreover, the synthesis of POMs, based on the reactions of lacunary Keggin structures and transition metal ions is well documented.⁵⁵ Regarding the catalytic features of Mn-substituted polyoxometalates in oxygen

Table 3 Results of eucalyptus kraft pulp delignification with oxygen catalysed by HPA-5-*x*Mn^{II} ^{a,60}

Delignification system	Kappa number	Intrinsic viscosity/cm ³ g ⁻¹	Delignification degree (%) ^b
Kraft pulp	13.9	1290	—
O ₂ (without catalyst)	8.5	1030	39
HPA-5/O ₂	5.8	920	58
HPA-5-1.0Mn ^{II} /O ₂	6.0	1000	57
HPA-5-1.5Mn ^{II} /O ₂	6.2	1050	55
HPA-5-2.0Mn ^{II} /O ₂	6.1	1060	56
HPA-5-3.0Mn ^{II} /O ₂	6.0	1050	57
HPA-5-1.5Mn ^{III} /O ₂	5.8	1060	58

^a Consistency = 3%; 100 °C; 2 h; *p*^o(O₂) = 0.5 MPa; [HPA-5-*x*Mn^{II}] = 2.0 mmol L⁻¹; pH = 3.0. ^b Estimated as the decrease of kappa number.

delignification,⁵⁶ the use of a lacunary structure of HPA-5 acting as a multidentate ligand to the manganese ions (HPA-5-Mn^{II}) on the oxygen delignification catalysis was investigated.

The delignification degree achieved with HPA-5/O₂ or HPA-5-Mn^{II}/O₂ systems was considerably higher than that obtained by oxygen without a catalyst (Table 3).⁵⁴ Comparing the two reaction systems HPA-5/O₂ and HPA-5-Mn^{II}/O₂, the latter showed a slightly lower delignification efficiency but a remarkably improved selectivity, proving a positive influence of the presence of manganese in the substituted HPA-5.

The VO₂⁺ ions present in the acidic HPA-5 solution play a key role in the oxidative delignification because they were considered as the main active species in the catalytic oxidation of lignin.^{47,57} At the same time, however, VO₂⁺ ions oxidise the polysaccharides, thus decreasing the selectivity of the delignification.⁵⁸ The introduction of Mn in the synthesis of HPA-5-Mn^{II} could control, to some extent, the VO₂⁺ ions released. The lower concentrations of VO₂⁺ in the HPA-5-Mn^{II} solution could explain the slightly lower delignification efficiency but better selectivity. The molar ratio between HPA-5 and Mn²⁺ ions used in the synthesis of HPA-5-Mn^{II} also influenced the delignification results. The selectivity of the lignin oxidation was fairly constant when the ratio [HPA-5]/[Mn²⁺] was higher than 1.5 (Table 3).⁵⁴

The catalyst HPA-5-1.5Mn^{II} ([HPA-5]/[Mn²⁺] = 1.5) was suggested as being the best for the catalytic needs.⁵⁴ About 15–20% higher viscosity of the delignified pulp was achieved with HPA-5-1.5Mn^{II} when compared with HPA-5 catalysis at the same degree of delignification. Delignification parameters in the system HPA-5-1.5Mn^{II}/O₂ were also optimized. The best delignification selectivity with HPA-5-1.5Mn^{II} was observed at a pH between 3 and 4. The temperature of 100 °C seemed to be a good compromise for selective delignification. After 4 h of reaction at 100 °C, it was possible to reach up to 70% of residual lignin removal with a viscosity drop of only 26%.

6.2.2. Catalytic oxidative mechanisms. Reactions of phenolic and non-phenolic lignin monomeric model compounds (homovanillyl and homoveratryl alcohol, respectively) in the HPA-5-Mn^{II}/O₂ system were considered and compared with those in the HPA-5/O₂ system.⁵⁹ The chromatograms of the oxidation products of homovanillyl alcohol in both HPA-5/O₂ and HPA-5-Mn^{II}/O₂ systems were very similar. Oxidation of homoveratryl alcohol in both systems also gave similar

chromatograms. It was concluded that Mn^{II} incorporation into the HPA-5 structure does not have a significant influence on the oxidative degradation of phenolic or non-phenolic lignin structures. HPA-5 and HPA-5-Mn^{II} are suggested to originate identical lignin oxidative mechanism pathways. The proposed mechanisms for the oxidative degradation of homovanillyl alcohol and homoveratryl alcohol are presented elsewhere.⁵⁹ The first one-electron oxidation by the catalyst yielding the formation of the corresponding cation-radical was assumed as the rate-limiting oxidation step of both of the model compounds with HPA-5 or HPA-5-Mn^{II}. Comparing the conversion degree of around 16% for homoveratryl alcohol with that of more than 99% for homovanillyl alcohol, it was shown that the contribution of the non-phenolic lignin structural units in the oxidative degradation must be lower than that of phenolic ones.

The reactions of eucalyptus dioxane lignin adsorbed on cellulose in the HPA-5-Mn^{II}/O₂ system were considered, in order to analyse the possible structural modifications in lignin. Changes were followed by 1D quantitative ¹³C NMR and 2D ¹H-¹³C NMR techniques.⁵⁹ Several oxidised functional groups (carboxyls, aldehydes and ketones) appeared in the lignin structure during the delignification procedure. Demethoxylation was also a significant reaction that took place. These changes are supported by studies with lignin model compounds. The cleavage of β-O-4 structures was suggested as the main way of lignin depolymerization. On the other hand, carbon-carbon linkage as the β-β and β-5 bonds seemed to decrease during the oxidative process. Another interesting feature that occurs during the delignification procedure applied to the dioxane lignin was the formation of Cα-O-polysaccharide linkages in the β-O-4 structures of lignin.

6.2.3. HPA-5-Mn^{II} stages in short bleaching sequences. The catalysis by HPA-5-Mn^{II} in the oxygen delignification stage (O_{POM}) and in the ozone stage (Z_{POM}) was tested in short bleaching sequences such as O_{POM}E_pO_{POM} and Z_{POM}E_pO_{POM}.⁵⁴ The effect of HPA-5-catalysed delignification with ozone has been previously discussed.⁵² This experiment was extended to the HPA-5-Mn^{II} catalytic delignification, and the delignification trials showed the high potential of HPA-5-1.5Mn^{II}-catalysed delignification both with dioxygen and ozone. Two O_{POM} stages of 2 h each, with intermediate alkaline extraction, demonstrated better delignification for the same final viscosity of the pulp when compared with the one-stage, 4 h delignification. About 80% of the delignification was reached while the viscosity decreased 26%. The substitution of one O_{POM} stage in O_{POM}E_pO_{POM} by Z_{POM} in the Z_{POM}E_pO_{POM} sequence allowed a delignification degree higher than 70% to be reached with a decrease of pulp viscosity of only about 20%. These results are rather attractive when compared to those previously obtained with HPA-5 for the same delignification trials.⁶⁰

6.3. Pilot plant trials including oxygen stages catalysed by HPA-5-Mn^{II}

The oxygen stage catalysed by HPA-5-Mn^{II} can be carried out in a 'closed loop' mode since the solution of the catalyst may

be re-used. This possibility was confirmed in a series of 16 delignification experiments, carried out using as delignification solutions the filtrates from the previous delignification experiment.⁶⁰ No significant changes occurred in kappa number and viscosity after 16 delignification cycles, showing that no catalytic deactivation took place in the performed experiments.

Pilot-scale delignification and bleaching trials, including oxygen stages catalysed by HPA-5-1.5Mn^{II}, were carried out at the technical facilities of the Centre Technique du Papier (CTP, Grenoble, France). The scheme of the pilot plant has been presented elsewhere.⁶¹ The kinetics of delignification with oxygen catalysed by HPA-5-Mn^{II} was two times faster in the pilot plant scale ($K_{\text{obs}} = 5.97 \times 10^{-3} \text{ min}^{-1}$)⁶¹ than in the laboratory experiments ($K_{\text{obs}} = 3.07 \times 10^{-3} \text{ min}^{-1}$).⁵⁴ This better performance was explained by better mixing of the pulp with the catalyst and oxygen in the pump, dynamic mixer and in the high pressure reactor. It was also suggested that the live steam should have a crucial effect on mass/heat transfer, allowing a better delignification rate. On the other hand, the delignification kinetics of the alkaline O stage, at the pilot plant scale, in the first 45 min ($K_{\text{obs}} = 5.48 \times 10^{-3} \text{ min}^{-1}$), was slightly slower than that observed for the O_{POM} stage.⁶¹ For longer than those 45 min, the delignification development was negligible for the O stage, while for the O_{POM} stage it could be largely extended without a significant decrease of viscosity. In contrast, the oxidation selectivity for the first hour of reaction was slightly lower in the O_{POM} than in the alkaline O stage. However, the selectivity in the O_{POM} stage can be improved if the concentration of the catalyst is higher and if the reactor loading could be carried out with the pulp, catalyst solution, vapour injection and oxygen at the same time, preventing the higher extent of POM reduced form in the initial instants of the O_{POM} stage.

Oxygen delignified pulps after both catalytic (O_{POM}) or alkaline (O) stages were submitted to further delignification with chlorine dioxide in an aim to estimate their delignification response in W_AO_{POM}DED and WODED sequences (W_A stands for an acid washing stage and W for a washing stage).⁶¹ These data were compared with those obtained for the pulp bleached by the industrial DEDED process. The consumption of chlorine dioxide was reduced by 56% for the W_AO_{POM}DED sequence and by 53% for the WODED sequence (similar pulp brightness), compared with the typical DEDED sequence (Table 4). In spite of the noted differences in the viscosity of

Table 4 Physical properties of eucalyptus kraft pulp bleached with W_AO_{POM}DED, WODED and DEDED sequences (65 g m⁻² a,⁶⁰)

	W _A O _{POM} DED	WODED	DEDED
ClO ₂ charge (as active chlorine)/kg ton ⁻¹	24	26	55
Pulp viscosity/cm ³ g ⁻¹	755	900	980
Brightness (% ISO)	85.1	86.7	89.5
Revolution PFI number	1800	2000	1250
Beating degree/°SR	30	30	30
Burst index/kPa m ² g ⁻¹	4.16	4.24	5.30
Tensile index/Nm g ⁻¹	62.1	64.8	77.1
Tear index/mNm ² g ⁻¹	7.75	8.20	8.6
Opacity (%)	72.0	71.5	70.4

^a Industrially bleached DEDED kraft pulp supplied by Soporcel pulp mill.

the pulps bleached by the $W_{AOPOM}DED$ and $WODED$ sequences (Table 4), their strength properties were very similar. Both pulps showed on average 10–20% lower strength indexes when compared with conventional pulp bleached by the $DEDED$ sequence. The pulp bleached by $W_{AOPOM}DED$ showed better beatability and opacity than the pulp bleached by $WODED$.

The analyses on toxicity have supported the idea that the final bleached pulp is not toxic and the effluents from the $W_{AOPOM}DED$ sequence can be biologically treated by conventional modes. Moreover, the absorption of POM composition elements in the pulp after the O_{POM} stage occurred only in residual amounts. More than 99% of the catalyst was recovered after using two washing steps.

6.4. Mn(III)-substituted polyoxometalates (and others)

Oxygen delignification experiments in the presence of Mn(III)-substituted polyoxotungstates with the Keggin structure such as $[XW_{11}Mn^{III}(H_2O)O_{39}]^{m-}$, with $X = P, Si, B$ ($XW_{11}Mn^{III}$)⁵⁶ and $[SiW_{10}Mn_2^{III}(H_2O)_2O_{40}]^{10-}$ ($SiW_{10}Mn_2^{III}$),⁶² or sandwich-type polyoxotungstates $[(PW_9O_{34})_2Mn^{III}_xMn^{II}_{4-x}]^{p-}$, where $x = 1, 3$ [$(PW_9)_2Mn_4$]⁶² were performed. A comparison of the kappa number decrease and the delignification selectivity in a conventional oxygen-alkaline delignification process and in the $SiW_{11}Mn^{III}/O_2$ or $(PW_9)_2Mn^{III}_3Mn^{II}/O_2$ systems showed significant advantages of the latter process.⁶² Moreover, these systems proved to be more selective than the $HPA-5/O_2$ and even the $HPA-5-Mn/O_2$ systems for the delignification of kraft pulp.^{46,62} With the $SiW_{11}Mn^{III}/O_2$ system, the kappa number was reduced from 12.4 to 5.1 (59%) while the viscosity drop was of only 11%.

As mentioned before (Section 6), the final state of the POM after the delignification experiments is an important point to address. It was found that POMs such as $SiW_{11}Mn^{III}$ or $SiW_{10}Mn_2^{III}$ were presented at the end of the delignification experiments in a partially oxidised form (about 15 and 40%, respectively).^{56,62} For the sandwich-type anions, no re-oxidation was detected and only the reduced form (Mn^{II}_4) was observed at the end of the reaction.⁶² In fact, this correlated with their redox potentials and the irreversibility of the $Mn^{III/II}$ pair in the following order: $SiW_{10}Mn_2^{III} < SiW_{11}Mn^{III} < (PW_9)_2Mn^{III}_4$. In spite of the high selectivity on delignification the incomplete re-oxidation of such POMs after the delignification experiments may be a limitation for their application in a single-stage delignification experiment which is the ideal and simplest system for the delignification purpose. A second stage is required (see heading 7).

Studies on the oxidation of model compounds with stoichiometric amounts of $SiW_{11}Mn^{III}$ under O_2 confirmed its reactivity with phenolic structures (oxidation of homovanillyl alcohol gave mainly vanilethanediol and dehydrodihomovanillyl alcohol), showing that phenolic units of lignin are easily oxidised by $SiW_{11}Mn^{III}$ via two- and one-electron abstraction mechanisms, respectively.⁵⁶ As expected from earlier studies, very poor conversion of homoveratryl alcohol (non-phenolic structure) was achieved with $SiW_{11}Mn^{III}$. A mechanism was proposed in which a fast period of delignification began by a fast reaction of $SiW_{11}Mn^{III}$ with phenolic

structures. Then, the delignification rate decreased due to the occurrence of coupling reactions that did not favour the lignin depolymerization, and possibly due to more difficult reaction with non-phenolic structures and partially oxidised lignin substructures.⁵⁶

One of the most effective POMs for the oxygen delignification of kraft pulp was $[SiW_{11}Co^{III}(H_2O)O_{39}]^{5-}$ ($SiW_{11}Co^{III}$). However, as for the sandwich-type anions, only the reduced form of $SiW_{11}Co^{II}$ was detected after the delignification experiments.⁶² Heteropolyanions of the series $[SiW_{12-x}V_xO_{40}]^{(4+x)-}$ ($x = 1-4$) were also evaluated as catalysts in the oxygen delignification of eucalyptus kraft pulps.⁶³ The best delignification results were achieved using $[SiW_8V_4O_{40}]^{8-}$ (SiW_8V_4) at pH 3–4. With the SiW_8V_4/O_2 system, about 50% delignification was obtained but with a high viscosity drop of around 30%.

7. Oxygen delignification with polyoxometalates and laccase

Polyoxometalates such as $SiW_{11}V$ and $SiW_{11}Mn$ are proved to be among the most effective and selective oxidants for the delignification of pulp under anaerobic conditions (as shown in Sections 5.1 and 6.4). In spite of possessing a redox potential $M^{(n+1)/n}$ (+0.7 to +0.8 V vs. NHE) lower than that of oxygen reduction to water they are hardly re-oxidised by oxygen even at vigorous conditions of temperature and oxygen pressure, which is attributed mainly to kinetic factors. This fact limits their application in oxygen delignification catalysis. A solution was found by using bio-catalytic re-oxidation of POMs by laccase of *Trametes versicolor*. Two different approaches were considered.

In a first approach, POMs were used as inorganic mediators to laccase-catalysed delignification of pulp at temperatures typically around 45–60 °C.^{64–67} This followed observation that some of the POMs that were hardly re-oxidised by oxygen, such as $SiW_{11}Mn^{II}$ and $SiW_{11}V^{IV}$, could be re-oxidised by the enzyme even at room temperature ($T \approx 25$ °C) and atmospheric pressure (ca. 0.02 MPa).⁶⁷ When using POMs as inorganic mediators for pulp delignification (laccase-mediator system – LMS), the POM oxidises the residual lignin in the pulp and the reduced POM is re-oxidised by laccase at the same stage. Finally, the cycle is completed by re-oxidation of the copper centres of the prosthetic group of laccase in the presence of oxygen. The application of the LMS to the delignification of kraft pulps has not produced high delignifications. No more than 35% delignification was achieved, even after 48 h of reaction.⁶⁴ The low delignification rate was suggested to be due to the scarce reactivity of the POM with the substrate under the applied conditions.⁶⁷ In fact, the optimal conditions required for kraft pulp delignification with the POM are typically around 90–110 °C, in contrast to the applied temperatures lower than 60 °C.

In a second approach, an alternative multi-stage process was developed in which the pulp is treated with a POM at high temperature (100–110 °C) in a first stage, followed by the POM re-oxidation with laccase at moderate temperatures (30–60 °C) in a separate stage.^{66,67} The application of this multi-stage process brought delignifications around 50% when applied to

Table 5 Results of eucalyptus kraft pulp delignification catalysed by POM and laccase^{a,67}

System	Kappa number	Viscosity/ cm ³ g ⁻¹	Delignification (%) ^b	Viscosity loss (%)
Kraft pulp	12.3	1185	—	—
SiW ₁₁ Mn ^{III}				
POM	9.5	1130	23	5
POM-L	8.9	1080	28	9
POM-L-POM	6.9	1075	44	9
POM-L-POM-L-POM	6.0	1020	52	14
SiW ₁₁ V ^V				
POM	9.0	1055	26	11
POM-L	8.2	1035	33	13
POM-L-POM	6.9	1005	44	15

^a Consistency = 6%; POM stage: 110 °C, 2 h, $p^{\circ}(\text{O}_2) = 0.6$ MPa, [POM] = 3.6 mmol L⁻¹, pH 4.5; laccase stage: 45 °C, 4 h, $p^{\circ}(\text{O}_2) = 0.3$ MPa, laccase 380 U l⁻¹. ^b Estimated as the decrease of kappa number.

SiW₁₁Mn^{III} and SiW₁₁V^V. SiW₁₁Mn^{III} was found to be more selective, while SiW₁₁V^V was more effective in the oxidative delignification (Table 5).⁶⁷ After the laccase stage (POM-L) the complete (or almost complete) re-oxidation of polyoxometalates SiW₁₁V (and SiW₁₁Mn, respectively) was verified. Furthermore, no indications of degradation of the Keggin structure were found under the experimental conditions used.

Recently, a novel integrated system was developed in which the delignification of pulp by a POM and the re-oxidation of the POM by laccase occur in separate reactors.⁶⁸ This is based on three main components: a delignification reactor operating at temperatures around 85–90 °C under atmospheric pressure where the reaction of SiW₁₁V^V with lignin occurs; a bio-reactor containing laccase operating at temperatures of around 45 °C under atmospheric pressure where the reduced POM SiW₁₁V^{IV} coming from the delignification reactor is re-oxidised back to SiW₁₁V^V; and an ultrafiltration membrane in which the SiW₁₁V^V is separated from the enzyme and returned to the delignification reactor. With this continuous system, delignification approaching 70% for only a 15% viscosity loss is obtained. Further ClO₂ stages confirmed high quality bleached pulps and allowed a saving of about 60% of ClO₂.⁶⁸ The principles of the POM-laccase integrated delignification system can be applied in the conventional multistage displacement bleaching tower, where reduced POM is withdrawn from different zones, continuously re-oxidised by laccase under aerobic conditions in a bioreactor and the re-oxidised catalyst returned to the tower after separation of laccase using suitable devices.

Three extracellular metalloenzymes are involved in the depolymerization of native lignin by wood-rotting fungi: laccase, manganese peroxidase and lignin peroxidase. In the biological delignification, manganese peroxidase, a protoheme-containing enzyme, oxidises Mn(II), abundant in the cell wall, to Mn(III); this species is stabilized by α -hydroxy acids. The formed Mn(III) complexes oxidise the phenolic groups within the lignin.⁶⁹ It is possible that manganese peroxidase could be used for the re-oxidation of the manganese-substituted Keggin anion, SiW₁₁Mn, and other related species. This could be an area to explore in the future.

8. Concluding remarks

In the past 10–15 years significant efforts toward the substitution of chlorine dioxide by environmentally friendly pulp delignification systems employing polyoxometalates have been made. The most effective and selective polyoxometalates found for the delignification process were SiW₁₁V^V, SiW₁₁Mn^{III}, AlW₁₁V^V, SiW₁₀V₂, 'SiW_{10.1}Mo_{1.0}V_{0.9}O₄₀' and the above-mentioned HPA-5-Mn^{II}.

Two general approaches were applied. One, where in a first stage the POM is used as a reagent for the pulp delignification under anaerobic conditions and in a different stage the re-oxidation of the POM takes place. Another, under aerobic conditions, where the POM in catalytic amounts is used to delignify the pulp and is continuously re-oxidised by oxygen in the same stage. Very interesting results could be obtained, the best approaching 70–80% of delignification with a viscosity loss of 20–30%. Pilot plant trials with HPA-5-Mn^{II} followed by further delignification with chlorine dioxide and analyses of the physical properties of the final bleached pulps showed that the polyoxometalate-catalysed oxygen delignification may represent a new and interesting tool for pulp delignification with practical feasibility. A saving of 56% of chlorine dioxide was achieved.

For those polyoxometalates (especially those most selective on delignification) where the re-oxidation step by oxygen is the limiting step, the incorporation of other oxidising reagents such as appropriate enzymes or even non-chemical oxidation processes is required. Incorporation of laccase for the re-oxidation of a few polyoxometalates has resulted in a new, clean biotechnological delignification process. These processes may be of practical interest, especially if the POM and enzyme can be both re-used for pulp delignification in a sustainable overall process.

New directions in the future may be towards the application of other polyoxometalates, searching for more powerful and selective oxidants/catalysts for the delignification process. Alternatively, the development/optimization of new/known processes incorporating delignification and re-oxidation of the POM in different stages should be considered. Up to date it is not possible to totally substitute the chlorine dioxide by POM-based systems (whether or not they employ oxygen). However, under appropriate conditions, POMs may be used to save 70% of the chlorine dioxide without losing out on the quality of the final cellulose fibres.⁶⁸ In the future, these processes should be optimized and costs evaluated and compared with those of industrial processes in order to evaluate the possibility of incorporating new POM-based delignification processes into industrial applications.

References

- 1 *Pulp Bleaching – Principles and Practice*, ed. C. W. Dence and D. W. Reeve, Tappi Press, Atlanta, 1996.
- 2 *Wood and Cellulosic Chemistry*, ed. D. N.-S. Hon and N. Shiraishi, Marcel Dekker, New York and Basel, 1991.
- 3 *Heteropoly and Isopoly Oxometalates*, ed. M. T. Pope, Springer Verlag, Berlin, 1983.
- 4 M. T. Pope and A. Müller, *Angew. Chem., Int. Ed. Engl.*, 1991, **30**, 34.
- 5 *Polyoxometalates: from platonic solids to anti-retroviral activity*, ed. M. T. Pope, and A. Müller, Kluwer Academic Publishers, Dordrecht, 1994.

- 6 C. L. Hill, *Chem. Rev.*, 1998, **98**, 1 (special issue).
- 7 *Polyoxometalate Chemistry. From Topology via Self-assembly to Applications*, ed. M. T. Pope and A. Müller, Kluwer, Dordrecht, 2001.
- 8 C. L. Hill and C. M. Prosser-McCarthy, *Coord. Chem. Rev.*, 1995, **143**, 407.
- 9 I. Kozhevnikov, *Chem. Rev.*, 1998, **98**, 171.
- 10 M. Misono, *Chem. Commun.*, 2001, 1141.
- 11 R. Neumann, *Prog. Inorg. Chem.*, 1998, **47**, 317.
- 12 *Wood chemistry, fundamentals and applications*, ed. E. Sjöström, Academic press, San Diego, 2nd edn, 1992.
- 13 *Wood: Chemistry, Ultrastructure, Reactions*, ed. D. Fengel and G. Wegener, Walter de Gruyter, New York, 1984.
- 14 *Pulp and Paper. Chemistry and Chemical Technology*, ed. J. P. Casey, Wiley-Interscience, New York, 3rd edn, 1980, vol. 1.
- 15 *Handbook for Pulp & Paper Technologists*, ed. G. A. Smook, Angus Wilde Publications Inc., Vancouver, 2nd edn, 1997.
- 16 T. J. McDonough, in: *Pulp Bleaching – Principles and Practice*, ed. C. W. Dence and D. W. Reeve, Tappi Press, Atlanta, 1996, sect. IV, ch. 1, p. 215.
- 17 L. C. W. Baker and D. C. Glick, *Chem. Rev.*, 1998, **98**, 3.
- 18 A. Müller, E. Krickemeyer, H. Bogge, M. Schmidtman, C. Beugholt, P. Kogerler and C. Lu, *Angew. Chem., Int. Ed.*, 1998, **37**, 1220.
- 19 A. Müller, E. Krickemeyer, H. Bogge, M. Schmidtman and F. Peters, *Angew. Chem., Int. Ed.*, 1998, **37**, 3360.
- 20 I. A. Weinstock, C. L. Hill and J. L. Minor, in *Proceedings of 2nd European Workshop on Lignocellulosics and Pulp*, held Grenoble, France, 2–4 Sep. 1992, p. 33.
- 21 R. Neumann and M. Levin, *J. Am. Chem. Soc.*, 1992, **114**, 7278.
- 22 D. V. Evtuguin, C. Pascoal Neto, H. Carapuça and J. Soares, *Holzforchung*, 2000, **54**, 511.
- 23 *Inorganic Chemistry. A guide to advance study*, ed., R. B. Heslop and K. Jones, Elsevier, Amsterdam, 1976.
- 24 I. A. Weinstock, C. L. Hill and R. H. Atalla, *US Pat.*, 5552019, issued: 3 September 1996; R. H. Atalla, I. A. Weinstock, C. L. Hill and R. S. Reiner, *US Pat.*, 5549789, issued: 27 August 1996; I. A. Weinstock, R. H. Atalla and C. L. Hill, *WO Pat.*, 9526438, issued: 5 October 1995; I. A. Weinstock and C. L. Hill, *WO Pat.*, 9405849, issued: 17 March 1994.
- 25 I. A. Weinstock, R. H. Atalla, R. S. Reiner, M. A. Moen, K. E. Hammel, C. J. Houtman and C. L. Hill, *New J. Chem.*, 1996, **20**, 269.
- 26 I. A. Weinstock, R. H. Atalla, R. S. Reiner, M. A. Moen, K. E. Hammel, C. J. Houtman, C. L. Hill and M. K. Harrup, *J. Mol. Catal.*, 1997, **116**, 59.
- 27 I. A. Weinstock, R. H. Atalla, R. S. Reiner, C. J. Houtman and C. L. Hill, *Holzforchung*, 1998, **52**, 304.
- 28 I. A. Weinstock, K. E. Hammel, M. A. Moen, L. L. Landucci, S. Ralph, C. E. Sullivan and R. S. Reiner, *Holzforchung*, 1998, **52**, 311.
- 29 R. H. Atalla, I. A. Weinstock, R. S. Reiner, C. J. Houtman, C. J. Hill and C. L. Hill, in *Proceedings of the 4th European Workshop on Lignocellulosics and Pulp*, held Stresa, Italy, 8–11 Sep. 1996, p. 189.
- 30 M. D. Sonnen, R. S. Reiner, R. A. Atalla and I. A. Weinstock, *Ind. Eng. Chem. Res.*, 1997, **36**, 4134.
- 31 I. A. Weinstock, R. H. Atalla, R. S. Reiner, M. A. Moen, K. E. Hammel, C. L. Hill and C. J. Houtman, in *Proceedings of International Pulp Bleaching Conference*, held Washington DC, USA, 14–18 Apr. 1996, 481.
- 32 R. H. Atalla, I. A. Weinstock, J. S. Bond, R. S. Reiner, D. M. Sonnen, C. J. Houtman, R. A. Heintz, C. G. Hill, C. L. Hill, M. W. Wemple, Y. V. Geletii and E. M. G. Barbuzzi, in *Oxidative delignification chemistry: fundamentals and catalysis*, ed. D. S. Argyropoulos, ACS Symposium Series, No. 785, American Chemical Society, San Francisco, CA, 2001, ch. 19, p. 313.
- 33 I. A. Weinstock, E. M. G. Barbuzzi, M. W. Wemple, J. J. Cowan, R. S. Reiner, D. M. Sonnen, R. A. Heintz, J. S. Bond and C. L. Hill, *Nature*, 2001, **414**, 6860.
- 34 R. H. Atalla, I. A. Weinstock, J. S. Bond, R. S. Reiner, C. J. Houtman, S. E. Reichel, D. M. Sonnen, C. G. Hill and C. L. Hill, in *Proceedings of TAPPI Pulping/Process and Product Quality Conference*, held Boston, MA, USA, 5–8 Nov. 2000, p. 113.
- 35 R. H. Atalla, I. A. Weinstock, R. S. Reiner, E. L. Springer, C. G. Hill, Y. Geletii and C. L. Hill, in *Proceedings of TAPPI Fall Technical Conference: Engineering, Pulping & PCE&I*, held Chicago, IL, USA, 26–30 Oct. 2003, p. 857.
- 36 R. H. Atalla, I. A. Weinstock, R. S. Reiner, E. L. Springer, C. G. Hill, Y. Geletii and C. L. Hill, in *Proceedings of TAPPI Paper Summit – Spring Technical and International Environmental Conference*, held Atlanta, GA, USA, 3–5 May 2004, p. 55.
- 37 I. A. Weinstock, R. H. Atalla, U. P. Agarwal, J. L. Minor and C. Petty, *Spectrochim. Acta, Part A*, 1993, **49**, 819.
- 38 G. Kang, Y. Ni and A. V. Heiningen, *Appita J.*, 1997, **50**, 313.
- 39 J. Gierer, E. Yang and T. Reitberger, *Holzforchung*, 1992, **46**, 495.
- 40 M. Lissel, H. Jansen in de Wal and R. Neumann, *Tetrahedron Lett.*, 1992, **33**, 1795.
- 41 T. Yokoyama, H.-m. Chang, I. A. Weinstock, R. S. Reiner and J. F. Kadla, in *Proceedings of 12th International Symposium on Wood and Pulping Chemistry*, held Madison, WI, USA, 2003, vol. II, p. 43.
- 42 T. Yokoyama, H.-m. Chang, R. S. Reiner, R. J. Atalla, I. A. Weinstock and J. F. Kadla, *Holzforchung*, 2004, **58**, 116.
- 43 K. Ruuttunen, PhD Thesis, Helsinki University Of Technology, Helsinki, 2006.
- 44 K. Ruuttunen and T. Vuorinen, *Ind. Eng. Chem. Res.*, 2005, **44**, 4284.
- 45 K. Ruuttunen, V. Tarvo, J. Aittamaa and T. Vuorinen, *Nord. Pulp Pap. Res. J.*, 2006, **21**, 303.
- 46 D. V. Evtuguin and C. Pascoal Neto, *Holzforchung*, 1997, **51**, 338.
- 47 D. V. Evtuguin, C. Pascoal Neto, J. Rocha and J. D. Pedrosa de Jesus, *Appl. Catal., A*, 1998, **167**, 123.
- 48 D. V. Evtuguin and C. Pascoal Neto, *PT Pat.*, 101857, issued 31 Oct. 1997.
- 49 D. V. Evtuguin and C. Pascoal Neto, in *Proceedings of 5th European Workshop on Lignocellulosics and Pulp*, held Aveiro, Portugal, 30 Aug.–2 Sep. 1998, p. 589.
- 50 D. V. Evtuguin, C. Pascoal Neto and J. D. Pedrosa de Jesus, *J. Pulp Pap. Sci.*, 1998, **24**, 133.
- 51 D. V. Evtuguin, C. Pascoal Neto and J. Rocha, *Holzforchung*, 2000, **54**, 381.
- 52 D. V. Evtuguin and C. Pascoal Neto, in *Proceedings of International Pulp Bleaching Conference*, held Helsinki, Finland, 1–5 Jun. 1998, p. 487.
- 53 D. V. Evtuguin, C. Pascoal Neto, V. M. Marques and F. P. Furtado, in *Proceedings of International Pulp Bleaching Conference*, held Helsinki, Finland, 1–5 Jun. 1998, p. 493.
- 54 A. Gaspar, D. V. Evtuguin and C. Pascoal Neto, in *Proceedings of 11th International Symposium on Wood and Pulping Chemistry*, held Nice, France, 11–14 Jun. 2001, vol. I, p. 227.
- 55 C. M. Tourné, G. F. Tourné, S. A. Malik and T. J. R. Weakley, *J. Inorg. Nucl. Chem.*, 1970, **32**, 3875.
- 56 A. Gaspar, D. V. Evtuguin and C. Pascoal Neto, *Appl. Catal., A*, 2003, **239**, 157.
- 57 D. V. Evtuguin and C. Pascoal Neto, in *Oxidative delignification processes: fundamentals and catalysis*, ed. D. S. Argyropoulos, ACS Symposium Series, No. 785, American Chemical Society, San Francisco, CA, 2001, ch. 20, p. 327.
- 58 A. A. Shatalov, D. V. Evtuguin and C. Pascoal Neto, *Carbohydr. Polym.*, 2000, **43**, 23.
- 59 A. Gaspar, D. V. Evtuguin and C. Pascoal Neto, *Holzforchung*, 2004, **58**, 640.
- 60 A. R. Gaspar, PhD Thesis, University of Aveiro, Portugal, 2002.
- 61 A. R. Gaspar, D. V. Evtuguin and C. Pascoal Neto, *Ind. Eng. Chem. Res.*, 2004, **43**, 7754.
- 62 J. A. F. Gamelas, A. R. Gaspar, D. V. Evtuguin and C. Pascoal Neto, *Appl. Catal., A*, 2005, **295**, 134.
- 63 A. Gaspar, D. V. Evtuguin and C. Pascoal Neto, *Appita J.*, 2004, **57**, 386.
- 64 M. Balaskshin, D. V. Evtuguin, C. Pascoal Neto and A. Cavaco-Paulo, *J. Mol. Catal. B: Enzym.*, 2001, **16**, 131.
- 65 A. I. R. P. Castro, D. V. Evtuguin and A. M. B. Xavier, *J. Mol. Catal. B: Enzym.*, 2003, **22**, 13.
- 66 A. P. M. Tavares, J. A. F. Gamelas, A. R. Gaspar, D. V. Evtuguin and A. M. R. B. Xavier, *Catal. Commun.*, 2004, **5**, 485.
- 67 J. A. F. Gamelas, A. P. M. Tavares, D. V. Evtuguin and A. M. B. Xavier, *J. Mol. Catal. B: Enzym.*, 2005, **33**, 57.
- 68 J. A. F. Gamelas, A. S. N. Pontes, D. V. Evtuguin, A. M. R. B. Xavier and A. P. Esculcas, *Biochem. Eng. J.*, 2007, **33**, 141.
- 69 M. Sundaramoorthy, K. Kishi, M. H. Gold and T. L. Poulos, *J. Biol. Chem.*, 1994, **269**, 32759 and refs cited therein.

Highly efficient production of 2,3,5-trimethyl-1,4-benzoquinone using aqueous H₂O₂ and grafted Ti(IV)/SiO₂ catalyst

Oxana A. Kholdeeva,*^a Irina D. Ivanchikova,^a Matteo Guidotti^b and Nicoletta Ravasio^b

Received 23rd November 2006, Accepted 15th February 2007

First published as an Advance Article on the web 27th February 2007

DOI: 10.1039/b617162a

The oxidation of 2,3,6-trimethylphenol with aqueous H₂O₂ over titanium(IV) grafted on commercial mesoporous silica produces 2,3,5-trimethyl-1,4-benzoquinone, with nearly quantitative yield.

The vitamin E precursor, 2,3,5-trimethyl-1,4-benzoquinone (TMBQ), is currently produced in industry *via* oxidation of 2,3,6-trimethylphenol (TMP) with molecular oxygen in the presence of a copper chloride catalyst used in amounts close to stoichiometric.¹ The evident shortcomings of the CuCl₂/O₂ homogeneous system are corrosiveness and product contamination with transition metal (Cu) and chlorine-containing compounds, even if the process is operated under two-phase conditions. The development of green alternatives for the production of TMBQ is thus a challenging goal of fine chemistry.

Recently, some of us have suggested the production of TMBQ *via* oxidation of TMP with aqueous H₂O₂ over a mesoporous titanium-silicate catalyst (Scheme 1).²

Both well-ordered mesostructured materials and amorphous TiO₂-SiO₂ mixed oxides were found to operate as true heterogeneous catalysts in this reaction when acetonitrile was used as a solvent.³ The highest yield of TMBQ (up to 98%) was attained over TiO₂-SiO₂ aerogels with titanium loading in the range of 1.7–6.5 wt%. However, despite the fact that the catalysts did not suffer from titanium leaching into solution, the catalytic activity dramatically decreased after the first run because of the hydrolytic instability of the porous structure and irreversible titanium oligomerization on the surface.³ The progress in solving the problem of the hydrothermal instability of mesoporous titanium-silicates is related to the synthesis of mesoporous TS-1,⁴ Ti-MMM-1⁵ and Ti-MMM-2⁶ materials. Meanwhile, the selectivity to TMBQ attained with Ti-MMM-2 does not exceed 80%,⁶ which is not enough to make this process commercially attractive. Furthermore, the synthesis of the catalyst requires the use of the

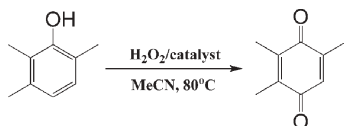
expensive and toxic ionic surfactant, cetyltrimethylammonium bromide.

Tuel and Hubert-Pfalzgraf have reported that nanometric monodispersed titanium oxide particles supported on meso-structured silicates, such as SBA-15, MCM-41 and HMS, using the hexanuclear cluster [Ti₆(μ₃-O)₆(μ-O₂CC₆H₄OPh)₆(OEt)₆] are highly active and selective in the H₂O₂-based TMP oxidation to TMBQ.⁷ Unfortunately, the catalyst stability and recycling tests were not provided.

Some of us showed that titanium-grafted materials obtained from non-ordered commercially available silicas are efficient catalysts for the epoxidation of unsaturated terpenes and fatty acid derivatives.⁸ These systems can be prepared by a less expensive and time-consuming method than the ordered template-based molecular sieves and can provide comparable, or even superior, performances. In this work we demonstrate that titanium catalysts (Ti/SiO₂) prepared by grafting titanocene dichloride onto the surface of commercial silicas, adapting the procedure developed by Maschmeyer *et al.*,⁹ are highly efficient in TMBQ production.

The catalytic performance of titanium grafted onto non-ordered mesoporous (A) and pyrogenic non-porous (B) silica supports was assessed in TMP oxidation with H₂O₂ in acetonitrile under optimal reaction conditions determined previously.³ The results of the catalytic tests are presented in Table 1. The results obtained with the mesostructured Ti-MMM-2 catalyst prepared by hydrothermal synthesis⁶ are given for comparison.

The non-porous pyrogenic silica-grafted catalyst shows a rather low activity compared to the mesoporous materials, and TMBQ



Scheme 1

Table 1 TMP oxidation with H₂O₂ over Ti,Si-catalysts^a

Catalyst ^b (Ti, wt%)	TMP conversion (%)	TMBQ selectivity ^c (%)	TOF ^d /min ⁻¹
Ti/SiO ₂ (A) ^e (1.97)	100	96 (100) ^f	2.0 (2.0)
Ti/SiO ₂ (A) ^e (0.92)	100	79	1.4 (2.0)
Ti/SiO ₂ (B) ^e (1.78)	85	47	0.7 (1.0)
Ti-MMM-2 ^h (2.00)	98	76	1.3 (1.9)

^a Reaction conditions: TMP, 0.1 M; H₂O₂, 0.4 M; catalyst, 0.006 mmol of Ti; MeCN, 1 mL, 80 °C, 30 min. ^b All the catalysts were calcined at 560 °C for 5 h in air directly before experiments.

^c GC yield based on TMP consumed. ^d TOF = (moles of TMBQ formed)/(moles of Ti) × (time), determined from the initial rates of TMBQ formation; in parentheses, (moles of TMP consumed)/(moles of Ti) × (time), determined from the initial rates of TMP consumption. ^e Surface area of the support, A, 290 m² g⁻¹, volume of mesopores, V, 1.48 cm³ g⁻¹, mean pore diameter, d, 20.4 nm. ^f The catalyst amount was increased twice. ^g Non-porous, A 268 m² g⁻¹. ^h A 1120 m² g⁻¹, V 0.57 cm³ g⁻¹, d 3.2 nm.

^a Borekov Institute of Catalysis, Pr. Ac. Lavrentieva 5, Novosibirsk, 630090, Russia. E-mail: khold@catalysis.nsk.su; Fax: +73833309573; Tel: +73833309573

^b CNR-ISTM, Centro CIMA and Dip. Chimica IMA, via G. Venezian 21, Milano, 20133, Italy. E-mail: m.guidotti@istm.cnr.it; Fax: +39 02 50314405; Tel: +39 02 50314428

yield does not exceed 40% based on the initial substrate. The activities of the Ti/SiO₂ catalysts grafted onto the non-ordered mesoporous silica and of Ti-MMM-2 expressed in TOF values determined from the initial rates of TMP consumption are similar, and 98–100% TMP conversion is reached after 15–20 min. Acetonitrile is the solvent of choice for this reaction. In methanol or *iso*-propanol, the reaction rate is several times slower and TMBQ selectivity significantly decreases.

It is worth noting that Ti/SiO₂ containing about 2 wt% of Ti reveals superior selectivity in TMBQ formation, TMBQ yields as high as 96–100% being attained (Table 1). Both Ti-MMM-2 and Ti/SiO₂ with a lower titanium loading (0.92 wt%) have a higher degree of isolation of Ti(IV) sites, which is clearly indicated¹⁰ by the higher energy position of the band in the DR-UV spectra (Fig. 1).

Meanwhile, these two catalysts are less selective, and only 76–79% yield of TMBQ is achieved (Table 1). Comparing the TOF values determined from the initial rates of TMBQ production and TMP consumption, which are given in Table 1, we may conclude that titanium site isolation is crucial for the activity of the Ti,Si-catalysts but not for the high selectivity of the TMBQ formation. Oppositely, a high surface concentration of well-dispersed, probably dimeric,¹¹ titanium species, which is manifested by a broad maximum of the band in the DR-UV spectrum in the range of 220–270 nm (Fig. 1), favours the formation of the monoquinone at the expense of the typical by-product of TMP oxidation, biphenol. This conclusion is in agreement with the results reported earlier by Tuel and Hubert-Pfalzgraf⁷ and by some of us.³ Importantly, no bands in the range of 300–330 nm are present in the DR-UV spectra of all the titanium catalysts studied in this work, indicating the lack of anatase-like oligomeric species, which are known to be responsible for a low activity of Ti,Si-catalysts in selective oxidations with H₂O₂.¹⁰

To better fulfil the green chemistry guidelines and to assess the propensity of the materials to be recovered and reused, the Ti/SiO₂ catalyst was recycled in two consecutive catalytic runs. In contrast to the TiO₂-SiO₂ aerogels, the grafted Ti/SiO₂ catalyst is considerably more stable and can be used repeatedly without a significant loss in both the activity and selectivity (Fig. 2).

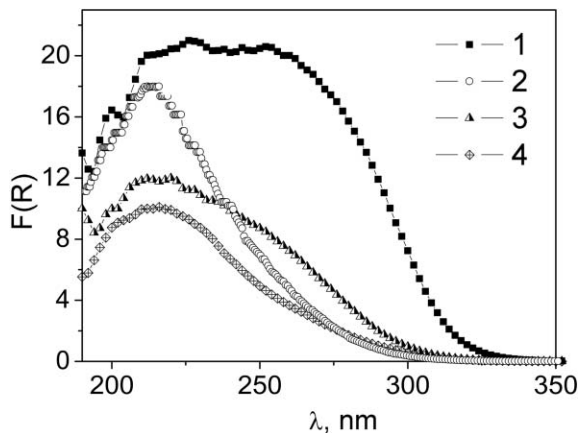


Fig. 1 DR-UV spectrum of Ti/SiO₂ (A) (Ti 1.97 wt%) (1), Ti/SiO₂ (B) (Ti 1.78 wt%) (2), Ti/SiO₂ (A) (Ti 0.92 wt%) (3), Ti/SiO₂ (Ti-MMM-2) (Ti 2.00 wt%) (4).

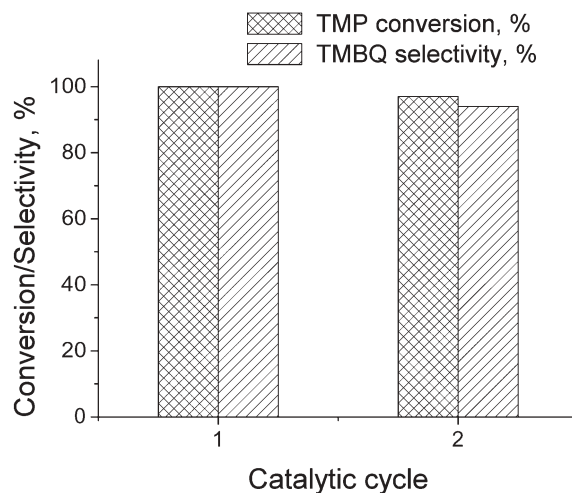


Fig. 2 Recycling of Ti/SiO₂ (A) (Ti 1.97 wt%) in TMP oxidation with H₂O₂. Reaction conditions: TMP, 0.1 M; H₂O₂, 0.4 M; catalyst, 0.013 mmol of Ti; MeCN, 5 mL, 80 °C, 30 min.

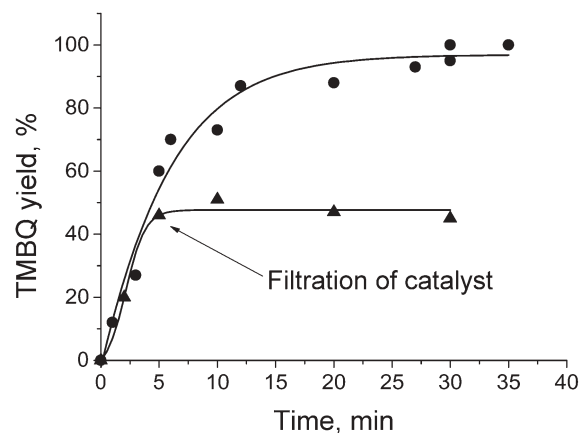


Fig. 3 Oxidation of TMP with H₂O₂ over Ti/SiO₂ (A) (Ti 1.97 wt%). Reaction conditions as in Table 1.

Typically for Ti,Si-catalysts,³ no further TMP conversion is observed in the filtrate after fast hot catalyst filtration at about 50% of TMP conversion, indicating a true heterogeneous nature of catalysis over Ti/SiO₂ (Fig. 3). Elemental analysis data confirm that no titanium leaching from the solid catalyst occurs under the conditions of TMP oxidation.

The catalysts prepared by grafting titanium onto non-ordered commercial mesoporous silica combine excellent activity, very high selectivity to the desired product and good recyclability in the TMP oxidation by aqueous H₂O₂. In addition, these solids are prepared by a simple, affordable and cheap synthesis methodology. All these facts allow us to view them as prospective heterogeneous catalysts for the clean and sustainable synthesis of TMBQ.

Acknowledgements

We thank M. P. Vanina for preliminary results and T.V. Larina for DRS-UV measurements. OAK thanks CNR for the Short Term Mobility Program grant (N 30212, year 2006)

Notes and references

- W. Bonrath and T. Netscher, *Appl. Catal., A*, 2005, **280**, 55.
- O. A. Kholdeeva, V. N. Romannikov, N. N. Trukhan, V. N. Parmon, *RU Patent* 2196764, 2001.
- N. N. Trukhan, V. N. Romannikov, E. A. Paukshtis, A. N. Shmakov and O. A. Kholdeeva, *J. Catal.*, 2001, **202**, 110; O. A. Kholdeeva, N. N. Trukhan, M. P. Vanina, V. N. Romannikov, V. N. Parmon, J. Mrowiec-Bialon and A. B. Jarzebski, *Catal. Today*, 2002, **75**, 203.
- I. Schmidt, A. Krogh, K. Wienberg, A. Carlsson, M. Brorson and C. J. H. Jacobsen, *Chem. Commun.*, 2000, 2157.
- R. H. P. R. Poladi and C. C. Landry, *Microporous Mesoporous Mater.*, 2002, **52**, 11.
- O. A. Kholdeeva, M. S. Melgunov, A. N. Shmakov, N. N. Trukhan, V. V. Kriventsov, V. I. Zaikovskii and V. N. Romannikov, *Catal. Today*, 2004, **91–92**, 205.
- A. Tuel and L. G. Hubert-Pfalzgraf, *J. Catal.*, 2003, **217**, 343.
- M. Guidotti, N. Ravasio, R. Psaro, G. Ferraris and G. Moretti, *J. Catal.*, 2003, **214**, 247; M. Guidotti, N. Ravasio, R. Psaro, E. Gianotti, L. Marchese and S. Coluccia, *Green Chem.*, 2003, **5**, 421; M. Guidotti, N. Ravasio, R. Psaro, E. Gianotti, L. Marchese and S. Coluccia, *J. Mol. Catal. A: Chem.*, 2006, **250**, 218.
- T. Maschmeyer, F. Rey, G. Sankar and J. M. Thomas, *Nature*, 1995, **378**, 159; M. Guidotti, L. Conti, A. Fusi, N. Ravasio and R. Psaro, *J. Mol. Catal. A: Chem.*, 2002, **182–183**, 149.
- B. Notari, *Adv. Catal.*, 1996, **41**, 253; A. Corma, *Chem. Rev.*, 1997, **97**, 2373; O. A. Kholdeeva and N. N. Trukhan, *Russ. Chem. Rev.*, 2006, **75**(5), 411.
- E. Gianotti, A. Frache, S. Coluccia, J. M. Thomas, T. Maschmeyer and L. Marchese, *J. Mol. Catal. A: Chem.*, 2003, **204–205**, 483.



STOP!

searching...

Save valuable time searching for that elusive piece of vital chemical information.

Let us do it for you at the Library and Information Centre of the RSC.

We are your chemical information support, providing:

- Chemical enquiry helpdesk
- Remote access chemical information resources
- Speedy response
- Expert chemical information specialist staff

Tap into the foremost source of chemical knowledge in Europe and send your enquiries to

library@rsc.org

RSC Publishing

www.rsc.org/library

12120515

Enzymatic resolution of Indinavir precursor in ionic liquids with reuse of biocatalyst and media by product sublimation†

Nuno M. T. Lourenço,^b Susana Barreiros^b and Carlos A. M. Afonso^{*a}

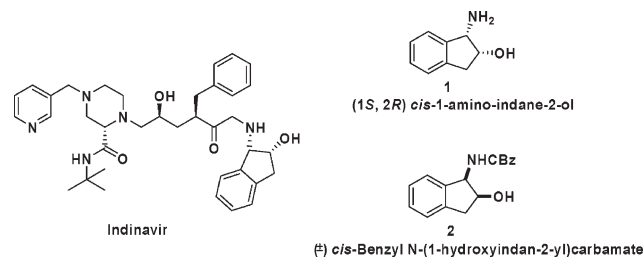
Received 10th January 2007, Accepted 20th February 2007

First published as an Advance Article on the web 6th March 2007

DOI: 10.1039/b700406k

Efficient enzymatic resolution of (\pm)-*cis*-benzyl *N*-(1-hydroxyindan-2-yl)carbamate in [aliq][N(CN)₂] by acylation using CALB as a biocatalyst was achieved, with the possibility of catalyst and medium reuse. The reaction proceeds to the formation of the corresponding acetate in moderate yield and high enantiomeric excess for the first and second cycles. Additionally, the biocatalyst can be recovered by filtration and reaction products can be easily removed from the ionic liquid by direct sublimation under high vacuum.

The development of efficient routes to obtain chiral pure compounds is the subject of considerable interest. Among many others, (1*S*, 2*R*) *cis*-1-amino-indan-2-ol **1** is an important unit present in drugs with physiological activity such as Indinavir (under the trade name of Crixivan[®]). Researches at Merck first demonstrated in 1990¹ the utility of **1** as an effective ligand for an HIV protease inhibitor.² In the last few years, a new class of HIV protease inhibitors have been developed³ using the same key unit **1**.^{4–7} Efficient chiral auxiliaries and catalysts have also been prepared from **1** and used in asymmetric synthesis.^{8–12}



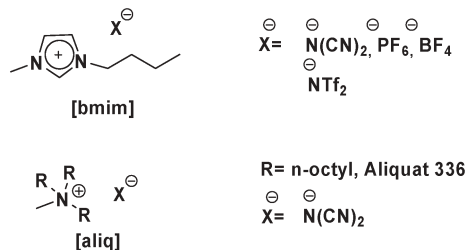
Enzymatic resolution is a powerful methodology to obtain chiral active compounds used as precursors of pharmaceutical drugs.^{13,14} In the past few years, several enzymatic and non-enzymatic procedures have been described for the synthesis of enantiomerically pure *cis*-1-amino-indan-2-ol **1**.^{8,12,15–23}

In 1999, Luna *et al.*²¹ reported the enzymatic resolution of (\pm)-*cis*-benzyl *N*-(1-hydroxyindan-2-yl)carbamate **2** in 1,4-dioxane using *Pseudomonas cepacia* lipase (PSL). Under these reaction conditions, PSL exhibited high enantioselectivity, providing the

substrate (1*R*, 2*S*)-**2** in 78% ee, and the corresponding acetate (1*S*, 2*R*)-**3** in 99% ee. However, the long reaction times (9 days) reported are probably due to low solubility of the substrate in the organic solvent. In the same year, Anilkumar *et al.*²³ described the enzymatic alcoholysis of an *N,O*-diacetyl derivative of **1** in several organic solvents using *Candida antarctica* lipase B (CALB). A 1 : 1 diisopropyl ether : 1,4-dioxane solvent mixture and *n*-butanol proved to be a good combination to perform this reaction. After 76 h of reaction, the product was obtained in 43% yield with an ee >99%. Water-miscible hydrophilic solvents, such as 1,4-dioxane, normally induce enzyme denaturation and deactivation to some extent, and thus most researchers prefer to use water-immiscible lipophilic solvents such as hexane or toluene to perform enzymatic resolutions.²⁴ The use of ionic liquids (ILs) in enzymatic resolutions has been the object of recent interest by different laboratories.^{25–28} Ionic liquids provide a stable and friendly environment for the enzymes where they retain their catalytic activity even after several cycles. The high stability of IL media and the ease of product recovery combined with enzyme reuse makes ILs a powerful tool for biocatalysis.

Herein, we report the use and reuse of ILs and biocatalysts for the efficient enzymatic resolution of (\pm)-*cis*-Benzyl *N*-(1-hydroxyindan-2-yl)carbamate **2**, where the products are easily recovered from the IL by sublimation.

Initially, we compared the performance of PSL and CALB (Novozym 435[®]) in the resolution of (\pm)-**2**²⁰ in 1-*n*-butyl-3-methylimidazolium hexafluorophosphate [bmim][PF₆], using vinyl acetate as an acyl donor. Reaction conversions up to 28% prompted us to perform a screening of different ILs at a constant water activity (*a_w*, the most convenient parameter to correlate enzymatic activity, here set to 0.2), as summarized in Table 1 (entries 1–5).



As shown in Table 1, all ILs based on the imidazolium cation (entries 1–4) showed low product **3** conversions at 35 °C over 72 h reaction. Interestingly, no enantioselectivity was observed in [bmim][N(CN)₂] (entry 4), in which the enzymatic preparation was physically altered in the course of reaction. We observed that **2** was also poorly soluble in the majority of the ILs tested as well in

^aCQFM, Departamento de Engenharia Química e Biológica, Instituto Superior Técnico, 1049-001 Lisboa, Portugal.

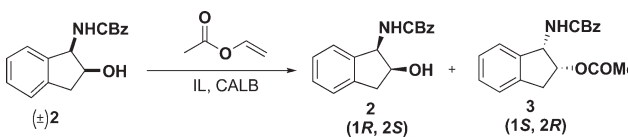
E-mail: carlosafonso@ist.utl.pt; Fax: + 351 21 8464455;

Tel: +351218417627

^bREQUIMTE, Departamento de Química, Faculdade de Ciências e Tecnologia, Universidade Nova de Lisboa, 2829-516 Caparica, Portugal

† Electronic supplementary information (ESI) available: Detailed experimental procedures, spectral data and pictures of sublimation apparatus. See DOI: 10.1039/b700406k

Table 1 Effect of different ionic liquids on the enzymatic resolution of (\pm)-*cis*-benzyl *N*-(1-hydroxyindan-2-yl)carbamate **2** using CALB (Novozym 435[®]) as biocatalyst



Entry ^a	Solvent	Temp./°C	Time/h	Conv. ^b (%)	ee ^c 2 (%)	ee ^d 3 (%)
1	[bmim][PF ₆] ^e	35	24	8	10	99
			72	19	20	85
2	[bmim][BF ₄] ^e	35	24	7	9	99
			72	12	14	99
3	[bmim][NTf ₂] ^e	35	24	5	5	90
			72	8	9	96
4	[bmim][N(CN) ₂] ^f	35	24	13	0	0
			72	19	<1	3
5	[aliqu][N(CN) ₂] ^f	35	24	36	42	77
			72	56	87	69
6	[aliqu][N(CN) ₂] ^f	35	96	61 (56)	94 (76)	60 (61)
7	[aliqu][N(CN) ₂] ^f	35	24	48	77	83
8	[aliqu][N(CN) ₂] ^f	25	24	31	43	98
			48	45	74	92
			72	53	90	80
9	[aliqu][N(CN) ₂] ^g	25	24	29	34	83
10	[aliqu][N(CN) ₂] ^f	25	60	48 (44)	80 (65)	88 (83)

^a All reactions were carried out in 0.5 ml solvent with 0.07 mmol of substrate, 10 eq. of vinyl acetate and 20 mg of CALB. For entries 7–10, reactions were carried out in 1 ml solvent with 0.36 mmol of substrate, 10 eq. of vinyl acetate and 100 mg of CALB. Results in brackets correspond to reactions with reused biocatalyst (entry 6) or with both reused IL and biocatalyst (entry 10). ^b Conversion determined by HPLC. ^c Optical purity of **2** determined by HPLC. ^d Optical purity of **3** calculated on the basis of the observed conversion and ee of **2** by HPLC. The calculated ee value is on average 4% lower than the ee observed for derived isolated product **2** (measured after hydrolysis). ^e Water activity of $a_w = 0.2$. ^f Water content of 3.3 μ g H₂O per μ L [aliqu][N(CN)₂]. ^g Water activity of $a_w = 0.2$ (6.1 μ g H₂O per μ L [aliqu][N(CN)₂]).

1,4-dioxane. We identified [aliqu][N(CN)₂] as the solvent in which the solubility of **2** was highest, making this IL a suitable alternative to organic media. In [aliqu][N(CN)₂], up to 56% conversion of enzymatic resolution was observed, with ee values of 87% and 69% for **2** and **3**, respectively (entry 5). Enzyme stability in this IL was

tested by performing two reactions at 35 °C over 4 days where the enzyme was reused (entry 6). The product **3** was obtained in 60% ee for the first run and in 61% ee for the second run at a conversion of 61% and 56%, respectively. These results demonstrates excellent enzyme stability in [aliqu][N(CN)₂].

As a result of further optimization of the reaction conditions, the concentration of the substrate was increased, temperature was decreased and water content in the ionic liquid was reduced (entries 7–10). Both reaction conversion and ee were found to depend on these three parameters. The use of high substrate concentration and lower water content led to an increase in reaction conversion (48% vs. 36% after 24 h, entry 7 vs. entry 5), and the ee values for both substrate and product increased as well (entry 7 vs. entry 5). The effect of temperature is consistent with the observation that this parameter can be a useful tool to modulate enzyme enantioselectivity.²⁹ The water content in reaction mixture is another important issue when enzymatic reactions are performed. At lower water contents, (where the ionic liquid is not equilibrated at $a_w = 0.2$) a higher ee was obtained (entry 8 vs. entry 9).

At optimal conditions, in the first and in the second cycle **3** was obtained in 48% conversion with 88% ee, and in 44% conversion with 83% ee, respectively (entry 10).

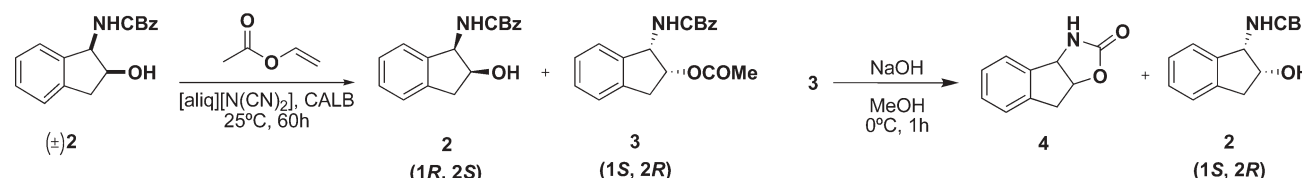
There is still no consensus on the use of ILs, mainly because of their cost and availability. However, in this case neither condition is applicable, since [aliqu][N(CN)₂] is readily obtained from a commercial source (Aliquat 336[®]) and at relatively lower cost than the imidazolium ILs.

By taking advantage of the IL being almost non-volatile,³¹ our main objective was to isolate the products directly from the IL by sublimation, as has already been demonstrated for the Fischer indole reaction.³² To this end, preparative-scale enzymatic reactions were performed, as shown in Table 2.

As before the effect of water content was noted. At lower water contents, better yields and ee were achieved (entry 1 vs. entry 2).

After 60 h of reaction, the products **2** and **3** can be directly recovered as a mixture from the IL by sublimation. After column separation, **3** was obtained in 36% yield (entry 3). The ee of **3** was assigned after basic hydrolysis to the corresponding alcohol **2** providing an ee of 92%. Nevertheless, another cyclization can occur during hydrolysis with the formation of side products.

Table 2 Preparative enzymatic resolution of (\pm)-*cis*-benzyl *N*-(1-hydroxyindan-2-yl)carbamate **2** using CALB (Novozym 435[®]) in [aliqu][N(CN)₂] at 25 °C for 60 h reaction time



Entry ^a	Time/h	Isolation method	Conv. (%)	Yield 2 (%)	ee ^b 2 (%)	Yield 3 (%)	ee ^c 3 (%)
1	24	Column	28	71	34	27	90
2	24	Column	31	67	40	28	97
3	60	Sublimation ^d	48	47 ^e	80	36	92
4 (reuse) ^f	60	Column	44	55	65	40	88

^a All reactions were carried out in 1 ml of [aliqu][N(CN)₂] (water content 3.3 μ g H₂O per μ L IL) using 0.36 mmol of substrate, 10 eq. of vinyl acetate and 100 mg CALB.³⁰ For entry 1, water content 6.1 μ g H₂O per μ L IL. ^b Optical purity of **2** determined by HPLC. ^c Optical purity of **3** determined by HPLC (measured after hydrolysis). ^d Sublimation under high vacuum (2 h, 130–140 °C, 3×10^{-5} mbar). ^e Isolated as a mixture of **2** (5%) and **4** (42%). ^f Experiment performed using enzyme recovered by filtration and the IL recovered after sublimation (entry 3).

Hydrolysis must be performed under low concentration of base, to prevent formation of the cyclic carbamate **4**, as shown in Table 2. Regardless of the substrate, **2** was isolated in 5% with an ee of 80%, this low yield is due to the cyclisation of substrate during sublimation, with formation of cyclic carbamate **4**. Since an efficient sublimation was achieved, the reaction medium was reused and a second cycle was performed under the same reaction conditions (25 °C, 60 h, entry 4). After column separation, **3** was collected in 40% yield and an ee of 88% was observed after hydrolysis to the corresponding alcohol.

In conclusion, we have demonstrated an efficient enzymatic resolution of Indinavir precursor **2** in [aliq][N(CN)₂], where the products can be easily recovered from the reaction medium by direct sublimation. This approach, that allows the reuse of the reaction medium (solvent and biocatalyst) and avoids the use of organic solvents in both reaction and separation processes, should be readily applied to other substrates that can also be removed from the IL by sublimation.

Acknowledgements

We thank Fundação para a Ciência e Tecnologia and FEDER (SFRH/BD/18487/2004; POCTI/QUE/35437/1999, POCI/QUI/57735/2004; POCTI/BIO/57193/04) for financial support.

Notes and references

- 1 T. A. Lyle, C. M. Wiscount, J. P. Guare, W. J. Thompson, P. S. Anderson, P. L. Darke, J. A. Zugay, E. A. Emini, W. A. Schleif, J. C. Quintero, R. A. F. Dixon, I. S. Sigal and J. R. Huff, *J. Med. Chem.*, 1991, **34**, 1228–1230.
- 2 J. P. Vacca, B. D. Dorsey, W. A. Schleif, R. B. Levin, S. L. McDaniel, P. L. Darke, J. Zugay, J. C. Quintero, O. M. Blahy, E. Roth, V. V. Sardana, A. J. Schlabach, P. I. Graham, J. H. Condra, L. Gotlib, M. K. Holloway, J. Lin, I. W. Chen, K. Vastag, D. Ostovic, P. S. Anderson, E. A. Emini and J. R. Huff, *Proc. Natl. Acad. Sci. U. S. A.*, 1994, **91**, 4096–4100.
- 3 K. Izawa and T. Onishi, *Chem. Rev.*, 2006, **106**, 2811–2827.
- 4 J. K. Ekegren, N. Ginman, A. Johansson, H. Wallberg, M. Larhed, B. Samuelsson, T. Unge and A. Hallberg, *J. Med. Chem.*, 2006, **49**, 1828–1832.
- 5 A. B. Smith, A. K. Charnley, H. Harada, J. J. Beiger, L. D. Cantin, C. S. Kenesky, R. Hirschmann, S. Munshi, D. B. Olsen, M. W. Stahlhut, W. A. Schleif and L. C. Kuo, *Bioorg. Med. Chem. Lett.*, 2006, **16**, 859–863.
- 6 A. G. Myers, J. K. Barbay and B. Y. Zhong, *J. Am. Chem. Soc.*, 2001, **123**, 7207–7219.
- 7 M. Rouquayrol, W. Gaucher, J. Greiner, A. M. Aubertin, P. Vierling and R. Guedj, *Carbohydr. Res.*, 2001, **336**, 161–180.
- 8 A. K. Ghosh, S. Fidanze and C. H. Senanayake, *Synthesis*, 1998, 937–961.
- 9 L. Lin, Q. Fan, B. Qin and X. Feng, *J. Org. Chem.*, 2006, **71**, 4141–4146.
- 10 R. V. Wisman, J. G. de Vries, B. J. Deelman and H. J. Heeres, *Org. Process Res. Dev.*, 2006, **10**, 423–429.
- 11 H. Takikawa, Y. Hachisu, J. W. Bode and K. Suzuki, *Angew. Chem., Int. Ed.*, 2006, **45**, 3492–3494.
- 12 I. Gallou and C. H. Senanayake, *Chem. Rev.*, 2006, **106**, 2843–2874.
- 13 R. N. Patel, *Food Technol. Biotechnol.*, 2004, **42**, 305–325.
- 14 M. Breuer, K. Ditrich, T. Habicher, B. Hauer, M. Kessler, R. Sturmer and T. Zelinski, *Angew. Chem., Int. Ed.*, 2004, **43**, 788–824.
- 15 C. H. Senanayake, G. B. Smith, K. M. Ryan, L. E. Fredenburgh, J. Liu, F. E. Roberts, D. L. Hughes, R. D. Larsen, T. R. Verhoeven and P. J. Reider, *Tetrahedron Lett.*, 1996, **37**, 3271–3274.
- 16 A. Mitrochkine, F. Eydoux, M. Martres, G. Gil, A. Heumann and M. Reglier, *Tetrahedron: Asymmetry*, 1995, **6**, 59–62.
- 17 R. N. Patel, K. Ogasawara, *Synthesis*, 1996, 954–958.
- 18 A. K. Ghosh, J. F. Kincaid and M. G. Haske, *Synthesis*, 1997, 541–544.
- 19 Y. Igarashi, S. Otsutomo, M. Harada and S. Nakano, *Tetrahedron: Asymmetry*, 1997, **8**, 2833–2837.
- 20 Y. Igarashi, S. Otsutomo, M. Harada, S. Nakano and S. Watanabe, *Synthesis*, 1997, 549–552.
- 21 A. Luna, A. Maestro, C. Astorga and V. Gotor, *Tetrahedron: Asymmetry*, 1999, **10**, 1969–1977.
- 22 S. Nakano, Y. Igarashi and H. Nohira, *Tetrahedron: Asymmetry*, 2001, **12**, 59–62.
- 23 A. T. Anilkumar, K. Goto, T. Takahashi, K. Ishizaki and H. Kaga, *Tetrahedron: Asymmetry*, 1999, **10**, 2501–2503.
- 24 C. Laane, S. Boeren, K. Vos and C. Veeger, *Biotechnol. Bioeng.*, 1987, **30**, 81–87.
- 25 F. van Rantwijk, R. M. Lau and R. A. Sheldon, *Trends Biotechnol.*, 2003, **21**, 131–138.
- 26 S. Park and R. J. Kazlauskas, *Curr. Opin. Biotechnol.*, 2003, **14**, 432–437.
- 27 U. Kragl, M. Eckstein and N. Kaftzik, *Curr. Opin. Biotechnol.*, 2002, **13**, 565–571.
- 28 S. Garcia, N. M. T. Lourenco, D. Lousa, A. F. Sequeira, P. Mimoso, J. M. S. Cabral, C. A. M. Afonso and S. Barreiros, *Green Chem.*, 2004, **6**, 466–470.
- 29 T. Sakai, *Tetrahedron: Asymmetry*, 2004, **15**, 2749–2756.
- 30 To a stirred solution of (±)-*cis*-benzyl *N*-(1-hydroxyindan-2-yl)carbamate, (±)-**2**, (100 mg, 0.36 mmol) in 1 mL of [aliq][N(CN)₂] (water content: 3.3 µg H₂O per µL ionic liquid) at 25 °C in a thermostatic bath was added Novozyme 435[®] (100 mg) and vinyl acetate (35.5 mmol, 327 µL). The reaction was left running for 60 h, after which the enzyme was filtered off and washed with Et₂O (10 mL). The reaction mixture was submitted to sublimation under high vacuum provided with a diffusion pump (2h, 130–140 °C, 3 × 10^{−5} mbar), giving a mixture of compounds (Figure ESI-1†) that were further purified by flash column chromatography.
- 31 M. J. Earle, J. Esperanca, M. A. Gilea, J. N. C. Lopes, L. P. N. Rebelo, J. W. Magee, K. R. Seddon and J. A. Widegren, *Nature*, 2006, **439**, 831–834.
- 32 R. C. Morales, V. Tambyrajah, P. R. Jenkins, D. L. Davies and A. P. Abbott, *Chem. Commun.*, 2004, 158–159.

Functionalized chiral ionic liquid as recyclable organocatalyst for asymmetric Michael addition to nitrostyrenes†

Bukuo Ni, Qianying Zhang and Allan D. Headley*

Received 9th February 2007, Accepted 1st March 2007

First published as an Advance Article on the web 9th March 2007

DOI: 10.1039/b702081c

A new type of pyrrolidine-based chiral ionic liquid has been developed. This chiral ionic liquid was found to catalyze the Michael addition reaction of aldehydes and nitrostyrenes to give moderate yields, good enantioselectivities, high diastereoselectivities, and recyclability.

During the past decade, room temperature ionic liquids (RTILs) have received considerable attention due to their ability to serve as effective reaction media for a wide variety of organic reactions and other applications in chemistry.¹ By modifying the structures of the cations or anions of ionic liquids, it has been shown that their properties can be altered to influence the outcomes of reactions.

Ionic liquids that contain specific functionalities and are capable of carrying out specific tasks have received considerable attention. There have been a limited number of task-specific ionic liquids that have been designed and synthesized that are capable of controlling the outcomes of asymmetric organic reactions.² Task-specific ionic liquids have shown limited success when used as solvents for reactions, such as the Baylis–Hillman reaction,³ the enantioselective photoisomerisation,⁴ Michael additions,⁵ and Heck oxyarylation.⁶ Most task-specific ionic liquids that are capable of influencing the outcomes of asymmetric reactions contain the proline moiety. It is well known that pyrrolidine-based catalytic systems have been very effective for asymmetric Michael addition reactions, often yielding high enantioselectivities.⁷ The pyrrolidine structure of these compounds is now regarded as one of the essential backbones for asymmetric catalysis and has been incorporated into the design of task-specific ionic liquids, examples are shown in Fig. 1 (I–III).⁸

It appears that the presence of an acidic hydrogen is essential for the activity and selectivity of proline derived catalysts; for example, reactions in which II is used as the catalyst, poor yields were obtained, compared to yields observed when III is used. For reactions involving II, an acid, such as trifluoroacetic acid, is typically added in order to improve enantioselectivities.

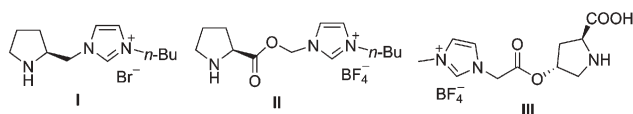


Fig. 1 The known chiral ionic liquids.

Department of Chemistry, Texas A&M University-Commerce, Commerce, TX, 75429-3011, USA.

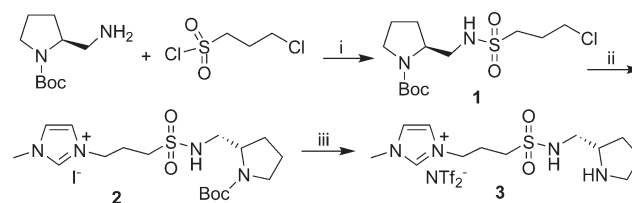
E-mail: allan_headley@tamu-commerce.edu

† Electronic supplementary information (ESI) available: Experimental details and compound characterisation. See DOI: 10.1039/b702081c

One aspect of our research involves the design and synthesis of functionalized chiral RTILs that exhibit the ability to form hydrogen bonds with reactants and intermediates in an effort to influence the outcomes of asymmetric reactions.⁹ In this study, we report the design, synthesis, characterization, and application of a new type of task-specific ionic liquid, which is derived from proline and contains an acidic hydrogen. Catalyst 3, shown in Scheme 1, contains a fairly acidic N–H hydrogen; its acidity is due to the presence of the adjacent electron-withdrawing group. Thus, our functionalized ionic liquid, not only introduces a chiral pyrrolidine moiety into an imidazolium ionic liquid, but also includes a protonic functionality. A major advantage of our current design is that this functionalized IL can not only serve as organocatalyst, but also is easily recovered from the reaction mixture, making it a recyclable green ionic liquid.

Scheme 1 shows the synthesis of the pyrrolidine-based chiral imidazolium ionic liquid 3. The reaction of 3-chloropropanesulfonyl chloride with (S)-2-amino-1-N-Boc-pyrrolidine¹⁰ provided 1, which was converted to imidazolium iodide 2 in 86% overall yield via two steps, involving iodation with NaI and alkylation of the corresponding pyrrolidine sulfonamide with 1-methylimidazole in CH₃CN. The chiral ionic liquid (CIL) 3 was obtained by removal of the Boc group, followed by anion exchange with NTf₂ in 88% overall yield.

Catalyst 3 was next used as an organocatalyst for a series of asymmetric Michael addition reaction of aldehydes with nitroolefins. The organocatalytic direct asymmetric Michael reaction has been recognized as one of the most powerful carbon–carbon bond-forming reactions in modern organic synthesis, and has been explored intensively in recent years.¹¹ The reactions of ketones and aldehydes as nucleophiles with nitroolefins are catalyzed by proline and their derivatives, such as pyrrolidine-pyridine,¹² aminomethylpyrrolidine,¹³ 2,2'-bipyrrolidine,¹⁴ and pyrrolidinylerazole,¹⁵ with high diastereoselectivities and enantioselectivities. Very recently, Tang reported a pyrrolidine-thiourea as



Scheme 1 Synthesis of chiral ionic liquid 3. Reaction conditions: (i) Et₃N, CH₂Cl₂, 72%; (ii) (1) NaI, acetone, 96%; (2) 1-methylimidazole, CH₃CN; 86% for 2 steps; (iii) (1) CF₃COOH, CH₂Cl₂; (2) LiNTf₂, H₂O; 88% for 2 steps.

a highly diastereo- and enantioselective catalyst for Michael reactions of ketones with nitroolefins.^{7b} Wang *et al.*^{7a} and Hayashi *et al.*¹⁶ independently reported remarkably effective catalysts for asymmetric Michael reaction of aldehydes. However, all organocatalysts reported to date for asymmetric Michael reactions are not easily recycled. The development of new effective asymmetric organocatalysts for Michael reaction while facilitating catalyst recovery and reuse remains a challenging task.^{8a,17}

Initially, the Michael reaction of isobutyraldehyde and nitrostyrene in various solvents was examined at room temperature using CIL **3** as organocatalyst; the results are shown in Table 1. In polar solvents, such as MeOH and *i*-PrOH, the reaction proceeds smoothly and gave the desired Michael adduct **4a** in good yields (62–80%) and enantioselectivities (66–67% ee) (Table 1, entries 1–2). Using CH₃CN as a solvent resulted in a poor yield and similar enantioselectivity (Table 1, entry 3). Higher enantioselectivities (74–78% ee) were observed in solvent-free conditions or by using THF and CH₂Cl₂ as solvents, but the yields were poor (Table 1, entries 4–6). The addition of a catalytic amount of organic acid or using ethyl acetate as solvent did not enhance the yields (Table 1, entries 7–9). However, when the less polar solvents Et₂O and CHCl₃ were used in conjunction with IL **3**, the Michael addition adduct was afforded in moderate yields (43–52%) and good enantioselectivities (76–78% ee) (Table 1, entries 10–11). Moreover, at a lower temperature (4 °C), the adduct **4a** was obtained in 82% ee and 58% yield (Table 1, entry 12).¹⁸ In addition, catalyst **3** could be recycled twice without losing its activity and enantioselectivity (Table 1, entries 13–14).

As a result of the observations from Table 1, the reaction conditions of entry 12 were chosen to study the application of CIL **3** to the Michael addition reaction. The asymmetric Michael addition reaction with a series of aldehydes and nitrostyrenes under the catalysis of CIL **3** was investigated and the results are shown in Table 2. As demonstrated in Table 2, all aldehydes can undergo Michael reactions with different aryl-substituted nitrostyrenes in the presence of 20 mol% of **3** in Et₂O at 4 °C,

Table 2 Michael addition reactions of aldehydes to *trans*-nitrostyrenes catalyzed by **3**

Ar		H		catalyst 3 (20%)		4 °C, Et ₂ O, 6d		H		Ar	
NO ₂		R ₁						R ₁		R ₂	
Entry	Product	Yield (%) ^a		ee (%) ^b		dr (<i>syn</i> / <i>anti</i>) ^c					
1		58		82		—					
2		64		68		97 : 3					
3		60		67		96 : 4					
4		29 (85) ^d		67		92 : 8					
5		53		66		96 : 4					
6		64		73		97 : 3					
7		49 (87) ^d		64		89 : 11					
8		38 (90) ^d		68		96 : 4					
9 ^e		38 (88) ^d		88		95 : 5					

^a Yield of isolated product. ^b the ee values were determined by HPLC analysis on a chiral phase (chiralpak AS-H, AD, and chiralcel OD-H). ^c Determined by ¹H NMR spectroscopy (400 MHz). ^d Yield based on recovery of nitrostyrene. ^e the reaction was carried out in CH₃CN at room temperature.

Table 1 Optimization of the reaction conditions

Ph		H		catalyst 3 (20%)		solvent, 6 d		H		Ph	
NO ₂		R ₁						R ₁		R ₂	
Entry	Solvent	Additive	T	Yield (%) ^a		ee (%) ^b					
1	MeOH	—	rt	80		67					
2	<i>i</i> -PrOH	—	rt	62		66					
3	CH ₃ CN	—	rt	22		68					
4	neat	—	rt	22		74					
5	THF	—	rt	17		75					
6	DCM	—	rt	34		77					
7	THF	TsOH	rt	<10		— ^c					
8	DCM	TsOH	rt	<10		— ^c					
9	EtOAc	—	rt	<5		— ^c					
10	Et ₂ O	—	rt	52		78					
11	CHCl ₃	—	rt	43		76					
12	Et ₂ O	—	4 °C	58		82					
13	Et ₂ O	—	4 °C	57		81 ^d					
14	Et ₂ O	—	4 °C	55		82 ^e					

^a Yield of isolated product. ^b Determined by chiral HPLC analysis (chiralpak AS-H). ^c Not determined. ^d Second cycle of **3**. ^e Third cycle of **3**.

giving the corresponding Michael adducts **4b–h** in moderate yields (29–64%), good enantioselectivities (64–82% ee), and high diastereoselectivities (*syn*/*anti* ratio up to 97 : 3). Typically, substituents on aryl groups slightly influenced the diastereoselectivities and enantioselectivities as well as the yields. For example, nitrostyrenes bearing H used in the reaction with branched aldehyde isovaleraldehyde gave the desired product **4e** with moderate yield, enantioselectivity, and high diastereoselectivity (Table 2, entry 5), while the reaction of *trans*-4-methyl-β-nitrostyrene with isovaleraldehyde afforded adduct **4f** with an increased yield (64%) and enantioselectivity (73%) (Table 2, entry 6). The linear aldehyde *n*-pentanal and *n*-hexanal can serve as the Michael donor to produce the desired adducts **4b–d** and **4g–h** in moderate yields (29–64%) and enantioselectivities (64–68% ee) and high diastereoselectivities (*syn* : *anti* ratio up to 97 : 3) (Table 2,

entries 2–4 and 7–8). The reaction involving the asymmetric Michael addition of a ketone and nitrostyrene using CIL **3** as catalyst was also investigated. The reaction of cyclohexanone and *trans*- β -nitrostyrene in CH₃CN at room temperature gave the adduct **4i** in moderate yield and high selectivities (88% ee, *syn* : *anti* = 95 : 5) (Table 2, entry 9).

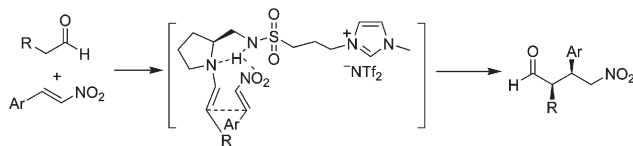


Fig. 2 Mechanism for the Michael addition using catalyst **3**.

As shown in Tables 1 and 2, modest yields were observed for the reactions, with good enantioselectivities. A possible mechanism to explain the results for the Michael addition is shown in Fig. 2. Based on the L-proline catalyst model, it is obvious that the N–H acidic hydrogen plays an important role in the reaction by forming hydrogen bonds to the nitrostyrene substrate in a manner that C–C bond formation would take place by the preferential enamine addition to the less hindered *Si* face of the nitrostyrene.^{7a} In addition, pyrrolidine-sulfonamide-based CIL **3**, being a bifunctional catalyst, is expected to stabilize the transition state and make the selectivity possible.

In summary, we have developed a new type of task-specific ionic liquid, which is capable of catalyzing Michael addition reaction of aldehydes and nitrostyrenes with moderate yields (up to 64%), good enantioselectivities (up to 82% ee), and high diastereoselectivities (*syn/anti* ratio up to 97 : 3). Apparently, the acidic N–H adjacent to the electron-withdrawing sulfonyl group plays an important role in the selectivity of the reaction. The newly designed ionic liquid tethered chiral pyrrolidine catalyst can be easily recycled without loss of activity. The design of similar catalysts, which influence the outcomes of asymmetric reactions is underway in our laboratory.

Acknowledgements

This work was supported by the Robert A. Welch Foundation (T-1460). We thank Mahsa Fardin, Jeffery Sun, and Carlos Kee for their assistance.

Notes and references

- For selective reviews see: (a) T. Welton, *Chem. Rev.*, 1999, **99**, 2071; (b) J. Dupont, R. F. de Souza and P. A. Z. Suarez, *Chem. Rev.*, 2002, **102**, 3667; (c) R. D. Rogers, K. R. Seddon and S. Volkov, *Green Industrial Applications of Ionic Liquids*, Kluwer Academic, Dordrecht, 2002; (d) J. Levillain, D. Cahard, A.-C. Gaumont and J. C. Plaquevent, *Tetrahedron: Asymmetry*, 2003, **14**, 3081.
- (a) J. Ding and D. W. Armstrong, *Chirality*, 2005, **17**, 281 and references cited therein; (b) C. Baudequin, D. Bérgeon, J. Levillain,

- Guillen, J.-C. Plaquevent and A.-C. Gaumont, *Tetrahedron: Asymmetry*, 2005, **16**, 3921; (c) R. Gausepohl, P. Buskens, J. Kleinen, A. Bruckmann, C. W. Lehmann, J. Klankermayer and W. Leitner, *Angew. Chem., Int. Ed.*, 2006, **45**, 3689; (d) S. T. Handy, *Chem.-Eur. J.*, 2003, **9**, 2938.
- B. Pégot, G. Vo-Thanh, D. Gori and A. Loupy, *Tetrahedron Lett.*, 2004, **45**, 6425.
- J. Ding, V. Desikan, X. Han, T. L. Xiao, R. Ding, W. S. Jenks and D. W. Armstrong, *Org. Lett.*, 2005, **7**, 335.
- Z. Wang, Q. Wang, Y. Zhang and W. Bao, *Tetrahedron Lett.*, 2005, **46**, 4657.
- L. Kiss, T. Kurtan, S. Antus and H. Brunner, *Arkivoc*, 2003, **5**, 69.
- (a) W. Wang, J. Wang and H. Li, *Angew. Chem., Int. Ed.*, 2005, **44**, 1369; (b) C.-L. Cao, M.-C. Ye, X.-L. Sun and Y. Tang, *Org. Lett.*, 2006, **8**, 2901.
- (a) S. Luo, X. Mi, L. Zhang, S. Liu, H. Xu and J.-P. Cheng, *Angew. Chem., Int. Ed.*, 2006, **45**, 3093; (b) W. Miao and T. H. Chan, *Adv. Synth. Catal.*, 2006, **348**, 1711.
- (a) B. Ni, A. D. Headley and G. Li, *J. Org. Chem.*, 2005, **70**, 10600; (b) B. Ni and A. D. Headley, *Tetrahedron Lett.*, 2006, **47**, 7331; (c) B. Ni, Q. Zhang and A. D. Headley, *J. Org. Chem.*, 2006, **71**, 9857; (d) B. Ni, S. Garre and A. D. Headley, *Tetrahedron Lett.*, 2007, **48**, 1999.
- N. Dahlin, A. Bøgevig and H. Adolfsson, *Adv. Synth. Catal.*, 2004, **346**, 1101.
- For selected reviews regarding of organocatalysis, see: (a) B. List, *Acc. Chem. Res.*, 2004, **37**, 548; (b) P. I. Dalko and L. Moisan, *Angew. Chem., Int. Ed.*, 2004, **43**, 5138; (c) W. Notz, F. Tanaka and C. F. Barbas, III, *Acc. Chem. Res.*, 2004, **37**, 580; (d) J. Seayad and B. List, *Org. Biomol. Chem.*, 2005, **3**, 719.
- T. Ishii, S. Fujioka, Y. Sekiguchi and H. Kotsuki, *J. Am. Chem. Soc.*, 2004, **126**, 9558.
- (a) N. Mase, R. Thayumanavan, F. Tanaka and C. F. Barbas, III, *Org. Lett.*, 2004, **6**, 2527; (b) J. M. Betancort, K. Sakthivel, R. Thayumanavan, F. Tanaka and C. F. Barbas, III, *Synthesis*, 2004, 1509.
- (a) A. Alexakis and O. Andrey, *Org. Lett.*, 2002, **4**, 3611; (b) O. Andrey, A. Vidonne and A. Alexakis, *Tetrahedron Lett.*, 2003, **44**, 7901; (c) O. Andrey, A. Alexakis, A. Tomassini and G. Bernardinelli, *Adv. Synth. Catal.*, 2004, **346**, 1147.
- (a) A. J. A. Cobb, D. A. Longbottom, D. M. Shaw and S. V. Ley, *Chem. Commun.*, 2004, 1808; (b) A. J. A. Cobb, D. M. Shaw, D. A. Longbottom, J. B. Gold and S. V. Ley, *Org. Biomol. Chem.*, 2005, **3**, 84.
- Y. Hayashi, H. Gotoh, T. Hayashi and M. Shoji, *Angew. Chem., Int. Ed.*, 2005, **44**, 4212.
- L. Zu, J. Wang, H. Li and W. Wang, *Org. Lett.*, 2006, **8**, 3077.
- Typical experimental procedure for Michael addition reaction. Synthesis of (*R*)-2,2-Dimethyl-4-nitrophenylbutanal **4a**: the catalyst CIL **3** (23 mg, 0.04 mmol) was added to a solution of isobutyraldehyde in Et₂O (1 mL) at 4 °C. The mixture was stirred for 20 min, and then *trans*- β -nitrostyrene (30 mg, 0.2 mmol) was added. After stirring at 4 °C for 6 d, the reaction mixture was diluted with Et₂O (10 mL) to precipitate the catalyst. The organic layer was separated and purified by flash chromatography on silica gel (hexane : ethyl acetate = 5 : 1) to afford the Michael adduct **4a** (26 mg, 58%) as a colorless oil. The catalyst was used directly for the next run after drying. $[\alpha]_D^{20} = -15.0$ deg cm³ g⁻¹ dm⁻¹ (*c* = 0.01, CH₂Cl₂); ¹H NMR (300 MHz, CDCl₃) δ 9.50 (s, 1H), 7.40–7.15 (m, 5H), 4.83 (dd, *J* = 13.0 and 11.4 Hz, 1H), 4.67 (dd, *J* = 13.0 and 4.0 Hz, 1H), 3.76 (dd, *J* = 11.4 and 4.0 Hz, 1H), 1.11 (s, 3H), 0.98 (s, 3H); ¹³C NMR (75 MHz, CDCl₃) δ 204.2, 135.3, 129.0, 128.7, 128.1, 76.3, 48.4, 48.2, 21.6, 18.8; HPLC (Chiralpak AS-H, i-Propanol–Hexane = 5/95, flow rate 0.5 mL min⁻¹, λ = 238 nm): *t*_{minor} = 33.1 min, *t*_{major} = 34.5 min; ee = 82%.

PEG-assisted solvent and catalyst free synthesis of 3,4-dihydropyrimidinones under mild reaction conditions

Suman L. Jain, Sweetly Singhal and Bir Sain*

Received 13th February 2007, Accepted 6th March 2007

First published as an Advance Article on the web 20th March 2007

DOI: 10.1039/b702311a

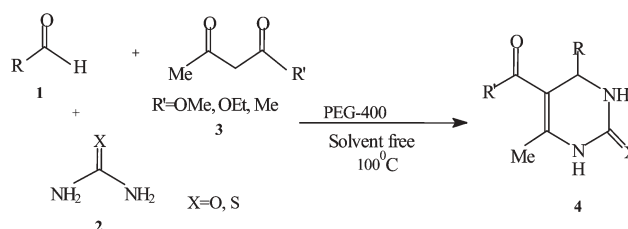
PEG-assisted solvent and catalyst free synthesis of 3,4-dihydropyrimidinones under mild and neutral reaction conditions is described.

In the recent years development of environmentally friendly chemical synthesis is gaining considerable interest both in academia and industrial research.¹ In this context, the replacement of toxic and volatile organic solvents as reaction media with environmentally acceptable alternatives such as water, ionic liquids and PEG and carrying out organic reactions under solvent-free conditions is an area of tremendous importance in modern organic synthesis.² 3,4-Dihydropyrimidinones, denoted as Biginelli compounds, and their derivatives are highly important heterocyclic units in the realm of natural and synthetic organic chemistry that possess diverse therapeutic and pharmacological properties, including anti-viral, anti-tumor, anti-bacterial and anti-inflammatory activities.³ Furthermore, these compounds have emerged as calcium channel blockers, anti-hypertensive agents and α -1a-adrenergic antagonists. Also, several alkaloids containing the dihydropyrimidine nucleus isolated from marine sources have been found to possess interesting biological activities.⁴ Owing to the wide range of pharmacological and biological activities, the synthesis of these compounds has become an important target in current years. The Biginelli reaction, first reported in 1893, is a direct and simple approach for the synthesis of 3,4-dihydropyrimidinones by one-pot cyclocondensation of ethyl acetoacetate, benzaldehyde and urea in the presence of strong acid.⁵ However, one serious drawback of this method is the low yield of the product, particularly in case of substituted aromatic and aliphatic aldehydes.⁶ This has led to the development of multistep syntheses of Biginelli compounds that produce higher yields, albeit lacking the simplicity of the one pot synthesis. Thus, the Biginelli reaction involving one step cyclocondensation for the synthesis of dihydropyrimidinones has received renewed interest, and several improved protocols, mainly using Lewis acids as well as protic acids, have been developed for accomplishing this reaction.⁷ Nevertheless, use of toxic organic solvents, expensive catalysts and harsh reaction conditions in these protocols leaves scope for further development of new environmentally clean syntheses. Very recently, Deng *et al.*⁸ reported an efficient ionic liquid catalyzed Biginelli reaction using [bmim]BF₄ and [bmim]PF₆ as catalysts under solvent-free conditions. However, ionic liquids especially imidazolium based systems containing PF₆ and BF₄ anions are toxic in nature as they liberate hazardous HF, and their high cost and disposability make their utility limited.⁹ Polyethylene glycol

and their monomethyl ethers are inexpensive, thermally stable, non-toxic, recyclable and find wide applications as media for phase transfer catalysts.¹⁰ However, their potential as reaction media and promoter for organic reaction does not appear to have been explored much. Recently, Wang *et al.*¹¹ have described a microwave assisted synthesis of 3,4-dihydropyrimidinones using PEG-SO₃H as catalyst and solvent. In continuation of our studies on developing improved methodologies for organic reactions, we reveal herein for the first time a PEG-assisted solvent and catalyst free synthesis of 3,4-dihydropyrimidinones under neutral reaction conditions (Scheme 1).

In a typical experimental procedure, a mixture containing aldehyde **1** (2 mmol), urea **2** (2 mmol), β -dicarbonyl compound **3** (2 mmol) and PEG (0.2 g) was heated at 100 °C for 45 min. After cooling at room temperature the reaction mixture was poured into water, the solid product thus obtained was filtered and recrystallized.¹² A variety of aldehydes, β -dicarbonyl compounds and ureas were reacted under these reaction conditions to afford corresponding 3,4-dihydropyrimidinones **4**. These results are presented in Table 1. A variety of heterocyclic, aliphatic and aromatic aldehydes both containing electron donating and withdrawing groups were smoothly converted to their corresponding 3,4-dihydropyrimidinones in excellent yields. Both β -ketoesters (ethyl and methylacetoacetate) and 1,3-dicarbonyl compound (acetylacetone) smoothly reacted under these reaction conditions. Further, the use of thiourea instead of urea gave corresponding 3,4-dihydropyrimidinones-2(1H)-thiones in comparable yields (Table 1, entries 18–22). All the products were characterized by comparing their physical and spectral (IR and ¹H NMR) data with those of authentic compounds reported in literature. Use of 0.2 g of PEG at 100 °C under these reaction conditions was found to be sufficient for optimum yields of the desired products and an increase in its amount did not improve the yields.

To evaluate the effect of PEG, a mixture of benzaldehyde, urea and ethylacetoacetate in molar ratio (1 : 1 : 1) was heated at 100 °C for 1 h in the absence of PEG. It was found that reaction did not proceed, indicating PEG to be an essential promoter for this



Scheme 1

Chemical and Biotechnology Division, Indian Institute of Petroleum, Dehradun, 248005, India

Table 1 PEG-promoted synthesis of 3,4-dihydropyrimidinones under solvent-free conditions^a

Entry	Product	R	R'	X	Yield (%) ^b
1	4a	C ₆ H ₅	OEt	O	98
2	4b	4-CH ₃ C ₆ H ₄	OEt	O	96
3	4c	4-CH ₃ OC ₆ H ₄	OEt	O	96
4	4d	4-NO ₂ C ₆ H ₄	OEt	O	95
5	4e	4-ClC ₆ H ₄	OEt	O	97
6	4f	2-ClC ₆ H ₄	OEt	O	94
7	4g	2-Pyridyl	OEt	O	86
8	4h	2-Furyl	OEt	O	90
9	4i	<i>n</i> -CH ₃ CH ₂ CH ₂	OEt	O	92
10	4j	(CH ₃) ₂ CH	OEt	O	94
11	4k	<i>n</i> -CH ₃ (CH ₂) ₂ CH ₂	OEt	O	94
12	4l	C ₆ H ₅ CH=CH	OEt	O	90
13	4m	C ₆ H ₅	OMe	O	96
14	4n	4-NO ₂ C ₆ H ₄	OMe	O	92
15	4o	4-CH ₃ OC ₆ H ₄	CH ₃	O	90
16	4p	4-ClC ₆ H ₄	CH ₃	O	92
17	4q	C ₆ H ₅	CH ₃	O	94
18	4r	C ₆ H ₅	OEt	S	98
19	4s	4-CH ₃ C ₆ H ₄	OEt	S	96
20	4t	4-NO ₂ C ₆ H ₄	OEt	S	94
21	4u	<i>n</i> -CH ₃ CH ₂ CH ₂	OEt	S	90
22	4v	2-Furyl	OEt	S	89

^a Reaction conditions: aldehyde (2 mmol), urea/thiourea (2 mmol), β-dicarbonyl compound (2 mmol), PEG-400 (0.2 g) at 100 °C for 45 min. ^b Isolated yields.

Table 2 Effect of various solvents^a

Entry	Solvent	Reaction time/min	Yields (%) ^b
1	Acetonitrile	60	80
2	Toluene	60	70
3	Water	60	50
4	Neat	45	98 ^c

^a Reaction conditions: benzaldehyde (2 mmol), urea (2 mmol), ethyl acetoacetate (2 mmol), PEG-400 (0.2 g), solvent (1 ml) under refluxing condition. ^b Isolated yields. ^c Reaction conditions as in Table 1.

reaction. We also studied the PEG promoted Biginelli condensation of benzaldehyde, urea and ethylacetoacetate in the presence of various solvents, such as water, acetonitrile, and toluene (1 ml). These results are presented in Table 2. However, in the presence of these additional solvents, the yields of 3,4-dihydropyrimidinone were found to be comparatively lower, probably due to the reduced efficiency of PEG because of dilution. The reaction did not proceed in the presence of acetonitrile or toluene (0.2 ml) without PEG-400. However, in water (0.2 ml), the reaction did proceed but the yields obtained remained low even after longer reaction times (3 h).

The mechanism for Biginelli condensation is well explored in the literature.¹³ The exact role played by PEG in this reaction remains unclear and should be further explored.

In the present procedure PEG, a cheap, cost effective, eco-friendly reagent, is employed as a promoter, without the aid of any co-solvent and precautions, for the Biginelli reaction.

In summary, we have described the first example of the use of PEG-400 as a promoter for the synthesis of 3,4-dihydropyrimidinones under mild and neutral solvent-free conditions. This procedure offers several advantages, such as (i) PEG is a cost

effective and environmentally benign reagent, (ii) green synthesis (avoiding hazardous and toxic organic solvents for work up) and (iii) applicability to a wide range of substituted aldehydes. Furthermore, better yields, simple reaction conditions, shorter reaction times and easy work up make this a green, facile and superior method for the synthesis of 3,4-dihydropyrimidinones.

We are grateful to the Director, IIP for his kind permission to publish these results. Suman L. Jain and Sweetly Singhal are thankful to CSIR, New Delhi for the award of Research Fellowships.

Notes and references

- (a) P. T. Anastas and J. C. Warner, *Green Chemistry, Theory and Practice*, Oxford University Press, Oxford, 1998; (b) J. Clark, D. M. A. Macquarrie, *Handbook of Green Chemistry & Technology*, Blackwell, Oxford, 2002.
- (a) *Green Reaction Media for Organic Synthesis*, ed. M. Kochi, Blackwell, Oxford, 2005; (b) T. Welton, *Chem. Rev.*, 1999, **99**, 2071; (c) P. Wasserscheid and W. Keim, *Angew. Chem., Int. Ed.*, 2000, **39**, 3772; (d) R. Sheldon, *Chem. Commun.*, 2001, 2399; (e) P. A. Grieco, *Organic Synthesis in Water*, Blackie Academic and Professional, London, 1998; (f) R. Breslow, *Acc. Chem. Res.*, 1991, **24**, 159; (g) S. Chandrasekar, C. Narsihmulu, S. S. Shameem and N. R. Reddy, *Chem. Commun.*, 2003, 1716; (h) K. Tanemura, T. Suzuki, Y. Nishida and T. Horaguchi, *Chem. Lett.*, 2005, **34**, 576.
- (a) C. O. Kappe, *Tetrahedron*, 1993, **43**, 6937; (b) C. O. Kappe, *Acc. Chem. Res.*, 2000, **33**, 879; (c) C. O. Kappe, *Eur. J. Med. Chem.*, 2000, **35**, 1043.
- (a) K. S. Atwal, G. C. Rovnyak, S. D. Kimball, D. M. Floyd, S. Moreland, B. N. Swanson, J. Z. Gougoutas, J. Schwartz, K. M. Smillie and M. F. Malley, *J. Med. Chem.*, 1990, **33**, 2629; (b) K. S. Atwal, B. N. Swanson, S. E. Unger, D. M. Floyd, S. Moreland, A. Hedberg and B. C. O'Reilly, *J. Med. Chem.*, 1991, **34**, 806; (c) H. Cho, M. Ueda, K. Shima, A. Mizuno, M. Hayashimatu, Y. Ohnaka, Y. Takechi, M. Hamaguchi, K. Aisaka, T. Hidaka, M. Kawai, M. Takeda, T. Ishihara, K. Funahashi, F. Satah, M. Morita and T. Noguchi, *J. Med. Chem.*, 1989, **32**, 2399.
- P. Biginelli, *Gazz. Chim. Ital.*, 1893, **23**, 360.
- J. Barleunga, M. Tomas, A. Ballesteros and L. A. Lopez, *Tetrahedron Lett.*, 1989, **30**, 4573.
- (a) C. V. Reddy, M. Mahesh, P. V. K. Raju, T. R. Babu and V. V. N. Reddy, *Tetrahedron Lett.*, 2002, **43**, 2657; (b) K. Ramalinga, P. Vijayalakshmi and T. N. B. Kaimal, *Synlett*, 2001, 1341; (c) F. Bigi, S. Carloni, B. Frullanti, R. Maggi and G. Sartori, *Tetrahedron Lett.*, 1999, **40**, 3465; (d) J. S. Yadav, B. V. S. Reddy, E. J. Reddy and T. Ramalingam, *J. Chem. Res.*, 2000, S354.
- J. Peng and Y. Deng, *Tetrahedron Lett.*, 2001, **42**, 5917–5919.
- A. Kamal, D. R. Reddy and Rajendar, *Tetrahedron Lett.*, 2005, **46**, 7951.
- (a) V. N. Vasudevan and S. V. Rajender, *Green Chem.*, 2001, **3**, 146; (b) A. Haimov and R. Neumann, *Chem. Commun.*, 2002, 876; (c) L. Heiss and H. J. Gais, *Tetrahedron Lett.*, 1995, **36**, 3833; (d) S. Chandrasekar, Ch. Narsihmulu, S. S. Shameem and N. R. Reddy, *Chem. Commun.*, 2003, 1716; (e) T. J. Dickerson, N. N. Reed and K. D. Janda, *Chem. Rev.*, 2002, **102**, 3325; (f) A. Kamal, D. R. Reddy and Rajendar, *Tetrahedron Lett.*, 2006, **47**, 2261.
- X. Wang, Z. Quan, F. Wang, M. Wang, Z. Zhang and Z. Li, *Synth. Commun.*, 2006, **36**, 451.
- General experimental procedure: a stirred mixture containing the aldehyde (2 mmol), urea/thiourea (2 mmol), β-dicarbonyl compound (2 mmol) and PEG-400 (0.2 g) was heated at 100 °C for 45 min. After completion, the reaction mixture became a solid with a yellow color, which was separated and washed with water. The resulting crude product was recrystallized with ethanol to afford pure 3,4-dihydropyrimidinones. All the products were characterized by comparing their physical and spectral data with those of reported compounds.
- E. H. Hu, D. R. Sidler and U.-H. Dolling, *J. Org. Chem.*, 1998, **63**, 3454.

The first Au-nanoparticles catalyzed green synthesis of propargylamines *via* a three-component coupling reaction of aldehyde, alkyne and amine†

Mazaahir Kidwai,*^a Vikas Bansal,^a Ajeet Kumar^b and Subho Mozumdar^b

Received 13th February 2007, Accepted 14th March 2007

First published as an Advance Article on the web 23rd March 2007

DOI: 10.1039/b702287e

Recyclable Au-nanoparticles provide an efficient, economic, novel route for multi component A³ coupling reaction of aldehyde, amine and alkyne. This method provides the wide range of substrate applicability. This protocol avoids the use of heavy metals, co-catalyst and gives the propargylamine in excellent yields.

Introduction

Propargylamines are major skeletons¹ or synthetically versatile and key intermediates² for the preparation of many nitrogen-containing biological active compounds, such as β -lactams, oxotremorine analogues, conformationally restricted peptides, isosteres and important structural elements of natural products and therapeutics drug molecules.³ Propargylamines were synthesized by three component one-pot coupling reaction (A³ coupling) of aldehydes, alkynes and amines.

One-pot multi component coupling reactions (MCRs) are an attractive strategy in organic synthesis⁴ and are highly valued among synthetic methodologies, as several elements of diversity can be introduced in a single step into a molecule. There are several transition metal catalysts able to carry out multi component A³ coupling reactions of aldehyde, alkynes and amines *via* C–H activation. These include Ag(I) salts,⁵ Au(I)/Au(III) salts,⁶ Au(III) salen complexes,⁷ Cu(I) salts,⁸ iridium complexes,⁹ Hg₂Cl₂¹⁰ and a Cu/Ru¹¹ bimetallic system under homogenous conditions.

Recently, an A³ coupling reaction has been reported through C–H activation in water using Au(I) salts,⁶ immobilization of Ag salts in ionic liquid,¹² and Cu-supported hydroxyapatite,¹³ although the scope is generally limited for cyclic amines. In addition, more sophisticated alternative energy sources like microwave^{8,14} and ultrasonic¹⁵ radiation have been used in the presence of a Cu(I) salt.

However, these reagents, used in stoichiometric amounts, are highly moisture sensitive, and require strictly controlled reaction conditions. Using the above-mentioned protocol, reactions were carried out either in toxic solvent like toluene⁵ or in the presence of expensive solvents, such as ionic liquids¹⁶ or required drastic

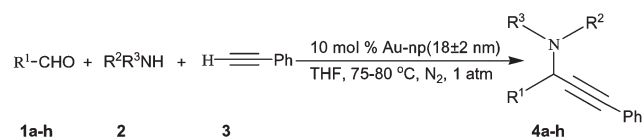
reaction conditions. It is a considerable drawback that an expensive metal catalyst is often lost at the end of the reaction, as there were no reports on the recyclability of catalyst. Metal nanoparticles are employed as a heterogenous catalyst and could be recycled, which overcomes the serious limitation of the non-recyclability of the catalyst.

In continuation of our studies on the development of new synthetic methods¹⁷ and the role of transition metal nanoparticles¹⁸ in organic transformations, we report here in an efficient recyclable A³ coupling reaction (*via* C–H activation) catalyzed by Au-nanoparticles (An-np).

Result and discussion

Initially, to examine the catalytic activity of Au-nanoparticles on the traditional Mannich reaction, benzaldehyde (1 mmol), piperidine (1 mmol) and phenylacetylene (1.5 mmol) in methanol (5 ml) were stirred under a nitrogen atmosphere at 35 °C in the presence of 10 mol% of Au-nanoparticles for 12 h (Scheme 1). 91% conversion of phenylacetylene was found on the basis of ¹H-NMR analysis of the crude reaction mixture, and propargylamine was isolated in 78% yield.

Increasing the loading of Au-nanoparticles up to 50 mol% gave desired propargylamine in 96% yield (Table 1, entry 5) with 93%



Scheme 1 Gold nanoparticles catalysed A³ coupling reaction of aldehyde, secondary amines, and alkyne.

Table 1 Optimization of Au-nanoparticles for A³ coupling^a

Entry	Au-np (18 ± 2 nm)/mol%	Time/h	Conversion (%) ^b	Yield (%) ^c
1	0	18	54	0
2	5	12	66	83
3	10	5	97	92
4	30	3.5	88	95
5	50	2	93	96

^a Reaction conditions: 1.0 equiv. of benzaldehyde, 1.0 equiv. of piperidine, 1.5 equiv. of phenylacetylene, x mol% Au-np (18 ± 2 nm); solvent MeOH; temperature 75–80 °C; N₂; 1 atm. ^b Conversions were determined by ¹H NMR of crude reaction mixture. ^c Isolated and unoptimized yields.

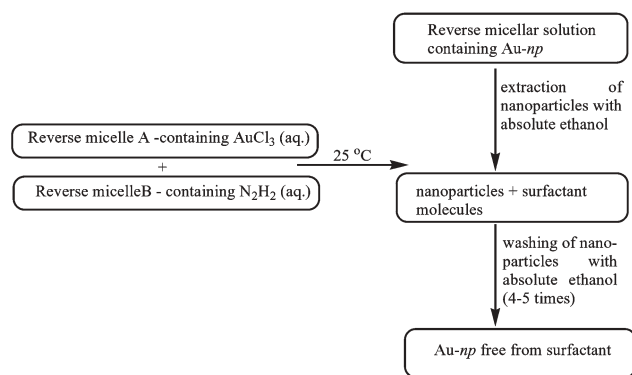
^aGreen Chemistry Research Laboratory, Department of Chemistry, University of Delhi, Delhi, 110007, India.

E-mail: kidwai.chemistr@gmail.com; Fax: +91 11 27666235;

Tel: +91 11 27666235

^bLaboratory of Nanobiotechnology, Department of Chemistry, University of Delhi, Delhi, 110007, India

† Electronic supplementary information (ESI) available: Experimental details and compound characterisation. See DOI: 10.1039/b702287e



Scheme 2 Preparation of Au-nanoparticles.

conversion. However, the increase in the concentration of catalyst not only promotes the reaction but also results in an increase of the yield.

In addition, it was found that at higher temperatures Au-np show good catalytic activity; at 75–80 °C, a 92% yield were obtained, however at room temperature lower yields are obtained even after longer reaction times. Comparable results were obtained when the reaction was carried out at 75–80 °C with 10 mol% of Au-np. Thus, to reduce the amount of catalyst, all optimizations are carried out at 75–80 °C with 10 mol% of Au-np. Further, to optimize the reaction conditions, Au-nanoparticles of different sizes, ranging from 15 nm to 70 nm in diameter, were prepared in an aqueous core of reverse micellar droplets (Scheme 2)^{19–21} and size was confirmed as 10–17 nm through quasi elastic light scattering data (QELS) (Fig. 1a) and transmission electron microscopy (TEM) (Fig. 1b). The studies shows that mechanism of catalytic action nanoparticles is dependent on the nanoparticles size (Table 2).

The maximum reaction rate has been observed for an average particle of diameter of about 20 nm. With a decrease in a particle size, a trend of decreasing reaction rate has been found for particles with a diameter of less than 20 nm, while those above this diameter shows a steady decline of reaction rate with increasing size. It has been postulated that in the case of particles of average size less than a 20 nm, a downward shift of the Fermi level takes place, with a consequent increase of band gap energy. As a result, the particles require more energy to pump electrons to the adsorbed ions for electron transfer reaction. This leads to a reduction in reaction rate when catalysed by smaller particles. On the other hand, for nanoparticles >20 nm in diameter, the change of Fermi level is not appreciable. As these particles exhibit less surface area for adsorption with increased particle size, a decrease in catalytic efficiency results.

It is important to stress that the catalyst was recycled and reused for five or seven runs with only slight drop in activity. Additional starting material was added into the reaction mixture and the reaction proceeded for an additional 10 h, and it results in the formation of **4a** (Table 5) in 80% yield. The results in Table 3 showed that after every run the yield was excellent while the reaction time was delayed.

We supposed that this result was induced by conglomeration of Au-nanoparticles, which was size dependent. Au-nanoparticles were separated from the reaction mixture by mild centrifugation at 2000–3000 rpm, at 10 °C for 5 min. QELS data (Figure 2) clearly

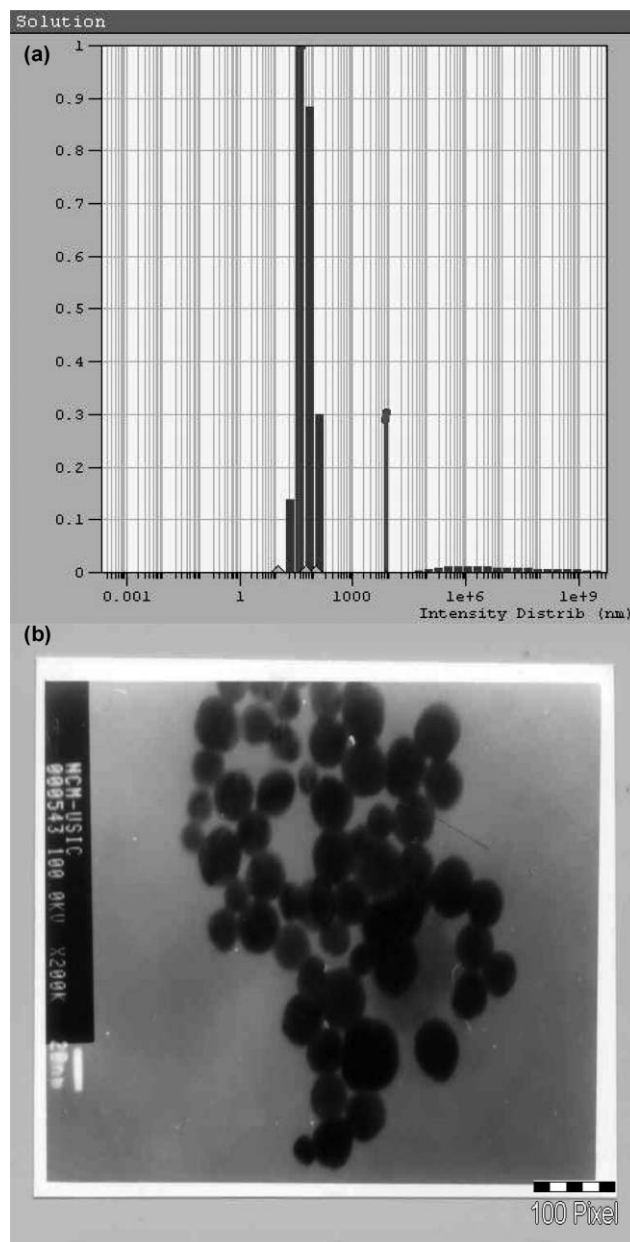


Fig. 1 (a) QELS data of Au-nanoparticles: plot of population distribution in percentile versus size distribution in nanometres (nm); (b) TEM image of Au-nanoparticles. The scale bar corresponds to 100 nm in the TEM image.

Table 2 Size screening of Au-nanoparticles on A³ coupling of benzaldehyde, phenylacetylene, and piperidine^a

Entry	Particle size (±2)/nm	Time/h	Conversion (%) ^b	Yield (%) ^c
1	10	11	94	87
2	20	5	97	92
3	30	8	87	85
4	50	12	91	73
5	70	15	78	67

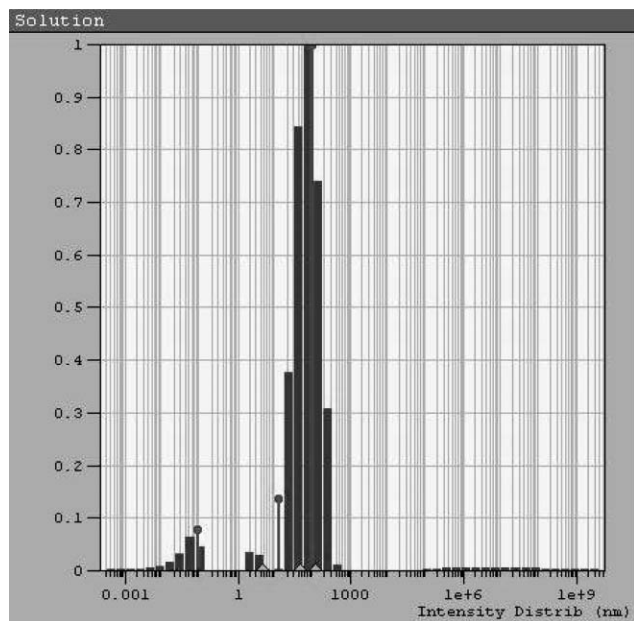
^a Reaction conditions: 1.0 equiv. of benzaldehyde, 1.0 equiv. of piperidine, 1.5 equiv. of phenylacetylene, 10 mol% Au-np ($x \pm 2$ nm); solvent MeOH; temperature 75–80 °C; N₂; 1 atm.

^b Conversions were determined by ¹H NMR of crude reaction mixture. ^c Isolated and unoptimized yields.

Table 3 Recycling of Au-nanoparticles

No. of cycles ^a	Fresh	Run 1	Run 2	Run 3	Run 4
Yield (%) ^b	92	87	81	72	63
Time/h	5	7	10	12	18

^a Reaction conditions: 1.0 equiv. of benzaldehyde, 1.0 equiv. of piperidine, 1.5 equiv. of phenylacetylene, 10 mol% Au-np (18 ± 2 nm); solvent MeOH; temperature 75–80 °C; N₂; 1 atm. ^b Isolated and unoptimized yields.

**Fig. 2** QELS data of recycled Au-nanoparticles: plot of population distribution in percentile versus size distribution in nanometres (nm).

showed that there was conglomeration of Au-nanoparticles. In addition, the reaction remained very clean without side product formation, thus Au-nanoparticles are 'green'.

The nature of reaction media has an important role in A³ coupling reactions in the presence of Au-nanoparticles (10 mol%). Among the various solvent investigated, CH₃CN was found to be the best solvent of choice (Table 4, entry 1), and no products were obtained when the reaction was carried out in C₆H₁₂ or CH₂Cl₂. This may be due to the high polarity associated with CH₃CN, which may result in the stabilization of the alkenyl–Au intermediate.

After all the standardisation, we chose a variety of structurally different aldehydes, and amines possessing a wide range of

Table 4 Effect of polarity of the solvent on A³ coupling^a

Entry	Solvent	Time/h	Yield (%) ^b
1	Acetonitrile	5	96
2	Methanol	5	92
3	Tetrahydrofuran	5	87
4	Dichloromethane	5	0 (unidentified product)
5	Cyclohexane	5	0 (unidentified product)

^a Reaction conditions: 1.0 equiv. of benzaldehyde, 1.0 equiv. of piperidine, 1.5 equiv. of phenylacetylene, 10 mol% Au-np (18 ± 2 nm); temperature 75–80 °C; N₂; 1 atm. ^b Isolated and unoptimized yields.

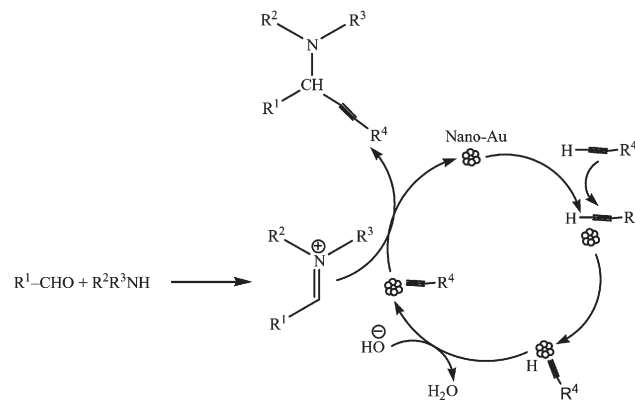
Table 5 A³ coupling of aldehyde, alkynes and secondary amines by Au-nanoparticles as catalyst^a

Entry	Aldehyde R ¹	Amines	Product	Time/h	Conv. (%) ^b	Yield (%) ^c
1	C ₆ H ₅ –	Piperidine	4a	5	97	94
2	4-MeC ₆ H ₄ –	Piperidine	4b	11	76	81
3	4-MeOC ₆ H ₄ –	Piperidine	4c	8	78	87
4	3-ClC ₆ H ₄ –	Piperidine	4d	4	94	96
5	4-Br C ₆ H ₄ –	Piperidine	4e	7	92	95
6	2-Furfuryl	Piperidine	4f	3	85	84
7	2-Thiophenyl	Piperidine	4g	5	88	96
8	3-Pyridinyl	Piperidine	4h	6	91	93
9	C ₆ H ₅ –	Morpholine	5a	7	79	82
10	4-MeC ₆ H ₄ –	Morpholine	5b	8.5	73	88
11	C ₆ H ₅ –	Pyrolidine	6a	6	82	67
12	4-MeC ₆ H ₄ –	Pyrolidine	6b	13	88	71

^a Reaction conditions: 1.0 equiv. of aldehyde, 1.0 equiv. of secondary amine, 1.5 equiv. of phenylacetylene, 10 mol% Au-np (18 ± 2 nm); solvent: CH₃CN; temperature 75–80 °C; N₂; 1 atm.; ^b Conversions were determined by ¹H NMR of crude reaction mixture. ^c Isolated and unoptimized yields.

functional group to understand the scope and generality of the Au-nanoparticles promoted A³ coupling reaction. A variety of aromatic aldehydes were coupled with a piperidine and phenylacetylene and it was found that aryl aldehydes possessing electron withdrawing groups (Table 5, entries 4, 5) afforded a better yield, with good reactivity, than that with an electron donating group (Table 5, entry 2, 3) bound to the benzene ring, which required longer reaction times. Heterocyclic aldehydes (Table 5, entry 6,7,8) also displayed high reactivities with good yields. To expand the scope of amine substrate, we used phenylacetylene as a model substrate and examined various amines with different aldehydes. The coupling proceeded smoothly with morpholine and pyrolidine to afford the corresponding propargylamine in good yields under standard conditions, and it was found that piperidine gave better results in term of yields and reaction time than morpholine.

In general, the formation of propargylamine *via* A³ coupling proceeded smoothly to afford the corresponding propargylamine *via* A³ coupling proceeding through C_{sp}–H bond activation of terminal alkynes. A tentative mechanism (Figure 3) was proposed involving the activation of the C–H bond of alkyne by Au-nanoparticles. The alkenyl–Au intermediate thus formed reacted with the iminium ion generated *in situ* from aldehyde and secondary amines to give the corresponding propargylamine and

**Fig. 3** Tentative mechanism of Au-nanoparticles catalysed A³ coupling.

regenerated the Au-nanoparticles for further reaction. In the literature it was reported that metal nanoparticles act as a redox catalyst by a free radical mechanism²² and thus the reaction may proceed by a free radical mechanism.

Conclusions

Overall this methodology offers the competitive advantages of recyclability of the catalyst without significant loss of catalytic activity; ready availability; it can be used or reused without further purification, and without using additives or cofactor; it requires lower catalyst loading, has broad substrate applicability, gives high yields in short reaction times, and is simple and easy to carry out.

In conclusion, we have successfully developed a novel, facile, economic, practical and green method for the synthesis of propargylamines. The catalyst can be readily recovered and reused, thus making this procedure more environmentally acceptable and no catalyst has widespread use in organic synthesis for preparation of propargylamines.

Experimental

In a 50 ml round bottom flask, aromatic aldehydes/heterocyclic aldehydes **1a–h** (1 mmol), secondary amine (1 mmol) and phenylacetylene (1.5 mmol) in CH₃CN (5 ml) were mixed and stirred under a nitrogen atmosphere. To this, Au-nanoparticles (10 mol%, 18 ± 2 nm) were added. The resulting solution was refluxed at 75–80 °C for the appropriate time mentioned in Table 5. The progress of reaction was monitored by TLC. After completion of the reaction, the reaction mixture was centrifuged at 2000–3000 rpm, at 10 °C for 5 min. The organic layer was decanted out and remaining Au-nanoparticles were reused for further reactions. The organic layer was dried over anhydrous Na₂SO₄ and the solvent was removed *in vacuo*. The crude product was subjected to purification by silica gel column chromatography using 15% ethyl acetate, 5% methanol and 80% petroleum ether as an eluent to yield the propargylamine **4a–h**. The structures of all the products were unambiguously established on the basis of their spectral analysis (IR, ¹H NMR and GC/MS mass spectral data). All the products are known compounds (see ESI).†

Acknowledgements

S.M. gratefully acknowledges financial support from the Department of Science and Technology, Govt of India, for this work.

Notes and references

- 1 A. A. Boulton, B. A. Davis, D. A. Durden, L. E. Dyck, A. V. Juorio, X. M. Li, I. A. Paterson and P. H. Yu, *Drug Dev. Res.*, 1997, **42**, 150;

- M. A. Huffman, N. Yasuda, A. E. DeCamp and E. J. J. Grabowski, *J. Org. Chem.*, 1995, **60**, 1590; M. Konishi, H. Ohkuma, T. Tsuno, T. Oki, G. D. VanDuyne and J. Clardy, *J. Am. Chem. Soc.*, 1990, **112**, 3715.
- 2 M. Miura, M. Enna, K. Okuro and M. Nomura, *J. Org. Chem.*, 1995, **60**, 4999; A. Jenmalm, W. Berts, Y. L. Li, K. Luthman, I. Csoregh and U. Hacksell, *J. Org. Chem.*, 1994, **59**, 1139; B. Nilsson, H. M. Vargas, B. Ringdahl and U. Hacksell, *J. Med. Chem. Soc.*, 1992, **35**, 285.
- 3 G. Dyker, *Angew. Chem.*, 1999, **38**, 1698; I. Naota, H. Takaya and S. I. Murahashi, *Chem. Rev.*, 1998, **98**, 2599.
- 4 C. Cao, Y. Shi and A. L. Odom, *J. Am. Chem. Soc.*, 2003, **125**, 2880; S. Kamijo and Y. Yamamoto, *J. Am. Chem. Soc.*, 2002, **124**, 11940; A. Domling and I. Ugi, *Angew. Chem.*, 2000, **112**, 3300; I. Ugi, A. Domling and B. Werner, *J. Heterocycl. Chem.*, 2000, **37**, 647; R. W. Armstrong, A. P. Combs, P. A. Tempst, S. D. Brown and T. A. Keating, *Acc. Chem. Res.*, 1996, **29**, 123.
- 5 W. Yan, R. Wang, Z. Xu, J. Xu, L. Lin, Z. Shen and Y. Zhou, *J. Mol. Catal. A: Chem.*, 2006, **255**, 81; Y. Zhang, A. M. Santos, E. Herdtweck, J. Mink and F. E. Kuhn, *New J. Chem.*, 2005, **29**, 366; C. Wei, Z. Li and C. J. Li, *Org. Lett.*, 2003, **5**, 4473.
- 6 M. L. Kantam, B. V. Prakash, C. Reddy, V. Reddy and B. Sreedhar, *Synlett*, 2005, 2329; C. Wei, Z. Li and C. J. Li, *Synlett*, 2004, 1472; C. Wei and C. J. Li, *J. Am. Chem. Soc.*, 2003, **125**, 9584.
- 7 V. K. Y. Lo, Y. Liu, M. K. Wong and C. M. Che, *Org. Lett.*, 2006, **8**, 1529.
- 8 L. Shi, Y. Q. Tu, M. Wang, F. M. Zhang and C. A. Fan, *Org. Lett.*, 2004, **6**, 1001; H. Z. S. Syeda, R. Halder, S. S. Karla, J. Das and J. Iqbal, *Tetrahedron Lett.*, 2002, **43**, 6485; G. W. Kabalka, L. Wang and R. M. Pagni, *Synlett*, 2001, 676; Y. Ju, C. J. Li and R. S. Varma, *QSAR Comb. Sci.*, 2004, 23.
- 9 C. Fischer and E. M. Carreira, *Org. Lett.*, 2001, **3**, 4319.
- 10 L. P. Hua and W. Lei, *Chin. J. Chem.*, 2005, **23**, 1076.
- 11 C. J. Li and C. Wei, *Chem. Commun.*, 2002, 268.
- 12 L. Zhang, C. Wei, R. S. Varma and C. J. Li, *Tetrahedron Lett.*, 2004, **45**, 2443.
- 13 B. M. Choudary, C. Sridhar, M. L. Kantam and B. Sridhar, *Tetrahedron Lett.*, 2004, **45**, 7319.
- 14 N. E. Leadbeater, H. M. Torenus and H. Tye, *Mol. Diversity*, 2003, **7**, 135.
- 15 B. Sreedhar, P. S. Reddy, B. V. Prakash and A. Ravindra, *Tetrahedron Lett.*, 2005, **46**, 7019.
- 16 S. B. Park and H. Alper, *Chem. Commun.*, 2005, 1315.
- 17 M. Kidwai, R. Venkataramanan and B. Dave, *Green Chem.*, 2001, **3**, 278; M. Kidwai, V. Bansal and P. Mothra, *J. Mol. Catal. A: Chem.*, 2007, **268**, 76; M. Kidwai, P. Mothra, V. Bansal, R. K. Somvanshi, A. S. Ethayathulla, S. Dey and P. Singh Tej, *J. Mol. Catal. A: Chem.*, 2006, **265**, 177; M. Kidwai and P. Mothra, *Tetrahedron Lett.*, 2006, **47**, 5029; M. Kidwai, P. Mothra, V. Bansal and R. Goyal, *Monatsh. Chem.*, 2006, **137**, 1189.
- 18 M. Kidwai, V. Bansal, A. Saxena, S. Aerry and S. Mozumdar, *Tetrahedron Lett.*, 2006, **47**, 8049; M. Kidwai, V. Bansal, A. Saxena, R. Shankar and S. Mozumdar, *Tetrahedron Lett.*, 2006, **47**, 4161; A. Saxena, A. Kumar and S. Mozumdar, *Appl. Catal., A*, 2007, **317**, 210.
- 19 M. Boutonnet, J. Kizling, R. Touroude, G. Marie and P. Stenius, *Catal. Lett.*, 1991, **9**, 347.
- 20 M. Boutonnet, J. Kizling and G. S. P. Marie, *Colloids Surf.*, 1982, **5**, 209.
- 21 M. P. Pileni and I. Lisiecki, *J. Am. Chem. Soc.*, 1993, **115**, 3887.
- 22 K. Mallick, M. Witcomp and M. Scurrall, *Mater. Chem. Phys.*, 2006, **97**, 283.

Polyelectrolyte-functionalized ionic liquid for electrochemistry in supporting electrolyte-free aqueous solutions and application in amperometric flow injection analysis†

Yanfei Shen,^a Yuanjian Zhang,^a Xuepeng Qiu,^{‡a} Haiquan Guo,^{‡a} Li Niu^{*a} and Ari Ivaska^b

Received 10th November 2006, Accepted 30th January 2007

First published as an Advance Article on the web 15th March 2007

DOI: 10.1039/b616452h

As a green process, electrochemistry in aqueous solution without a supporting electrolyte has been described based on a simple polyelectrolyte-functionalized ionic liquid (PFIL)-modified electrode. The studied PFIL material combines features of ionic liquids and traditional polyelectrolytes. The ionic liquid part provides a high ionic conductivity and affinity to many different compounds. The polyelectrolyte part has a good stability in aqueous solution and a capability of being immobilized on different substrates. The electrochemical properties of such a PFIL-modified electrode assembly in a supporting electrolyte-free solution have been investigated by using an electrically neutral electroactive species, hydroquinone (HQ) as the model compound. The partition coefficient and diffusion coefficient of HQ in the PFIL film were calculated to be 0.346 and $4.74 \times 10^{-6} \text{ cm}^2 \text{ s}^{-1}$, respectively. Electrochemistry in PFIL is similar to electrochemistry in a solution of traditional supporting electrolytes, except that the electrochemical reaction takes place in a thin film on the surface of the electrode. PFILs are easily immobilized on solid substrates, are inexpensive and electrochemically stable. A PFIL-modified electrode assembly is successfully used in the flow analysis of HQ by amperometric detection in solution without a supporting electrolyte. The results indicate a green electrochemical methodology in supporting electrolyte-free solution and a potential application in amperometric detection in a flow system without any supporting electrolyte in the solution, such as the high performance liquid chromatography electrochemical detection (HPLC-ECD) system.

1. Introduction

Ionic liquids (ILs), or more specifically cation–anion pairs that form a stable fluid near room temperature, are playing an increasingly practical role as ‘green’ chemical reaction solvents, electrolytes, and heat-transfer media on scales ranging from the laboratory bench to industrial manufacturing processes. Their advantages include minuscule vapor pressure, high polarity, and relative inertness.^{1,2} In particular, in electrochemistry, they show relatively wide potential windows and high conductivity, and allow studies to be undertaken without any additional supporting electrolyte.^{3–7} Therefore, there is the possibility of using ILs to develop ion-conductive materials. As pioneers, the groups of Murray and also of Wrighton have extensively investigated the solid-state electrochemistry of another class of ILs, namely, undiluted melts of hybrids of lithium electrolytes or redox materials and polyethers.^{8–16} Heller and co-workers have also successfully developed

another kind of semi-solid hydrogel based on the hybrids of polyvinylimidazole or polyvinylpyridine and Ru^{2+} or Os^{2+} complexes.^{17,18} When an electrode surface is modified with these kinds of polymer, the attached layer would function as a supporting electrolyte for electrochemistry in a solution without additional supporting electrolytes. However, studies to use the ionic conductive melts or hydrogels for electrochemistry in aqueous solution without a supporting electrolyte are few in number.^{19,20}

It is common practice that electrochemical experiments should be conducted in the presence of supporting electrolytes. This is due to the recommendation that the ionic strength and conductivity of the solution must be high and constant.^{21–24} In general, supporting electrolytes are usually applied to (i) decrease the *Ohmic* potential drop, (ii) eliminate changes in ionic strength due to electrochemically consumed or generated ionic species, and (iii) eliminate migration as a mode of mass transport.^{22,23} However, within last few years, the general necessity to add an excess of supporting electrolyte has been questioned, and it is desirable to consider even the necessity of using a supporting electrolyte in various cases.^{19,20,25–31} The reasons are numerous, such as: (i) to eliminate the need of an expensive electrolyte, particularly in experiments performed in organic media, which is also highly anticipated for *green chemistry*; (ii) to eliminate the possible interference of any supporting electrolytes in electrochemical synthesis; and (iii) to detect species of interest in gas or non-conductive

^aState Key Laboratory of Electroanalytical Chemistry, Changchun Institute of Applied Chemistry, and Graduate School of the Chinese Academy of Sciences, Chinese Academy of Sciences, Changchun 130022, P. R. China. E-mail: lniu@ciac.jl.cn; Fax: +86-431-526 2800.

^bLaboratory of Analytical Chemistry, Process Chemistry Centre, Åbo Akademi University, FI-20500, Åbo-Turku, Finland

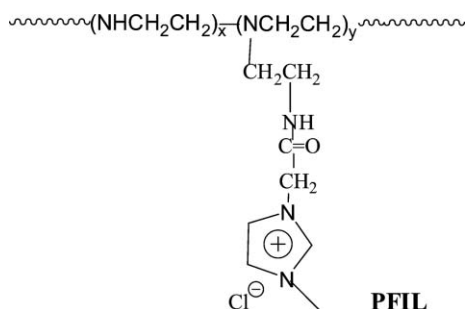
† Electronic supplementary information (ESI) available: Application of HPLC-ECD and FAQ of HPLC-ECD. See DOI: 10.1039/b616452h

‡ In State Key Laboratory of Polymer Physics and Chemistry in CIAC, CAS, P. R. China.

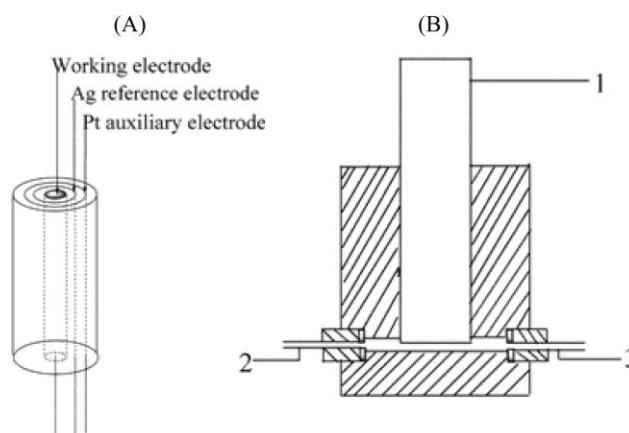
fluids.^{19,20,26–31} Moreover, sometimes the need to use supporting electrolytes for electrochemical detection creates problems. For example, the high performance liquid chromatography electrochemical detection (HPLC-ECD) system has become a powerful tool in chemical, clinical, pharmaceutical and environmental analysis due to its excellent sensitivity and selectivity to electroactive species.^{32–35} However, the supporting electrolytes might precipitate in the HPLC system after long-time use causing, for example, high back-pressure and ghost peaks.³⁶

Some promising methods for electrochemical detection in flow systems have successfully been developed. In these applications, the detection is done with ultramicroelectrodes (UMEs) or their modifications with moist ion-exchange membranes such as Nafion.^{19,26,37–43} Fuchigami and Tajima have developed another novel method to generate *in situ* the supporting electrolyte during the electro-organic synthesis. This procedure not only eliminates the use of expensive supporting electrolytes in organic media, but also makes the product separation very simple.^{30,31}

As part of our ongoing research in developing immobilized ILs,⁴⁴ in this paper, we report a straightforward approach towards electrochemistry in supporting electrolyte-free solutions based on a polyelectrolyte-functionalized ionic liquid (PFIL, as illustrated in Scheme 1) where the imidazolium part functions as the ionic liquid. Our previous results have indicated that the PFIL combines the individual advantages of each functional part in the material: high ionic conductivity, solvation properties originating from the ionic liquid part in the molecule, and good immobilization properties and stability in aqueous solution originating from the polyelectrolyte.⁴⁴ Moreover, when the polyelectrolyte was used for the electrochemical detection of analytes, owing to the high chemical and electrochemical stability, the detection with the PFIL modified on the electrode would not be interfered with by the redox behaviour of polyelectrolyte itself. Therefore, the PFIL is an interesting material to be used for electrochemical measurements in supporting electrolyte-free solutions. Furthermore, two aspects of green chemistry would be involved: one is the elimination of supporting electrolytes for electrochemistry, which are often corrosive and expensive; the other originates from the ionic liquid part of PFIL, such as chemical and thermal stability. The experiments in this work are to develop a simple ion-conductive polyelectrolyte-modified electrode for electrochemistry in aqueous solutions without any supporting



Scheme 1 Structure of the polyelectrolyte-functionalized ionic liquid (PFIL) used in this study.



Scheme 2 (A) Illustration of the assembly electrode; (B) the detection cell (cross-section view): (1) electrode assembly; (2) inlet; (3) outlet.

electrolyte. The electrochemical performance of the PFIL-modified electrode assembly [as shown in Scheme 2(A)] in supporting electrolyte-free solution will be studied, and further applied to flow analysis in supporting electrolyte-free aqueous solutions as an example of the potential applications of the developed concept.

2. Experimental

Chemicals and materials

Polyethylenimine (PEI; $M_w = 25\,000$) was obtained from Aldrich. The polyelectrolyte-functionalized ionic liquid (PFIL, Scheme 1) was prepared according to our previous report.⁴⁴ Unless otherwise stated, reagents were of analytical grade and used as received. All aqueous solutions were prepared with double-distilled water from a Millipore system ($>18\text{ M}\Omega\text{ cm}$).

Preparation of electrode assembly and detection cell

The structure of the electrode assembly is shown in Scheme 2(A). The working electrode is a glassy carbon electrode ($d = 3\text{ mm}$), and coaxial Pt and Ag rings are used as counter and quasi-reference electrodes, respectively. The electrodes are a three concentric circle on the same plane. The three parts were encapsulated with epoxy resin and assembled into an integrated electrode.

The detection cell used in this study is schematically shown in Scheme 2(B). The electrode assembly, the inlet and outlet tubes are inserted into their corresponding preset access holes and connected to the cell body with screws. The solutions are pumped through a microinjection pump.

Modification of the electrode assembly with PFIL

The electrode assembly was polished with aqueous slurries of fine alumina powders (1, 0.3 and $0.05\text{ }\mu\text{m}$) on a polishing cloth. Then this electrode assembly was finally rinsed with double-distilled water in an ultrasonic bath for 5 min. Because the PFIL is a kind of hydrogel, it can form a rather stable film on the electrode surface simply by traditional casting. Typically, *ca.* $15\text{--}60\text{ }\mu\text{L}$ of aqueous solution of 3 mg mL^{-1} PFIL was evenly spread onto the surface of the electrode assembly. Then

the electrode assembly was dried overnight in air to form a uniform film. The thickness of the PFIL film was estimated from the volume of PFIL used for modification and the geometry of the electrode. For example, when 30 μL of aqueous solution of 3 mg mL^{-1} PFIL was cast onto the electrode, the film thickness was *ca.* 1.4 μm .

Determination of diffusion coefficient and partition coefficient

The diffusion coefficient and partition coefficient of HQ in the PFIL film was obtained by chronoamperometry. The experiment was carried out in a conventional three-electrode electrochemical cell. The working electrode was a PFIL-modified Pt microelectrode ($d = 20 \mu\text{m}$), the auxiliary electrode was a Pt wire, and the reference electrode was Ag|AgCl (saturated KCl). The thickness of the PFIL film was *ca.* 1.4 μm .

Instruments

All electrochemical experiments were performed using the CHI 660A and CHI 900 electrochemical workstations (CHI Inc., USA).

3. Results and discussion

3.1 Electrochemical performance of the PFIL-modified electrode assembly

3.1.1 Electrochemical microenvironment provided by the PFIL. The electrochemical performance of the PFIL-modified electrode assembly in supporting electrolyte-free solution was investigated by using an electrically neutral electroactive species hydroquinone (HQ) as the model compound. Fig. 1 shows a study where cyclic voltammograms (CVs) of a 20 μM HQ solution have been recorded with different electrode assemblies. As can be seen in curve 'a', in the absence of HQ there are no redox peaks at the PFIL-modified electrode assembly in pure water. Upon addition of HQ to the pure water, a pair of well-defined redox peaks of the HQ can clearly

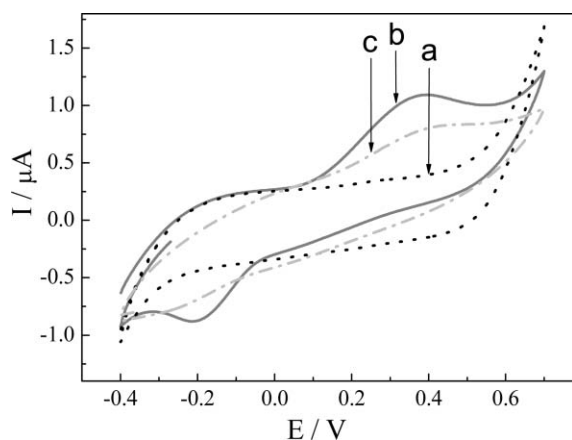


Fig. 1 Cyclic voltammograms (CVs) in supporting electrolyte-free aqueous solutions: (a) pure water at the 1.4 μm thick PFIL-modified electrode assembly, (b) 20 μM HQ at the 1.4 μm thick PFIL-modified electrode assembly, and (c) 20 μM HQ at a bare glassy carbon electrode. Scan rate: 0.1 V s^{-1} .

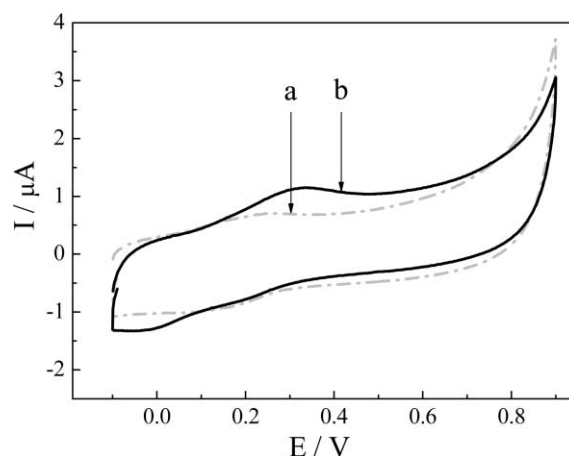


Fig. 2 Cyclic voltammograms (CVs) at a bare glassy carbon electrode in 1 M KCl aqueous solution: (a) without, and (b) with HQ (20 μM). Scan rate: 0.1 V s^{-1} .

be seen (curve 'b').⁴⁵ Those redox peaks can also be found at a bare glassy carbon electrode (curve 'c'), but are much smaller than at the PFIL-modified electrode (curve 'b'). These results indicate that the PFIL film on the modified electrode provides a good electrochemical microenvironment for the redox reaction of HQ.

To further demonstrate the essential role of the PFIL film, two control experiments were also performed. Cyclic voltammograms (CVs) in a traditional manner with a supporting electrolyte were recorded. Fig. 2 shows the CVs at the bare glassy carbon electrode in 1 M KCl aqueous solution. Curve 'a' is recorded in the presence of the supporting electrolyte only and curve 'b' after making the solution 20 μM with respect to HQ. When comparing curve 'b' in Fig. 2 and curve 'b' in Fig. 1, we can conclude that the current recorded at the PFIL-modified electrode is enhanced. This indicates that the PFIL on the electrode assembly not only exhibits the properties of an electrolyte, but also shows a good affinity towards HQ. If HQ, however, is irreversibly absorbed on the PFIL film, similar results would also be obtained. Therefore, we performed an additional experiment where the CVs at the PFIL-modified electrode assembly in HQ solution were recorded. The electrode was briefly rinsed with water and the CVs at the same electrode in pure water were collected. It was found that no redox peaks of HQ were observed, which indicated that although PFIL exhibited a good affinity towards HQ, there was no irreversible absorption in the film. Therefore, these results showed that the PFIL on the electrode assembly offered a suitable electrochemical microenvironment for electrochemical reaction.

3.1.2 Effect of film thickness on the electrochemical performance. The film thickness was expected to influence the electrochemical signal of HQ, because both the ionic conductance of the PFIL film and the diffusion of HQ in the film depend on the film thickness. On the one hand, an increase in the film thickness increases the amount of ionic species in the electrode assembly, thus improving its ionic conductance; on the other hand, the thick film also limits the

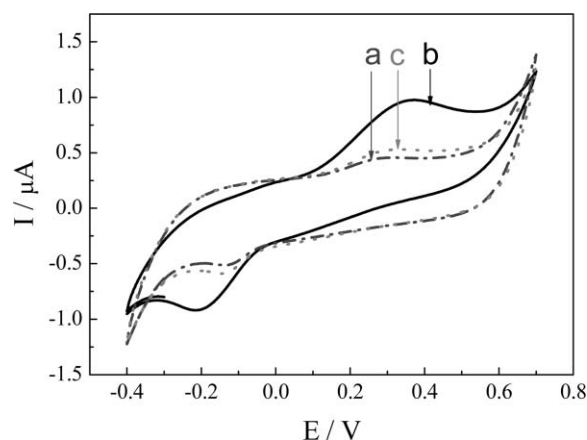


Fig. 3 Cyclic voltammograms for HQ (20 μM) in supporting electrolyte-free solution at an electrode assembly modified with (a) 0.7 μm , (b) 1.4 μm and (c) 2.8 μm PFIL film. Scan rate: 0.1 V s^{-1} .

diffusion of HQ from the solution into the PFIL film matrix and further to the electrode. Therefore, the effect of film thickness was investigated by potential cycling measurements. As shown in Fig. 3 (curve 'a'), a small current peak was obtained on the electrode assembly modified with a *ca.* 0.7 μm PFIL film. When the thickness of the PFIL was increased to *ca.* 1.4 μm , a significant growth in the peak current was observed (curve 'b'). However, when the film thickness was increased to *ca.* 2.8 μm , a decrease in the current peak was observed (curve 'c'), and the control experiments showed that the current did not increase with the incubation times. As a conclusion, the film thickness significantly affected the CVs signal and an optimized film thickness should be adopted for the potential applications. It was also noted that the background currents in Fig. 3(a) and 3(c) were almost the same, which might be due to the fact that in the present experimental conditions there was a balance between film porosity, thickness and ionic conductivity on the influence of the background currents.

3.1.3 Electrochemical dynamics of HQ at the PFIL-modified electrode. To further investigate the electrochemical process of HQ at the PFIL-modified electrode assembly, the relationship between the scan rate and the peak current was studied. Fig. 4 shows the voltammetric scans with different scan rates recorded in 20 μM HQ in supporting electrolyte-free solution at the electrode assembly modified with a *ca.* 1.4 μm PFIL film. As shown in Fig. 4, the peak current was found to be directly proportional to the square root of the scan rate, confirming a diffusion-controlled process. Such a linear relationship may also indicate that there was no significant irreversible adsorption of HQ or its oxidation product, quinone, onto the electrode surface during the potential cycling.

The relationship between the concentration of HQ and the peak current was also studied (Fig. 5). As shown in Fig. 5(B), the peak current is proportional to the concentration of HQ, and the line goes through zero. It indicated that the partition coefficient of HQ was not related to the concentration of HQ in solution. And it again suggested that the electrochemical process was well diffusion-controlled.

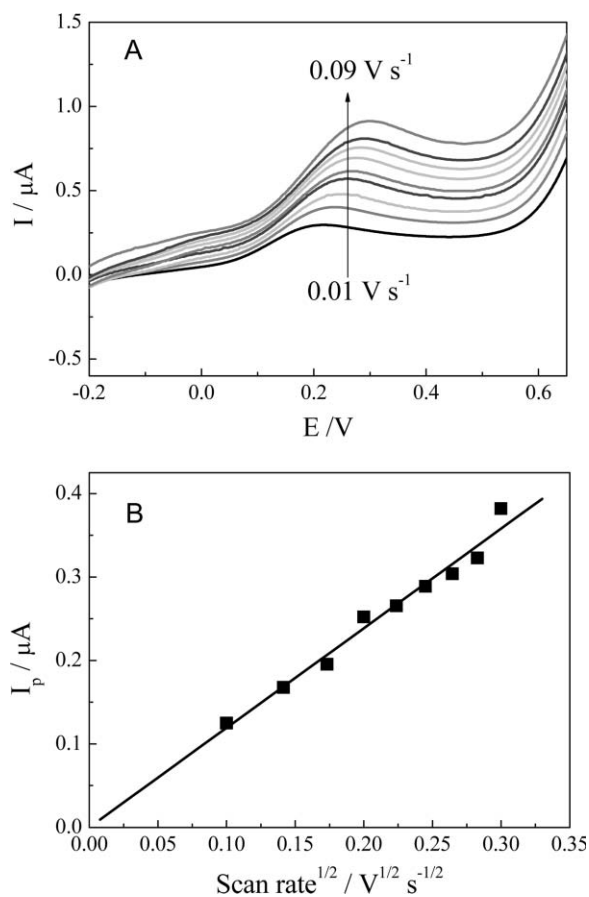


Fig. 4 (A) Linear sweep voltammograms for an aqueous solution of 20 μM HQ without any supporting electrolyte at a 1.4 μm thick PFIL-modified electrode assembly. Scan rate: 0.01, 0.02, 0.03, 0.04, 0.05, 0.06, 0.07, 0.08, 0.09 V s^{-1} . (B) Plot of I_p vs. $v^{1/2}$ for HQ at the PFIL-modified integrated electrode.

The peak potential experiences a positive shifts with the increase in HQ concentration, as shown in Fig. 5(A). The positive shift should originate from the good solubility of the PFIL film to the oxidized product – quinone. The resulting quinone species is enriched in the PFIL film matrix and is hard to diffuse into the solution. It is quite similar to the case where the product is insoluble in the solution. Then, at this time the peak potential should not be constant any more, but shifted to a more positive value for an increase in the concentration of HQ in the body of the solution.

Chronoamperometry was used to determine the diffusion coefficient and the partition coefficient of HQ in PFIL film (Fig. 6). The experiment was performed by holding the potential at 0.1 V for 20 s, and then a step to 0.45 V (which is sufficient for oxidation of HQ) for 5 s [Fig. 6(A)]. By plotting the current, I , vs. the reciprocal of the square root of time, $t^{-1/2}$ [Fig. 6(B)], a straight line was found corresponding to the modified Cottrell equation,⁴⁶

$$I(t) = \frac{nFAD^{1/2}C_m}{\pi^{1/2}t^{1/2}} + \pi nFDC_m r \quad (1)$$

where A is the geometric area of the microelectrode, r is the radius of the microelectrode, D is the diffusion coefficient of

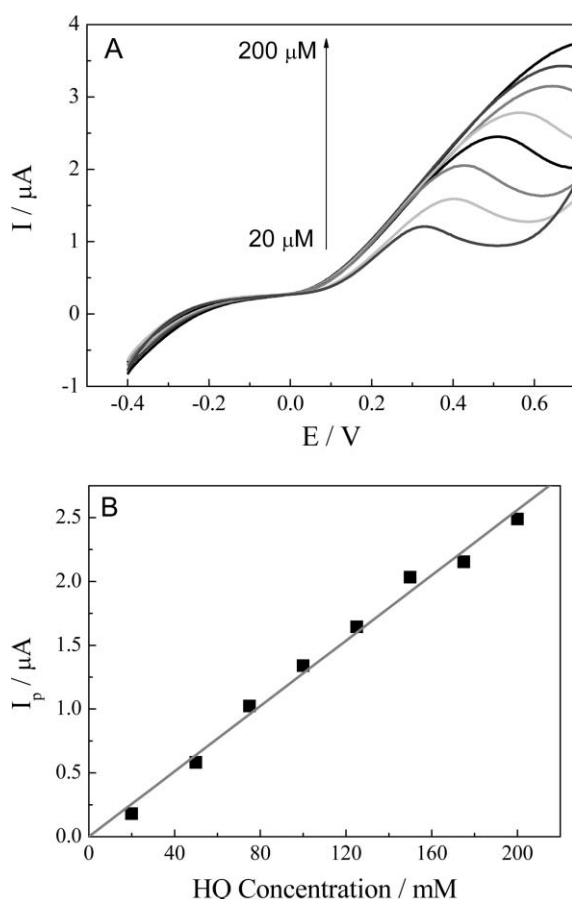


Fig. 5 (A) Linear sweep voltammograms for a supporting electrolyte-free aqueous solution of 20, 50, 75, 100, 125, 150, 175 and 200 μM HQ at a 1.4 μm thick PFIL-modified electrode assembly. (B) Relationship between the current and the concentration of HQ.

HQ in the PFIL film, and C_m is the concentration in the PFIL film. D and C_m values were obtained from the slope and intercept of the linear regression line. The partition coefficient, K_p , is defined as the following way,

$$K_p = \frac{C_m}{C_0} \quad (2)$$

where C_0 is the concentration of HQ in the solution. From this experiment, the following values were obtained: $D = 4.74 \times 10^{-6} \text{ cm}^2 \text{ s}^{-1}$ and $K_p = 0.346$, which were comparable to the reported values of ions in traditional membranes, such as Nafion film.^{47,48}

Based on all these results, the electrochemical process of HQ at the PFIL-modified electrode assembly is summarized and illustrated in Scheme 3: First, the conductive PFIL film connects the working (WE), counter (CE) and reference (RE) electrodes, giving an electrolytic contact between these electrodes. Second, the good affinity towards HQ and the sufficient diffusion of HQ through the PFIL film to the electrode assembly surface are also crucial factors for the electrochemical process. But it should be pointed out that the thickness of the PFIL film on electrodes should be optimized in order to obtain the high conductivity of the film and effective diffusion of analytes through the film.

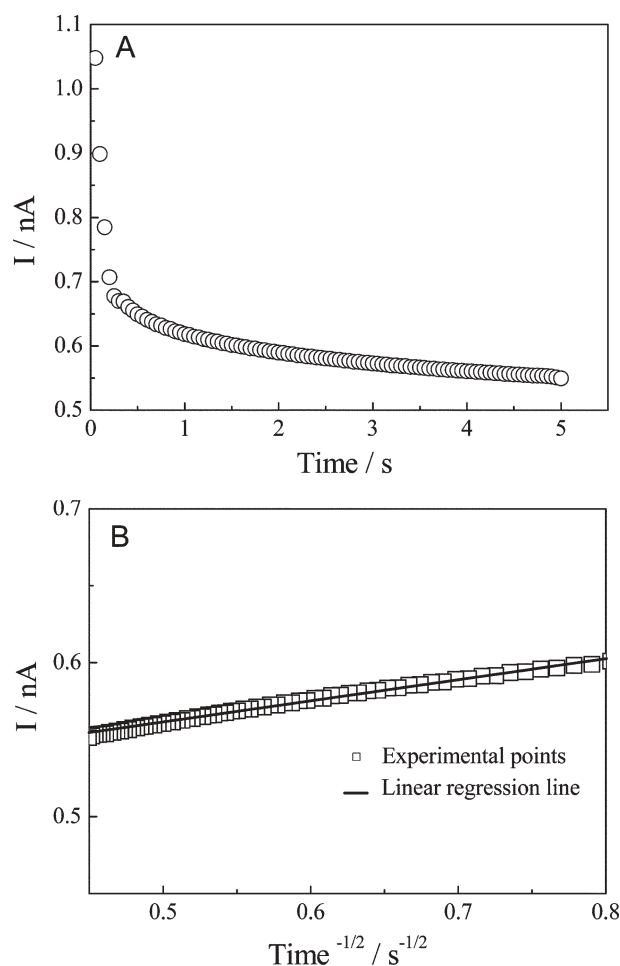
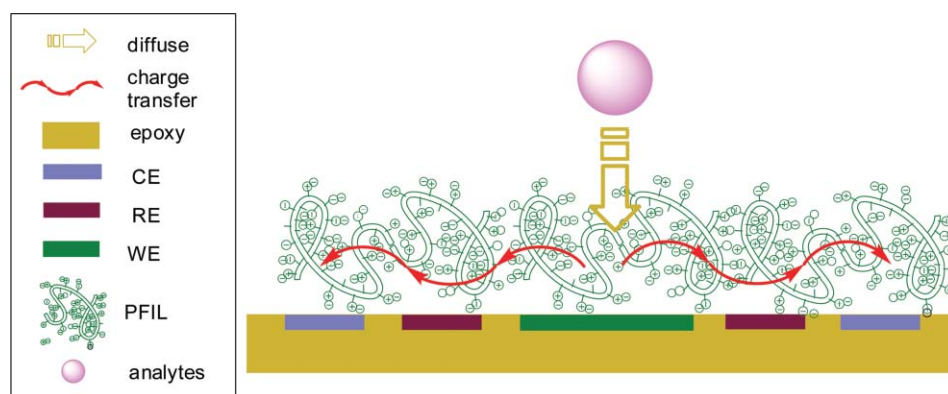


Fig. 6 (A) Chronoamperometry for HQ oxidation at the Pt micro-electrode/PFIL interface in 1 mM HQ solution. The potential was first held at 0.1 V for 20 s, then stepped to 0.45 V for 5 s. (B) The resulting I vs. $t^{-1/2}$ plots.

3.2 Application in amperometric flow analysis

Within the past years, the amperometric detection in supporting electrolyte-free solution in a flow system has received increasing interest.^{49–52} In this work, we will demonstrate how the PFIL-modified electrode assembly can be used in flow injection analysis (FIA) in supporting electrolyte-free solutions.^{37–43} The structure of a detection cell for the flow system was shown in Scheme 2(B).

Fig. 7(A) displays the amperometric responses of the repeated injection of 20 μM HQ in a supporting electrolyte-free solution. The potential of the electrode was held at +0.3 V. The current response remained almost unchanged upon continuous running for several hours. The relative standard deviation was 0.66% ($n = 11$). It should be noted that even after hundreds of repeated cycles; only a small decrease in current response was observed, indicating that the PFIL film on the electrode assembly is rather stable. The response time was determined by the passage of the sample zone over the PFIL-modified electrode assembly.⁵³ As can be seen in Fig. 7, the response time is rather long, even at a few minutes. This is due to the flow cell design where all three electrodes had to be covered by the PFIL film (the



Scheme 3 Illustration of the electrochemical process of the analytes at the PFIL-modified electrode assembly in a supporting electrolyte-free solution.

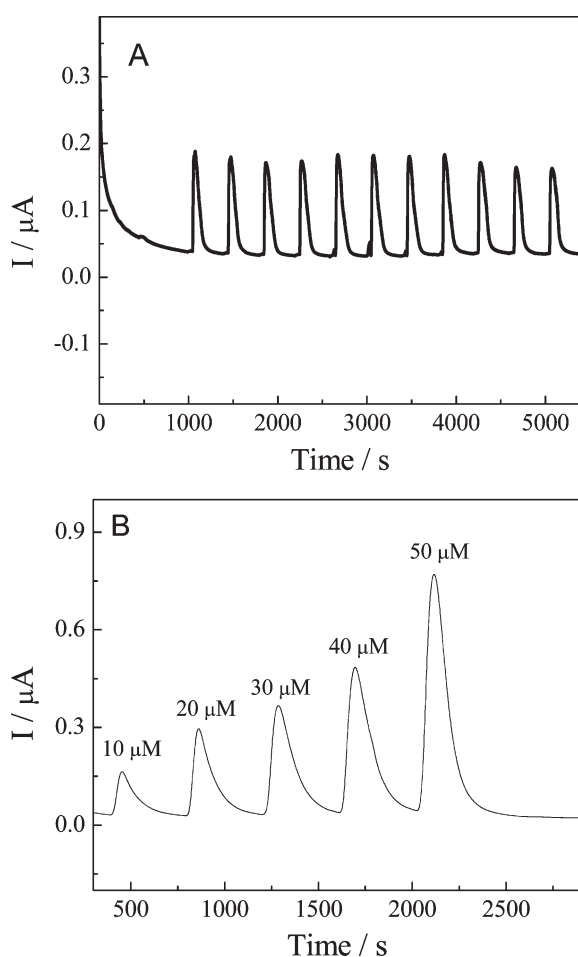


Fig. 7 (A) Amperometric responses of repeated injection of a 20 μM HQ solution. (B) Amperometric response of HQ at different concentrations. The signal was recorded at the 1.4 μm thick PFIL-modified electrode assembly at +0.3 V. Double-distilled water was used as the carrier solution. Flow rate: 1 mL min^{-1} .

diameter of the glassy carbon electrode was 3 mm and the diameter of the electrode assembly was 10 mm). This construction resulted in a rather big dead volume of the cell. For practical assay work, the cell design and flow rate should be optimized.

Fig. 7(B) shows successive injections of HQ at different concentrations. The current is linear with the concentration of HQ. Similar results have been obtained with some other ion-exchange membranes employed in electrochemical flow systems without any added supporting electrolyte.^{37–43} The advantage of our approach is that we do not need any internal electrolyte in the flow cell construction. Another advantage in our system is that the PFIL film has good dissolving properties for many analytes. The FIA results obtained clearly show the good properties of the PFIL-modified electrode in amperometric detection. The same system can certainly also be used in the HPLC-electrochemical detection (HPLC-ECD) system in supporting electrolyte-free solutions.

3.3 Electrochemical behavior with charged analytes

It should be admitted that the PFIL we have demonstrated here is a cationic polyelectrolyte and some special attention should be paid when PFIL is applied to cationic analytes in practical analytical work. For example, $\text{Fe}(\text{CN})_6^{3-/4-}$ exhibits surface-enhanced redox waves at the PFIL-modified electrode assembly (Fig. 8). The peak current increased little with time, indicating the enrichment behavior of $\text{Fe}(\text{CN})_6^{3-/4-}$ at the PFIL-modified electrode assembly [Fig. 8(A)]. And when this electrode was put back into pure water, the current decreased gradually with time [Fig. 8(B)]. Therefore, it is beneficial for the detection of negative analyte species at low-concentration due to significant enrichment of the analyte species in the PFIL film. In contrast, no redox response was found for $\text{Ru}(\text{NH}_3)_6^{3+/2+}$ at the PFIL-modified electrode assembly due to electrostatic expulsion [Fig. 8(C)]. Fortunately, the structure of this kind of PFIL can be designed to be a cationic or an anionic polyelectrolyte if necessary.³ The tunable design makes this IL suitable for the detection of most cationic or anionic analytes. Therefore, this PFIL material can be used in electrochemical studies in supporting electrolyte-free solutions.

4. Conclusions

The results presented in this work show how a simple polyelectrolyte-functionalized ionic liquid (PFIL) covering the electrode assembly can be used in electrochemical studies

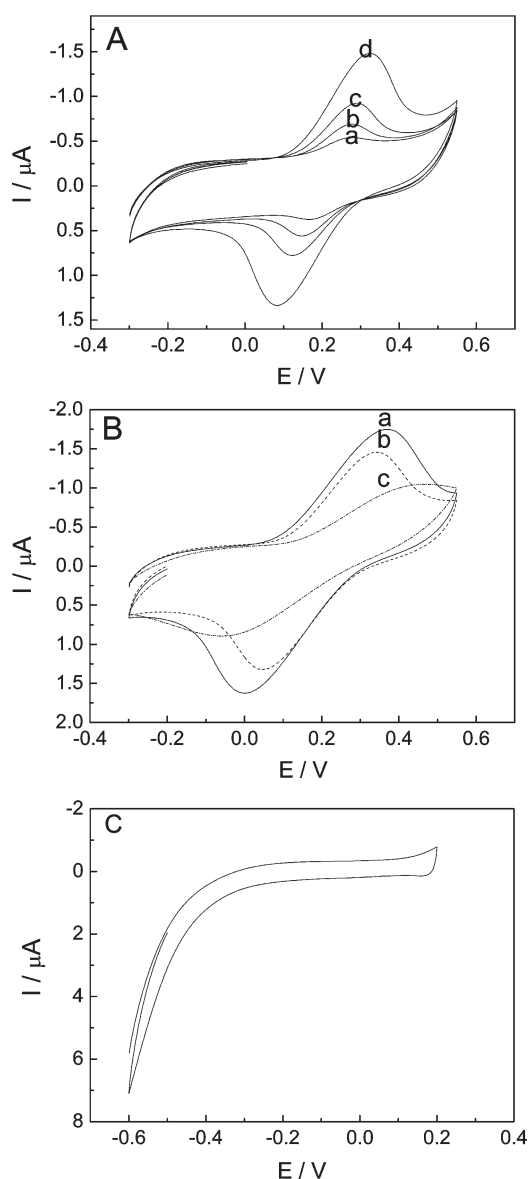


Fig. 8 (A) Cyclic voltammograms (CVs) at the PFIL-modified electrode assembly in 20 μM $\text{K}_3\text{Fe}(\text{CN})_6$ with different immersion times: (a) 0, (b) 4, (c) 7, and (d) 28 min. (B) CVs at the PFIL-modified electrode assembly which has been enriched with $\text{K}_3\text{Fe}(\text{CN})_6$ with different immersion times in H_2O : (a) 0, (b) 10, and (c) 28 min. (C) CV of 1 mM $\text{Ru}(\text{NH}_3)_6\text{Cl}_3$ at the PFIL-modified electrode assembly.

in aqueous solution without a supporting electrolyte. The electrochemical performance of the PFIL-modified electrode assembly in supporting electrolyte-free aqueous solutions was tested with hydroquinone (HQ) as the model compound. The electrochemical reactions take place in the thin PFIL film covering the three electrodes. The analyte has first to enter the PFIL film before any electrochemical reaction can take place. By proper design of the polyelectrolyte, either anionic or cationic species can be excluded in entering the film, and in that way selectivity can also be enhanced. Because the ionically conductive PFIL film covers all of the three electrodes, it is not necessary to have any supporting electrolyte in the carrier solution in amperometric flow injection analysis (FIA)

experiments. The PFIL film can prevent any possible short cuts in amperometric detection, e.g. air bubbles entering the flow system. The same detection concept can also be used in the HPLC-electrochemical detection (HPLC-ECD) system in supporting electrolyte-free solution. The electrochemical system developed in this work can be used in other fields of electrochemistry in supporting electrolyte-free solutions as a green process, such as electrochemical synthesis, and electrolysis in industry. To realize the full potential of such polyelectrolytes grafted with ionic liquid for electrochemistry in supporting electrolyte-free solutions, we are currently investigating the influence of different kinds of ionic liquid polyelectrolytes, such as anionic and cationic ionic liquid polyelectrolytes.

Acknowledgements

The authors would like to thank the referees for their helpful comments on the manuscript. The authors are most grateful to the NSFC, China (No.20475053 and No. 20673109) and to Department of Science and Technology of Jilin Province (No.20050102) for the financial supports. In addition, the joint project between Chinese and Finnish research groups sponsored by NSFC, China and Academy of Finland should also be acknowledged.

References

- 1 J. G. Huddleston, A. E. Visser, W. M. Reichert, H. D. Willauer, G. A. Broker and R. D. Rogers, *Green Chem.*, 2001, **3**, 156–164.
- 2 *Ionic Liquids: Industrial Applications for Green Chemistry*, ed. R. D. Rogers and K. R. Seddon, American Chemical Society, Washington, DC, 2002.
- 3 H. Ohno, *Electrochemical Aspects of Ionic Liquids*, Wiley-VCH, Weinheim, 2005.
- 4 J. L. Anderson, D. W. Armstrong and G.-T. Wei, *Anal. Chem.*, 2006, **78**, A2892–2902.
- 5 Y. Gao, N. Li, L. Q. Zheng, X. Y. Zhao, S. H. Zhang, B. X. Han, W. G. Hou and G. Z. Li, *Green Chem.*, 2006, **8**, 43–49.
- 6 J. H. Li, Y. F. Shen, Y. J. Zhang and Y. Liu, *Chem. Commun.*, 2005, 360–362.
- 7 M. C. Kroon, W. Buijs, C. J. Peters and G. J. Witkamp, *Green Chem.*, 2006, **8**, 241–245.
- 8 T. Hatazawa, R. H. Terrill and R. W. Murray, *Anal. Chem.*, 1996, **68**, 597–603.
- 9 T. T. Wooster, M. L. Longmire, H. Zhang, M. Watanabe and R. W. Murray, *Anal. Chem.*, 1992, **64**, 1132–1140.
- 10 L. Geng, R. A. Reed, M. Longmire and R. W. Murray, *J. Phys. Chem.*, 1987, **91**, 2908–2914.
- 11 J. F. Parcher, C. J. Barbour and R. W. Murray, *Anal. Chem.*, 1989, **61**, 584–589.
- 12 J. W. Long, C. S. Velazquez and R. W. Murray, *J. Phys. Chem.*, 1996, **100**, 5492–5499.
- 13 M. Morita, M. L. Longmire and R. W. Murray, *Anal. Chem.*, 1988, **60**, 2770–2775.
- 14 V. Cammarata, D. R. Talham, R. M. Crooks and M. S. Wrighton, *J. Phys. Chem.*, 1990, **94**, 2680–2684.
- 15 T. E. Mallouk, V. Cammarata, J. A. Crayston and M. S. Wrighton, *J. Phys. Chem.*, 1986, **90**, 2150–2156.
- 16 R. Balasubramanian, W. Wang and R. W. Murray, *J. Am. Chem. Soc.*, 2006, **128**, 9994–9995.
- 17 F. Mao, N. Mano and A. Heller, *J. Am. Chem. Soc.*, 2003, **125**, 4951–4957.
- 18 T. J. Ohara, R. Rajagopalan and A. Heller, *Anal. Chem.*, 1993, **65**, 3512–3517.
- 19 F. Opekar and K. Stulik, *Anal. Chim. Acta*, 1999, **385**, 151–162.
- 20 G. Schiavon, G. Zotti, R. Toniolo and G. Bontempelli, *Anal. Chem.*, 1995, **67**, 318–323.

- 21 M. Ciszowska and Z. Stojek, *Anal. Chem.*, 2000, **72**, 754A–760A.
- 22 A. M. Bond and S. W. Feldberg, *J. Phys. Chem. B*, 1998, **102**, 9966–9974.
- 23 W. Hyk and Z. Stojek, *Anal. Chem.*, 2002, **74**, 4805–4813.
- 24 M. B. Rooney, D. C. Coomber and A. M. Bond, *Anal. Chem.*, 2000, **72**, 3486–3491.
- 25 J. Szymanska, M. J. Palys and B. Van den Bossche, *Anal. Chem.*, 2004, **76**, 5937–5944.
- 26 A. W. E. Hodgson, P. Jacquinot and P. C. Hauser, *Anal. Chem.*, 2000, **72**, 2206–2210.
- 27 N. P. C. Stevens, M. B. Rooney, A. M. Bond and S. W. Feldberg, *J. Phys. Chem. A*, 2001, **105**, 9085–9093.
- 28 P. Jacquinot, A. W. E. Hodgson and P. C. Hauser, *Anal. Chim. Acta*, 2001, **443**, 53–61.
- 29 R. Toniolo, N. Comisso, G. Schiavon and G. Bontempelli, *Anal. Chem.*, 2004, **76**, 2133–2137.
- 30 T. Tajima and T. Fuchigami, *Angew. Chem., Int. Ed.*, 2005, **44**, 4760–4763.
- 31 T. Tajima and T. Fuchigami, *J. Am. Chem. Soc.*, 2005, **127**, 2848–2849.
- 32 Z. Liu, J. Li, S. Dong and E. Wang, *Anal. Chem.*, 1996, **68**, 2432–2436.
- 33 U. Rückert, K. Eggenreich, R. Wintersteiger, M. Wurglics, W. Likussar and A. Michelitsch, *J. Chromatogr., A*, 2004, **1041**, 181–185.
- 34 See ESI† for the application of HPLC-ECD accessed from http://www.esainc.com/applications/esa_applications.htm on 14 September 2006.
- 35 C. Y. Kuo and S.-M. Wu, *J. Chromatogr., A*, 2005, **1088**, 131–135.
- 36 See ESI† for the application of HPLC-ECD accessed from http://www.esainc.com/products/ECD_faqs.htm on 14 September 2006.
- 37 T. W. Kaaret and D. H. Evans, *Anal. Chem.*, 1988, **60**, 657–662.
- 38 D. W. D. Wulf and A. J. Bard, *J. Electrochem. Soc.*, 1988, **135**, 1977–1985.
- 39 X. K. Xing and C. C. Liu, *Electroanalysis*, 1991, **3**, 111–117.
- 40 L. R. Jordan and P. C. Hauser, *Anal. Chem.*, 1997, **69**, 2669–2672.
- 41 C. A. Paddon, G. J. Pritchard, T. Thiemann and F. Marken, *Electrochem. Commun.*, 2002, **4**, 825–831.
- 42 D. Lee, J. C. Hutchison, A. M. Leone, J. M. DeSimone and R. W. Murray, *J. Am. Chem. Soc.*, 2002, **124**, 9310–9317.
- 43 R. Horcajada, M. Okajima, S. Suga and J. Yoshida, *Chem. Commun.*, 2005, 1303–1305.
- 44 Y. F. Shen, Y. J. Zhang, Q. X. Zhang, L. Niu, T. Y. You and A. Ivaska, *Chem. Commun.*, 2005, 4193–4195.
- 45 S. Wang and D. Du, *Sensors*, 2002, **2**, 41–49.
- 46 L. Zhang, C. Hampel and S. Mukerjee, *J. Electrochem. Soc.*, 2005, **152**, A1208–A1216.
- 47 K. L. Huang, T. M. Holsen and J. R. Selman, *Ind. Eng. Chem. Res.*, 2003, **42**, 3620–3625.
- 48 A. Goswami, A. Acharya and A. K. Pandey, *J. Phys. Chem. B*, 2001, **105**, 9196–9201.
- 49 E. F. Sullenberger, S. F. Dressmen and A. C. Michael, *J. Phys. Chem.*, 1994, **98**, 5347–5354.
- 50 R. Toniolo, N. Comisso, G. Bontempelli, G. Schiavon and S. Sitran, *Electroanalysis*, 1998, **10**, 942–947.
- 51 I. Lahdesmaki, A. Lewenstam and A. Ivaska, *Talanta*, 1996, **43**, 125–134.
- 52 I. Lahdesmaki, J. Ruzicka and A. Ivaska, *Analyst*, 2000, **125**, 1889–1895.
- 53 H. Kahlert, J. R. Porsen, I. Isildak, M. Andac, M. Yolcu, J. Behnert and F. Scholz, *Electroanalysis*, 2005, **17**, 1085–1090.

Synthesis of a novel cardanol-based benzoxazine monomer and environmentally sustainable production of polymers and bio-composites

Emanuela Calò,^a Alfonso Maffezzoli,^a Giuseppe Mele,^{*a} Francesca Martina,^a Selma E. Mazzetto,^b Antonella Tarzia^c and Cristina Stifani^c

Received 23rd November 2006, Accepted 27th February 2007

First published as an Advance Article on the web 19th March 2007

DOI: 10.1039/b617180j

A novel pre-polymer deriving from cardanol—a well known renewable organic resource and harmful by-product of the cashew industry—in combination with cellulose based materials (*i.e.* jute fibres) has been used to produce bio-composites having a high percentage of renewable materials. Cardanol and its derivatives are considered nowadays very attractive precursors to developing new materials from renewable bio-sources to use in eco-friendly processes. This paper deals with the synthesis and characterization of a novel cardanol based benzoxazine monomer used for the preparation of new bio-composites. The new cardanol-based benzoxazine was characterised by ¹H and ¹³C NMR, FT-IR spectroscopies and LC mass spectrometry analysis, while a differential scanning calorimeter was used to study and monitor the polymerization process. Different bio-composites have been obtained by thermal cure of jute fibres impregnated with a cardanol based benzoxazine resin.

Introduction

Phenol–formaldehyde resins were the first fully synthetic commercial polymer resins and were first described over 100 years ago. Because of their relatively low cost and their dimensional stability, the resole type resins are still largely used in the industry of polymeric materials.

More recently, the development of the benzoxazine-based family of phenolic resins has attracted significant attention. Particular attention was devoted to the synthesis of polybenzoxazines, one of a series of phenolic-type polymers with good thermal and mechanical properties. In fact, these new materials combine the thermal properties and flame retardance of phenolics and the mechanical performance and molecular design flexibility of advanced composites.^{1,2} For this reason, the new polybenzoxazines showed physical and mechanical properties comparable with those of conventional phenolic and epoxy resins. Benzoxazines are bicyclic heterocycles (see Fig. 1) generated by the Mannich-like condensation of a phenol, formaldehyde and an amine.^{3–8} Moreover,

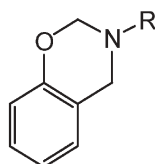


Fig. 1 Structure of a 3,4-dihydro-2H-1,3-benzoxazine.

^aDipartimento di Ingegneria dell'Innovazione, Università del Salento, Via Arnesano, 73100, Lecce, Italy. E-mail: giuseppe.mele@unisalento.it; Fax: +39 0832 297279; Tel: +39 0832 297281

^bDepartamento de Química Orgânica e Inorgânica – Universidade Federal do Ceará-UFC, Caixa Postal 12.200, 60455-760, Fortaleza, CE, Brazil

^cCimtecLab s.r.l, via Piave n 10, Monteroni, LE

polybenzoxazines, one of a series of phenolic-type polymers, which are generated upon thermal polymerization from various types of substituted 3,4-dihydro-2H-1,3-benzoxazines, offer excellent mechanical, physical and thermal properties due to the phenolic groups, Mannich base linkages and the existence of extensive inter- and intramolecular hydrogen bonds. A great deal of effort was expended towards the understanding the curing chemistry of these resins.

On the other hand, the development of new polymers, especially those based on renewable organic raw materials using alternative sustainable processes, deserve the attention of both academic and industrial research.

Cardanol is an industrial grade yellow oil obtained by vacuum distillation of “cashew nut shell liquid” (CNSL), the international name of the alkyl phenolic oil contained in the spongy mesocarp of the cashew nut shell from the cashew tree *Anacardium occidentale* L. (Fig. 2).

CNSL derived from the most diffused roasted mechanical processes of the cashew industry represents nearly 25% of the total nut weight, and its production worldwide (Africa, Asia, and South America being the main producer areas) is estimated to be about 300 000 tons per year. In addition, CNSL represents a powerful phenolic pollutant of the cashew agro industry.

CNSL, indeed, is a mixture of anacardic acid, cardanol, and traces of cardol and 2-methylcardol, as shown in Fig. 3. The alkyl side chain (R) of each of them may be saturated, monolefinic (8), diolefinic (8, 11) or triolefinic (8, 11, 14), with a high percentage of the components having one or two double bonds per molecule.^{9,10}

Due to the easy thermic decarboxylation of anacardic acid during the distillation process, cardanol is the main component of distilled CNSL (see Table 1).¹¹

CNSL, as well as cardanol, can be considered a sustainable, low cost and largely available natural resource by-product of



Fig. 2 Picture of cashew tree with fruits and nuts.

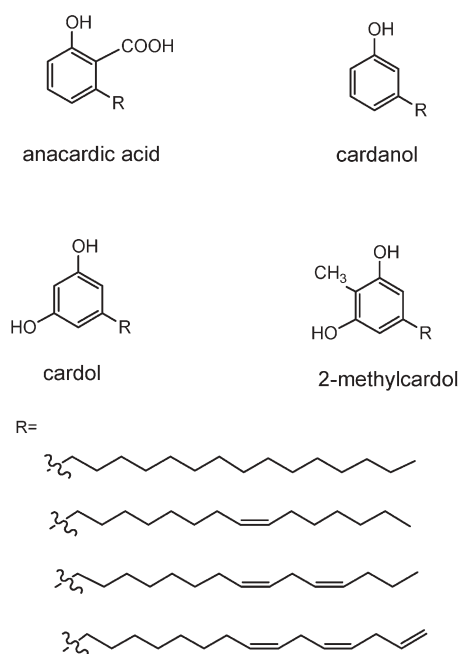


Fig. 3 Main components of CNSL.

the cashew industry. Therefore, CNSL, as well as cardanol and its derivatives, are becoming important starting materials having possible industrial utilizations, such as additives for lubricants, diesel engine fuels, pour point depressant,

Table 1 Chemical composition of CNSL *in natura* and technical grade

Components	Room temperature extraction	High temperature (80–200 °C) extraction
Anacardic acid	71.7	1.1
Cardol	18.7	18.2
Cardanol	4.7	67.8
Methyl cardol	2.7	3.3
Unidentified products	2.2	2.2
Polymerised products	—	7.4

antioxidants, stabilizers, flame retardants, resins, inks, hydro-repellents as well as fine chemicals and intermediates.^{12–23}

The increasing interest to develop renewable cardanol-cellulose based materials prompted us to investigate the synthesis and characterization of a novel cardanol-based resin having a benzoxazine structure, thermal and cationic catalyzed polymerization of the benzoxazine monomer, as well as its formulation for the production of cellulose-based bio-composites, pursuing the strategies to minimise the environmental impact of new materials and processes.

Experimental

Materials and methods

Cardanol was kindly supplied by Oltremare Spa (Bologna, Italy).

The aqueous solutions of ammonia (30% w/w) and formaldehyde (37% w/w) were purchased from Aldrich Chemical Co. and used as received. Silica gel (Merck) was used in the chromatographic separations. Jute fibres were supplied by Companhia Jauense Industrial (Jaú, Brazil). The fibres were previously cut (40 cm × 35 cm in length), washed with water and neutral detergent to remove residue, and washed with distilled water at room temperature. The fibres were dried and kept in a desiccator to avoid humidity excess. Solutions of NaOH and NaClO (both Aldrich) were prepared for fiber bleaching and were used without any previous treatment. Mercerization: dried jute fibres were treated with 5% and 10% NaOH solutions respectively, at temperature intervals of 60–70 °C, for 6 hours for removal of lignin, cellulose and other residues. After this period, the fibres were submitted to washing several times with distilled water to remove sodium hydroxide excess from the surface.

Measurements

FT-IR spectra were obtained on a Jasco 430; ¹H and ¹³C NMR spectra were taken on a Bruker 400 Ultrashield™ spectrometer with proton frequency of 400 MHz and with deuterated chloroform as solvent.

Mass spectrometry analyses were carried out by using an LC mass spectrometer (LC-MS) 1100 Series (Agilent) equipped with electrospray ionization interface (ESI).

The samples, dissolved in chloroform, were injected into the mass spectrometer by an auto sampler spraying an acetonitrile–water (90 : 10) solution at a flow rate of 0.6 mL min^{−1}. Positive ions were extracted *via* a heated capillary to a skimmer lens arrangement at reduced pressure and transferred by an octapole to the main analytical quadrupole assembly. The instrumental conditions were: drying gas (nitrogen) 10 L min^{−1}, nebulizer pressure 60 psi, drying gas temperature 350 °C, mass range 100–1000 a.m.u.

Viscosity measurements were carried out using a strain-controlled rheometer Rheometric ARES and repeated twice to assess the reproducibility of the results. The viscosity of the freshly prepared benzoxazine was 0.43 Pa s measured at 28 °C using a shear rate of 0.8–100 s^{−1}.

A Perkin Elmer DSC-7 Differential Scanning Calorimeter (DSC) was employed, in order to monitor the polymerization

reactions of benzoxazine and to measure the polymer glass transition temperature (T_g). Each dynamic scan was performed by heating a sample at $10\text{ }^\circ\text{C min}^{-1}$ under nitrogen purge at a constant flow rate of 20 ml min^{-1} .

Synthesis of the benzoxazine (Bz)

136.46 g of cardanol, 12.80 g of aqueous solution of ammonia (30% w/w) and 54.95 g of formaldehyde (37% w/w in aqueous solution) were placed in a 500 ml three-neck round flask equipped with magnetic stirrer, thermometer and reflux condenser. The mixture was heated under stirring at $75\text{--}80\text{ }^\circ\text{C}$ for 3 hours. The crude of the reaction, conveniently diluted by addition of chloroform was thoroughly washed by distilled water using a separating funnel; then, the organic phase was collected, dried with anhydrous sodium sulfate and filtered. The solvent was removed under vacuum and the crude product was purified by column chromatography using chloroform as eluent. A consistent amount of benzoxazine was isolated and characterised by ^1H and ^{13}C NMR, FT-IR spectroscopies and LC-MS analysis.

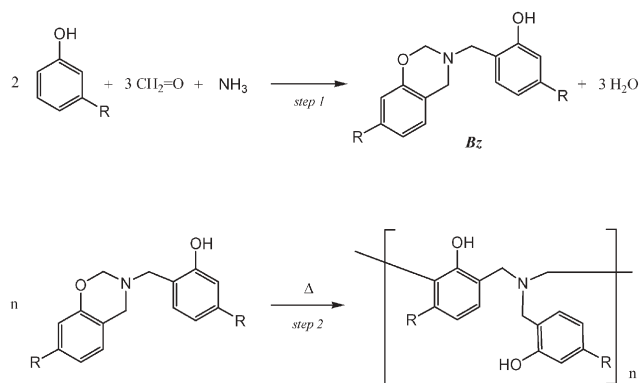
Selected data for Bz. Elemental analysis: C, 82.24; H, 10.76; N, 2.13; O, 4.87. LC-MS (ESI interface—positive ions): cluster of signals due to $(\text{Bz} + \text{H})^+$ adducts centered respectively at m/z 652, 654, 656, 658, 660 amu. ^1H NMR (400 MHz, CDCl_3): δ = 6.90–6.63 (aromatic protons), 5.45–5.37 (vinylic protons, $=\text{C}-\text{H}$), 4.89 (s, $-\text{OCH}_2\text{N}-$), 4.07 (s, $\text{ArCH}_2\text{N}-$), 4.03 (s, $\text{ArCH}_2\text{N}-$), 2.90–2.70 (aliphatic CH_2 protons), 2.57 (t, J = 7.8 Hz, benzylic CH_2), 2.20–2.00 (aliphatic CH_2 protons), 1.70–1.50 (aliphatic CH_2 protons), 1.29 (aliphatic CH_2 protons), 0.90–1.00 (CH_3 protons) ppm. ^{13}C NMR (100.64 MHz, CDCl_3): δ = 157.87, 153.54, 144.96, 143.74, 130.83, 130.80, 130.56, 130.40, 130.37, 130.28, 130.25, 129.75, 129.55, 128.62, 128.46, 128.43, 128.05, 128.02, 127.89, 127.25, 121.99, 120.14, 118.50, 116.73, 116.19, 115.14, 81.10, 55.87, 54.94, 49.37, 36.15, 36.11, 32.37, 32.23, 31.96, 31.75, 31.70, 30.20, 30.18, 30.15, 30.11, 30.07, 29.86, 29.85, 29.81, 29.77, 29.74, 29.66, 29.43, 27.64, 26.10, 26.02, 23.24, 23.10, 14.54, 14.24. FT-IR (cm^{-1}): 1578, 1505, 1240, 1164, 1107, 978.

Results and discussion

The novel cardanol based benzoxazine (Bz) used as monomeric starting material for the polymerization reaction was prepared by a condensation reaction of cardanol with formaldehyde, in the presence of ammonia, as shown in Scheme 1 (step 1).

Cardanol and, consecutively, the aqueous solutions of ammonia and formaldehyde were placed in a 500 ml three-neck round flask. The mixture was heated under stirring at $75\text{--}80\text{ }^\circ\text{C}$ for 3 hours; after appropriate work-up, a consistent amount of benzoxazine was isolated and characterised (see Experimental). The ^1H NMR spectrum was consistent with the proposed benzoxazinic structure; it shows three typical singlets centered respectively at 4.89, 4.08 and at 4.03 ppm due to the hydrogen atoms of the three nitrogen bonded methylene groups.

^{13}C resonances at 49.37, 54.94 and 81.10 ppm present in the spectrum for Bz monomer are also diagnostic for benzoxazine systems.²⁴ The FT-IR spectrum of the benzoxazine shows



Scheme 1

significant bands respectively at 1578, 1505, 1107, 978 cm^{-1} , some of which are typical of benzoxazine structures.²⁵

The liquid mass spectrum of Bz, showed a cluster of signals of the positively charged benzoxazinic $(\text{Bz} + \text{H})^+$ adducts centered, respectively, at m/z 652, 654, 656, 658, 660 amu, as expected by using the ESI interface and corresponding to the molecular ion peaks of variously unsaturated benzoxazinic adducts.

The typical polymerisation process to obtain polybenzoxazines is based on the ring opening of benzoxazine monomer.

In this work, the Bz monomer was polymerised using different processes: (a) thermal polymerization, (b) catalytic polymerization by phosphorus pentachloride (PCl_5), (c) thermal polymerization of Bz impregnated jute fibres to produce bio-composites.

Thermal polymerization of Bz

Thermal polymerization was achieved, as shown in the Scheme 1 (step 2), by heating—in the DSC instrument (Fig. 4)—the Bz monomer at $10\text{ }^\circ\text{C min}^{-1}$ in nitrogen atmosphere from $25\text{ }^\circ\text{C}$ to $300\text{ }^\circ\text{C}$. A second scan was carried out, on the cured sample, at $10\text{ }^\circ\text{C min}^{-1}$ from $-60\text{ }^\circ\text{C}$ to $140\text{ }^\circ\text{C}$, for the measurement of T_g . The first scan was used to calculate a heat of reaction of 61 J g^{-1} using the baseline

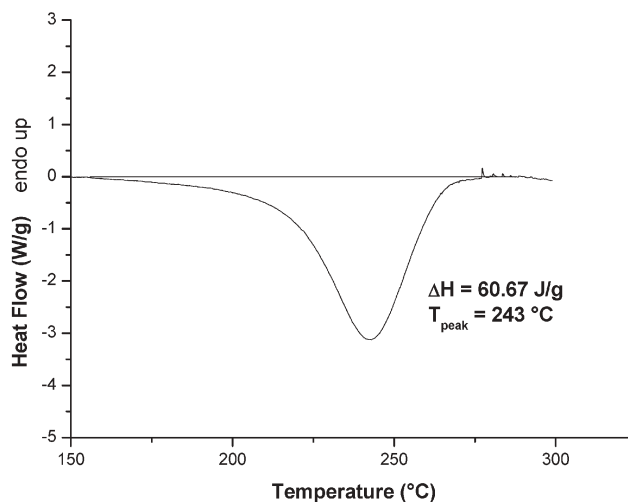


Fig. 4 DSC thermogram of the cure of Bz monomer.

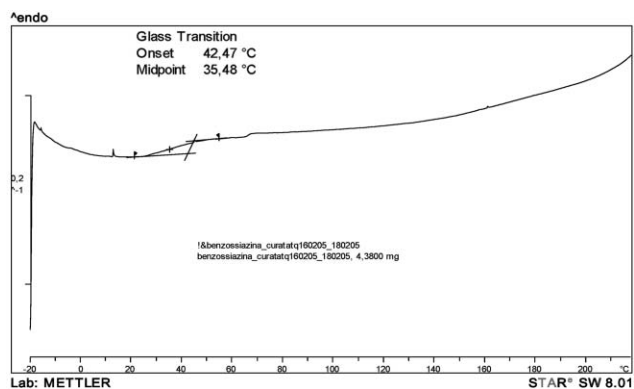


Fig. 5 Thermogram of thermally polymerised Bz (second scan) for T_g determination.

reported in Fig. 4. The obtained polymer is solid at room temperature and it was characterised by a T_g of 36 °C, as revealed by a second DSC scan (Fig. 5).

In accordance with that reported in the literature,^{1,2,25,26} thermal treatment of Bz produced the ring opening typical of benzoxazines, by ring cleavage of the $\text{CH}_2\text{-O}$ bond and successive polymerization as reported in Scheme 2 as also confirmed by FT-IR analysis (see Fig. 6).

As shown in Fig. 6, the disappearance of the peak at 3006 cm^{-1} —typical of the C–H vinylic stretching present in the cardanol chain in Bz monomer—confirms the reactivity of the double bond(s) at high temperature occurring after the thermal treatment of Bz, with the possible production of a network of cross linked material.

The formation of imine groups (-N=CH-)—also observed during the thermal cure of novolac resins with hexamethylenetetramine²⁷—as well the formation of carbonyl groups evidenced for the thermo-oxidative degradation of polybenzoxazines²⁸ can not be excluded. In this way, the presence of a large peak in the range of $1640\text{--}1760\text{ cm}^{-1}$ was justified (see dotted line in Fig. 6).

Catalytic polymerization of Bz. A number of catalysts as initiators have been used in order to induce the ring-opening (cationic, anionic, and radical) polymerization of benzoxazines. Recently, Ishida *et al.* reported the cationic ring-opening polymerisation of benzoxazines.

Among the various cationic initiators, phosphorus pentachloride (PCl_5) was used efficiently for the polymerisation reaction of benzoxazine monomers in chloroform solution.²⁵

In particular, in our case, the polymerisation reaction was carried out as shown in Scheme 2 (step 1), following a

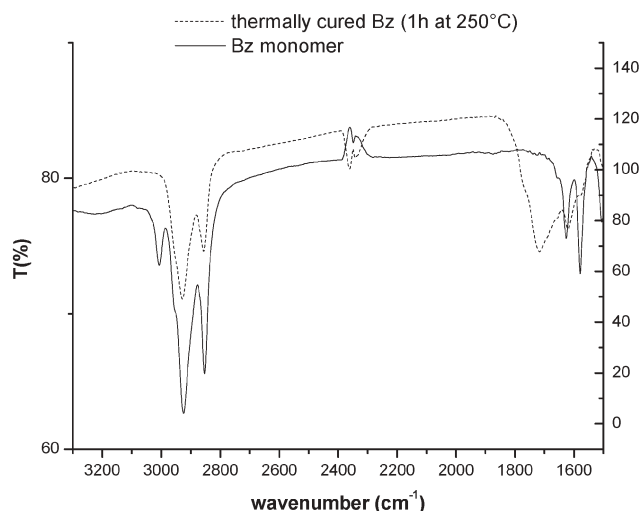


Fig. 6 Comparison of a portion of FT-IR spectra of Bz monomer (solid line) and thermally polymerised Bz (dotted line).

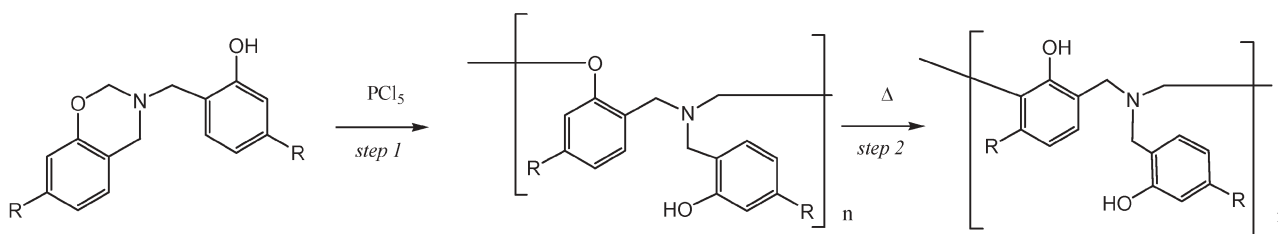
procedure similar to that already reported in literature²⁵ (molar ratio of PCl_5 : Bz was 1 : 100) using a dry glove box under nitrogen atmosphere to reduce the high reactivity of PCl_5 with wet air and/or oxygen. The initiator was added at room temperature and the reaction continued at the same temperature for a few minutes, leading to polymerised thermoplastic material after chloroform was removed by rotavapor under vacuum.

The FT-IR spectrum of the cationically polymerised benzoxazine showed the disappearance of the peak centered at 1575 cm^{-1} as well as the presence of typical signals at 1625, 1463, 1421, 1307, 1240, 1105, 994 cm^{-1} .

A relatively weaker band in the range $3200\text{--}3500\text{ cm}^{-1}$ due to the stretching of -O-H groups could be ascribed to the “free” OH groups, many of which are in the polymer chain (Scheme 2, step 1).

The thermal treatment of the catalytic polymerization product of Bz (carried out by DSC at 10 °C min^{-1} from 25 °C to 300 °C under nitrogen atmosphere) evidenced a feeble exothermic reaction peak (8.97 J g^{-1} at 220 °C), ascribed to structural changes of the catalytically obtained polymer converted into the thermal obtained one as shown in Scheme 2 (step 2).

The comparison of FT-IR spectra demonstrates that different polymeric structures were produced by PCl_5 catalyzed ring opening or thermal cure of Bz monomer, as well as the structural analogies existing for the thermally cured polymer and cationically polymerised polymer after a thermal post-cure.



Scheme 2



Fig. 7 Jute fibres after alkali treatment.

The post-cure polymer spectrum shows a large peak in the range of $1750\text{--}1580\text{ cm}^{-1}$, also observed in Fig. 6, and not detected in the PCl_5 polymerised Bz. As expected, in the thermally cured polymer spectrum, the band at 1307 cm^{-1} arising from the CH_2 wagging mode disappears as well the band at 1107 cm^{-1} characteristic of C–O stretching, demonstrating that a different structure is obtained upon thermal treatment of the cationic polymerised Bz; a new band ascribable to the stretching of C–OH appears at 1086 cm^{-1} . These results suggest that the cationically polymerised Bz heated up to $260\text{ }^\circ\text{C}$ is transformed in a structure similar to that obtained after thermal polymerization of Bz (Scheme 2, step 2).

In light of these considerations, as well taking into account the fact that PCl_5 has a relatively high toxicity, although its catalytic properties gave rapid polymerization at ambient temperature, the bio-composites materials were prepared only by thermal cure of natural fibres impregnated with the cardanol based benzoxazine resin.

Preparation of composite materials reinforced with natural jute fibres

Part of the present work is aimed at the preparation and characterization of cardanol based benzoxazine matrix composites, reinforced by jute fibres.

It is well known that plant fibres are renewable and biodegradable natural cellulosic materials.

In particular, fibres are an important alternative, offering several advantages such their abundance, biodegradability, light weight, renewability, negligible toxicity, low cost and properties comparable with those of glass, carbon and aramid fibres. Moreover, they can be modified by a number of chemical treatments.

In our case, the surface modification on the fibres was carried out through alkali treatment (see Fig. 7), NaOH 5% and NaOH 10% ($75\text{ }^\circ\text{C}$), and bleaching with sodium hypochlorite ($\text{NaClO-H}_2\text{O}$ 1 : 1) ($60\text{ }^\circ\text{C}$).



Fig. 8 Jute fibres based composite.

The alkali treatment removed non-cellulosic components from the fiber surface, exposing their internal fibrillar structure. As a consequence, the treatment promoted an increase on interfacial adhesion between jute fibres with the benzoxazine matrix.

Subsequently, the cardanol based benzoxazine resins were used as building blocks for the development of a thermosetting matrix for composites. Bio-composites based on natural components were prepared by open mold and hand lay up impregnation of the fibres with the thermally polymerizable cardanol-based resin cured at a moderately high temperature.

Fig. 8 shows a bio-composite obtained by thermal cure of jute fibres impregnated with freshly prepared cardanol based benzoxazine resin. The results of the surface treatments on jute fibres resulted in an increase of mechanical properties of corresponding composites. The best mechanical performance was generally obtained for composites of jute after NaOH 5% and NaOH 10% treatment, showing an enhancement of mechanical properties, such as resistance at break (28% and 48%, respectively).

Moreover, a higher elongation to break and a lower void content indicate that the fiber treatment improves the composite quality. The reduced properties of the composite obtained with NaOH treated fibres can be explained by the lower fiber content (Table 2).

The final content of natural originating material in the benzoxazine resin is more than 75%, reaching more than 90% in the composite loaded with 33% by weight of natural fibres. Also, if a development route is successfully explored, more work is still needed in order to improve the mechanical properties of the resin, at the same time improving its glass transition temperature and further lowering the curing temperature. Future research efforts will be also devoted to the construction, by filament winding, of composites reinforced with long natural fibres in the form of a non-woven or rope like yarn, and to the improvement of their wettability with the cardanol based resin.

Conclusions

In this work, a new cardanol-based benzoxazine (Bz) was synthesised from cardanol—a well known renewable organic

Table 2 Composite properties depending on fiber treatment

Composite type	Fibre content (wt%)	Void content (%)	Density/ g cm^{-3}	Tensile modulus/MPa	Tensile strength/MPa	Elongation to break (%)
Benzoxazine/untreated jute fibres	33	15	0.930	4890	20.6	2.9
Benzoxazine/(5%) NaOH treated jute fibres	26	7	1.002	2006	13.07	6.6

resources and harmful by-product of the cashew industry—and successively polymerised to produce different polybenzoxazines depending on the polymerization method. Bz was characterised by analytical and spectral data.

Thermal polymerization of the Bz monomer during a DSC scan showed a polymerization reaction starting at 150 °C and characterised by a heat of polymerisation of about 61 J g⁻¹. A glassy polymer, characterised by a *T_g* of 36 °C, as revealed by a second DSC scan, is obtained at room temperature. Catalytic polymerization of Bz was obtained at ambient temperature by using PCl₅ as catalyst. Moreover, the catalytically polymerised Bz can be converted into in the thermally polymerised polymer by the subsequent thermal cure. Bz was also used as pre-polymer in combination with cellulose based materials (jute fibres) to produce novel bio-composite materials having a high percentage of renewable materials. In the light of these results, cardanol and its derivatives could be considered nowadays very attractive renewable bio-sources to use in eco-friendly processes.

Acknowledgements

Authors wish to thank the “Ministero dell’Istruzione, Università e Ricerca” (MIUR) for financial support of the project N. 8206. L. 297, D.M. 593.

The authors wish to thank Prof. Orazio Attanasi and Prof. Paolino Filippone for the useful discussions and suggestions.

References

- 1 X. Ning and H. Ishida, *J. Polym. Sci., Part A: Polym. Chem.*, 1995, **58**, 1751.
- 2 D. Ru Yei, H. K. Fu, W.-Y. Chen and F. C. Chang, *J. Polym. Sci., Part B: Polym. Phys.*, 2005, **44**, 347.
- 3 F. W. Holly and A. C. Cope, *J. Am. Chem. Soc.*, 1944, **66**, 1875.
- 4 W. J. Burke, *J. Am. Chem. Soc.*, 1949, **71**, 609.
- 5 W. J. Burke and C. Weatherbee, *J. Am. Chem. Soc.*, 1950, **72**, 4691.
- 6 W. J. Burke and C. W. Stephens, *J. Am. Chem. Soc.*, 1952, **74**, 1518.
- 7 W. J. Burke and K. C. Murdoch, *J. Am. Chem. Soc.*, 1954, **76**, 1677.
- 8 W. J. Burke, E. L. M. Glennie and C. Weatherbee, *J. Org. Chem.*, 1964, **24**, 909.
- 9 J. H. P. Tyman, *Synthetic and Natural Phenols*, Elsevier, Amsterdam, 1996.
- 10 O. A. Attanasi and P. Filippone, *Chim. Ind. (Milano)*, 2003, **85**, 11.
- 11 W. N. Milfont Jr, E. Monteiro and J. Dweck, *III Encontro Regional de Polimeros da ABPol Regional leste*, 2000.
- 12 O. A. Attanasi, S. Buratti and P. Filippone, *Org. Prep. Proced. Int.*, 1995, **27**, 653.
- 13 M. Coletta, P. Filippone, C. Fiorucci, S. Marini, E. Mincione, V. Neri and R. Saladino, *J. Chem. Soc., Perkin Trans. 1*, 2000, 581.
- 14 R. Amorati, G. F. Pedulli, L. Valgimigli, O. A. Attanasi, P. Filippone, C. Fiorucci and R. Saladino, *J. Chem. Soc., Perkin Trans. 2*, 2001.
- 15 G. John, M. Masuda, Y. Okada, K. Yase and T. Shimizu, *Adv. Mater.*, 2001, **13**, 715.
- 16 P. Filippone, V. Neri, E. Mincione and R. Saladino, *Tetrahedron*, 2002, **58**, 8493.
- 17 R. Amorati, O. A. Attanasi, B. El Ali, P. Filippone, G. Mele, J. Spadavecchia and G. Vasapollo, *Synthesis*, 2002, **18**, 2749.
- 18 O. A. Attanasi, G. Ciccarella, P. Filippone, G. Mele, J. Spadavecchia and G. Vasapollo, *J. Porphyrins Phthalocyanines*, 2003, **7**, 52.
- 19 O. A. Attanasi, P. Filippone, V. Neri, E. Mincione and R. Saladino, *Pure Appl. Chem.*, 2003, **75**, 261.
- 20 A. Maffezzoli, E. Calò, S. Zurlo, G. Mele, A. Tarzia and C. Stifani, *Comput. Sci. Technol.*, 2004, **64**, 839–845.
- 21 O. A. Attanasi, R. Del Sole, P. Filippone, R. Ianne, S. E. Mazzetto, G. Mele and G. Vasapollo, *Synlett*, 2004, **5**, 799–802.
- 22 G. Mele, R. Del Sole, G. Vasapollo, E. Garcia-López, L. Palmisano, S. E. Mazzetto, O. A. Attanasi and P. Filippone, *Green Chem.*, 2004, **6**, 604.
- 23 O. A. Attanasi, R. Del Sole, P. Filippone, S. E. Mazzetto, G. Mele and G. Vasapollo, *J. Porphyrins Phthalocyanines*, 2004, **08**, 1276.
- 24 Y. X. Wang and H. Ishida, *Macromolecules*, 2000, **33**, 2839.
- 25 Y. X. Wang and H. Ishida, *Polymer*, 1999, **40**, 4563.
- 26 C. P. Reghunadhan Nair, *Prog. Polym. Sci.*, 2004, **29**, 401–498.
- 27 Z. Xiaoping, M. G. Looney, D. H. Solomon and A. K. Whittaker, *Polymer*, 1997, **38**, 5835.
- 28 L. H. Yee and H. Ishida, *Polymer*, 1999, **40**, 4365.

Effects of different head groups and functionalised side chains on the cytotoxicity of ionic liquids†

Stefan Stolte,^a Jürgen Arning,^a Ulrike Bottin-Weber,^a Anja Müller,^a William-Robert Pitner,^b Urs Welz-Biermann,^b Bernd Jastorff^a and Johannes Ranke^{*a}

Received 20th October 2006, Accepted 14th February 2007

First published as an Advance Article on the web 9th March 2007

DOI: 10.1039/b615326g

To enlarge the restricted knowledge about the hazard potentials of ionic liquids to men and the environment we have concentrated on systematically analysing the effects of 7 head groups, 10 side chains (mainly containing functional groups) and 4 anions on cytotoxicity. For our investigations, we used the promyelotic leukemia rat cell line IPC-81 as test system, with the reduction of the WST-1 dye as an indicator of cell viability. Our results show that most of the tested 100 ionic liquids generally exhibit a low cytotoxicity compared to previously investigated ionic liquids in consequence of their polar ether, hydroxyl and nitrile functional groups within the side chains. Those functional groups hamper cellular uptake by membrane diffusion and reduce lipophilicity based interactions with the cell membrane.

In general, a low influence of the head group and a clear anion effect of the $[(CF_3SO_2)_2N]^-$ anion could be observed. Furthermore, we could confirm the general dependency between ionic liquid cation lipophilicity and cytotoxicity using a HPLC derived lipophilicity parameter. For one head group and for one side chain, deviations were obtained concerning this general dependency. This can be interpreted as a first hint for a more specific mode of action for these structural elements.

Introduction

Especially because of the imminent intensification of the EU chemicals legislation (REACH project), increasing importance is attached to the knowledge of (eco)toxicological hazard potentials of chemical substances. This requires efficient testing strategies to generate data sets leading to a profound insight in modes of toxic action and target sites of chemicals. Regarding this issue we follow a T-SAR^{1,2} (thinking in terms of structure activity relationships) guided strategy to:

- Systematically select test compounds and structural elements according to the “testkit concept”.^{2,3}
- Test the selected substances in a flexible (eco)toxicological test battery at different levels of biological complexity (*e.g.* enzymes, cells, microorganisms and organisms).³
- Identify toxicophore substructures in chemicals and to use this knowledge in the prospective design of inherently safer chemical products.
- Improve the molecular understanding of (eco)toxicological results by relating them to physicochemical properties.⁴

Following this concept, we are aiming to assess the hazard potential of ionic liquids. The interest in ionic liquids and in their promising physical and chemical properties is still growing rapidly. Diverse applications of ionic liquids in

different fields have been recently described.^{5–10} They are discussed as “green” or “sustainable” chemicals just based on their negligible vapour pressure, resulting in reduced inhalatory exposure and the absence of flammability. However, the knowledge about their (eco)toxicity is still very basic and restricted to only a few chemical entities out of the enormous pool of available ionic liquids.

To handle this structural variability, we subdivide ionic liquids into the following sub-structural elements: the cationic head group, the side chain and the corresponding anion. Following this classification we systematically examine the (toxic) effects of these structural elements on different test systems out of our flexible (eco)toxicological test battery. Recently we described the effects of the alkyl side chain length,¹¹ the cation lipophilicity⁴ and the anion¹² *inter alia* on the cytotoxicity.

The test kit presented here was assembled to identify the impact of further head groups and functionalised side chains on biological effects.

To attain the goal of producing more sustainable ionic liquids, which imply an optimum of technical applicability on the one hand and a minimum of hazard potentials for man and the environment on the other hand, we formed a university–industry partnership. Sustainable chemicals cannot be developed in academia alone because of the need for knowledge on current industrial products and processes. The Merck KGaA synthesised a set of ionic liquids—guided by the test kit concept and T-SAR—with the result of 100 new ionic liquids, which allows the systematic investigation of the impact of 7 different head groups, 10 side chains and 4 anions in (eco)toxicological studies.

^aUFT - Centre for Environmental Research and Technology, University of Bremen, Leobener Straße, Bremen, D-28359, Germany.

E-mail: jranke@uni-bremen.de

^bMerck KGaA, Frankfurter Straße 250, Darmstadt, D-64293, Germany

† Electronic supplementary information (ESI) available: Confidence intervals of the EC₅₀ values and a complete listing of the parameters of the fitted dose response models. See DOI: 10.1039/b615326g

Table 1 Structures of the tested head groups, side chains and their abbreviations. List of all EC₅₀ values as halides with the exact anion species in brackets

R	EC ₅₀ /μM (anion)							
Structure								
	Abbreviation	"Py-4NMe2"	"Py"	"IM1"	"Mor1"	"Pip1"	"Pyr1"	"N112"
-C ₂ H ₅	2	790 (Br)						
-CH ₂ CH ₂ -OH	2OH		14 300 (I)	>20 000 (I)	>20 000 (I)	>20 000 (I)	>20000 (I)	>20 000 (I)
-CH ₂ CN	1CN		6100 (Cl)	>20 000 (Cl)	>20 000 (Cl)	>20 000 (Cl)	17 100 (Cl)	>20 000 (Cl)
-C ₄ H ₉	4	85 (Cl)	8000 (Br)	3600 (Cl)	>20 000 (Br)	11 000 (Br)	>20 000 (Cl)	>20 000 (Cl)
-CH ₂ CH ₂ CH ₂ -OH	3OH		>20 000 (Cl)	>20 000 (Cl)	>20 000 (Cl)	>20 000 (Cl)	>20 000 (Cl)	
-CH ₂ -O-CH ₂ CH ₃	1O2		2100 (Cl)	4000 (Cl)	3300 (Cl)	17 200 (Cl)	850 (Cl)	3900 (Cl)
-CH ₂ CH ₂ -O-CH ₃	2O1		>20 000 (Cl)	>20 000 (Cl)	>20 000 (Cl)	>20 000 (Br)	>20 000 (Cl)	>20 000 (Cl)
-CH ₂ CH ₂ -O-CH ₂ CH ₃	2O2		17 500 (Br)	13 800 (Br)	>20 000 (Br)	>20 000	>20 000 (Br)	>20 000 (Cl)
-CH ₂ CH ₂ CH ₂ -O-CH ₃	3O1		>20 000 (Cl)	>20 000 (Cl)	>20 000 (Cl)	>20 000 (Cl)	>20 000 (Cl)	>20 000 (Cl)
-C ₆ H ₁₃	6	9 (Cl)						

For our first screening investigations, we used the promyelocytic leukemia rat cell line IPC-81¹³ as a test system, with the reduction of the WST-1^{14–16} dye as an indicator of cell viability. This test system has proven to provide reproducible results for measuring cytotoxicity of various industrial chemicals.^{11,17–19}

Furthermore, we are aiming to correlate the obtained cytotoxicity data with a HPLC derived lipophilicity parameter, which is described in detail by Ranke *et al.*,⁴ for some of the test kit compounds. In this previous study, a good correlation between the lipophilicity parameter of the cation and the observed cytotoxicity for a set of approximately 70 ionic liquids was found.⁴ In general, the lipophilicity of chemical substances is considered to be the mediator of non-specific toxic effects evoked by membrane interactions, termed narcosis (polar and non polar)^{20–23} or baseline toxicity^{24,25} when applied to mammals or in aquatic toxicology, respectively.

In this context, several recent publications^{4,11,12,26–35} outline that the acute toxic effects of ionic liquids can be attributed to side chain length or lipophilicity of the compounds as descriptive parameters. Due to this fact, we suggest that in the absence of more specific modes of actions, a type of baseline toxicity similar to polar narcosis is assumed to be the predominant mode of toxic action for ionic liquid cations.

The test kit compounds

The test kit comprised three aromatic head groups (4-(dimethylamino)pyridinium, pyridinium and imidazolium), three non aromatic heterocycles (4-methylmorpholinium, 1-methylpiperidinium, 1-methylpyrrolidinium), and one non-cyclic quaternary ammonium head group (*N,N*-dimethylethylammonium).

The seven head groups (Table 1, second row) are combined with eight different aliphatic side chains containing ether (in different positions), terminal hydroxyl and nitrile functions (Table 1, first column).

For all cationic head groups one halide (chloride, bromide, or iodide; Table 1) and the [(CF₃SO₂)₂N][−] anion was tested (Table 2).

Acronyms for ionic liquids

A detailed description of the following system of acronyms will be published elsewhere. The cation is abbreviated according to the type of the head group as "Py-4NMe2" (dimethylamino)pyridinium, "Py" (pyridinium), "IM" (imidazolium), "Mor" (morpholinium), "Pip" (piperidinium), "Pyr" (pyrrolidinium) and as "N" (quaternary ammonium). The substituents at the nitrogen atom(s) of the head group are given as numbers corresponding to their alkyl chain length. For example the

Table 2 Structures of the tested head groups, side chains and their abbreviations. List of all EC₅₀ values as [(CF₃SO₂)₂N][−] anion

R	EC ₅₀ /μM (anion = [(CF ₃ SO ₂) ₂ N] [−])							
Structure								
	Abbreviation	"Py-4NMe2"	"Py"	"IM1"	"Mor1"	"Pip1"	"Pyr1"	"N112"
-C ₂ H ₅	2	700						
-CH ₂ CH ₂ -OH	2OH		6200	5800	1500	4500	5200	6300
-CH ₂ CN	1CN		3200	8000	3400	10 000	6400	7300
-C ₄ H ₉	4	50		500	2700	2600	1000	2700
-CH ₂ CH ₂ CH ₂ -OH	3OH		3500	4600	3400	4200	4000	6700
-CH ₂ -O-CH ₂ CH ₃	1O2		1300	1600	2300	2600	1800	6300
-CH ₂ CH ₂ -O-CH ₃	2O1		1500	1800	6500	1900	2000	2000
-CH ₂ CH ₂ -O-CH ₂ CH ₃	2O2		1800	1500	4900	2200	1600	2000
-CH ₂ CH ₂ CH ₂ -O-CH ₃	3O1		2400	2200	5900	1900	2500	6700
-C ₆ H ₁₃	6	9						

1-butyl-3-methylimidazolium cation has the shorthand notation IM14. Ether containing side chains are indicated by splitting the chain in alkyl units with the symbol “O” for the oxygen in between (*e.g.* IM11O2 for 1-(ethoxymethyl)-3-methylimidazolium). Terminal hydroxyl or nitrile groups are shortened as OH (*e.g.* IM14OH is 1-(4-hydroxybutyl)-3-methyl-imidazolium) or CN (*e.g.* IM11CN is 1-cyanomethyl-3-methylimidazolium). The acronyms used for the halides are as in the periodic table. The bis(trifluoromethylsulfonyl)imide is written as $[(CF_3SO_2)_2N]^-$ according to its structural formula. The identifiers for the cation and for the anion—separated by a white space—give the whole acronym for an ionic liquid.

Results

All fitted EC_{50} values are shown in Table 1 and Table 2 and are described in the following sections. Confidence intervals and a complete listing of the parameters of the fitted models are given in the ESI.†

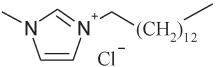
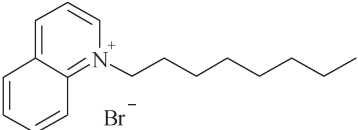
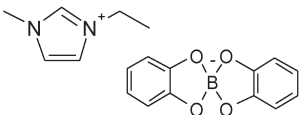
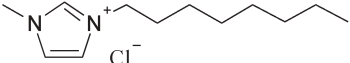
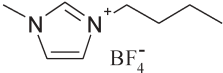
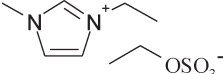
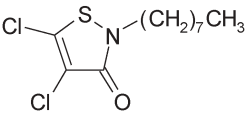
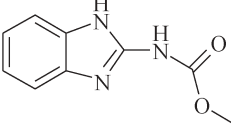
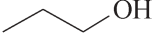

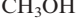
Range of cytotoxicity

To illustrate the range of cytotoxicity covered by the test kit compounds, we composed a set of reference chemicals consisting of ionic liquids tested in earlier studies, antifouling biocides and conventional solvents (Table 3).

Looking at the cytotoxicity of the ionic liquid reference substances we can demonstrate that in general, EC_{50} values of ionic liquids cover five orders of magnitude. This range can be interpreted to result from the contributions of different head groups, side chain lengths and anions. We consider substances showing EC_{50} values lower than 100 μM to be significantly cytotoxic. As demonstrated earlier, ionic liquids can reach drastic cytotoxicities ($EC_{50} < 1 \mu M$) comparable with commonly used and highly active biocides such as carbendazim and 4,5-dichloro-2-*n*-octyl-3(2*H*)-isothiazolone (DCOIT).

On the other hand the 1-ethyl-3-methyl-imidazolium ethyl sulfate is introduced in our lab as a reference ionic liquid exhibiting a comparatively low cytotoxicity ($EC_{50} \sim 10\,000 \mu M$) but which is still some orders of magnitude more

Table 3 Reference compounds to demonstrate the range of cytotoxicity of ionic liquids, biocides, and common solvents

Structure	Name	$EC_{50}/\mu M$
	1-Methyl-3-tetradecyl-imidazolium chloride	0.4
	1-Octyl-quinolinium bromide	1
	1-Ethyl-3-methyl-imidazolium [bis(1,2-benzendiolate)] borate	10
	1-Methyl-3-octyl-imidazolium chloride	100
	1-Butyl-3-methyl-imidazolium tetrafluoroborate	1300
	1-Ethyl-3-methyl-imidazolium ethyl sulfate	8500
	4,5-Dichloro-2- <i>n</i> -octyl-3(2 <i>H</i>)-isothiazolone (DCOIT)	1
	Carbendazim	10
	Propanol	100 000
	Ethanol	700 000
	Methanol	1 600 000

cytotoxic than ordinary polar organic solvents, *e.g.* methanol, ethanol or propanol.

Midway in the above described cytotoxicity spectrum ($EC_{50} \sim 1000 \mu M$) one can find ionic liquids such as the 1-butyl-3-methyl-imidazolium tetrafluoroborate showing neither a significant nor a negligible cytotoxicity.

Ranking our results for the test kit compounds (Table 1 and Table 2) due to this scheme, 45 of the 100 ionic liquids showed a lower cytotoxicity than the 1-ethyl-3-methyl-imidazolium ethyl sulfate reference for a low cytotoxicity. Furthermore, 52 out of the test substance pool are located around the 1-butyl-3-methyl-imidazolium tetrafluoroborate reference for moderate cytotoxicity. Significant cytotoxicity ($EC_{50} < 100 \mu M$) was only found for 4 compounds.

In the following sections the influence of the different structural features (anion, head group and side chain) on the observed biological effects are illustrated.

Influence of the anion

The halides (chloride, bromide and iodide) do not exhibit an intrinsic anion effect up to a concentration range of $5000 \mu M$.¹² Thus, it was concluded that all observed cytotoxic effects for compounds with these anions (Table 1) can be exclusively attributed to the cation.

In a recent paper from our group, the intrinsic cytotoxic effect of the $[(CF_3SO_2)_2N]^-$ anion is described.¹² Comparing the EC_{50} values of the halides (Table 1) with the cytotoxicity data of the corresponding $[(CF_3SO_2)_2N]^-$ anion (Table 2) this observation could be confirmed for nearly all investigated ionic liquids (with the exception of Py6-4NMe₂, Pyr11O2 and N1121O2).

Influence of the head group

The influence of the 7 investigated head groups on cytotoxicity is analysed by comparing the results obtained with ionic liquids containing the same fixed side chain and halides as counter ions (Table 1).

As mentioned above, most of the ionic liquids tested in this study have a relatively low cytotoxicity (high EC_{50} values). There are no clear differences in the EC_{50} values within the rows (Table 1) indicating a generally low influence of the head group itself on cytotoxicity. Only for the butyl substituted head groups and for one further compound (Py1CN Cl) one can observe a more general pattern in the EC_{50} values. By comparing the different head groups with the butyl side chain, a clear head group effect on cytotoxicity can be found for the 4-(dimethylamino)pyridinium cations. For this head group, no functionalised side chains were available. Thus, the test kit was supplemented by the ethyl and the hexyl side chain for a comparison with the corresponding imidazolium moieties. For all three side chains, the 4-(dimethylamino)pyridinium cation shows a remarkably lower EC_{50} value (by 1–2 orders of magnitude) than the corresponding imidazolium head group. Additionally, the well known side chain length effect (decrease in EC_{50} values with elongation of the alkyl side chain) could also be confirmed for the 4-(dimethylamino)pyridinium cation (Fig. 1).

For the cations with the $[(CF_3SO_2)_2N]^-$ anion (Table 2) the general pattern observed for the halides is still present, but

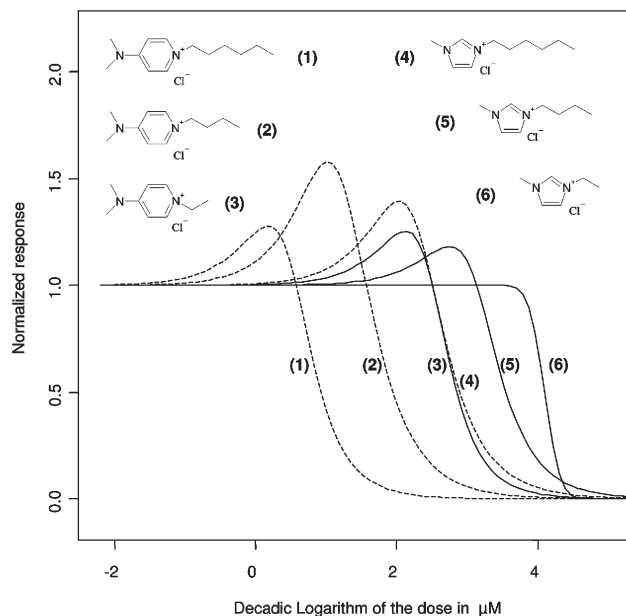


Fig. 1 Dose response curves of the 4-(dimethylamino)pyridinium (dashed lines) and imidazolium (bold line) head group with different alkyl chain length. Most of the dose response curves show a hormetic effect (response > 1) to which no significance is attributed in the context of the present study.

higher deviations within the head groups can be found. However, a consistently higher cytotoxicity for one head group over the other, except for the 4-(dimethylamino)-pyridinium compounds, was not found.

Influence of the side chain

The impact of the side chains on the cytotoxicity of an ionic liquid can be analysed by comparing the results for one head group and one anion, only varying the ten side chains.

For the ionic liquids with the halides, in general, a low cytotoxicity was observable. However, the ethoxymethyl ($-CH_2OCH_2CH_3$) side chain clearly increases the cytotoxicity for all head groups with exception of the piperidinium cation (Table 1) as compared to the isomeric methoxyethyl ($-CH_2CH_2OCH_3$) side chain. This finding could also be confirmed for most of the ionic liquids containing the $[(CF_3SO_2)_2N]^-$ anion but the effect is negligibly low (Table 2).

Furthermore, the increased cytotoxicity of the ionic liquids with the $[(CF_3SO_2)_2N]^-$ anion allows for a more differentiated interpretation of the observed effects and the influence of the side chains. Generally, the butyl side chain has the strongest cytotoxic influence on all head groups except for the morpholinium head group. Taking a closer look at the imidazolium compounds, it can be found that the introduction of oxygen into the side chain results in a lower cytotoxicity (Fig. 2). In particular, the terminal hydroxyl group and the nitrile function reduce the cytotoxicity by about one order of magnitude.

For the other head groups, a resembling trend is perceptible but not consistent for all compounds (*e.g.* Mor12OH ($CF_3SO_2)_2N$).

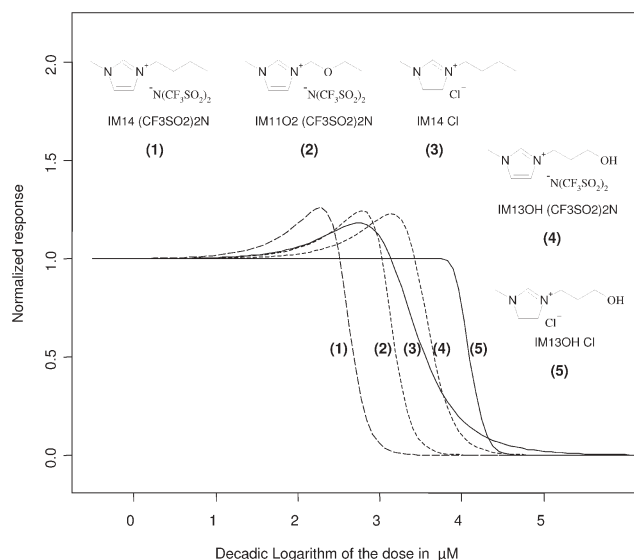


Fig. 2 Dose response curves of imidazolium ionic liquids to demonstrate the shift in EC_{50} values for the functionalised side chains compared to the alkyl side chain. Furthermore, the anion effect of the $[(CF_3SO_2)_2N]^-$ species (dashed lines) is demonstrated by comparison with the chlorides (bold line). The presented curves illustrate that cations containing terminal hydroxy functions in their side chain are able to equalise the anion effect of the $[(CF_3SO_2)_2N]^-$ moiety.

Correlation of cytotoxicity with HPLC lipophilicity data

First of all, the results from the HPLC based lipophilicity determination of selected ionic liquid cations are presented. As expected, one can find increasing $\log k_0$ values (increasing lipophilicity) with elongation of the alkyl chain (Table 4). For the functionalised side chains the pattern is similar. The short

Table 4 Lipophilicity parameter $\log k_0$ and $\log EC_{50}$ values for all compounds shown in Fig. 3. Previously published data are marked with an asterisk

Compound	$\log k_0$	$\log EC_{50}$	
		Halides	$[(CF_3SO_2)_2N]^-$
IM11CN	-0.29	>4.3	3.9
IM12OH	-0.28	>4.3	3.76
IM13OH	-0.23	>4.3	3.66
IM12O1	-0.02	>4.3	3.25
Mor14	0.18	>4.3	3.48
IM11O2	0.21	3.6	3.2
IM12O2	0.45	4.14	3.18
Pyr14*	0.51	3.77	3.01
Py4*	0.57	3.9	—
IM14	0.63	3.55	2.68
Pip14	0.68	>4.3	3.41
N1124	0.51	>4.3	3.43
Py2-4NMe2	0.51	2.9	2.85
Py4-4NMe2	1.08	1.94	1.85
Py6-4NMe2	1.8	0.95	1
IM13*	0.42	>4.3	—
IM14*	0.63	3.55	2.68
IM15*	0.92	>3	—
IM16*	1.24	2.85	2.24
IM17*	1.57	2.53	—
IM18*	1.85	2.01	1.59
IM19*	2.1	1.4	—
IM1-10*	2.37	1.34	—

and polar $-CH_2CN$ side chain exhibits the lowest $\log k_0$, whereas for the long and relatively non-polar $-CH_2-CH_2-O-CH_2-CH_3$ ether side chain, the highest $\log k_0$ value can be found. Additionally, the terminal hydroxyl groups are to be found more polar than the ether functions (e.g. IM13OH versus IM12O1) as predicted from T-SAR. One can find even significant differences in the $\log k_0$ values of IM12O1 and IM11O2. Responsible for this observation are electronic and steric effects due to the vicinity of the oxygen atom to the positively charged imidazolium core which increases the lipophilicity of the $-CH_2-O-CH_2-CH_3$ chain.

Focusing on the cationic head groups with the butyl side chain, the 4-(dimethylamino)pyridinium moiety exhibits the highest lipophilicity ($\log k_0 = 1.08$) due to the broadly delocalised positive charge and the lipophilicity of the dimethylamino group. On the other hand the non-aromatic and oxygen containing morpholinium head group is found to be the most polar moiety with a $\log k_0$ of 0.18. The remaining cations are located with their $\log k_0$ in between the polar morpholinium and lipophilic 4-(dimethylamino)pyridinium moiety (Table 4).

Plotting the logarithm of the EC_{50} values derived from the cytotoxicity assay versus the logarithm of the HPLC derived lipophilicity parameter, k_0 reveals that ionic liquid cations in general span several orders of magnitude considering their lipophilicity and cytotoxicity (recently published data⁴ supplemented with results from this study, Fig. 3).

Taking a closer look at the results obtained in this study for the ionic liquids containing the $[(CF_3SO_2)_2N]^-$ anion versus those with the small halides (with the same cation), an anion effect becomes obvious (Fig. 3). The halides can be described by a good linear correlation between cytotoxicity and lipophilicity, whereas for the corresponding compounds

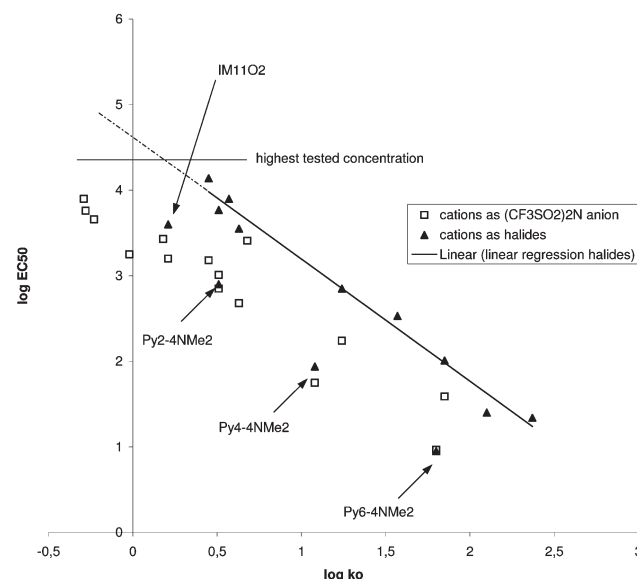


Fig. 3 The correlation between lipophilicity $\log k_0$ and cytotoxicity $\log EC_{50}$ is demonstrated for the cations as halides (closed symbols) and for the $[(CF_3SO_2)_2N]^-$ anions (open symbols). The linear regression ($R^2 = 0.9825$) relates to all cations with halides as anion (except IM11O2 Cl, Py2-4NMe2 Cl, Py4-4NMe2 Cl and Py6-4NMe2 Br).

containing the $[(CF_3SO_2)_2N]^-$ anion, an increasing deviation to higher cytotoxicities from this linear correlation is observed with decreasing lipophilicity of the ionic liquid cation. For the 4-(dimethylamino)pyridinium compounds combined with $[(CF_3SO_2)_2N]^-$ no, or just a small anion effect, was observable.

However, it must be noted that for the ionic liquids cations with low $\log k_0$ values no EC_{50} data are presented in Fig. 2 for the halides because no cytotoxic effects were detectable up to concentrations of 20 mM.

Additionally, four data points (IM11O2 Cl, Py2-4NMe2 Cl, Py4-4NMe2 Cl and Py6-4NMe2 Br) for the halides exhibit a significant deviation to higher cytotoxicities from the above mentioned linear correlation.

Discussion

The correlation of our cytotoxicity data with the HPLC derived lipophilicity parameter gives a more detailed view on the effect of the substructural elements on cytotoxicity and leads to the following inferences.

A good linear correlation ($R^2 = 0.9825$) for all halides (different head groups and side chains) from Table 4 can be found, which demonstrates the interdependency of lipophilicity and cytotoxicity for ionic liquids cations. Only for one head group (4-(dimethylamino)pyridinium) and one side chain ($-CH_2-O-CH_2-CH_3$) is an obvious deviation from this regression observed. These compounds exhibit a higher cytotoxicity than could be expected from the measured lipophilicity parameter $\log k_0$. In general, the $-CH_2-O-CH_2-CH_3$ side chain (with the sole exception of the piperidinium head group) and the 4-(dimethylamino)pyridinium head group show this relative decrease in their EC_{50} values. In consequence, beside the lipophilicity based toxic interaction with membranes, the possibility of further and more specific modes of toxic action (*i.e.* reactive interactions, inhibition of certain enzymes, interaction with signal transduction pathways) has to be taken into account.

The lipophilicity, and concomitantly the cytotoxicity, of the investigated ionic liquid cations are mainly affected by the polarity of the side chain ($\log k_0$ in the range of -0.29 to 2.37). Thus, the side chains of the ionic liquid cations should be considered as one of the key structural elements when identifying toxicophore substructures.

In support of this thesis we could show that the structure of the cationic head group itself—apart from the 4-(dimethylamino)pyridinium moiety—plays only an inferior role in altering the lipophilicity/cytotoxicity of the entire cation ($\log k_0$ from 0.18 to 0.68).

The data points for the cations combined with the $[(CF_3SO_2)_2N]^-$ anion show two trends. For high $\log k_0$ and for the 4-(dimethylamino)pyridinium compounds, the cation is dominating the cytotoxicity of the ionic liquid, which can be demonstrated by an approximation of the EC_{50} values for the ionic liquids with either the $[(CF_3SO_2)_2N]^-$ anion and the halides. On the other hand, the intrinsic cytotoxicity of the $[(CF_3SO_2)_2N]^-$ anion represents the minimal cytotoxicity for ionic liquids containing cations with low $\log k_0$ values (low cytotoxicity). It is proposed that the intrinsic (cyto)toxicity of this anion species is also based on its lipophilicity ($\log k_0 > 2$,

unpublished data). More detailed studies of toxic effects of the $[(CF_3SO_2)_2N]^-$ on microorganisms, aquatic and terrestrial plants and on terrestrial invertebrates are described by Matzke *et al.*³⁶ and Jufferholz and co-workers.³⁷

Conclusion

We used the WST-1 cytotoxicity assay for a preselection of toxicologically favourable structural elements for a large number of ionic liquids. Therefore, we analysed 100 ionic liquids with different head groups, side chains and anions. We could confirm a previously found linear correlation between ionic liquid cation lipophilicity and cytotoxicity using an HPLC derived lipophilicity parameter.

Considering the structural design of ionic liquids cations, the side chain is the main effector to alter cytotoxicity. According to their relatively low lipophilicity, short functionalised side chains can diminish the observed cytotoxicity compared to non-polar alkyl chains.

Our HPLC data revealed that the head groups are of minor concern—compared to the side chain—regarding their influence on the lipophilicity and therefore on the ionic liquid cytotoxicity.

Thus, our investigations support the general hypothesis that the cytotoxic effects of ionic liquids can be attributed to lipophilic interactions with cell membranes and cellular proteins, leading to disruption of membrane or protein function. Furthermore, the uptake rates of ionic liquids into the cells, and thereby their intracellular effect concentrations, are closely related to the lipophilicity of the compounds.

However, the 4-(dimethylamino)pyridinium head group in general and the ethoxymethyl ($-CH_2OCH_2CH_3$) side chain exhibit a significant deviation to higher cytotoxicities from the above mentioned linear correlation. This can be interpreted as a first hint for a more specific mode of action not only based on lipophilicity.

Furthermore, the clear influence of the $[(CF_3SO_2)_2N]^-$ anion on cytotoxicity could be verified. However, combined with a polar cationic species this anion effect is shifted to a moderate cytotoxicity.

Nevertheless, the following arising questions concerning the structural design and hazard potentials of ionic liquids are still unanswered and need additional investigations:

- Is the design with respect to beneficial toxicological properties of ionic liquids compatible to their technical applicability?
- Can the observation that the anion effect of the $[(CF_3SO_2)_2N]^-$ is reduced by choosing a cation with negligible cytotoxicity be expanded to other intrinsically toxic anions?
- Can the toxic effects be verified in higher level test systems (*e.g.* plants, animals)?

In general, the used acute cell viability assay and the tested IPC-81 cell line provide a useful tool for the screening of a large number of compounds, allowing the identification of possible toxicophore substructures. However, since *in vitro* assays are lacking toxicokinetic and toxicodynamic parameters and some major metabolic pathways, for a detailed (eco)toxicological risk assessment further testing with different organisms and endpoints is required.

Experimental

Cell viability assay

The cytotoxicity assay using the WST-1 reagent was described in detail in.¹¹ Briefly, promyelocytic rat cells from the IPC-81 cell line are incubated for 4 hours in 96-well plates with 2-(4-iodophenyl)-3-(4-nitrophenyl)-5-(2,4-disulfophenyl)-2H-tetrazolium monosodium salt (WST-1) reagent. Each plate contained blanks (no cells) and controls (no toxicant). The cell viability assays were generally carried out for a 1:1 dilution series. Each dose response curve was recorded for at least 9 parallel dilution series on three different 96-well plates. Positive controls with Carbendazim were checked in regular intervals.

Dose-response curve parameters and plots were obtained using the drfit package (version 0.05-86) for the R language and environment for statistical computing (www.r-project.org).³⁸

The HPLC system

The HPLC system used for deriving the lipophilicity parameters was a Hewlett Packard system Series 1100, with gradient pump, online degasser, autosampler and a Bruker esquire ESI-MS ion trap detector. The column was a MetaChem Polaris Ether bridged RP-18 column with 150 mm length, 3 mm inner diameter and 3 μ m particle size. A guard column with octadecylsilica material was also used (both Varian, Inc.). The eluent was composed of 0.25% acetic acid (*p.a.*) in Milipore (TM) water (pH = 3.2), mixed with gradient grade acetonitrile. The column dead time t_0 was calculated from retention time difference of thiourea with and without the column. The equipment dwell volume t_D was quantified by switching from water to 0.1 mM NaNO₃ in 10 minutes. Cation retention times from a single gradient run with a gradient time t_G of 10 min were obtained for all substances listed in Table 4. The theoretical background and the calculation of the log k_0 values were recently described in detail.⁴

Chemicals

All tested ionic liquids were received from Merck KGaA (Darmstadt, Germany), with the exception of 1-ethyl-3-methyl-imidazolium ethyl sulfate, which was obtained from Solvent Innovation (Köln, Germany) and 1-octyl-quinolinium bromide, which was prepared at the ITUC in Jena, Germany. The 4,5-dichloro-2-*n*-octyl-3(2*H*)-isothiazolone (DCOIT) was donated by Rohm and Haas (Philadelphia, USA). Carbendazim, acetic acid, acetonitrile, methanol, ethanol, propanol and dimethylsulfoxide were purchased from the Sigma-Aldrich Corporation (Germany).

Cell culture media, sera, and phosphate buffer were purchased from GIBCO BRL Life Technologies (Eggenstein, Germany). Antibiotics and glutamine were obtained from PAA Laboratories (Cölbe, Germany), and the WST-1 reagent was purchased from Roche Diagnostics (Mannheim, Germany).

Acknowledgements

The authors gratefully thank Prof. Detmar Beyersmann, Marianne Matzke, Tanja Juffernholz and Karen Thiele for

helpful discussions. Furthermore, thanks are given to Annegret Stark for providing the 1-octyl-quinolinium bromide and Rohm and Haas for donating DCOIT.

References

- 1 B. Jastorff, R. Störmann and U. Wölke, *Struktur-Wirkungs-Denken in der Chemie*, Universitätsverlag Aschenbeck & Isensee, Bremen, Oldenburg, 2004.
- 2 B. Jastorff, K. Mölter, P. Behrend, U. Bottin-Weber, J. Filser, A. Heimers, B. Ondruschka, J. Ranke, M. Schaefer, H. Schröder, A. Stark, P. Stepnowski, F. Stock, R. Störmann, S. Stolte, U. Welz-Biermann, S. Ziegert and J. Thöming, *Green Chem.*, 2005, 7, 362–372.
- 3 B. Jastorff, R. Störmann, J. Ranke, K. Molter, F. Stock, B. Oberheitmann, W. Hoffmann, J. Hoffmann, M. Nuchter, B. Ondruschka and J. Filser, *Green Chem.*, 2003, 5(2), 136–142.
- 4 J. Ranke, F. Stock, A. Müller, S. Stolte, R. Störmann, U. Bottin-Weber and B. Jastorff, *Ecotoxicol. Environ. Saf.*, 2006, DOI: 10.1016/j.ecoenv.2006.08.008.
- 5 J. L. Anderson, D. W. Armstrong and G. T. Wei, *Anal. Chem.*, 2006, 78(9), 2892–2902.
- 6 F. Endres, *ChemPhysChem*, 2002, 3(2), 144–154.
- 7 W. M. Liu, C. F. Ye, Q. Y. Gong, H. Z. Wang and P. Wang, *Tribol. Lett.*, 2002, 13(2), 81–85.
- 8 T. Welton, *Coord. Chem. Rev.*, 2004, 248(21–24), 2459–2477.
- 9 H. Zhang, J. Wu, J. Zhang and J. He, *Macromolecules*, 2005, 38(20), 8272–8277.
- 10 H. Zhao, *J. Mol. Catal. B: Enzym.*, 2005, 37, 16–25.
- 11 J. Ranke, K. Molter, F. Stock, U. Bottin-Weber, J. Poczbott, J. Hoffmann, B. Ondruschka, J. Filser and B. Jastorff, *Ecotoxicol. Environ. Saf.*, 2004, 58(3), 396–404.
- 12 S. Stolte, J. Arning, U. Bottin-Weber, M. Matzke, F. Stock, K. Thiele, M. Uerdingen, U. Welz-Biermann, B. Jastorff and J. Ranke, *Green Chem.*, 2006, 8(7), 621–629.
- 13 N. Lacaze, G. Gombaud-Saintonge and M. Lanotte, *Leuk. Res.*, 1983, 7(2), 145–154.
- 14 M. V. Berridge, A. S. Tan, K. D. McCoy and R. Wang, *Biochimica*, 1996, 4, 14–19.
- 15 M. Ishiyama, M. Shig. M. Mizoguchi and P. G. He, *Chem. Pharm. Bull.*, 1993, 44(6), 1118–1122.
- 16 M. V. Berridge, P. M. Herst and A. S. Tan, *Biotechnol. Annu. Rev.*, 2005, 11, 127–152.
- 17 C. A. Dose, J. Ranke, F. Stock, U. Bottin-Weber and B. Jastorff, *Green Chem.*, 2004, 6(5), 259–266.
- 18 A. Siol, *Ph.D. Thesis*, University of Bremen, 2002.
- 19 F. Stock, *Ph.D. Thesis*, University of Bremen, 2004.
- 20 B. Antkowiak, *Naturwissenschaften*, 2001, 88(5), 201–213.
- 21 H. H. Meyer, *Arch. Exp. Pathol. Pharmacol.*, 1899, 42, 109–118.
- 22 C. E. Overton, *Studien über die Narkose, zugleich ein Beitrag zur allgemeinen Pharmakologie*, Gustav Fischer, Jena, 1901.
- 23 J. Saarikoski and M. Viluksela, *Ecotoxicol. Environ. Saf.*, 1982, 6(6), 501–512.
- 24 J. DeJongh, H. J. Verhaar and J. L. Hermens, *Toxicol. Sci.*, 1998, 45(1), 26–32.
- 25 B. I. Escher and R. P. Schwarzenbach, *Aquat. Sci.*, 2002, 64(1), 20–35.
- 26 R. J. Bernot, E. E. Kennedy and G. A. Lamberti, *Environ. Toxicol. Chem.*, 2005, 24(7), 1759–1765.
- 27 D. J. Couling, R. J. Bernot, K. M. Docherty, J. K. Dixon and E. J. Maginn, *Green Chem.*, 2006, 8, 82–90.
- 28 K. M. Docherty and C. F. Kulpa, *Green Chem.*, 2005, 7(4), 185–189.
- 29 M. T. Garcia, N. Gathergood and P. J. Scammells, *Green Chem.*, 2005, 7(1), 9–14.
- 30 A. Latala, P. Stepnowski, M. Nedzi and W. Mrozk, *Aquat. Toxicol.*, 2005, 73(1), 91–98.
- 31 C. Pretti, C. Chiappe, D. Pieraccini, M. Gregori, F. Abramo, G. Monni and L. Intorre, *Green Chem.*, 2005, 8(3), 238–240.
- 32 J. Ranke, M. Cox, A. Müller, C. Schmidt and D. Beyersmann, *Toxicol. Environ. Chem.*, 2006, 88(2), 273–285.
- 33 P. Stepnowski, A. C. Skladanowski, A. Ludwiczak and E. Laczynska, *Hum. Exp. Toxicol.*, 2004, 23(11), 513–517.

- 34 F. Stock, J. Hoffmann, J. Ranke, R. Störmann, B. Ondruschka and B. Jastorff, *Green Chem.*, 2004, **6**(6), 286–290.
- 35 R. P. Swatloski, J. D. Holbrey, S. B. Memon, G. A. Caldwell, K. A. Caldwell and R. D. Rogers, *Chem. Commun.*, 2004(6), 668–669.
- 36 M. Matzke, S. Stolte, T. Juffernholz, K. Thiele, J. Arning, J. Filser and B. Jastorff, *Der Einfluss des Anions auf die Toxizität von Ionischen Flüssigkeiten: Bewertung verschiedener Ionischer Flüssigkeiten mit Hilfe einer flexiblen (öko)-toxikologischen Testbatterie*, Conference Proceeding, 11. Jahrestagung der SETAC GLB e.V. Landau, Germany, 2006, pp. 36–37.
- 37 T. Juffernholz, K. Thiele, M. Matzke, S. Stolte, J. Arning, J. Filser and B. Jastorff, *Der Einfluss des Anions auf die Toxizität von Ionischen Flüssigkeiten: Auswirkung auf terrestrische Systeme*, Conference Proceeding, 11. Jahrestagung der SETAC GLB e.V. Landau, Germany, 2006, pp. 88–89.
- 38 R. Ihaka and R. Gentleman, *J. Comput. Graph. Stat.*, 1996, **5**(3), 299–314.

Find a SOLUTION

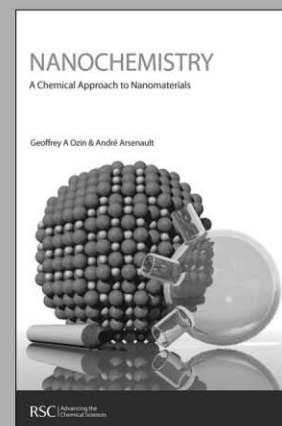
... with books from the RSC

Choose from exciting textbooks, research level books or reference books in a wide range of subject areas, including:

- Biological science
- Food and nutrition
- Materials and nanoscience
- Analytical and environmental sciences
- Organic, inorganic and physical chemistry

Look out for 3 new series coming soon ...

- RSC Nanoscience & Nanotechnology Series
- Issues in Toxicology
- RSC Biomolecular Sciences Series



RSCPublishing

www.rsc.org/books

28040542

A novel approach to the synthesis of SiO₂–PVAc nanocomposites using a one-pot synthesis in supercritical CO₂

Paul A. Charpentier,* William Z. Xu and Xinsheng Li

Received 5th December 2006, Accepted 12th February 2007

First published as an Advance Article on the web 7th March 2007

DOI: 10.1039/b617634h

Inorganic–polymer nanocomposites are of significant interest for emerging materials due to their improved properties and unique combination of properties. A novel one-step synthesis route has been developed for making the polymer nanocomposites silica–poly(vinyl acetate) (SiO₂–PVAc) in supercritical CO₂ (scCO₂), wherein all raw chemicals, tetraethoxysilane (TEOS)/tetramethoxysilane (TMOS), vinyltrimethoxysilane (VTMO), vinyl acetate, initiator, and hydrolysis agent were introduced into one autoclave. *In-situ* ATR-FT-IR was applied to monitor the process in scCO₂, and the parallel reactions of free radical polymerization, hydrolysis/condensation, and linkage to the polymer matrix, were found to take place. The nanocomposites were also studied by transmission electron microscopy (TEM) and EDX element Si-mapping. Well-dispersed nanoparticles of 10–50 nm were formed. This process provides a significant improvement by providing a one-step synthesis route where the potentially recyclable scCO₂ works as a solvent, a modification agent, and a drying agent. This green process has potentially many advantages in producing new and unique materials, along with waste-reduction and energy-saving properties. Production of metal-oxide–polymer nanocomposites from non-inhalable liquid precursors also has significant potential for non-toxicity in biomedical and other fields.

1. Introduction

Significant progress has been achieved in recent years for developing new green chemical processes to meet the ever stringent governmental policies for environmental protection.^{1,2} The main criteria for developing a green chemical process is producing the required (or superior) materials either by a waste-free process or with a significant reduction in the amount of generated waste.^{3–7} Generally, the development in green chemical processes can be divided into two scopes: reaction route alternatives^{3–5} and solvent alternatives.^{6–8} It is widely accepted that reducing the number of synthesis steps can significantly reduce the amount of waste and energy consumption. Hence, changing the reaction route to lower the number of synthetic steps is of significant environmental and economic advantage.³ As well, alternative synthesis design and approaches utilizing green solvents for pollution prevention are highly desirable.^{6–8} Regulation of the use of hazardous organic solvents is becoming increasingly stringent and has spurred the development of environmentally conscious, economical reaction media.

Supercritical carbon dioxide (scCO₂) has emerged as a viable ‘green’ alternative to organic solvents for several applications since carbon dioxide is inexpensive, non-toxic, non-flammable, and environmentally benign.⁹ In the supercritical state ($T_c = 31.1\text{ }^\circ\text{C}$, $P_c = 73.8\text{ bar}$), it can have unique properties such as a liquid-like density and a gas-like diffusivity, and these properties are ‘tunable’ by varying the

pressure and/or temperature.⁹ Previously, DeSimone and co-workers have shown that scCO₂ is a promising alternative medium for free radical, cationic, and step-growth polymerizations, and continuous processes.^{10–12} Indeed, DuPont has recently commissioned a plant to manufacture various grades of polymers based on polytetrafluoroethylene (TeflonTM), using scCO₂ as the solvent instead of 1,1,2-trichloro-1,2,2-trifluoroethane.¹³ In addition to polymer synthesis, scCO₂ has also been developed as an enabling solvent in various chemical processes such as particle formation,^{14,15} extraction, coating,¹⁶ cleaning,⁷ drying, and media for organic and inorganic reactions including nanomaterials,^{17,18} many of which are unique with exciting properties.

Polymer nanocomposites are finding widespread industrial, household and biomedical applications in both existing and several new areas.^{19–21} In comparison with the virgin plastics, polymer nanocomposites often have unique morphologies, physical and chemical properties, and exhibit marked improvements of fuel and gas (oxygen and CO₂) barriers, flame resistance, stiffness, thermal and structural stabilities. The polymer nanocomposites normally contain fine inorganic particles or inorganic fibers well dispersed in the polymer matrix, with the particle size of the inorganic particles/fibers having a significant effect on the mechanical properties.²² However, controlling the particle size at the nanometer level is a challenging project.¹⁹ Of additional challenge is the successful coupling of the nanoparticles to the matrix, which is highly desirable to maximize mechanical properties.¹⁹ Generally, the conventional methods for the synthesis of polymer composites are through complex multi-step synthetic processes, including:^{21,23–29} (1) formation of inorganic particles or polymer; (2) modification of the obtained inorganic particles or the

Department of Chemical and Biochemical Engineering, Faculty of Engineering, University of Western Ontario, London, Ontario, Canada N6A 5B9. E-mail: pcharpentier@eng.uwo.ca; Fax: +1 (519) 661-3498; Tel: +1 (519) 661-3466

polymer; and (3) introducing the inorganic particles into the polymer matrix. The most popular method is simply by mixing the two obtained parts of polymer and inorganic particles, either by melt compounding, which adds inorganic particles into a polymer melt,^{23,24,30} or by a solution obtained by dissolving the polymer in an organic solvent,^{25,26,31} then evacuating the solvent after mixing with the inorganic particles. In addition, usually the inorganic particles or the applied polymer requires further modification by adding a coupling agent to enhance the interaction of the inorganic part with the organic polymer for coupling to the polymer matrix.^{32,33} In these multi-step synthetic processes, each synthesis step consumes energy, time and labor, and results in significant waste. Hence, a green approach to polymer nanocomposite synthesis that provides small, nanometer-size particles, good distribution of the nanofiller throughout the matrix, chemical attachment of the nanofiller to the matrix, along with reducing the number of synthesis steps while using a green solvent, is extremely desirable.

In the present work, we applied *in-situ* FT-IR to analyze free radical polymerization and hydrolysis in scCO_2 , respectively, to generate polymer nanocomposites. A novel one-step synthesis route of SiO_2 -PVAc polymer composites was discovered by combining parallel reactions of free radical polymerization and hydrolysis, and subsequent linkage of the particles to the polymer chain.

2. Experimental

2.1 Materials

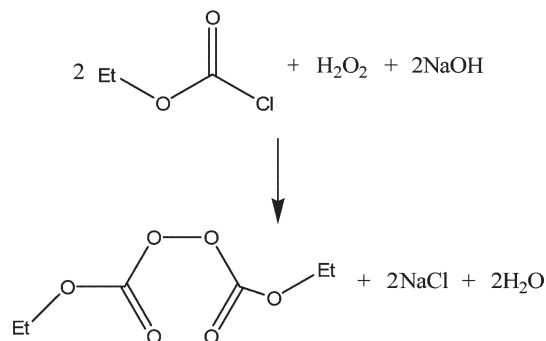
High purity CO_2 (from BOC Gases, 99.99%, with dip-tube) and high purity N_2 (BOC, 99.99%) were further purified by passing through columns filled with 5 Å molecular sieves and reduced 20% copper oxide/ Al_2O_3 to remove the moisture and oxygen, respectively. Heptane and vinyl acetate were purchased from Aldrich Canada (ACS grade) and were distilled under vacuum. NaOH, 30% H_2O_2 , ethyl chloroformate, 0.1 N sodium thiosulfate solution, sodium bicarbonate, sodium sulfate, glacial acetic acid, potassium iodide, tetraethoxysilane (TEOS), tetramethoxysilane (TMOS), and vinyltrimethoxysilane (VTMO) were purchased from Aldrich Canada and used as received.

2.2 Initiator preparation

The initiator diethyl peroxydicarbonate (DEPDC) was synthesized as previously described,³⁴ and the yield of DEPDC was measured using the standard iodometric analysis technique (ASTM E298-91) to exceed 90%. The reaction mechanism for the synthesis of DEPDC is shown in Scheme 1.

2.3 Polymerization procedure

Synthesis was conducted in a 100 mL high-pressure stainless steel autoclave (Parr 4842) coupled with a digital pressure transducer. The stirring speed was controlled at 400 rpm. The designated chemicals were charged into the reactor, purging with a flow of nitrogen, then pumping CO_2 into the autoclave by means of a syringe pump (Isco 260D). After the



Scheme 1 Overall reaction of synthesis of DEPDC.

reaction, CO_2 was carefully vented leaving the formed sample in the autoclave.

In-situ Fourier transform infrared (FT-IR) monitoring of the solution concentration in the stirred 100 mL high-pressure autoclave was performed using a high-pressure immersion probe (Sentinel-Mettler Toledo AutoChem). The DiComp ATR probe consists of a diamond wafer, a gold seal and a ZnSe support/focusing element, housed in alloy C-276. The probe was attached to an FT-IR spectrometer (Mettler Toledo AutoChem ReactIR 4000) via a mirrored optical conduit, connected to a computer, supported by ReactIR 2.21 software (MTAC). This system uses a 24-hour HgCdTe (MCT) photoconductive detector. The light source is a glowbar from which the interferometer analyzes the spectral region from 650 to 4000 cm^{-1} . The beamsplitter inside the RIR4000 is ZnSe. Spectra were recorded at a resolution of 2 cm^{-1} and the absorption spectra were the results of 64 scans. *In-situ* ATR-FT-IR was applied to monitor the various chemistries studied in scCO_2 including: (i) thermal decomposition of DEPDC; (ii) homopolymerization of vinyl acetate; (iii) copolymerization of vinyl acetate and VTMO; (iv) hydrolysis of silicon alkoxides in the presence of a copolymer; and (v) the one-pot synthesis of nanocomposites.

2.4 Characterization

Transmission electron microscopy (TEM) images were recorded using a Philips CM10 Transmission Electron Microscope operated at 80 kV. The specimens were previously dissolved in THF, and then placed on a copper grid covered with carbon film. EDX elemental mapping was recorded using a Hitachi S-2600N Scanning Electron Microscope.

3. Results and discussion

3.1 Copolymerization

Diethyl peroxydicarbonate (DEPDC) was selected as the polymerization initiator for copolymer synthesis due to its relative ease of synthesis, its ability to polymerize acrylate monomers, its solubility in supercritical carbon dioxide (scCO_2) and the success in polymerizing under sol-gel hydrolysis conditions for nanoparticle formation, as described below. Fig. 1 displays a set of typical *in-situ* FT-IR spectra of the thermal decomposition of DEPDC. It was found that the characteristic peaks of DEPDC in scCO_2 at 1803 and

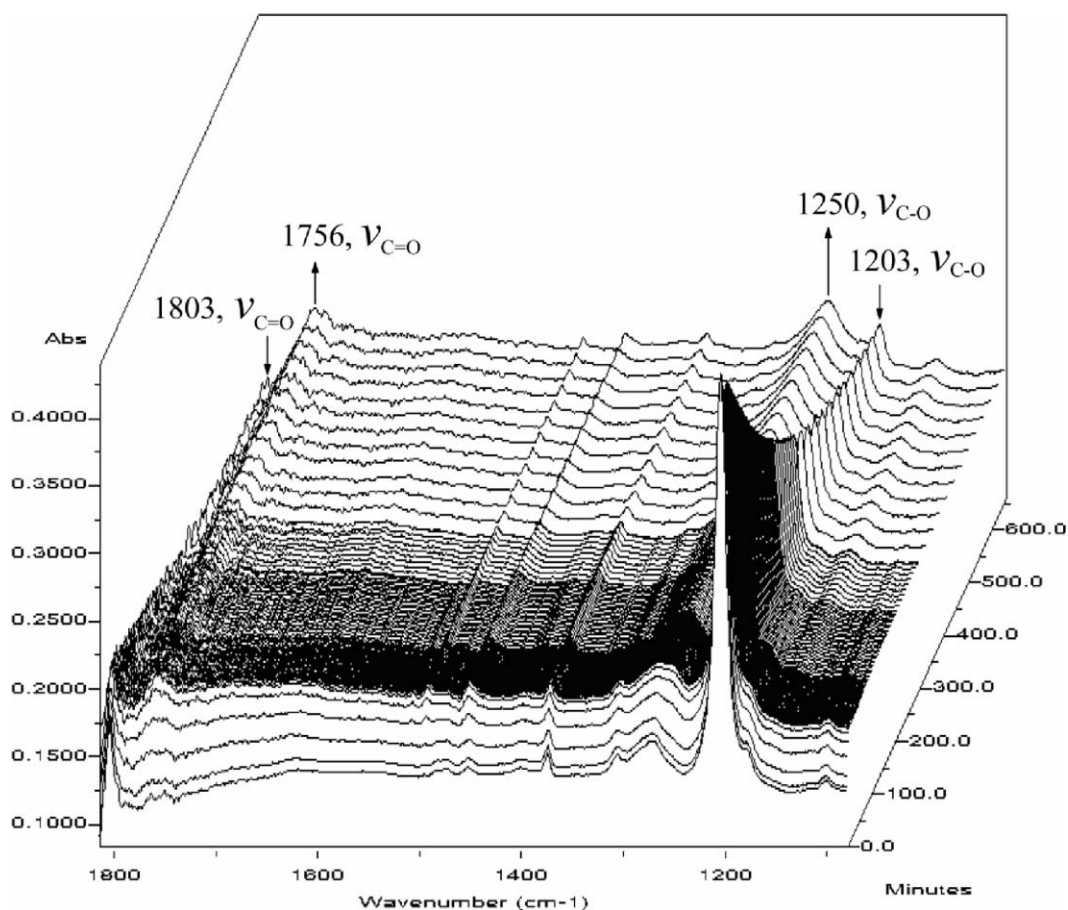


Fig. 1 *In-situ* FT-IR waterfall plot showing the decomposition of DEPDC initiator in scCO_2 (the experimental conditions are: 50°C , $P = 2850$ psi, DEPDC concentration 2.6 wt%).

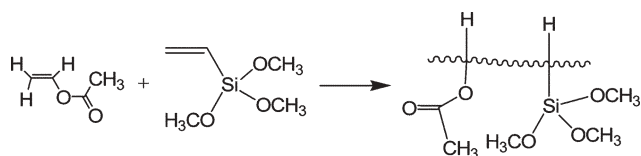
1203 cm^{-1} decreased following heating time, while new peaks gradually developed at 1756 and 1250 cm^{-1} . The thermal decomposition kinetics of DEPDC in scCO_2 were studied previously in both a batch reactor coupled with *in-situ* FT-IR³⁵ and a continuous stirred tank reactor (CSTR)³⁴ in the temperature range of 45 – 85°C .

Although this one-pot process can work with essentially any vinyl monomer and silane linker that are soluble in scCO_2 , vinyl acetate (VAc) was chosen as the monomer of interest due to its relatively high solubility in scCO_2 ,^{36,37} and the widespread industrial and biomedical applications of poly(vinyl acetate) (PVAc). Vinyltrimethoxysilane (VTMO) was applied as the second monomer for coupling to the sol-gel-derived nanoparticles, as shown in Scheme 2.

Fig. 2 shows the FT-IR spectra of the homopolymerization of vinyl acetate in scCO_2 . In order to identify clearly the change of absorbance peaks in the homopolymerization and

the copolymerization reactions, a transform was made in Fig. 2f by subtracting the spectrum at reaction time $t = 0$ (Fig. 2a) from the spectrum at reaction time $t = 300$ min (Fig. 2e). The absorbance intensities at 1766 , 1648 , 1212 , and 1140 cm^{-1} decreased during the polymerization, while those at 1729 and 1233 cm^{-1} increased. The decrease in height of the peaks at 1648 cm^{-1} (due to the C=C stretching vibration) and 1140 cm^{-1} (due to the O–C–C asymmetric stretching vibration of the $\text{CH}_3\text{C}(\text{O})\text{O}-\text{CH}=\text{CH}_2$ molecule) indicates the conversion of vinyl acetate to poly(vinyl acetate).³⁸ That the absorbance peaks changed from 1766 to 1729 cm^{-1} (due to the C=O stretching vibration) and from 1212 to 1233 cm^{-1} (due to the C–C–O asymmetric stretching vibration) indicates the transfer of the ester groups from the monomer molecules to the polymer chains. Depending on the molecular weight of the polymer chains, partial solubility is expected due to the acetate functionality.^{39,40}

The copolymerization of vinyl acetate and VTMO was carried out in scCO_2 by introducing the monomers, initiator, and CO_2 into the reactor, respectively. Fig. 3 shows the FT-IR spectra of a typical copolymerization at 60°C and 2440 psi. A transform was also made in Fig. 3f by subtracting the spectrum at reaction time $t = 0$ (Fig. 3a) from the spectrum at reaction time $t = 300$ min (Fig. 3e). Similar to Fig. 2, vinyl acetate consumption is indicated at 1764 , 1649 , 1214 and 1140 cm^{-1} . By contrast with the IR spectra of the homopolymerization of



Scheme 2 Copolymerization of vinyl acetate (VAc) and vinyltrimethoxysilane (VTMO) to form the copolymer.

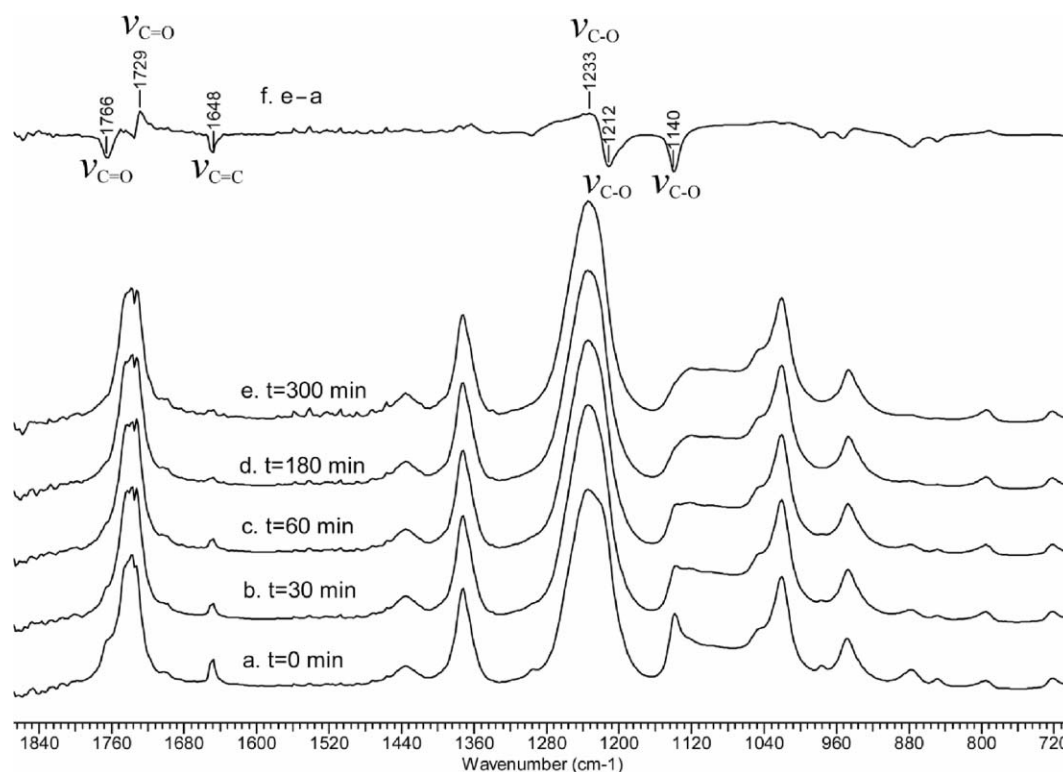


Fig. 2 *In-situ* FT-IR measurement of free radical polymerization of vinyl acetate in supercritical CO₂ (the experimental conditions are: 60 °C, $P = 3000$ psi).

vinyl acetate, it was found in Fig. 3 that the previously observed peaks during the homopolymerization of vinyl acetate drifted slightly and some peaks grew at 1368 and 1021 cm⁻¹, which are assigned to a CH₃ symmetric deformation vibration and

a Si-O stretching vibration, respectively.⁴¹ This silane-modified PVAc was further applied in the next step, where the hydrolysis of TMOS/TEOS to generate the inorganic part in the polymer composite was studied.

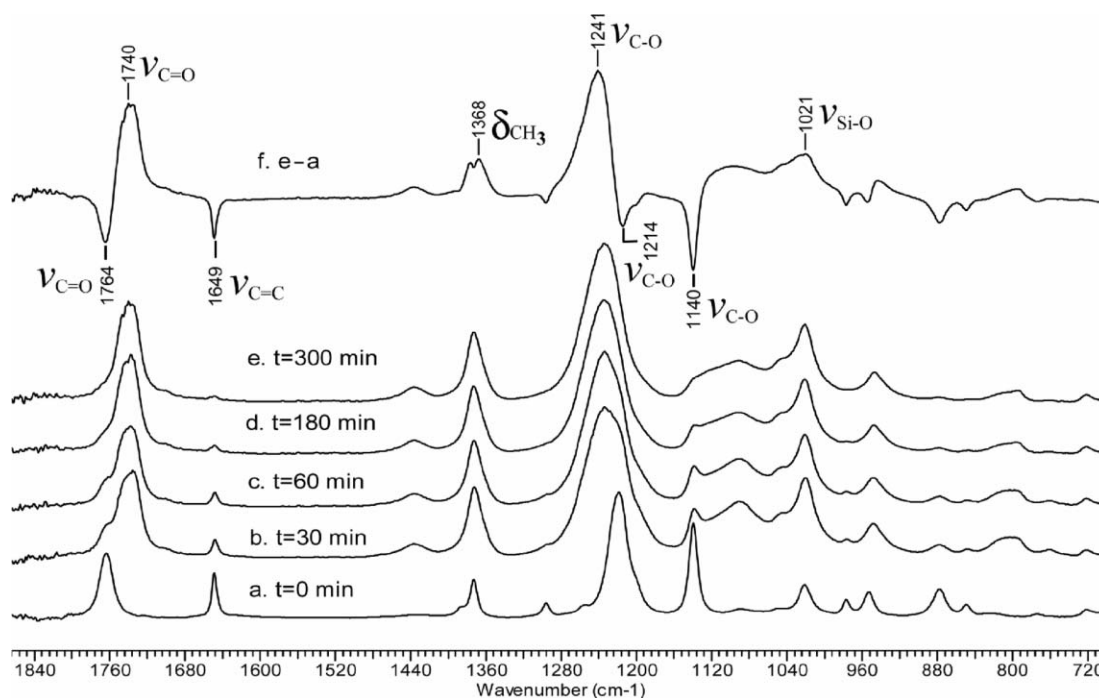


Fig. 3 *In-situ* FT-IR measurement of free radical copolymerization of vinyl acetate and VTMO in supercritical CO₂ (the experimental conditions are: 60 °C, $P = 2440$ psi, molar ratio: VAc : VTMO = 40 : 1).

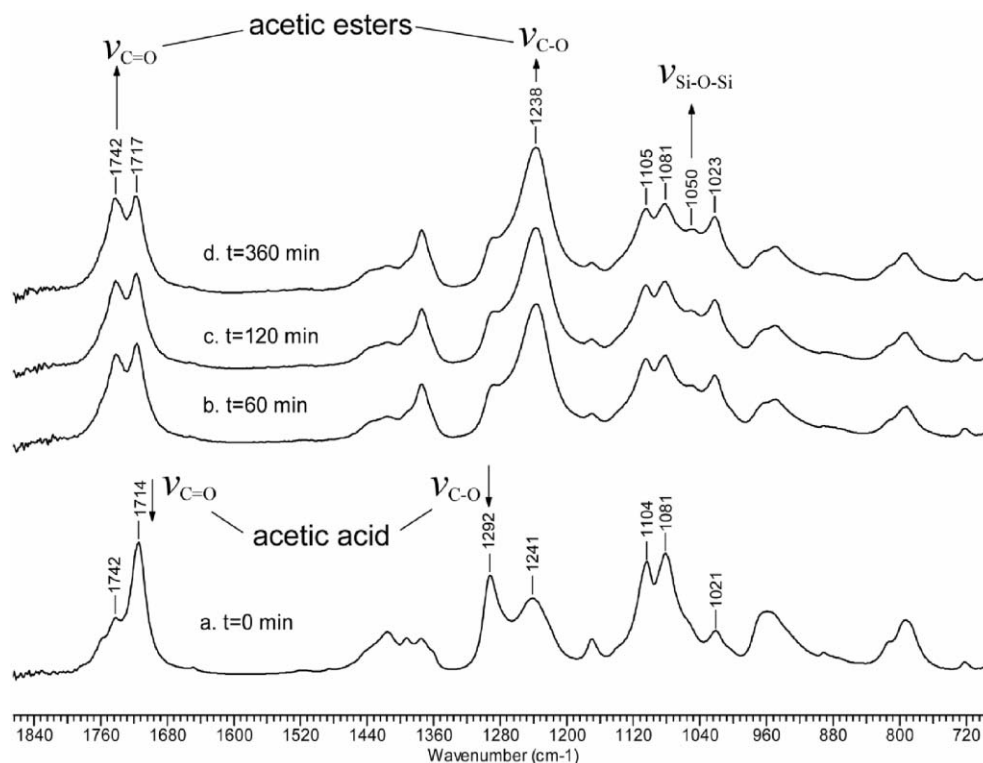


Fig. 4 *In-situ* FT-IR measurement of hydrolysis of TEOS in the silane-modified PVAc in scCO_2 (the experimental conditions are: 60 °C, $P = 2440$ psi, molar ratio: HAc : TEOS = 4.3 : 1).

3.2 Hydrolysis

Hydrolysis using sol-gel chemistry is one of the most important methods for producing fine particles such as nanometer-size inorganic particles.^{42,43} Supercritical CO_2 has previously been used to generate nanoparticles by drying the sample obtained from the sol-gel process,^{43,44} while our previous work has shown that a direct or 'one-pot' synthesis technique for the hydrolysis of metal alkoxides in scCO_2 was possible.^{44,45} We found that a variety of liquid metal alkoxides, such as tetraethoxysilane (TEOS) or tetramethoxysilane (TMOS), are relatively soluble in scCO_2 , particularly in the presence of a polar modifier/hydrolysis agent such as acetic acid. We also found that both TEOS and TMOS polycondensation could be carried out at a temperature above 35 °C in scCO_2 by using acetic acid.

Fig. 4 demonstrates the FT-IR spectra of the hydrolysis of TEOS mixed with the previously obtained copolymer of vinyl acetate and VTMO in scCO_2 at 60 °C, in which acetic acid was added as the hydrolysis agent. It is seen that the peaks grew with reaction time at 1742, 1238, 1050 and 1023 cm^{-1} but were lowered at 1714 and 1292 cm^{-1} . The growing peaks at 1742 and 1238 cm^{-1} are due to the formation of acetic esters from the polycondensation reaction. The growing peak at 1050 cm^{-1} is due to the formation of Si-O-Si, while the shrinking peaks at 1714 and 1292 cm^{-1} indicate the consumption of acetic acid. Fig. 5 displays a TEM image of the formed PVAc nanocomposite. The spherical nanoparticles of various sizes are well dispersed in the polymer matrix. The particle size range is approximately 50–150 nm.

3.3 One-pot synthesis

The goal of this research was not only to synthesize polymer nanocomposites, but also to explore a novel, green, one-pot technique. For this purpose, all the raw materials such as vinyl acetate, VTMO, TEOS/TMOS, acetic acid, and the initiator DEPDC were introduced into the autoclave. Then the

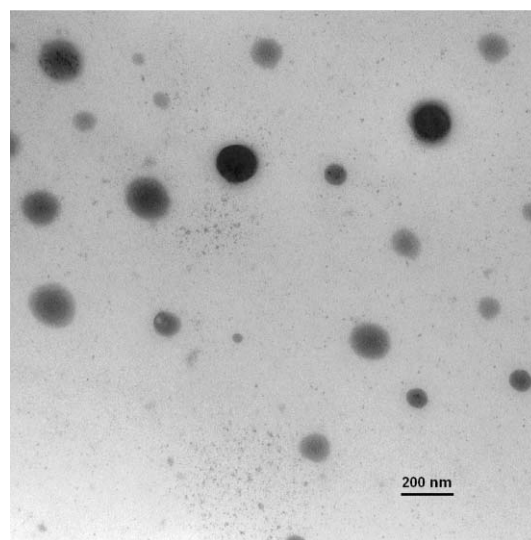


Fig. 5 TEM image of the PVAc nanocomposite from the hydrolysis of TEOS with acetic acid in the presence of the copolymer of vinyl acetate and VTMO in scCO_2 .

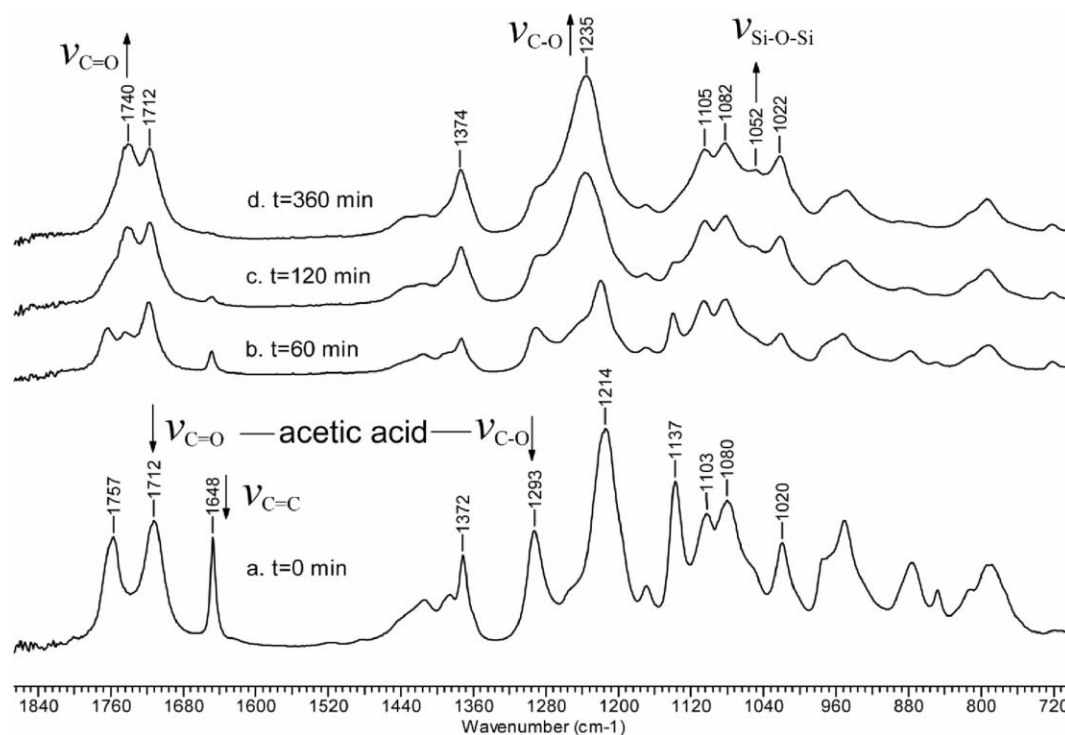


Fig. 6 Parallel reactions of the copolymerization of vinyl acetate and VTMO and hydrolysis of TEOS/VTMO with acetic acid in scCO_2 (the experimental conditions: 60°C , $P = 2440$ psi, molar ratio: VAc : VTMO : HAc : TEOS : DEPDC = 40 : 1 : 43 : 10 : 1).

compressed CO_2 was pumped into the autoclave and heated to reach the supercritical state. After 1080 min of reaction at 60°C and subsequent cooling and evacuation of CO_2 , a viscous liquid was collected from the autoclave and placed in a vacuum oven. A monolith product of SiO_2 -PVAc

nanocomposites was then obtained. Fig. 6 and 7 display the FT-IR spectra from the synthesis process by using TEOS and TMOS, respectively. Both the figures show the parallel reactions of copolymerization and hydrolysis proceeding simultaneously. Fig. 6 shows the consumption of the monomer

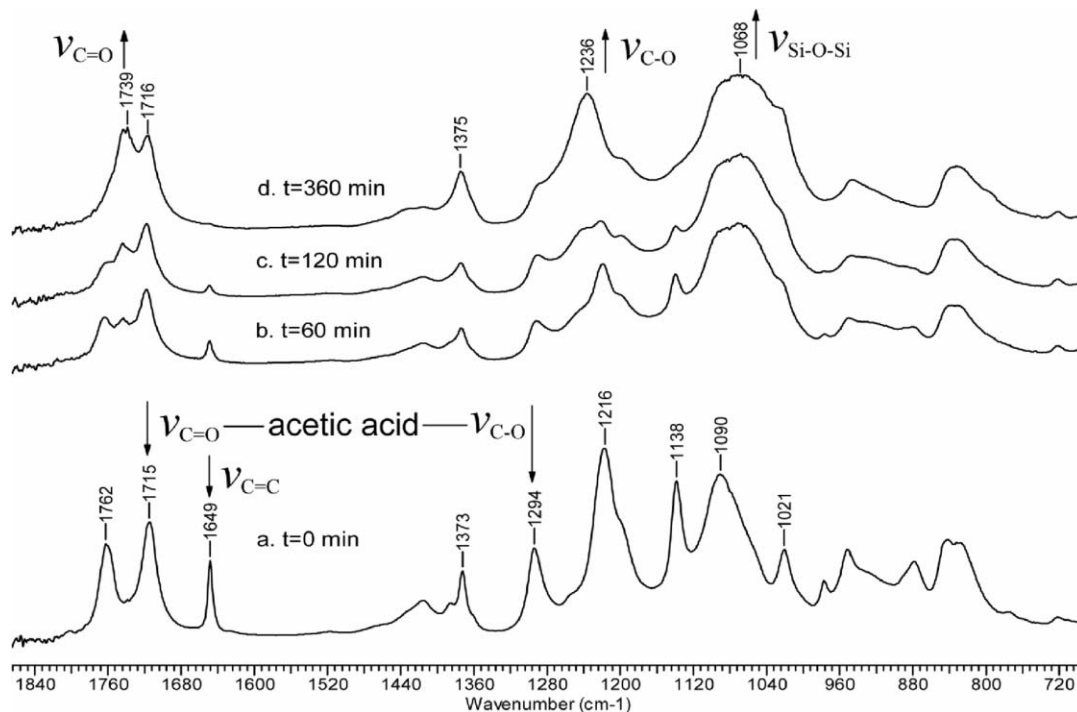


Fig. 7 Parallel reactions of the copolymerization of vinyl acetate and VTMO and hydrolysis of TMOS/VTMO with acetic acid in scCO_2 (the experimental conditions: 60°C , $P = 2440$ psi, molar ratio: VAc : VTMO : HAc : TMOS : DEPDC = 40 : 1 : 43 : 10 : 1).

from the decreasing intensity of the peak at 1648 cm^{-1} , by comparing with the spectra discussed previously. The growing peaks at 1740 and 1235 cm^{-1} are due to the formation of acetic esters from the polycondensation reaction, while the absorbance decreases at 1712 and 1293 cm^{-1} indicate the consumption of acetic acid. The formation of oxo bonds between silicon atoms can be noticed by the widening peak in the 1052 cm^{-1} region, which is similar to Fig. 4 where TEOS nanoparticles were attached to an existing vinyl acetate–VTMO copolymer. When using TMOS as the polycondensation agent, Fig. 7 also shows the parallel reactions occurring of copolymerization and hydrolysis. The consumption of the monomer is observed from the decreasing intensity of the peak at 1649 cm^{-1} , while the growing peaks at 1739 and 1236 cm^{-1} are due to the formation of acetic esters from the polycondensation reaction, and the absorbance decreases at 1715

and 1294 cm^{-1} indicate the consumption of acetic acid. The formation of oxo bonds between silicon atoms can be noticed by the widening peak in the 1068 cm^{-1} region.

Fig. 8 demonstrates the TEM images and particle size distribution histograms of the PVAc nanocomposites from the one-pot synthesis by using TMOS and TEOS, respectively. From the images, nanoparticles with a diameter of *ca.* 10–50 nm were well dispersed throughout the polymer matrix. The particle size distribution histograms show that the silica nanoparticles obtained when using TEOS have a smaller diameter and narrower size distribution than those obtained when using the TMOS precursor. This may be due to the lower reactivity of TEOS than TMOS in the sol–gel process.^{46,47} Low reaction rate could reduce agglomeration of particles and result in uniform and narrow distribution of particles.⁴⁴ Besides, these particles obtained from the one-pot synthesis

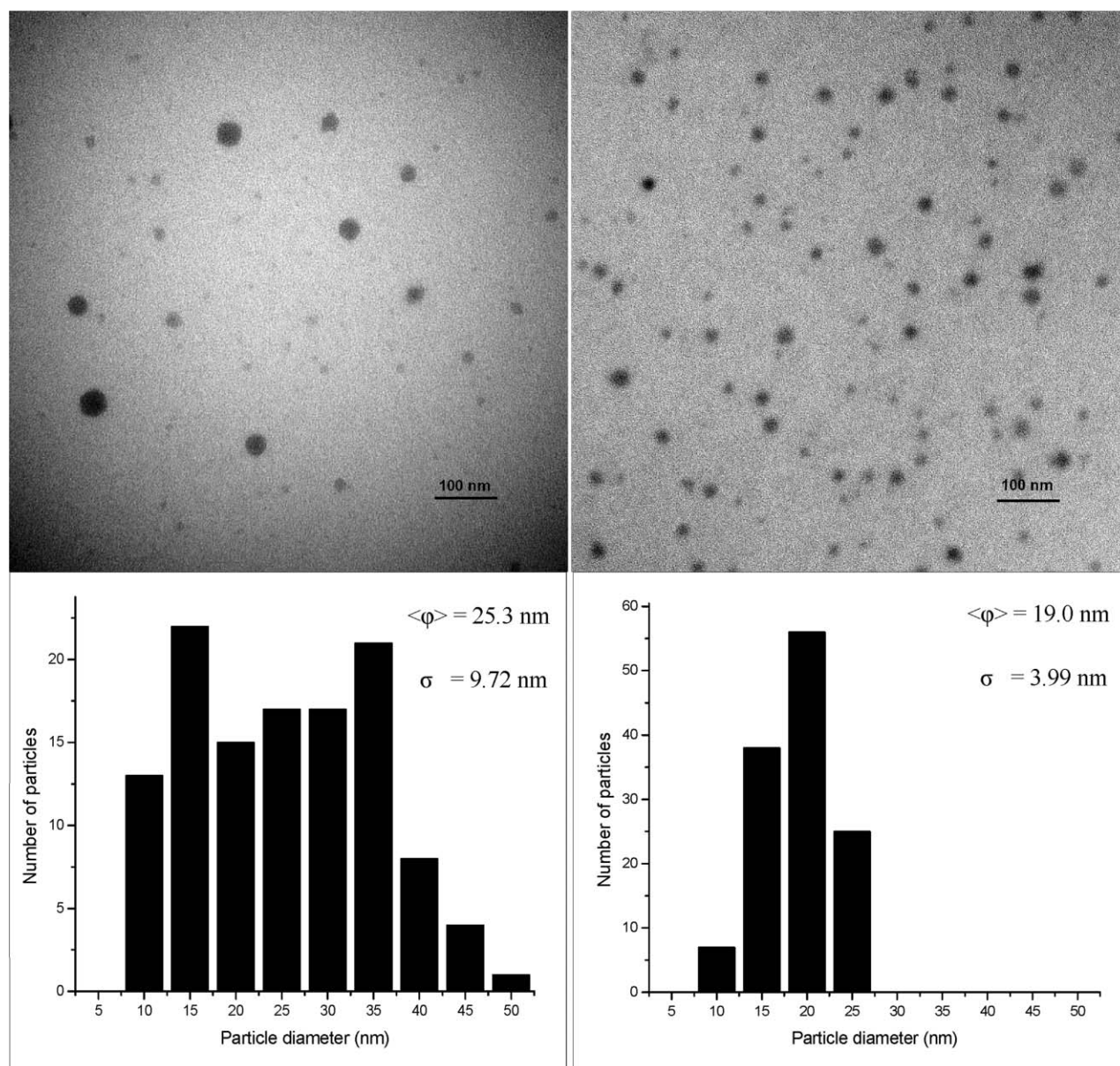


Fig. 8 TEM images and particle size distribution histograms of the PVAc nanocomposites from the one-pot synthesis in scCO_2 using TMOS (left) and TEOS (right).

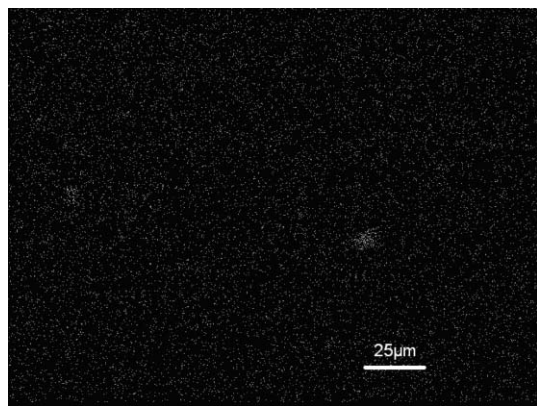


Fig. 9 EDX element Si-mapping of PVAc nanocomposite from the one-pot synthesis in scCO_2 using TMOS.

route are significantly smaller than those from the two-step synthesis route discussed above. This may be due to an enhanced interaction of the TEOS/TMOS alkoxide with the silane linker groups in the copolymer that forms during the one-pot synthesis, compared with that of the two-step procedure, where the previously synthesized copolymer was placed in the reactor before subsequent hydrolysis. One can envision that as the polymer chain grows and incorporates vinyltrimethoxysilane, the silane linkage is more accessible and easier to attach to the growing nanoparticles, hence slowing down the condensation reaction and subsequently providing smaller nanoparticles. The EDX Si-mapping (Fig. 9) also shows that the element Si was well dispersed within the material.

Hence, all the FT-IR evidence regarding the independent copolymerization and hydrolysis steps are found in the one-pot experiment, such as the conversion of monomers, polymer formation, consumption of acetic acid, and the formation of Si–O–Si bonding. Based on the knowledge developed on polymerization and hydrolysis, we have successfully achieved this goal: silica–poly(vinyl acetate) was synthesized by parallel reactions of the free radical copolymerization of vinyl acetate and VTMO and hydrolysis of TEOS/TMOS with acetic acid. This technique can be extended to other vinyl systems with solubility in scCO_2 , and hydrolysis of other metal alkoxides including TiO_2 , ZrO_2 , etc.

Several significant advantages of using scCO_2 as a green solvent for both polymerization and hydrolysis over conventional methods of using aqueous or organic solvents are likely. Small nanoparticles were formed that attach directly to the polymer matrix, which is extremely challenging using existing multi-step approaches. On the one hand, owing to the low heat of vaporization of CO_2 , energy costs can be substantially reduced relative to water-intensive or even solvent-based processes, which often demand a large amount of energy associated with drying operations.⁴⁸ On the other hand, using the parallel reactions of polymerization and hydrolysis in a one-pot reactor has significant advantages over multiple-step approaches which would require more time, labor and organic solvents. In addition, this process is amendable to a continuous process, with potential coupling to supercritical fluid extraction (SFE) for resin purification. Future work will further

explore the details of the one-pot mechanism in scCO_2 , and how to change the synthesis conditions to form desirable nanocomposites.

4. Conclusions

A green chemical process for the synthesis of polymer nanocomposites of SiO_2 –PVAc in supercritical carbon dioxide (scCO_2) was developed. *In-situ* ATR-FT-IR analysis showed that the steps of polymerization, hydrolysis, and coupling occurred simultaneously in scCO_2 in the autoclave. Nanoparticles in the 10–50 nm range were formed that were well distributed throughout the polymer matrix. A significant improvement has been made by reducing a complex multi-step procedure to a one-step synthesis route. As the recyclable supercritical carbon dioxide worked as solvent, modification agent, and drying agent, this green process demonstrated many advantages in waste-reduction and energy-saving.

Acknowledgements

This work was financially supported by the Canadian Natural Science and Engineering Research Council (NSERC), the Ontario Centres of Excellence (OCE) (through the EMK program), and the Canadian Foundation for Innovation (CFI). Special thanks go to Dr Alex Henderson and Dr Warren Baker at AT Plastics for fruitful discussions.

References

- 1 M. Poliakov, M. Fitzpatrick, T. R. Farren and P. Anastas, *Science*, 2002, **297**, 807–810.
- 2 W. Leitner, *Science*, 1999, **284**, 1780–1781.
- 3 B. Meunier, *Science*, 2002, **296**, 270–271.
- 4 R. F. Service, *Science*, 2002, **296**, 1784.
- 5 K. Ishihara, S. Ohara and H. Yamamoto, *Science*, 2000, **290**, 1140.
- 6 G. Chin, *Science*, 2001, **294**, 1243.
- 7 J. M. DeSimone, *Science*, 2002, **297**, 799–803.
- 8 T. E. Long and M. O. Hunt, *Solvent-free polymerizations and processes: minimization of conventional organic solvents*, American Chemical Society (distributed by Oxford University Press), Washington, DC, 1998.
- 9 M. A. McHugh and V. J. Krukonsis, *Supercritical Fluid Extraction: Principles and Practice*, Butterworth-Heinemann, Boston, 2nd edn, 1994.
- 10 J. M. DeSimone and W. Tumas, *Green Chemistry Using Liquid and Supercritical Carbon Dioxide*, Oxford University Press, Inc., New York, NY, 2003, p. 259.
- 11 J. L. Kendall, D. A. Canelas, J. L. Young and J. M. DeSimone, *Chem. Rev.*, 1999, **99**, 543–563.
- 12 P. A. Charpentier, K. Kennedy, J. M. DeSimone and G. W. Roberts, *Macromolecules*, 1999, **32**, 5973–5975.
- 13 *Chemical Week*, 2002, vol. **164**, p. 24.
- 14 E. Reverchon, *Ind. Eng. Chem. Res.*, 2002, **41**, 2405–2411.
- 15 J. Jung and M. Perrut, *J. Supercrit. Fluids*, 2001, **20**, 179–219.
- 16 F. E. Henon, R. G. Carbonell and J. M. DeSimone, *AIChE J.*, 2002, **48**, 941–952.
- 17 K. P. Johnston and P. S. Shah, *Science*, 2004, **303**, 482–483.
- 18 R. A. Pai, R. Humayun, M. T. Schulber, A. Sengupta, J.-N. Sun and J. J. Watkins, *Science*, 2004, **303**, 507–510.
- 19 J. Jordan, K. I. Jacob, R. Tannenbaum, M. A. Sharaf and I. Jasiuk, *Mater. Sci. Eng., A*, 2005, **A393**, 1–11.
- 20 *Polymer-clay nanocomposites*, ed. T. J. Pinnavaia and G. W. Beall, Wiley, Chichester, 2000.
- 21 S. Sinha Ray and M. Okamoto, *Prog. Polym. Sci.*, 2003, **28**, 1539–1641.

- 22 D. Qian, E. C. Dickey, R. Andrews and T. Rantell, *Appl. Phys. Lett.*, 2000, **76**, 2868.
- 23 S. Kumar, H. Doshi, M. Srinivasarao, J. O. Park and D. A. Schiraldi, *Polymer*, 2002, **43**, 1701–1703.
- 24 U. Wagenknecht, B. Kretzschmar and G. Reinhardt, *Macromol. Symp.*, 2003, **194**, 207–212.
- 25 P. K. Rana, S. K. Swain and P. K. Sahoo, *J. Appl. Polym. Sci.*, 2004, **93**, 1007–1011.
- 26 S. Sinha Ray, K. Yamada, M. Okamoto, Y. Fujimoto, A. Ogami and K. Ueda, *Polymer*, 2003, **44**, 6633–6646.
- 27 N. Salahuddin and A. Akelah, *Polym. Adv. Technol.*, 2002, **13**, 339–345.
- 28 X. Zhang, T. Liu, T. V. Sreekumar, S. Kumar, V. C. Moore, R. H. Hauge and R. E. Smalley, *Nano Lett.*, 2003, **3**, 1285–1288.
- 29 J. Pyun, S. Jia, T. Kowalewski, G. D. Patterson and K. Matyjaszewski, *Macromolecules*, 2003, **36**, 5094–5104.
- 30 M. Alexandre, G. Beyer, C. Henrist, R. Cloots, A. Rulmont, R. Jerome and P. Dubois, *Chem. Mater.*, 2001, **13**, 3830–3832.
- 31 Y.-Y. Yu, C.-Y. Chen and W.-C. Chen, *Polymer*, 2003, **44**, 593–601.
- 32 C. Sanchez, G. J. de Soler-Illia, F. Ribot, T. Lalot, C. R. Mayer and V. Cabuil, *Chem. Mater.*, 2001, **13**, 3061–3083.
- 33 S.-W. Zhang, S.-X. Zhou, Y.-M. Weng and L.-M. Wu, *Langmuir*, 2005, **21**, 2124–2128.
- 34 P. A. Charpentier, J. M. DeSimone and G. W. Roberts, *Chem. Eng. Sci.*, 2000, **55**, 5341–5349.
- 35 W. X. Xu, X. Li and P. A. Charpentier, *Polymer*, 2007, **48**, 1219–1228.
- 36 D. A. Canelas, D. E. Betts, J. M. DeSimone, M. Z. Yates and K. P. Johnston, *Macromolecules*, 1998, **31**, 6794–6805.
- 37 B. Baradie, M. S. Shoichet, Z. Shen, M. A. McHugh, L. Hong, Y. Wang, J. K. Johnson, E. J. Beckman and R. M. Enick, *Macromolecules*, 2004, **37**, 7799–7807.
- 38 G. Socrates, *Infrared and Raman Characteristic Group Frequencies: Tables and Charts*, John Wiley & Sons Ltd, Chichester, 3rd edn, 2001.
- 39 Z. Shen, M. A. McHugh, J. Xu, J. Belardi, S. Kilic, A. Mesiano, S. Bane, C. Karnikas, E. Beckman and R. Enick, *Polymer*, 2003, **44**, 1491–1498.
- 40 F. Rindfleisch, T. P. DiNoia and M. A. McHugh, *J. Phys. Chem.*, 1996, **100**, 15 581–15 587.
- 41 K. Nakamoto, *Infrared and Raman Spectra of Inorganic and Coordination Compounds*, Wiley-Interscience, New York, 5th edn., part B, 1997.
- 42 P. Raveendran and S. L. Wallen, *J. Am. Chem. Soc.*, 2002, **124**, 12 590–12 599.
- 43 M. Moner-Girona, A. Roig, E. Molins and J. Llibre, *J. Sol–Gel Sci. Technol.*, 2003, **26**, 645–649.
- 44 R. Sui, A. S. Rizkalla and P. A. Charpentier, *J. Phys. Chem. B*, 2004, **108**, 11 886–11 892.
- 45 R. Sui, A. S. Rizkalla and P. A. Charpentier, *Langmuir*, 2005, **21**, 6150–6153.
- 46 D. A. Loy, E. M. Russick, S. A. Yamanaka, B. M. Baugher and K. J. Shea, *Chem. Mater.*, 1997, **9**, 2264–2268.
- 47 K. G. Sharp, *J. Sol–Gel Sci. Technol.*, 1994, **2**, 35–41.
- 48 P. A. Charpentier, J. M. DeSimone and G. W. Roberts, ‘Continuous Polymerizations in Supercritical Carbon Dioxide’, in *Clean Solvents*, ed. M. A. Abraham and L. Moens, ACS Symposium Series 819, American Chemical Society, Washington, DC, 2002, ch. 9, pp. 113–135.

Formation and reaction of diazonium salts in a CO₂/H₂O system

Pietro Tundo,* Alessandro Loris and Maurizio Selva

Received 8th January 2007, Accepted 12th February 2007

First published as an Advance Article on the web 9th March 2007

DOI: 10.1039/b700207f

The formation of diazonium salts from the corresponding primary aromatic amines and their reaction with potassium iodide to give the corresponding aryl iodide have been performed in a CO₂/H₂O solvent system. The weak acidity of this system (pH about 3) allowed the formation of triazenes as an intermediate *via* a reversible reaction.

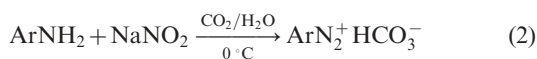
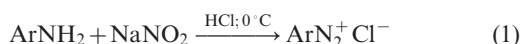
Furthermore, several aryl iodides have been synthesised with high purity. Their isolation was achieved by venting CO₂, without the utilization of organic solvents.

Introduction

In the last two decades, an enormous interest has been focused on CO₂ and H₂O as green alternatives to conventional organic solvents. Both water and CO₂ are non-toxic, non-flammable, do not release hazardous residues, are easy to handle, abundant and cheap.¹

In this context, mixtures of water and dense CO₂ have peculiar properties: when water is mixed with CO₂, the resulting pH remains constant (~ 2.9) over a wide range of pressures and temperatures.² Despite a limited acidity being obtained, the aqueous phase is substantially buffered by CO₂.

This behaviour prompted us to explore potential applications of such solvent systems for organic synthesis. It is well known that diazonium salts are obtained in the aqueous acidic phase by action of nitrous acid on anilines³ (eqn (1)). Since the required pH is not very low, conventional mineral acids (*e.g.* HCl, H₂SO₄)^{3,4} may, in principle, be safely replaced by an acidic CO₂/H₂O mixture. In this work, the diazotization of primary aromatic amines has been examined (eqn (2)).



An excellent test reaction for the formation and reaction of diazonium salts is the synthesis of aryl iodides from anilines and potassium iodide in the presence of an acid solution of NaNO_2 , according to classic procedures⁵ (eqn (3)). Moreover, aryl iodides are interesting compounds for their unique reactions,⁶ and are synthesized according to many non-conventional methods. For example, Smith and Ho employed isoamyl nitrite in an excess of diiodomethane to form aryl iodides in good yields from aryl amines.⁷



*Dipartimento di Scienze Ambientali, Università Ca' Foscari Venezia,
Italy, and Consorzio Interuniversitario Nazionale La Chimica per
l'Ambiente, Dorsoduro 2137 - 30123 Venezia, Italy.
E-mail: tundop@unive.it; Fax: +390412348620*

Results

In a preliminary series of reactions carried out at 0 °C, an aqueous solution of sodium nitrite (1.5 mmol), KI (1.5 mmol) and aromatic amine (1.0 mmol) were charged in an autoclave; it was then pressurised with 5 bar of CO₂. The autoclave was then introduced into an H₂O/ice bath to maintain the temperature at 0 °C. Under these conditions, conversion of anilines to phenyl iodides were low (~50% after 6 hours) which may be attributed to the relative stability of diazonium salts at this temperature. In these experiments, however, formation of biaryls (Ar–Ar [I]) was observed.⁸

More promising results were obtained working at room temperature (*ca.* 25 °C) and employing *p*-anisidine as substrate. The higher conversion observed and the easy detectability of this compound and its products by GC-MS prompted us to choose this substrate for further investigations.

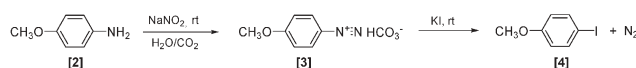
According to Scheme 1, *p*-anisidine was reacted at two different pressures of CO₂: 30 and 65 bar; in the former case carbon dioxide was gaseous, and in the latter a liquid.

Using these conditions (see Experimental), biphenyls [1] were no longer observed.

The yield of **[4]** was higher with liquid (65 bar) than for gaseous CO₂ (30 bar) (Table 1, entry 7 and 8, respectively). Since the difference in pH at the two pressures is negligible, the increased amount of **[4]** was attributed to the higher density of CO₂, which improves its solvent power.⁹ Additionally, organic compounds are more soluble in liquid CO₂ than in gaseous CO₂.

Since aryl iodides are completely soluble in liquid CO₂ (anilines are slightly soluble in this media and diazonium salts in aqueous solution only), separation of the product from the reaction mixture was carried out by simply venting CO₂.

However, since the acidity of the CO₂/H₂O system is limited, free aniline remains in the reaction media at high concentrations. This allows the diazonium cation to react with the amine and form the corresponding symmetric triazene [5] in

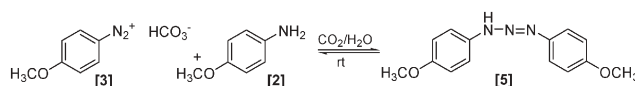
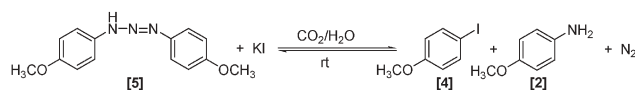


Scheme 1 Formation of diazonium salt and its reaction with I^- in $\text{CO}_2/\text{H}_2\text{O}$ system.

Table 1 Diazotization and iododediazotization of several *p*-substituted anilines

Entry	ArNH ₂	P(CO ₂)/bar	ArI (%)	Isolated yield (%)
1	Aniline	30	50	
2		65	58	45
3	<i>p</i> -Nitroaniline	30	69	
4		65	89	78
5	<i>p</i> -Chloroaniline	30	62	
6		65	65	58
7	<i>p</i> -Anisidine	30	85	
8		65	95	87

^a Aniline: 1.0 mmol, NaNO₂ 1.5 mmol, KI 1.5 mmol, H₂O 2.0 mL; time: 6 h, rt.

**Scheme 2** Formation of triazene.**Scheme 3** Reaction of triazene [5] in the presence of I[−] in the system CO₂/H₂O.

considerable amounts, according to Scheme 2. In fact, in the reaction of *p*-anisidine at 65 bar of CO₂ and in the absence of KI, [5] was isolated in nearly quantitative yield (see Experimental).

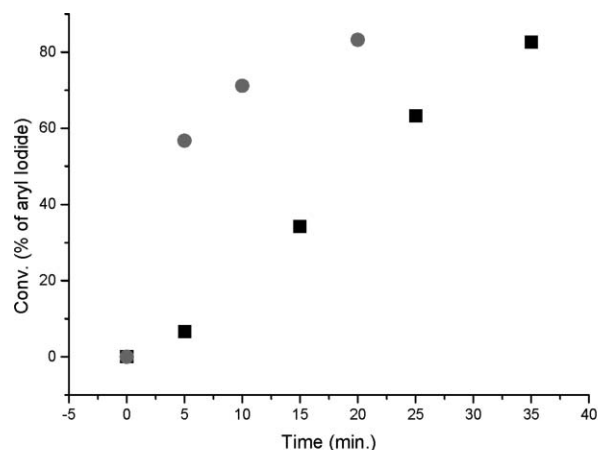
In order to establish the reaction pathway under these conditions, the isolated triazene [5] was treated with KI under the same conditions; however, in the absence of sodium nitrite, [4] and *p*-anisidine were obtained in the same amount (47 and 48%, respectively), thus showing that an equilibrium is established between [5], the amine and the diazonium salt (Scheme 3).

It is noteworthy that triazenes are very sensitive to strong acids as they decompose to nitrogen, anilines and phenols.¹⁰ In our case, the low acidity of carbonic acid might be responsible for the absence of phenols forming.

An additional kinetic investigation was performed in order to establish whether the reaction pathway occurred towards the formation of triazene exclusively (which afterwards reacts with I[−]), or if its formation was reversible with the diazonium salt acting as the reactive species.

Kinetics were conducted by drawing samples from the CO₂ phase by means of a sample loop connected to the autoclave with a valve (see Experimental). The reactions are carried out at 65 bar (liquid CO₂) and at room temperature.† For comparison another experiment was carried out under the usual procedure in a flask with an aqueous solution of HCl and *n*-heptane as the organic phase; this latter solvent was chosen because both its density and dielectric constant are

† In a small laboratory scale, the reaction products are more easily collected in a solvent like diethyl ether. In a larger scale many methods have been developed to collect pure products from CO₂ phase without the use of any organic solvent.¹¹



p-Anisidine: 1.0 mmol, NaNO₂: 1.5 Mol, KI: 1.5 mmol,
n-octane: 1.0 mmol, H₂O: 2.0 mL, CO₂: 65 bar, rt.

Fig. 1 Extent of conversion to form aryl iodide.

similar to liquid CO₂⁹ and can mimic what occurs in the autoclave. In Fig. 1 conversions vs. time are reported: in the case of the CO₂/H₂O system (squares) the trend is almost linear and does not look to be affected by the intermediate triazene; hence, this step is not rate determining. In the system HCl/*n*-heptane (circles), where triazene is not present, the reaction is faster, but the trend is consistent.

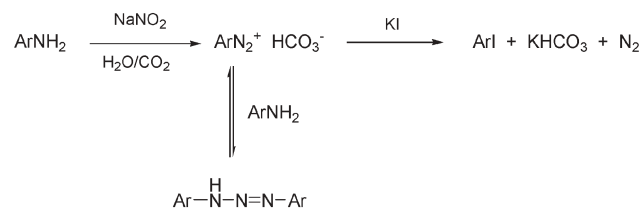
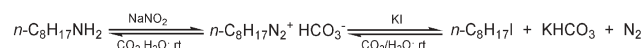
From such mechanistic investigations, it may be concluded that Scheme 4 supports the reaction pathway for the formation and reaction of diazonium salt in the CO₂/H₂O system.

According to the above reported conditions for *p*-anisidine, several primary aromatic amines (aniline, *p*-nitroaniline, *p*-chloroaniline) were reacted in the presence of gaseous and liquid CO₂.

As reported in Table 1, all conversions toward aryl iodides were higher when the pressure was 65 bar.

The diazotization of aliphatic amines was also considered. Similarly to the aforementioned experiments, *n*-octylamine was reacted with nitrite in the CO₂/H₂O system, in the presence of KI, according to Scheme 5.

After 15 min in the presence of liquid CO₂ (65 bar) all the starting amine disappeared from the reaction mixture; the products were 1-octyl iodide (77%), 2-octyl iodide (9%),

**Scheme 4** Proposed pathway for the formation of diazonium salt and its reaction with I[−] in CO₂/H₂O system.**Scheme 5** Diazotization and further substitution reactions of *n*-octylamine.

1-octanol (11%) and 2-octanol (3%). Such a distribution of products is comparable with previous reports in the literature¹² obtained under “classic” conditions: this low selectivity makes this method unsuitable for preparation of alkyl halides under CO₂/H₂O conditions.

Conclusions

Operating in a CO₂/H₂O system, at relatively mild pressure and at room temperature, yields of aryl iodides are comparable with those obtained in the classic procedures (mineral acids in water). The presence of triazenes as intermediates does not affect the rate of the reaction. Phenols were never observed as by-products, while formation of biaryls were avoided by operating at room temperature. Isolation of the products, aryl iodides, did not require organic solvents. The isolation process and the avoidance of inorganic acids makes this system “green”.

Experimental

All reagents were ACS grade and employed without any further purification.

Reactions mixtures were analyzed by a GC-MS (Agilent 5973 N) spectrometer and compared with authentic samples.

Typical experiment

Aniline (1.0 mmol), NaNO₂ (1.5 mol), KI (1.5 mol) and H₂O (2.0 mL) were charged in a 30 mL autoclave equipped with a sapphire window. CO₂ was pumped with a syringe pump (Isco 260 D) to the desired pressure (5, 30 and 65 bar); the autoclave was kept at rt the whole time and the mixture was stirred.

After 6 hours CO₂ was vented in a 50 mL beaker filled with diethyl ether; the same solution was employed to extract the organic phase from the reaction mixture.

Preliminary results

The autoclave was charged as above described, then immersed in an H₂O/ice bath. The pressure of CO₂ was 5 bar.

Preparation of triazene [5]

The aforementioned procedure was employed for the preparation of 1,3-bis(4-methoxyphenyl)-triazene [5] starting from *p*-anisidine, with the difference that KI was not used; the pressure of CO₂ was 65 bar. As triazene decomposes in the GC column, it was isolated by filtration on silica gel with a petroleum ether–diethyl ether mixture (20/80 V/V%), it was then analyzed by ¹H NMR, (CDCl₃), ppm 3.82 (s, 6H), 6.90 (d, 4H), 7.26 (dd, 4H), 9.40 (s, 1H).¹³

Reaction of triazene with KI

In the same conditions as above, 0.5 mmol of 1,3-bis(4-methoxy-phenyl)-triazene [5] were reacted with KI (1.5 mol) and H₂O (2.0 mL); 0.5 mmol of *n*-octane were introduced as

internal standard; the pressure of CO₂ was 65 bar. After 4 h, CO₂ was vented in diethyl ether, as explained above, and the solution was analyzed by GC-MS: conversion resulted to be 47% in *p*-iodoanisole and 48% in *p*-anisidine.

Kinetic investigation with CO₂/H₂O system

A 30 mL autoclave was equipped with a sample loop (vol. 1.1 mL) connected with a valve. *p*-Anisidine (1.0 mmol), NaNO₂ (1.5 mol), KI (1.5 mol), *n*-octane as internal standard (1.0 mmol) and H₂O (2.0 mL) were charged at rt; the autoclave was pressurised with CO₂ at 65 bar. Samples were withdrawn by stopping stirring and connecting the autoclave with the loop, 1.1 mL of liquid CO₂ were collected in the loop. After closing the connection, the loop was vented in diethyl ether, then washed with fresh diethyl ether: the solution containing *p*-iodoanisole and the standard was analyzed by GC-MS.

Kinetics with HCl

In a 50 mL round bottomed flask, aniline (1.0 mmol), NaNO₂ (1.5 mol), KI (1.5 mol), *n*-octane (1.0 mmol), *n*-heptane (30 mL) and 2.0 mL of HCl (10^{−3} M) were charged at rt. Samples were withdrawn by removing an aliquot of mixture which was then diluted and analyzed with GC-MS.

Diazotization and substitution reactions of *n*-octylamine

In the same conditions described for aromatic amines, *n*-octylamine was reacted for 15 min in the presence of liquid CO₂ (65 bar). The mixture was analyzed by GC-MS and the conversion was: 1-octyliodide (77%), 2-octyliodide (9%), 1-octanol (11%) and 2-octanol (3%).

References

- 1 P. G. Jessop and W. Leitner, *Supercritical Fluids as Media for Chemical Reactions*, in *Chemical Synthesis Using Supercritical Fluids*, Weinheim, Wiley-VCH, 1999.
- 2 K. L. Towes, R. M. Shrall and C. M. Wai, *Anal. Chem.*, 1995, **67**, 4040.
- 3 M. Bartle, S. T. Gore, R. K. Mackie and J. M. Tedder, *J. Chem. Soc., Perkin Trans. 1*, 1976, 1636.
- 4 H. G. Beaton, G. R. Willey and M. G. B. Drew, *J. Chem. Soc., Perkin Trans. 2*, 1987, 469.
- 5 P. Griess, *Ann. Chem. Pharm.*, 1866, **127**, 76.
- 6 E. Merkushev, *Synthesis*, 1988, 923.
- 7 W. B. Smith and O. Chenpu Ho, *J. Org. Chem.*, 1990, **55**, 2543.
- 8 If the aromatic ring contains an electron-withdrawing group, the main product is the biaryl, the presence of electron-donating group leads mainly the azo compound.
- 9 J. C. Giddings, M. N. Myers, L. McLaren and R. A. Keller, *Science*, 1968, **162**, 67.
- 10 M. Barra and N. Chen, *J. Org. Chem.*, 2000, **65**, 5739.
- 11 G. Brunner, *Gas extraction*, in *An Introduction to Fundamentals of Supercritical Fluids and their Application to Separation Processes*, Steinkopff, Darmstadt, Springer, New York, 1994.
- 12 F. C. Whitmore and D. P. Langlois, *J. Am. Chem. Soc.*, 1932, **54**, 3441; A. Streitweiser and W. D. Schaeffer, *J. Am. Chem. Soc.*, 1957, **79**, 2888.
- 13 N. Chen, M. Barra, I. Lee and N. Cahal, *J. Org. Chem.*, 2002, **67**, 2271.

Ionic liquids improve citronellyl ester synthesis catalyzed by immobilized *Candida antarctica* lipase B in solvent-free media†

Pedro Lozano,^a Rungtiwa Piamtongkam,^a Kevin Kohns,^a Teresa De Diego,^a Michel Vaultier^b and José L. Iborra^{*a}

Received 29th November 2006, Accepted 22nd February 2007

First published as an Advance Article on the web 14th March 2007

DOI: 10.1039/b617444b

Several citronellyl esters (acetate, propionate, butyrate, caprate and laurate) were synthesized by immobilized *Candida antarctica* lipase B (Novozym) in high yields (>99%) using equimolar mixtures of citronellol and alkyl vinyl ester as substrates in solvent-free medium. The best results were obtained for citronellyl butyrate synthesis ($17.4 \mu\text{mol min}^{-1} \text{mg IME}^{-1}$) at 70°C , which could be improved up to two-fold by coating the biocatalyst particles with alkyl imidazolium-based ionic liquids, which favoured partitioning of the substrate and product molecules.

Introduction

The use of enzymes in non-aqueous environments has increased recently as chemists attempt to broaden the applications of biocatalysis.¹ In the context of green chemistry, the technological utility of enzymes can be greatly enhanced by using them in neoteric solvents, *e.g.* ionic liquids (ILs) and supercritical carbon dioxide (scCO_2), due to their excellent solvent properties.² Water-immiscible ILs have been shown to be excellent non-aqueous media for enzyme-catalyzed reactions (especially for lipases), because of the high level of activity, stereoselectivity and stability displayed by enzymes in chemical transformations.³ Furthermore, the greenness of enzymatic reactions in neoteric solvents also arises from the fact that enzymes themselves are environmentally benign catalysts obtained from living systems. Also, in the same context of sustainable and ecologically friendly organic synthesis, a solvent-free strategy is another important alternative for avoiding the use of organic solvents, and one which has not been extensively studied in the core of enzyme-catalyzed chemical transformations.

Terpene esters of short-chain fatty acid are among the most important flavour and fragrance compounds used in the food, beverage, cosmetic and pharmaceutical industries (*e.g.* citronellyl acetate and citronellyl propionate are used in perfumery for a fresh fruity rose odor).⁴ Most flavour compounds are traditionally provided by chemical synthesis or extraction from natural sources. However, natural flavour esters extracted from plant materials are often too scarce or expensive for industrial uses, while terpene esters produced by chemical methods are not considered as natural products and present drawbacks, such as the formation of undesirable byproducts; furthermore, their market value is less than esters from natural

sources.⁵ The great interest for “natural” products has led industries to seek new methods for producing flavour compounds. However, even esters may be considered natural when produced by enzyme-mediated catalysis.⁶ Since the 1990’s, lipases have been used to synthesize citronellyl^{4–13} and geranyl^{14–16} esters by means of esterification or transesterification in organic solvents,^{5–7,10–13} supercritical fluids^{14,15} or ionic liquids¹⁶ as reaction media. In most cases, substrate solutions were used at concentrations lower than 0.5 M, and only for the best of them were acceptable conversion levels ($\leq 90\%$) reached after long reaction times ($>24 \text{ h}$). A solvent-free strategy has also been assayed to enzymatically synthesize citronellyl esters by direct esterification⁸ or transesterification⁹ (using ethyl acetate as an acyl donor) approaches. In both cases, the assayed citronellol : acyl donor mixture was in a 2 : 1 molar ratio, leading to a mixture of the synthetic product and the excess of unreacted citronellol. Furthermore, for the former approach, the best yield for the citronellol esterification was 74%, while the latter approach provided a 69% yield after 3 h, after which it was necessary to remove the formed ethanol by distillation, reaching a 91% yield after a new catalytic cycle of 3 h.

This paper describes, for the first time, a fast and efficient approach to synthesize citronellyl esters by Novozym-catalyzed transesterification from alkyl vinyl ester and citronellol in anhydrous solvent-free media (Fig. 1). The effect of temperature, the amount of enzyme and the alkyl chain length of the acyl donor (vinyl acetate, vinyl propionate, vinyl butyrate, vinyl caprate or vinyl laurate) on the enzyme activity was determined. Additionally, three different ionic liquids (ILs), based on alkyl-imidazolium cations, 1-butyl-3-methylimidazolium [bmim], 1-hexyl-3-methylimidazolium [hmim], and 1-methyl-3-octyl-imidazolium [omim], associated with the same anion (hexafluorophosphate, $[\text{PF}_6]$), were used to coat biocatalyst particles in order to improve both activity and stability.¹⁷

Results and discussion

Fig. 2A shows several time course graphs for the synthesis of citronellyl butyrate catalyzed by different amounts of enzyme and using a solvent-free equimolar (3.12 M) mixture of

^aDepartamento de Bioquímica y Biología Molecular B e Inmunología, Facultad de Química, Universidad de Murcia, P.O. Box 4021, Murcia, E-30100, Spain. E-mail: jliborra@um.es; Fax: +34-968-364148

^bUniversité de Rennes-1, Institut de Chimie, UMR-CNRS 6510, Campus de Beaulieu, Av. Général Leclerc, Rennes cedex, F-35042, France

† Electronic supplementary information (ESI) available: SEM images of Novozym particles. See DOI: 10.1039/b617444b

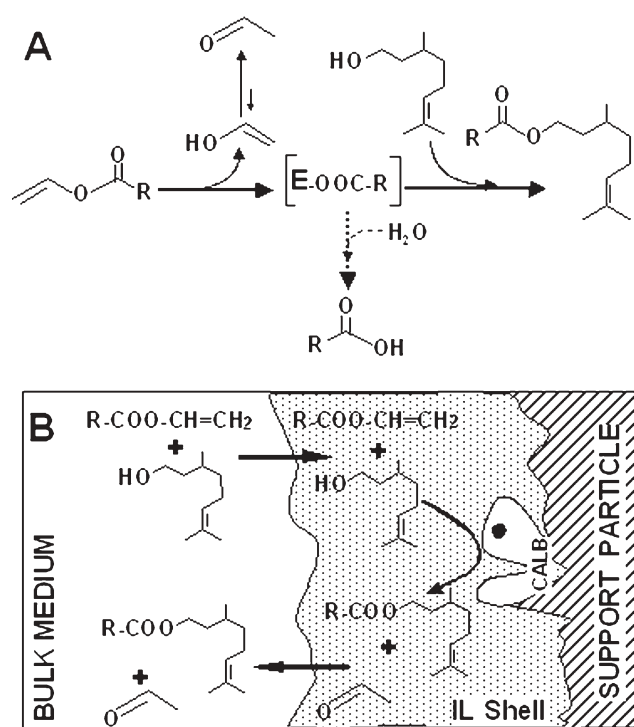


Fig. 1 (A) Kinetic mechanism of transesterification reaction. (B) Scheme of Novozym particles coated with ionic liquids catalyzing citronellyl alkyl ester synthesis in solvent-free medium.

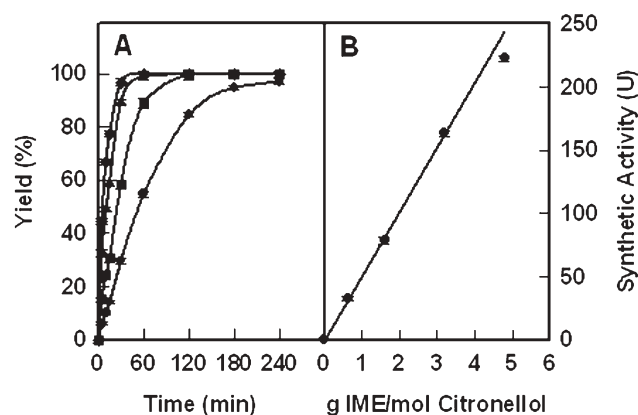


Fig. 2 (A) Time-course of citronellyl butyrate yields catalyzed by different amounts of Novozym: (●) 2 mg, (■) 5 mg, (▲) 10 mg and (◆) 15 mg, respectively. (B) Effect of the amount of immobilized enzyme (IME) on the initial synthetic rate of citronellyl butyrate at 50 °C.

citronellol and vinyl butyrate as reaction medium at 50 °C. The reaction mechanism occurs *via* a covalently linked acyl-enzyme intermediate, which deacylates through the nucleophilic attack of either water (hydrolytic pathway), or another nucleophile, such as citronellol (transesterification, see Fig. 1A). This latter synthetic pathway can be regarded as a kinetically controlled process, where both the rapid accumulation of the acyl-enzyme intermediate and the preferential nucleophilic attack by the alcohol are essential.^{3,13} The first condition is enhanced by the use of activated acid acyl-donors, such as vinyl esters,

because the vinyl alcohol released in the degradation of the vinyl ester tautomerizes to acetaldehyde, which cannot act as a substrate for the enzyme. The second condition arises from using anhydrous reaction media, resulting in the full conversion of the acyl donor to the desired citronellyl ester with high yield (>99%). The use of a solvent-free equimolar mixture of substrates allowed us to obtain citronellyl butyrate at 95% purity, which was identical to the assayed citronellol. The excellent suitability of Novozym for the proposed reaction was demonstrated by the linear increase in the synthetic activity with the amount of enzyme (see Fig. 2B), providing a maximum value of 15.3 U mg IME⁻¹. By this strategy, the full conversion of the offered citronellol was achieved for Novozym ≥ 1.6 g mol citronellol⁻¹ after 2 h, which is one half of the amount used for the previously reported transesterification approach in solvent-free medium.⁸ Vinyl esters were also used as acyl donors for the Novozym-catalyzed synthesis of terpene esters in organic solvents, resulting in 66–95% yields at 24 h, as a function of the log *P* of the solvent.¹³

Although the enzymatic synthesis of terpene esters has mainly focused on the acetate derivatives,^{6–9,11–14} other esters, such as citronellyl butyrate,^{4,12,13} citronellyl valerate,^{4,9} citronellyl methacrylate⁵ and citronellyl laurate^{10,11} have also attracted researchers because of the interest in developing perfumery compounds that are gradually released over long periods of time and/or in a controlled manner. Along these lines, we have determined the influence of the chain length of the acyl donor on Novozym-catalyzed citronellyl ester synthesis by using different vinyl esters as substrates at 50 °C (see Table 1). Because of the different molecular weight of the acyl donors, the concentration of each the assayed equimolar mixture of vinyl ester and citronellol was different. As can be seen, Novozym was able to catalyze the synthesis of all the proposed citronellyl esters, the synthetic activity increasing from acetate to butyrate, but then decreasing until laurate. In all cases, full conversion of the engaged citronellol was reached in 2 h, when the amount of immobilized enzyme was higher than 2.8 g IME per mol of citronellol. This behaviour is in agreement with the observed increase in synthetic yields, from citronellyl acetate to citronellyl valerate, obtained by transesterification in both solvent-free media⁹ and organic solvents.¹³ Acetate has been described as a powerful inhibitor of lipases in terpene ester synthesis by esterification, for which reason it is used at concentrations lower than 0.2 M.^{6–8,14–16} These facts emphasize the excellent suitability of our proposed transesterification approach, based on the use of equimolar

Table 1 Influence of the acyl donor chain length on the Novozym-catalyzed synthesis of citronellyl alkyl esters in solvent-free media based on equimolar substrate mixtures at 50 °C

Acyl donor	Alkyl chain length	[Acyl donor] ₀ /M	Activity/U mg IME ⁻¹	Yield at 2 h ^a (%)
Vinyl acetate	2	3.52	12.1 ± 0.4	100
Vinyl propionate	3	3.30	14.0 ± 0.8	100
Vinyl butyrate	4	3.12	15.3 ± 0.2	100
Vinyl caprate	10	2.34	13.7 ± 0.6	98.4 ± 0.4
Vinyl laurate	12	2.20	9.8 ± 0.5	100

^a Reaction system composed of 1 mL substrate (1 : 1 molar ratio of citronellol and vinyl alkyl ester) with 5 mg IME.

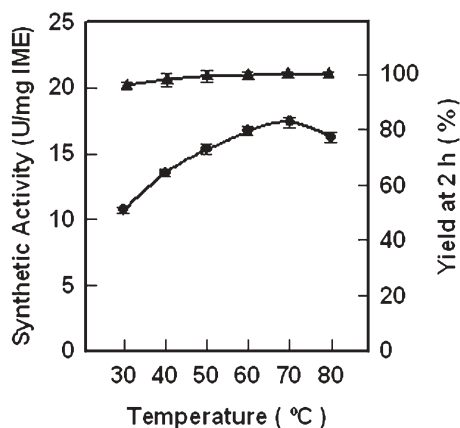


Fig. 3 Influence of temperature on both the activity (●) and yield at 2 h (▲) for Novozym-catalyzed citronellyl butyrate synthesis in solvent-free medium.

amount of vinyl esters as acyl donors and citronellol in solvent-free media, leading to product yields near to 100% and with high purity.

In order to improve the efficiency of the lipase-catalyzed synthesis of citronellyl esters, the influence of temperature, ranging from 30 to 80 °C, in the case of citronellyl butyrate, was also studied in solvent-free medium (see Fig. 3). As can be seen, the synthetic activity of Novozym shows a bell-shaped curve with a maximum level of activity ($17.4 \text{ U mg IME}^{-1}$) at 70 °C, which agrees with other works.^{10–12} It is worth noting how the yield in citronellyl butyrate after 2 h of reaction improved from 96 to 100% as the temperature was increased.

On the other hand, the stability of any enzyme to be reused is an essential aspect of the cost-effectiveness of a bioprocess. Therefore, the use of ILs to improve the activity and stability of the biocatalyst was also considered, since their ability to preserve active enzymes in non-aqueous media is recognized.^{2,3} Thus, three different alkyl imidazolium ILs ([bmim][PF₆], [hmim][PF₆] and [omim][PF₆]) were considered to improve lipase-catalyzed citronellyl butyrate synthesis. However, the proposed ILs are not miscible with citronellol. A 217.5 mM citronellol concentration in [bmim][PF₆] has been determined as the saturation limit at room temperature. Indeed, Barahona *et al.*¹⁶ report the Novozym-catalyzed synthesis of geranyl acetate by direct esterification of a 0.1 M geraniol and 0.1 M acetic acid solution in [bmim][PF₆], obtaining a very poor product yield (30% after 70 h). In this context, we have studied the influence of three different ILs ([bmim][PF₆], [hmim][PF₆] and [omim][PF₆]) on both the activity and the stability of supported Novozym on previously coated particles with these neoteric solvents, before testing for citronellyl butyrate synthesis during eight daily cycles at 50 °C under solvent-free conditions. It is also necessary to point out that the assayed ILs were unable to synthesize citronellyl butyrate in the absence of the enzyme. Synthetic activities were determined using low enzyme loading ($0.24 \text{ mg IME mol citronellol}^{-1}$), because of the first-order kinetics obtained for all the time-course profiles during the first hour of reaction (Fig. 4A). The synthetic activity shown by the immobilized enzyme for the first cycle was enhanced up to two-fold in the presence of ILs

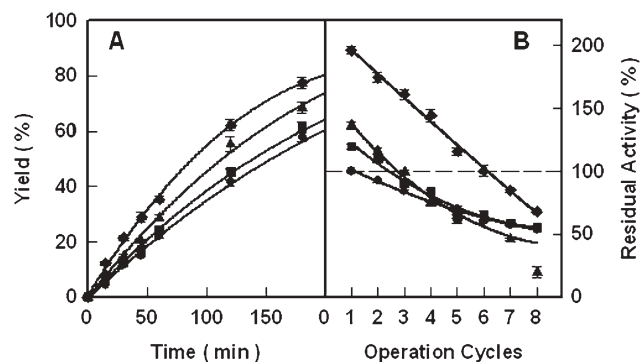


Fig. 4 (A) Time-course of citronellyl butyrate yields catalyzed by Novozym particles ($0.24 \text{ g IME mol citronellol}^{-1}$) coated with ionic liquids (●, None; ■ [bmim][PF₆]; ▲, [hmim][PF₆]; and ♦ [omim][PF₆], respectively) at 50 °C. (B) Residual activity profiles of reused Novozym particles coated with ionic liquids for citronellyl butyrate synthesis in free solvent medium at 50 °C.

(Fig. 4B). This increase follows the hydrophobicity of the alkyl-chain of the cation ([omim][PF₆] > [hmim][PF₆] > [bmim][PF₆]).

All immobilized biocatalysts showed a continuous decay in activity with the number of operation cycles to reach the same level (55–65% residual activity) after 8 cycles. The loss of activity observed in immobilized lipases during citronellyl ester synthesis in both organic solvents and solvent-free media was related with the direct interaction of the hydrophobic media (*e.g.*, organic solvents, citronellol, *etc*) resulting in protein denaturation.^{4,10,12} The important role played by the immobilization support material in encouraging preferential partition effects of substrates and/or products towards the enzyme microenvironment has been related with changes in enzyme activity.^{7,10} Similarly, the improvement in synthetic activity obtained by coating immobilized enzyme particles with ILs may also be related with an improvement in the transfer-rate of substrates/product from the bulk media to the enzyme microenvironment^{3d,17} (see Fig. 1B). To support this hypothesis, the partition coefficients (*P*) of both citronellol and citronellyl butyrate for three different IL/octane biphasic systems were determined by using initial solute concentrations

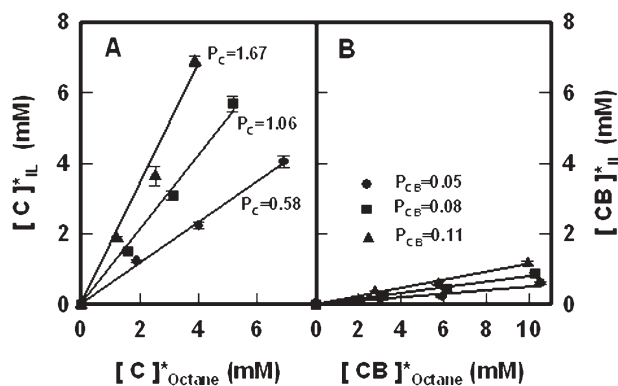


Fig. 5 Equilibrium concentration of citronellol (A, [C]*) and citronellyl butyrate (B, [CB]*) in the ionic liquid phase (●, [bmim][PF₆]; ■, [hmim][PF₆] or ▲, [omim][PF₆]) vs. their equilibrium concentration in the octane phase.

ranging from 0 to 10.6 mM at room temperature (see Fig. 5). After equilibrium was reached, the P parameter of each solute, defined as $P = C_{\text{IL}}^*/C_{\text{octane}}^*$, was calculated by linear regressions of experimental GC measurements. Fig. 5 shows that the P parameter of citronellol (P_{C}) was increased up to 3 times as the hydrophobicity of the alkyl side chain of the assayed ILs increased. Furthermore, P_{C} was 12-fold higher than the P parameter of citronellyl butyrate (P_{CB}) in all cases. These data clearly show how both the transport of substrate towards the enzyme microenvironment and the release of the product towards the bulk medium are favoured by the presence of ILs. Thus, both the synthetic activity and stability of the immobilized enzyme for reuse in citronellyl butyrate synthesis were improved by using [omim][PF₆] to coat the Novozym particles. Desorption of the IL shell coating the enzyme particle as a consequence of the magnetic stirring might have contributed to activity loss during reuse. This suggests that an appropriate selection of both the IL and the immobilization support may improve biotransformation efficiency.¹⁷

In conclusion, the proposed enzymatic transesterification approach, based on the use of vinyl alkyl esters as acyl donors in solvent-free media, is an excellent way of producing terpene esters with 100% yield and purity. Furthermore, coating immobilized enzyme particles with ILs is shown to be an excellent strategy for improving catalytic activity by favouring mass-transfer phenomena. These results clearly show how clean synthetic chemical processes directly providing pure terpene esters can be designed.

Experimental

Materials

Immobilized *Candida antarctica* lipase B (Novozym[®] 435, EC 3.1.1.3) was from Novozymes S.A. (DK), and was equilibrated to 0.11 Aw by over saturated LiCl solutions in a closed container at 25 °C for one week prior to use. 1-Butyl-3-methylimidazolium hexafluorophosphate ([bmim][PF₆], 99%), 1-hexyl-3-methylimidazolium hexafluorophosphate ([hmim][PF₆], 99%) and 1-methyl-3-octylimidazolium hexafluorophosphate ([omim][PF₆], 99%) were from Merck. Citronellol (95% GC), vinyl acetate (VA), vinyl propionate (VP) and vinyl caprate (VC) were from Aldrich, while vinyl butyrate (VB) and vinyl laurate (VL) were from Fluka. Solvents and other chemicals were purchased from Sigma–Aldrich–Fluka Chemical Co.

Adsorption of IL onto novozym particles

In a 5 mL capacity test tube, 40 µL of IL ([bmim][PF₆], [hmim][PF₆] or [omim][PF₆]) were dissolved in 1 mL acetonitrile. Then, 50 mg of Novozym were added, and the mixture was gently stirred for 30 min at room temperature. Finally, the acetonitrile was eliminated by continuous bubbling of N₂ for 30 min at room temperature. The resulting immobilized enzyme particles were equilibrated to 0.11 Aw by over saturated LiCl solutions in a closed container at 25 °C for one week. Particle morphology was not modified by coating with ILs (see ESI for SEM pictures†), and the coated particles behaved in a similar way to the uncoated ones in liquid media.

Drying of substrates

Water was removed from hexane, octane, vinyl esters and citronellol by adding molecular sieves (0.1 g mL^{−1}), shaking the resulting mixture for 24 h at room temperature, and finally storing them in the presence of the adsorbent.

Transesterification reactions

Transesterification reactions were carried out in 3 mL screw-capped vials with teflon-lined septa, containing 2 mL (1 : 1) molar ratio mixture of citronellol and vinyl alkyl ester (vinyl acetate, vinyl propionate, vinyl butyrate, vinyl caprate or vinyl laurate). The reaction was started by adding 5 mg of Novozym and magnetically stirred at 200 rpm and 50 °C in a glycerol bath for 24 h. In all cases, stirring speeds higher than 400 rpm resulted in the disruption of biocatalyst particles after 24 h. At regular time intervals, 10 µL aliquots were taken and suspended in 790 µL hexane, and then cooled in an ice bath. Then, 200 µL of 50 mM butyl butyrate (internal standard) solution in hexane were added, and finally analyzed by GC. One unit of synthetic activity was defined as the amount of enzyme that produces 1 µmol of citronellyl alkyl ester per min. All experiments were carried out in duplicate.

Operational stability

After one reaction cycle carried out as described above for citronellyl butyrate synthesis by using a 0.24 g IME mol citronellol^{−1}, the liquid medium was collected and the immobilized biocatalyst (coated or non-coated with IL) was recovered for reuse. First, it was washed twice with dry hexane (3 mL) to ensure that all the reaction products had been extracted. Then another reaction was started by adding 4 mL citronellol and vinyl butyrate mixture at (1 : 1) molar ratio to the immobilized enzyme derivative. This process was repeated eight times, the liquid phase being carefully collected every time to avoid loss of the biocatalyst. All experiments were carried out in duplicate.

GC analysis

Analyses were performed with a Shimadzu GC-2010 instrument equipped with FID detector. Samples were analyzed by a Beta DEX-225 column (30 m × 0.25 mm × 0.25 µm, Supelco), using butyl butyrate as internal standard and the following conditions: carrier gas (He) at 107 kPa (70 mL min^{−1} total flow); temperature program: 60 °C, 10 °C min^{−1}, 180 °C; split ratio, 50 : 1; detector, 300 °C.

Production of citronellyl alkyl esters

Five different mixtures (4 mL) of citronellol with vinyl acetate, vinyl propionate, vinyl butyrate, vinyl caprate or vinyl laurate, were added to screw-capped vials of 5 mL capacity with teflon-lined septa. Each reaction was started by adding 200 mg of Novozym and magnetically stirred at 200 rpm and 50 °C in a glycerol bath for 1 h. Then, the immobilized enzyme was separated from the reaction medium by centrifugation. The reaction mixture was collected and stored at 8 °C in a refrigerator for further studies. The GC analysis of each

reaction mixture showed one main peak corresponding to citronellyl acetate, propionate, butyrate, caprate or laurate, respectively, which represented 95–99% of the overall integrated area. GC-MS analyses were carried out at the S.A.C.E (University of Murcia), by using a GC-6890 (Agilent) coupled with a MS-5973 (Agilent) system. The GC was equipped with a HP-SMS column (30 m \times 0.25 mm \times 0.25 μ m), being used at the following conditions: carrier gas (He) at 1 mL min⁻¹; inlet split ratio, 1 : 60; temperature program: 60 °C, 10 °C min⁻¹, 310 °C; MS source ionization energy 70 eV; the scan time was 0.5 s covering a mass range of 50–800 amu. Each citronellyl alkyl ester was identified by comparison of its mass spectra with those in a computer library (NIST Library). Citronellyl acetate, retention time (R_t): 10.53 min; positive-ion (m/z) 55.2, 69.2, 81.2, 95.2, 109.2, 123.2, 138.2. Citronellyl propionate, R_t : 11.69 min; m/z : 55.2, 69.2, 81.2, 95.2, 109.2, 123.2, 138.2. Citronellyl butyrate, R_t : 12.79 min; m/z : 55.2, 69.2, 81.2, 95.2, 109.2, 123.2, 138.2. Citronellyl caprate, R_t : 18.85 min; m/z : 55.2, 69.2, 81.2, 95.2, 109.2, 123.2, 138.2, 155.2, 173.2; Citronellyl laurate, R_t : 20.65 min; m/z : 55.2, 69.2, 81.2, 95.2, 109.2, 123.2, 138.2, 183.2; 201.2.

Solubility of citronellol in [bmim][PF₆]

In a 1 mL test screw-capped vial with teflon-lined septum, 1.56 mmol citronellol (0.3 mL) were mixed 0.3 mL of [bmim][PF₆], and the resulting biphasic system was strongly shaken for 3 h at room temperature. When both phases were clearly separated, samples of 25 and 50 μ L of the IL phase were carefully withdrawn, and mixed with 975 and 950 μ L of hexane, respectively. For each sample, the new biphasic system was strongly shaken for 15 min to extract all the citronellol from the IL phase. Then, 100 μ L of the hexane phase were mixed with 400 μ L of 50 mM butyl butyrate (internal standard) solution in hexane, and finally analyzed by GC.

Partitions coefficients

In 3 mL test screw-capped vials with teflon-lined septa, 1 mL of IL (bmim)[PF₆], [hmim][PF₆] or [omim][PF₆] were mixed with 1 mL of either 3.1, 6.2 or 11.1 mM citronellol or citronellyl butyrate solutions in octane. The mixtures were vigorously shaken for 3 h at room temperature until reaching equilibrium. After this step, the mixture was centrifuged for 10 min at 8000 rpm to ensure phase separation. Samples of 50 μ L from the octane phase were diluted in 450 μ L of 10 mM butyl butyrate in octane, and then analyzed by GC. Samples of 50 μ L from the IL phase were mixed with 450 μ L octane, and then were strongly shaken for 15 min to extract all the citronellol or citronellyl butyrate from the IL phase. Finally, 350 μ L of the octane phase were mixed with 150 μ L of 30 mM

butyl butyrate (internal standard) solution in octane, and then analyzed by GC. The partition coefficient (P) of each compound between the IL and the octane phase was calculated as $P = C^*_{IL}/C^*_{octane}$, where C^*_{IL} and C^*_{octane} are the equilibrium solute molar concentrations in the IL and octane phase, respectively. All experiments were carried out in duplicate.

Acknowledgements

This work was partially supported by the CICYT (ref. CTQ2005-01571-PPQ), SENECA Foundation (ref.: 02910/PI/05) and BIOCARM (ref: BIO-BMC 06/01-0002) grants. R. Piamtongkam is a doctoral student from the Biotechnology Program of Chulalongkorn University (Bangkok, Thailand). K. Kohns is an Erasmus student from the University of Kaiserslautern (Germany). We thank Mr Ramiro Martínez from Novo España, S.A. for the gift of enzymes.

References

- (a) R. J. Kazlauskas, *Curr. Opin. Chem. Biol.*, 2005, **9**, 195–201; (b) M. T. Reetz, *Adv. Catal.*, 2006, **49**, 1–69.
- (a) C. E. Song, *Chem. Commun.*, 2004, 1033–1043; (b) R. A. Sheldon, *Green Chem.*, 2005, **7**, 267–278.
- (a) M. Eckstein, P. Wassercheid and U. Kragl, *Biotechnol. Lett.*, 2002, **24**, 763–767; (b) M. Persson and U. T. Bornscheuer, *J. Mol. Catal. B: Enzym.*, 2003, **22**, 21–27; (c) T. de Diego, P. Lozano, S. Gmouh, M. Vaultier and J. L. Iborra, *Biomacromolecules*, 2005, **6**, 1457–1464; (d) P. Lozano, T. de Diego, M. Larnicol, M. Vaultier and J. L. Iborra, *Biotechnol. Lett.*, 2006, **28**, 1559–1565.
- L. L. M. M. Melo, G. M. Pastore and G. A. Macedo, *Process Biochem.*, 2005, **40**, 3181–3185.
- V. Athawale, N. Manjrekar and M. Athawale, *Biotechnol. Prog.*, 2003, **19**, 298–302.
- P. A. Claon and C. C. Akoh, *Enzyme Microb. Technol.*, 1994, **16**, 835–838.
- H. F. De Castro, P. C. De Oliveira and E. B. Pereira, *Biotechnol. Lett.*, 1997, **19**, 229–232.
- F. Fonteyn, C. Blecker, G. Lognay, M. Marlier and M. Severin, *Biotechnol. Lett.*, 1994, **16**, 693–696.
- S. Gryglewicz, E. Jadownicka and A. Czerniak, *Biotechnol. Lett.*, 2000, **22**, 1379–1382.
- G. D. Yadav and P. S. Lathi, *J. Mol. Catal. B: Enzym.*, 2004, **27**, 113–119.
- N. A. Serri, A. H. Kamaruddin. and W. S. Long, *Bioprocess Biosyst. Eng.*, 2006, **29**, 253–260.
- Y. N. Yee, C. C. Akoh and R. S. Phillips, *J. Am. Oil Chem. Soc.*, 1997, **74**, 255–260.
- C. C. Akoh and L. N. Yee, *J. Mol. Catal. B: Enzym.*, 1998, **4**, 149–153.
- W. Chulalaksananukul, J. S. Condoret and D. Combes, *Enzyme Microb. Technol.*, 1993, **15**, 691–698.
- C. Peres, M. D. R. Gomes da Silva and S. Barreiros, *J. Agric. Food Chem.*, 2003, **51**, 1884–1888.
- D. Barahona, P. H. Pfromm and M. E. Rezac, *Biotechnol. Bioeng.*, 2005, **93**, 318–324.
- P. Lozano, T. de Diego, T. Sauer, M. Vaultier, S. Gmouh and J. L. Iborra, *J. Supercrit. Fluids*, 2007, **40**, 93–100.

Integral resource management by exergy analysis for the selection of a separation process in the pharmaceutical industry

J. Dewulf,^{*a} G. Van der Vorst,^a W. Aelterman,^b B. De Witte,^b H. Vanbaelen^b and H. Van Langenhove^a

Received 30th November 2006, Accepted 1st March 2007

First published as an Advance Article on the web 20th March 2007

DOI: 10.1039/b617505h

This paper reports a detailed analysis of the resource intake necessary for the separation of a mixture of diastereoisomers (2*R*,3*R*)-3-(3-methoxyphenyl)-*N,N*-2-trimethylpentanamine **6** and (2*R*,3*S*)-3-(3-methoxyphenyl)-*N,N*-2-trimethylpentanamine **7** in the production of an active pharmaceutical ingredient. The resource intake analysis is based on exergy calculations of both material (chemicals) and energy (utilities) requirements. For two separation processes, crystallisation and preparative chromatography, analysis is not only carried out at the process level (α level), but also at the plant level (β level) taking into account the 6 preceding synthesis steps towards the diastereoisomers and the supporting processes, *e.g.* for delivering heating media from natural gas or treating waste gases. Finally, exergetic life cycle analysis allowed the inclusion of the overall industrial metabolism (γ level) that is required to deliver all energy and materials to the plant to carry out the separation.

The results show that, in this example, the large scale chromatography process is not the most resource efficient option because of its high utilities requirement, despite its lower chemical requirement (180 MJ *versus* 122 MJ total requirement per mol of the *RR* stereoisomer (2*R*,3*R*)-3-(3-methoxyphenyl)-*N,N*-2-trimethylpentanamine monohydrochloride **8**) (α level). Due to its higher efficiency, the plant only requires 4.6% more resources when it selects chromatography instead of crystallisation (434 *versus* 415 MJ total requirement per mol of the *RR* stereoisomer **8**) (β level). Since the efficiencies of the overall industry depend on the type of materials and energy that it has to deliver to the plant, overall resource withdrawal from the environment differs by 4.2% for crystallisation and chromatography (883.7 and 920.6 MJ mol⁻¹ stereoisomer **8**).

The study has also shown that resource efficiency gain can be achieved by recycling solvents on the plant. Moreover, it is clear that there is more potential for resource efficiency improvement for the crystallisation than for chromatography because of the different nature of the resources consumed: chemicals, including solvents, *versus* utilities.

Introduction

Currently, there is no need to convince stakeholders of the necessity to shift towards greener chemical technology. The key to research in this area is twofold. First, innovative chemical reactions and better performing unit operations have to make the green concepts happen. Research efforts are numerous, but also industrial implementations have been achieved.¹ Second, there is a need for an adequate assessment of the “greenness” when decisions have to be taken, primarily in green technology development. At the same time, metrics also allow better communication of the efforts, be it for stimulating involvement of personnel or for external communication. Three major subgroups of indicators can be distinguished: (1) indicators for resource efficiency (*e.g.* reaction mass intensity, kg raw materials per kg product, kg water consumed per kg product, kg solvent loss per kg solvent used,

kg product recyclable per kg product, kg recycled feed per kg feed *etc.*); (2) indicators for energy efficiency (energy required per kg product, eventually normalized to the theoretical minimum); and (3) human and eco-toxicity indicators (*e.g.* ecotoxicity to aquatic life, photochemical ozone formation, acidification, human health effects *etc.*).² The latter toxicity type indicator is typically included in metrics used by large chemical, fine chemical and pharmaceutical manufacturers, *e.g.* in the tools used by Johnson & Johnson,³ GlaxoSmithKline⁴ and BASF.⁵ Also, the first type of indicators, dealing with mass resource efficiency, is introduced into practice. The second type of indicator is not that easy to implement for specific products in practice. Indeed, whereas mass resource use is product-specific, *e.g.* reagent and solvent need for a specific reaction, energy needs are ubiquitous in a fine chemical plant, making allocation to a specific product or process inconvenient. Therefore, energy resource requirements are often handled as ‘red light’ guidances, *e.g.* setting minimum and maximum operating temperatures and pressures, rather than quantifying specific energy limits in terms of J per kg of final product.

Apart from specific energy requirement quantification, green metrics today show two other shortcomings. First, there

^aResearch Group EnVOC, Ghent University, Coupure Links 653, Ghent, B-9000, Belgium. E-mail: Jo.Dewulf@UGent.be; Fax: +32 (0)92646243; Tel: +32 (0)92645949

^bJohnson & Johnson PRD, Janssen Pharmaceutica nv, Turnhoutseweg 30, Beerse, 2340, Belgium

is the frequently too narrow system boundary approach. For example, in metrics for resource efficiency, it is common practice to use the gate-to-gate system boundary, resulting in the omission of the overall resource intake upstream of the own facility. Put in a misleading way, this approach promotes outsourcing in order to reduce the environmental impact. A second limitation of the current environmental metrics, is splitting up resource and energy inputs. When looking to the overall production chain, numerous natural resources can fulfil both functions. For example, fossil oil is used both as fuel and feedstock in the petrochemical based industry. But this is also true for emerging renewable resources: bioresources can be either feedstock for renewables-based products and the source for biofuels.

Basically, the rather artificial subdivision of energy and raw materials can be overcome by exergy analysis.^{6,7,8} Exergy analysis provides a powerful tool for assessing the quality and quantity of a resource: it stands for the upper limit of the portion of the resource that can be converted into work, given the prevailing environmental conditions. The exergy value of resources diminishes each time they are used in a process. Exergy analysis, covering both utilities and feedstocks at the input, and products, waste streams and generated irreversibilities at the output, shows how efficient resources are employed towards products and not towards waste and lost work, *i.e.* the irreversibilities. Applications in the process industry from an economical and environmental point of view are huge today.^{9,10,11,12,13,14} For the chemical industry, the US Department of Energy investigated within its EERE programme (Energy Efficiency and Renewable Energy) the manufacturing processes for 25 bulk chemicals by exergy analysis in order to identify inefficiencies.¹⁵ However, applications within the pharmaceutical industry have not been reported so far.

The other limitation of currently used assessment tools, *i.e.* the system limits caused by, for example, the gate-to-gate approach, can be overcome through the life cycle approach. Indeed, detailed information on feedstocks and utilities going into a particular process, whether they are produced within the same facilities or supplied, should be taken into account if overall impact assessment is targeted. Here, for a large number of resources, one can make use of life cycle inventory data, as they are available from the US National Renewable Energy Laboratory or EMPA (Eidgenössische Materialprüfungs- und Forschungsanstalt) in Switzerland.

The scope of this paper is to evaluate resource use in two processes, covering energy and material resource requirements simultaneously. The processes are two alternative methods for the separation of two diastereoisomers that are intermediates in the chemical synthesis of an active pharmaceutical ingredient Tapentadol under investigation.¹⁶ One option consists of a separation by a classical batch crystallisation process, the other of industrial chromatographic separation (Fig. 1). The exergy and cumulative exergy approach is envisaged in order to evaluate the overall resource intake at three different levels. First, resource consumption evaluation at the process itself is carried out. Second, intake at the facility level, *i.e.* all resources necessary to deliver the intermediate to be separated and the mass and energy agents necessary to carry out the separation,

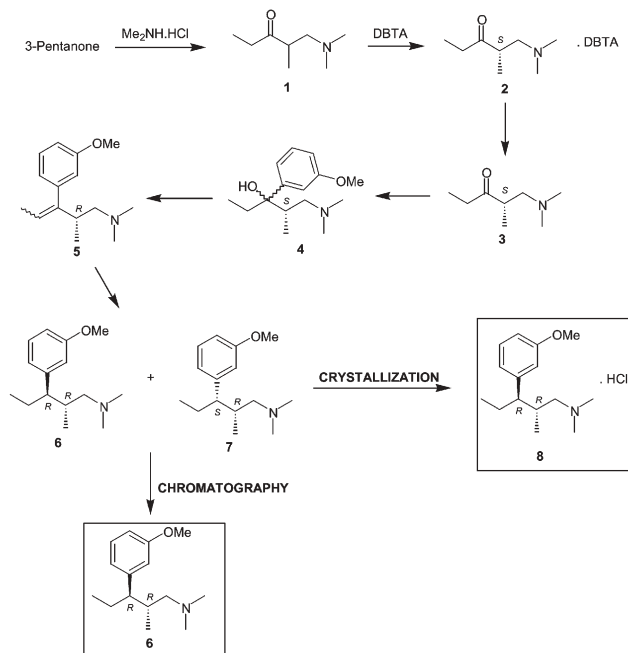


Fig. 1 Reaction scheme of the synthesis of the intermediate 8.

are quantified. Thirdly, the overall resource intake from the environment into the industrial metabolism to deliver the feedstocks and energy to the facility of Janssen Pharmaceutica to carry out the separation process are studied.

Results and discussion

Process level (α system boundary)

Chemical input, nitrogen gas input, electromechanical power for pumping and stirring, heating and cooling requirements and cleaning have been quantified per mol of **8** (crystallisation) or **6** (chromatography) in Table 1 and 2. Both products are

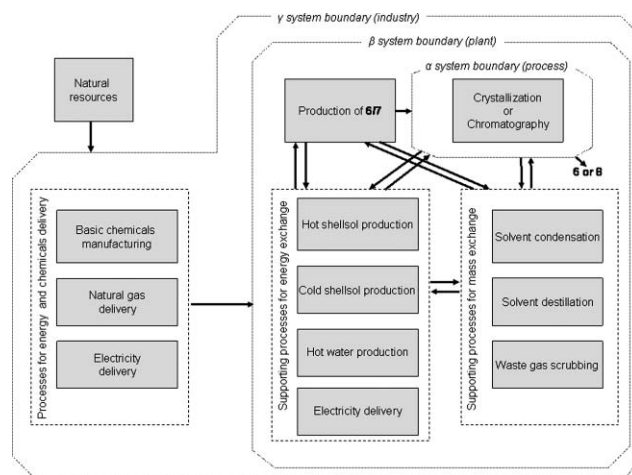
Table 1 Resource inputs for the crystallisation process ($\text{MJ}_{\text{exergy}} \text{ mol}^{-1}$ **8**)

Input	$\text{MJ}_{\text{exergy}} \text{ mol}^{-1}$ 8
Chemicals	110
Solution 6 + 7	92.7
HCl solution	6.9
THF	10.2
NaOH solution	0.036
Water	0
N₂ gas	0.0016
Electromechanical power	4.11
Pumping in fluids	0.0051
Stirring	3.38
Pumping heating media	0.201
Pumping cooling media	0.343
Circulation pumping	0.0074
Vacuum setting	0.133
Thermal inputs	0.186
Heating media	0.156
Cooling media	0.030
Cleaning agents	8.20
Water	0
Methanol	8.07
Acetone	0.13
Overall input	122

Table 2 Resource inputs for the chromatography process ($\text{MJ}_{\text{exergy}} \text{mol}^{-1} \mathbf{6}$)

Input	$\text{MJ}_{\text{exergy}} \text{mol}^{-1} \mathbf{6}$
Chemicals	107
Solution 6 + 7	70.3
EtAc	1.79
NaOH	0.0050
Water	0
EtAc–Et ₃ N	34.5
N₂ gas	0.0010
Electromechanical power	46.1
Pumping in liquids	9.96
Scraping	7.22
Stirring	0.646
Pumping cooling medium	16.4
Pumping heating medium	11.7
Vacuum setting	0.164
Thermal inputs	13.9
Cooling medium	7.57
Heating medium	6.28
Cleaning	13.2
Water	0
MeOH	2.52
EtAc	2.63
CH ₂ Cl ₂ –MeOH	4.08
EtOH	3.54
EtAc–Et ₃ N	0.438
Overall	180

suitable for the next step in the synthesis scheme of the drug. In both cases, it is obvious that chemicals are the major resource for the process: 89 and 57%, respectively. For crystallisation, thermal and inert gas inputs are negligible (<0.2%), the remaining 11% is mainly due to electromechanical power (3.6%) and cleaning agents (7.3%). For the chromatography process, only nitrogen consumption is negligible (0.01%). Cleaning agents have a share that is comparable to the crystallisation process (7.8%), but the heating and cooling requirements (8.1%) and especially the electromechanical power (27.3%) are higher than in the crystallisation process. Whereas chemicals, nitrogen gas and cleaning in absolute numbers are very similar for both processes, electromechanical power and thermal inputs increase by a factor 11 and 75, respectively, if one shifts from the crystallisation towards chromatography, ending up in an overall input increase of 48%. This is inherent in the batch chromatography process requiring significant pumping energy and heating and cooling for solvent volatilisation and condensation. In terms of efficiency, 7.54% of the exergy intake is found back in the target product in case of crystallisation; or 113 MJ is lost per mol of endproduct **6**. Cleaning agents and the mother liquor amount up to 108 MJ, with a share of 96 MJ for the mother liquor. These are, in principle, recoverable on the plant within the β -system boundary. In practice, part of the cleaning agents (solvents) are recuperated; the mother liquor is not. For chromatography, efficiency is 5.15% with a total loss of $170.4 \text{ MJ mol}^{-1} \mathbf{6}$, which is 51% higher than with crystallisation. However, 111 MJ are, in principle, recoverable (solvents). But the electromechanical power and thermal requirements are dissipated to the surroundings and are irreversibly lost. In conclusion, the higher electromechanical and thermal requirements mean that the chromatography process is less resource efficient.

**Fig. 2** Scheme for the analysis of the resource intake for the separation of the diastereoisomers **6** and **7** into **8** (= **6**·HCl) (crystallisation) or **6** (chromatography). Considered levels are the process level with its α system boundary, the Janssen Pharmaceutica plant with its β system boundary, and the overall industry with its γ system boundary.

Plant level (β system boundary)

For the calculation of the resource requirements for the plant to manufacture **6** or **8**, two kinds of processes have to be considered. First, there is the synthesis route from 3-pentanone towards **8** (Fig. 1), including the crystallisation or the chromatography as last step.

Secondly, there is the set of supporting processes for energy and mass exchange, as shown in Fig. 2. For the crystallisation process, the supporting processes are: cooling and heating agent production from electricity and natural gas, respectively, scrubbing of waste gases, condensation of solvents and distillation of methanol so that 90% can be reused within the β system boundary. It means that only 10% fresh methanol has to be taken in and will result in a significant resource saving on one hand; on the other hand resources for the distillation operation come in. With respect to chromatography, scrubbing waste gases, condensing solvents (ethyl acetate), methanol distillation and heating media production from natural gas have to be taken into account.

The inputs for the generation of **8** or **6** by crystallisation or chromatography are the chemicals purchased and introduced immediately at the synthesis steps themselves and the resources bought that are necessary for the supporting processes. From the analysis of the typical batch process used in the synthesis, it proves that chemicals going into the reaction chain are predominant with a share of 94% of the total intake. Energy requirements in the reaction chain and resources for the supporting processes are 6%.

A detailed inventory of all steps from 3-pentanone towards **6** and **7** shows that the exergy value of the purchased chemicals is 368 and 230 MJ to manufacture 1 mol **8** and **6** for crystallisation and chromatography, respectively. The difference can be explained by the higher active yield obtained with chromatography *versus* crystallisation: in order to produce 1 mole of **8** and **6**, crystallisation and chromatography require 2.61 ($92.7 \text{ MJ}_{\text{exergy}}$, Table 1) and 1.98 kg solution of the mixture

of **6** and **7** (70.3 MJ_{exergy}, Table 2), respectively. If one summarises the inputs to the plant for crystallisation, it turns out that 415 MJ are needed to deliver 1 mol of **8** (9.23 MJ) which is 2.22% efficiency. For chromatography, the result shows an overall intake of 434 MJ and an efficiency of 2.13%. This means that the plant has to take in 4.6% more resources in case of chromatography instead of the crystallisation case. Fig. 3 shows the shares of the intakes to the plant. Intake of chemicals is clearly lower for the chromatography case: 266 versus 385 MJ for crystallisation, which is basically the result of its higher yield (Table 1 and 2), resulting in lower chemical input in the overall chain. However, this advantage of chromatography cannot compensate the high electricity and natural gas inputs for power (56.2 MJ), cooling (31.2 MJ) and heating (67.3 MJ) that results in 35% of the total resource intake of the plant for the production of **6** by chromatography. These utilities are limited, respectively, to 20.0, 23.2 and 25.4 MJ in case of crystallisation, which is only 7% of the total (Fig. 3). The results show that cleaning solvents are not negligible, being in the order of 1 to 3% of the total. Nitrogen gas, scrubbing and solvent distillation are, however, negligible.

It is worth analysing the generated exergy losses in the two cases. Overall, with an exergy value of 9.2 MJ of the target product and a respective intake of 415 and 434, the exergy losses at the plant amount to 405.8 and 424.7 for crystallisation and chromatography, respectively, a difference limited to 4.6%. However, the nature of the losses is very different: whereas in crystallisation chemicals make up more than 90% of the losses, in chromatography their share is only 60%. This means that the potential of recoverable exergy losses is much higher in case of crystallisation. In other words, irreversible losses by heat and power utilities are more than six times higher with chromatography.

Moving from the process to the plant level can shift the results in two directions. First, if one has to include preceding processes, e.g. from 3-pentanone towards the mixture of **6** and **7** or heating media production from natural gas, exergy requirements drastically increase if one considers the plant instead of the process. The production of the heating fluid Shellsol necessary to produce **8** from **6** by crystallisation (0.156 MJ) requires 0.494 MJ of natural gas. Creating internal loops of solvents result in an opposite result. For example in case of crystallisation, 0.108 MJ are necessary for recovery of 90% of the methanol, allowing the reduction of the fresh methanol intake from 8.07 MJ down to 0.807 MJ. This means that the solvent intake drops from 8.07 down to 0.915 MJ if

one moves from the process to the plant level, emphasizing the high usefulness of closing cycles.

Industry level (γ system boundary)

In order to deliver the necessary materials and energy to the plant for the production of **8** and **6**, the industry has to extract a number of resources out of the environment. Basically, three main intakes have to be considered (Fig. 2). First, resources to feed the power stations to deliver electricity to the plant for electromechanical energy and cooling energy are required. Secondly, natural gas has to be supplied for heating media. Finally, there is the intake of fossil resources by the basic chemicals manufacturing industry to deliver the base chemicals, including solvents. Nitrogen gas can be omitted given its negligible share. The analysis of these supplying sectors shows efficiencies of 48, 34 and 85% for chemicals, electricity and natural gas delivery, respectively. It turns out that 883.7 and 920.6 MJ have to be extracted out of the environment to produce and isolate 1 mole of **8** or **6** through the industrial metabolism for crystallisation and chromatography, respectively. This is an overall efficiency of only 1.044 and 1.006% respectively. Fig. 4 summarises the shares of the three resource intake ways. If one focuses on materials intake (chemicals), chromatography is the process of choice. However, natural gas intake and especially electricity as utilities cannot be overlooked: it is specifically their weight that leads to another choice in terms of resource efficiency. In conclusion, the analysis emphasises the necessity to take into account both material and energy resource requirements at the same time.

Material and methods

Data inventory

The investigated process concerns the isolation of (2*R*,3*R*)-3-(3-methoxyphenyl)-*N,N*-2-trimethylpentanamine monohydrochloride **8** (Fig. 1). This is the 7th isolated intermediate in the synthesis of Tapentadol. For the isolation, both batch crystallisation and chromatography are considered. For both operations, a functional unit has to be chosen. In the case of batch crystallisation, involving a reactor, filter, dryer and a mother liquor tank, it is the net result of one batch: 199.77 kg of **8**. For batch chromatography, it is the net result from a sequence involving a solvent change in a batch reactor

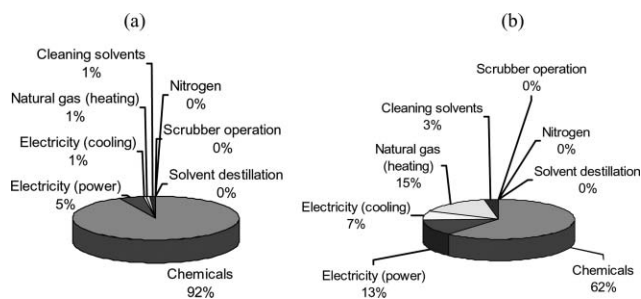


Fig. 3 Share of the overall intake of resources for the plant to produce (a) **8** by crystallisation and (b) **6** by chromatography

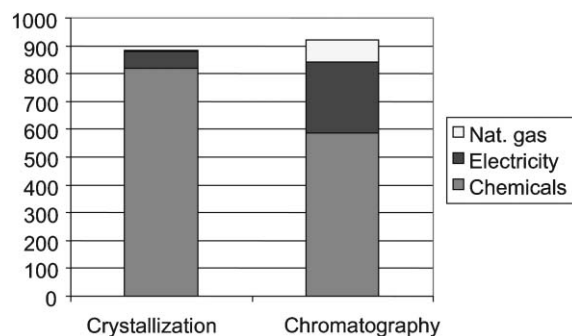


Fig. 4 Overall resource intake (MJ) of the whole industry necessary to deliver the 1 mol **8** (crystallisation) and **6** (chromatography)

Table 3 Detailed operations and related inputs and outputs for the batch crystallisation process

Operations	Inputs	Outputs
At the reactor:		
Inerting	9.73 kg N ₂ at 6 bar Pumping energy, 3300 kJ	
Pumping in solution 6 + 7	1915.25 kg solution 6 + 7 Pumping energy, 4950 kJ	9.73 kg N ₂
Stirring at 80 rpm (continuous)	6.99 kg N ₂ at 6 bar Stirring energy, 1 350 000 kJ	
Heating up to 46 °C	15 740 kg Shellsol at 170 °C Pumping energy 9000 kJ	15 740 kg Shellsol at 167.18 °C
Pumping in HCl in 2-propanol (6N)	197 kg HCl solution Pumping energy, 3300 kJ	6.99 kg N ₂ at 46 °C
Cooling to 46 °C	6.74 kg N ₂ at 6 bar 15 740 kg Shellsol at −10 °C Pumping energy, 9000 kJ	15 740 kg Shellsol at −6.34 °C
Adding seedling crystals 8	4.40 kg 8	
Stirring for 7 h		
Cooling to 40 °C over 3h	141 660 kg Shellsol at −10 °C Pumping energy, 81 000 kJ	141 660 kg Shellsol at −9.87 °C
Cooling to 32 °C over 3h	141 660 kg Shellsol at −10 °C Pumping energy, 81 000 kJ	141 660 kg Shellsol at −9.83 °C
Cooling to 22 °C over 3h	141 660 kg Shellsol at −10 °C Pumping energy, 81 000 kJ	141 660 kg Shellsol at −9.79 °C
Stirring for 7 h		
Emptying reactor		2116.65 kg to filter 6.74 kg N ₂
Cleaning reactor	80 kg water 59.25 kg MeOH Pumping energy for water, 264 kJ Pumping energy for MeOH, 247.5 kJ 7083 kg Shellsol at 170 °C Pumping Shellsol, 4050 kJ Stirring energy, 16 200 kJ	80 kg water 59.25 liquid MeOH at 65 °C 7083 kg Shellsol at 168.39 °C
At the filter:		
Inerting	6.87 kg N ₂ at 6 bar Pumping energy, 9900 kJ	
Pumping in product from reactor	2116.65 kg from reactor	3.00 kg N ₂
Filtering under pressure	11.67 kg N ₂ Stirring energy, 270 000 kJ	
Adding washing solvent	215.30 kg THF Pumping energy, 3300 kJ	15.54 kg N ₂
Filtering under pressure	15.54 kg N ₂	
Emptying filter		273.35 kg crystals to dryer 2058.60 kg mother liquor to tank 15.54 kg N ₂
Cleaning filter	80 kg water 79 kg MeOH Pumping energy for water, 264 kJ Pumping energy for MeOH, 330 kJ 3935 kg Shellsol at 170 °C Pumping energy, 13 500 kJ Stirring energy, 27 000 kJ	80 kg water 79 kg gaseous MeOH at 65 °C 3935 kg Shellsol at 159.00 °C
At dryer:		
Inerting	4.58 kg N ₂ at 6 bar Pumping energy, 9900 kJ	
Take in of crystals	273.35 kg crystals	
Vacuum setting	Pumping energy, 98 100 kJ	64.69 kg gaseous THF at 1 mbar 4.58 kg N ₂
Heating to 50 °C	47 220 kg Shellsol at 170 °C Pumping energy, 108 000 kJ Stirring energy, 792 000 kJ	47 220 kg Shellsol at 169.58 °C
Cooling to 22 °C		
Emptying		208.66 kg product 8 4.40 kg seedling crystals to reactor
Cleaning dryer	80 kg water 79 kg MeOH Pumping energy for water, 264 kJ Pumping energy for MeOH, 330 kJ 4722 kg Shellsol at 170 °C Pumping energy, 13 500 kJ Stirring energy, 27 000 kJ	80 kg water 79 kg gaseous MeOH at 65 °C 3935 kg Shellsol at 160.83 °C

Table 3 Detailed operations and related inputs and outputs for the batch crystallisation process (*Continued*)

Operations	Inputs	Outputs
At the mother liquor tank:		
Take in of mother liquor	2058.60 kg mother liquor	
Pumping in NaOH solution	50 L NaOH solution (50%) Pumping energy, 165.00 kJ	
Pumping in industrial water	100.00 kg industrial water Pumping energy, 330.00 kJ	
Emptying mother liquor tank		2234.85 kg mother liquor
Cleaning mother liquor tank	80 kg water 47.40 kg MeOH 3.16 kg Acetone Pumping energy for water, 264 kJ Pumping energy for MeOH, 648 kJ Pumping energy acetone, 463.20 kJ	80 kg water 47.40 kg MeOH 3.16 kg acetone

Table 4 Detailed operations and related inputs and outputs for the batch chromatography process

Operations	Inputs	Outputs
At the reactor:		
Inerting	9.73 kg N ₂ at 6 bar Pumping energy, 3300 kJ	
Pumping in solution 6 + 7	1040.57 kg solution 6 + 7 Pumping energy, 2750 kJ	9.73 kg N ₂
Stirring at 80 rpm (continuous)	8.59 kg N ₂ at 6 bar Stirring energy, 324 000 kJ	
Heating up to 66 °C	194 544.77 kg Shellsol at 170 °C Pumping energy 111 239.07 kJ	194 544.77 kg Shellsol at 168.96 °C 830.36 gaseous THF at 66 °C
Addition of ethyl acetate	3669.48 kg ethyl acetate Pumping energy, 11 825 kJ	8.59 kg N ₂
Soda liquor and industrial water addition	4.92 kg N ₂ at 6 bar 7.74 kg soda liquor 300 kg industrial water Pumping energy, 880 kJ 4.92 kg N ₂ at 6 bar	4.92 kg N ₂
Removal of water layer		310.95 kg water layer
Emptying reactor		3876.48 kg solution to column 4.92 kg N ₂
Cleaning reactor	80 kg water 59.25 kg MeOH Pumping energy for water, 264 kJ Pumping energy for MeOH, 247.5 kJ 7083 kg Shellsol at 170 °C Pumping shellsol, 4050 kJ Stirring energy, 16 200 kJ	80 kg water 59.25 kg liquid MeOH at 65 °C 7083 kg Shellsol at 168.39 °C
At the column:		
Pumping in solution from reactor	3876.48 kg solution	
Heating of solvent mixture and column	65 360.19 kg water at 60 °C Pumping energy, 4 153 248 kJ	65 360.19 kg water at 55 °C
Pumping in solvent mixture	70 794 kg EtAc/Et ₃ N Pumping energy, 4 968 000 kJ	47 220 kg Shellsol at 169.58 °C
Collection of fractions		74 670 kg fractions to evaporator
Cleaning column	9.00 kg EtAc–Et ₃ N 19.88 CHCl ₂ –MeOH 15.80 kg EtOH Pumping energy solvents, 3000 kJ	9.00 kg EtAc–Et ₃ N 19.88 CHCl ₂ –MeOH 15.80 kg EtOH
At the evaporator:		
Inerting	1.14 kg N ₂ at 6 bar Pumping energy, 1350 kJ	
Take in of fractions from column	74 670 kg fractions	
Heating to 55 °C	1 461 370 kg water at 60 °C Pumping energy, 1 895 481 kJ	1 461 370 kg water at 55 °C
Vacuum setting	Pumping energy, 86 158.25 kJ	73 718.85 kg EtAc/Et ₃ N 1.14 kg N ₂
Scraping	Scraping energy, 3 790 963 kJ	
Emptying		123.89 kg T2653RR 827.74 kg waste stream
Cleaning evaporator	Pumping energy for water, 264 kJ Pumping energy for MeOH, 5602 kJ	54 kg EtAc at 55 °C 119.88 kg CH ₂ Cl ₂ –MeOH at 40 °C 47.40 kg EtOH at 55 °C

(123.89 kg of **6**) that makes use of recycled (99%) ethyl acetate. The subsequent chromatographic system consists of chromatographic separation, solvent evaporation and condensation that recuperates the solvent for the chromatographic separation. Both products **8** (= **6**·HCl) from the crystallisation and **6** are suitable for the subsequent reaction. All operations, inputs and outputs are summarised in Table 3 and 4 for both processes. Notice that also cleaning procedures have been allocated to one batch.

Both processes, situated within the process system boundary α , are embedded in a network of related processes in the plant: manufacturing processes towards mixture of **6** and **7**, supporting processes for energy exchange (hot and cold media delivery, electricity delivery), and supporting processes for mass exchange (solvent condensation and distillation, waste gas scrubbing), all situated within the plant system boundary β in Fig. 2. Here, similar process analyses as in Table 3 and 4 have been made for solvent condensation and heat and cooling media delivery to quantify the energy and material inputs, where energy intake is electricity and natural gas (data not shown). For waste gas scrubbing and distillation, the flows to be treated have been considered taking energy and material requirement data for these operations as available from Dewulf *et al.*¹⁷ and Hamelinck *et al.*¹⁸ With respect to the manufacturing of mixture **6** and **7** starting from 3-pentanone, all required mass and energy inputs have been quantified. Finally, based on the life cycle data of Ecoinvent,¹⁹ the resources to be extracted out of the natural environment to deliver the mass and energy to the Janssen Pharmaceutica plant have been quantified.

Exergy and cumulative exergy calculations

All energy and material inputs and useful outputs to both crystallisation and chromatography and the supporting processes have been quantified in exergy terms. To do so, data available in the literature as such, data obtained by means of group contribution methods, and data obtained from Gibbs formation energy data have been employed.²⁰ Exergy data for waste gas treatment and for distillation were taken from Dewulf *et al.*¹⁷ and Hamelinck *et al.*¹⁸

Cumulative exergy consumption data for the overall industrial metabolism were obtained from the eXoinvent database developed by De Meester *et al.*²¹

Conclusion

First of all, this study has shown that it is possible to quantify energy and material resource intake simultaneously for industrial processes. Exergy analysis is here the unique scientifically sound tool that enables us to quantify all kinds of resources and products on the same scale. However, exergy analysis can only be done if detailed data inventory are available, which is not common practice today, particularly with energy resource intake. Next to data acquisition, setting appropriate system boundaries is critical. It is important to see to what extent the particular processes require supporting processes for energy and materials not only within the facility

itself, but also outside the facility in the overall industrial metabolism.

This study also illustrates the importance and usefulness of considering energy and materials at the same time. Considering the traditional material resource efficiency would lead erroneously towards selecting chromatography. However, the role of heat and power to the specific batch chromatography process is so important that it disfavours the chromatography option.

Furthermore, the study has also shown where efficiency gains can be made by identifying and quantifying the exergy losses. They can be either due to loss of chemicals that are considered as wastes, or related to dissipation of energy, typically heat and power, to the environment. The analysis has shown the potential for better resource efficiency by no longer considering chemicals, typically solvents, as waste but to recover them.

References

- 1 A. M. Rouhi, *Chem. Eng. News*, 2002, **80**, 30–33.
- 2 A. Lapkin, in *Renewables-Based Technology, Sustainability Assessment*, ed. J. Dewulf and H. Van Langenhove, Wiley, Chichester, 2006, pp. 39–53.
- 3 Johnson & Johnson, *Explorer*, August, 2002, vol. 2, p. 4.
- 4 A. D. Curzons, D. J. C. Constable, D. N. Mortimer and V. L. Cunningham, *Green Chem.*, 2001, **3**, 1–6.
- 5 P. Saling and A. Kicherer, in *Renewables-Based Technology, Sustainability Assessment*, ed. J. Dewulf and H. Van Langenhove, Wiley, Chichester, 2006, pp. 299–313.
- 6 J. Dewulf and H. Van Langenhove, in *Renewables-Based Technology, Sustainability Assessment*, ed. J. Dewulf and H. Van Langenhove, Wiley, Chichester, 2006, pp. 111–125.
- 7 J. Dewulf, H. Van Langenhove, J. Mulder, M. M. D. van den Berg, H. J. van der Kooi and J. D. Arons, *Green Chem.*, 2000, **2**, 108–114.
- 8 J. Szargut, *Exergy method: technical and ecological applications*, WIT Press, Southampton, 2005.
- 9 H. Chang and J. W. Li, *Chem. Eng. Sci.*, 2005, **60**, 2771–2784.
- 10 C. Haynes and W. J. Wepfer, *J. Energy Resour. Technol.*, 2002, **124**, 95–104.
- 11 K. Nishida, T. Takagi and S. Kinoshita, *JSME Int. J. Ser. B*, 2004, **47**, 786–794.
- 12 M. A. Rosen and I. Dincer, *Int. J. Energy Res.*, 2004, **28**, 917–930.
- 13 S. K. Som, S. S. Mondal and S. K. Dash, *J. Heat Transfer*, 2005, **127**, 1322–1333.
- 14 P. S. Yong, H. M. Moon and S. C. Yi, *J. Ind. Eng. Chem.*, 2002, **8**, 499–505.
- 15 US DOE, *Chemical bandwidth study. Exergy analysis: a powerful tool for identifying process inefficiencies in the US chemical industry*, Summary Report, U.S. Department of Energy, Industrial Technologies Program, Washington D. C., December 2004, p. 37.
- 16 H. Buschmann, W. Strassburger and E. Friderichs, *Eur. Pat.* EP 693475 B1, 1996.
- 17 J. Dewulf, H. Van Langenhove and J. Dirckx, *Sci. Tot. Environ.*, 2001, **273**, 41–52.
- 18 C. Hamelinck, P. J. A. M. Kerkhof and K. J. Ptasiński, *Energy Convers. Manage.*, 2002, **43**, 1445–1457.
- 19 Ecoinvent, *Ecoinvent data v1.1. Final reports ecoinvent 2000 No. 1–15*, Swiss Center for Life Cycle Inventories, Dübendorf, 2004, CD-ROM.
- 20 J. Szargut, D. R. Morris and F. R. Steward, *Exergy analysis of thermal, chemical and metallurgical processes*, Hemisphere Publishing, Berlin, 1998.
- 21 B. De Meester, J. Dewulf and H. Van Langenhove, *Exoinvent: the exergy of ecoinvent reference flows (version 1.0)*, Ghent University, 2006.

A highly efficient procedure for hydroformylation and hydroamino-vinylation of methyl acrylate

Matthew L. Clarke* and Geoffrey J. Roff

Received 20th November 2006, Accepted 27th February 2007

First published as an Advance Article on the web 20th March 2007

DOI: 10.1039/b616918j

Methyl acrylate has been hydroformylated to the branched aldehyde with essentially perfect regio-selectivity and extraordinarily high average turnover frequencies (up to 4000 h⁻¹). Using 1,3,5,7-tetramethyl-2,4,8-trioxo-6-phosphaadamantane based Rh catalyst with a substrate to catalyst ratio of 10 000, hydroformylation in excellent yield was achieved with complete branched selectivity in around 2 h. Performing this reaction in the presence of aromatic amines gave very high yields of the corresponding enamines in a quick one pot domino hydroaminovinylation reaction. Remarkably, this latter reaction works best under solvent-free conditions.

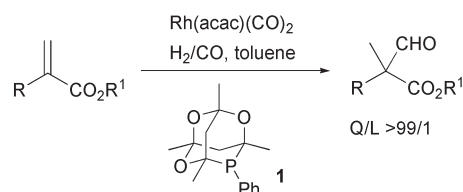
Introduction

Hydroformylation of alkenes represents a highly attractive method to prepare aldehydes, and is one of the most industrially important C–C bond forming reactions. Production is estimated at 7 million tonnes per year, with the majority of this being the production of commodity chemicals, such as *n*-butanal.¹ Due to their higher value, complexity, purity thresholds, and potentially shorter production lifetimes synthesis of fine, ultra-fine and pharmaceutical chemicals creates far more waste and is many times less efficient than commodity and bulk chemical processes. Although the volume of each reaction is comparatively small, the total volumes of waste produced by the many different processes being run worldwide is significant. Due to the different challenges in these industries, the focus is on developing new more efficient synthetic methods, minimising solvent use, and developing tandem procedures such that purification processes can be minimised. Although, many modern reactions are cleaner than their counterparts 20 years ago, there is a whole arsenal of cleaner synthetic chemistry that needs to be developed in order for fine and pharma chemical syntheses to approach the efficiency and lower environmental impact of current commodity chemical processes. Hydroformylation is an excellent example of a 100% atom efficient reaction, and as a result of the rising importance of greener organic synthesis, is now beginning to be recognised as a useful clean synthetic method.¹ There has been great interest in the hydroformylation of functionalised substrates such as vinyl acetate,^{2a} allyl cyanide,^{2b,c} allyl alcohol³ and *N*-vinyl amide derivatives.⁴ One substrate that has been the subject of many studies is methyl acrylate:⁵ hydroformylation of which can serve to provide a starting material for a range of products including heterocycles,⁶ the widely used enantio-pure building block methyl-3-hydroxy-2-methyl propionate,⁷ methyl methacrylate,⁸ and the β -amino acid, [MeC(H)(CH₂NH₂)(CO₂Me)].⁹

Methyl acrylate has been measured to be two orders of magnitude less reactive to H₂/CO relative to oct-1-ene.^{5a–d} However, both linear and branched products have practical and commercial value. In methyl acrylate hydroformylation, Trzeciak and Ziolkowski found rhodium/triphenylphosphite catalyst to give ~60% yield of pure linear aldehyde, along with significant amounts of hydrogenation products.¹⁰ Lee and Alper reported lower hydrogenation by-products (~5%) and high branched selectivity for this reaction using [Rh(COD)(η^6 -C₆H₅-BPh₃)] and dppb as catalyst.^{5f} Neibecker and coworkers demonstrated an effective use of a mono-phosphine derived catalyst for this reaction which gave a 70% conversion to branched aldehyde with no hydrogenation products.¹¹ There have also been several interesting papers on hydroformylation of this substrate in benign solvents or using supported catalysts which show enhanced results compared to standard solvents and conditions.⁵ Recently, Xiao and co-workers reported an important development in this reaction: using a fluoro-polymeric ligand in supercritical CO₂, excellent regio- and chemo-selectivity were observed.^{5b}

We have recently developed a protocol for hydroformylation of 1,1' disubstituted alkenes such as methyl atropate, (H₂C=C(Ph)CO₂Me), with quaternary regio-selectivity.¹² The key to this process has been the use of the ^{Me}CgPPh ligand, **1** (Scheme 1), that gives extremely reactive Rh hydroformylation catalysts.

This very active catalyst was not tested in methyl acrylate hydroformylation in our initial study, but it occurred to us that the high activity of the catalyst might allow a solvent-free hydroformylation of this non-viscous liquid. In this paper, we report how these studies have led to an optimised laboratory



Scheme 1 Hydroformylation of 1,1-disubstituted alkenes.

School of Chemistry, University of St. Andrews, EaStCHEM, St. Andrews, Fife, UK KY16 9ST. E-mail: mc28@st-andrews.ac.uk; Fax: (+44) 1334 463808; Tel: (+44) 1334 463850

scale (multi-gram) procedure for methyl acrylate hydroformylation. The high activity of the catalyst has also been exploited in a domino hydroformylation-enamine formation reaction. Remarkably, this gives highest yields under solvent-free conditions.

Results and discussion

A range of ligands were tested in the hydroformylation of methyl acrylate (Table 1) with most showing excellent branched to linear selectivity. It was found that at room temperature and a substrate to catalyst ratio (S/C) of 500, most ligands gave excellent chemo- and regioselectivity, but insufficient reactivity, giving between 3–15% conversion in 24 h. Tris-(3,5-bistrifluoromethyl)phenylphosphine **2**,¹³ tris-(2,4-di-*tert*-butyl) phenylphosphite, **3**, tris(2-benzofuryl)phosphine, **4**¹⁴ and the caged ligand **1** all proved extremely effective under such conditions giving much better conversion to the branched aldehyde, that exists as a mixture of aldehyde and enol tautomers. This is the first reported use of tris(2-benzofuryl) phosphine as a ligand in a hydroformylation reaction, and this result suggests some promise for this new catalyst system.

Using the most reactive ligand systems, the possibility of solvent free hydroformylation was explored. At lower temperatures and pressure using the cage phosphine, such reactions were extremely sluggish, with the resulting mixture consisting of very little aldehyde with a lot of hydrogenation, polymerisation and aldol products. It was found that increasing the catalyst loading resulted in a significant increase in linear aldehyde production (Table 2). Presumably, these reactions at higher loadings are limited by diffusion of CO to the Rh-catalyst resulting in greater levels of isomerisation from the branched Rh-alkyl intermediate to the linear Rh-alkyl that ultimately gives more linear aldehydes. By keeping the catalyst loading low and using increased pressure and temperature, NMR showed consumption of all starting material after only 5 h compared to the 70 h reactions under milder conditions, although the amount of aldehyde produced was found to be

Table 1 Hydroformylation of methyl acrylate using a range of ligands

Ligand	Yield ^a	B/L
PPh ₃	15	47/1
Ligand 3 ^b	87	>99/1
MeCgPPh, 1	87	63/1
Tris-(2-benzofuryl)phosphine, 4	90	>99/1
Tris-(pentafluorophenyl)phosphine	3	>99/1
Ligand 2	82	96/1
(2-Methylphenyl)diphenylphosphine	5	50/1
Tris-(4-methoxyphenyl)phosphine	4	4/1

^a Conversion based on total aldehydes produced as determined by NMR relative to internal standard. ^b Ligands are tris-(3,5-bistrifluoromethyl)phenylphosphine **2**, tris-(2,4-di-*tert*-butyl) phenylphosphite, **3**, tris(2-benzofuryl)phosphine, **4**. ^c Reaction conditions: Rh(acac)(CO)₂ (0.2%), P-Ligand (1.0%), toluene (1.0 ml per mg Rh), H₂/CO(1 : 1) (50 bar), room temperature, 20–24 h.

Table 2 Solvent free hydroformylation of methyl acrylate

Ligand	Conditions	Yield ^a	B/L
MeCgPPh	A	Low	1/1.7
MeCgPPh	B	8 ^b	6.0/1
MeCgPPh	C	9 ^b	45/1
MeCgPPh	D	35 ^c	35/1
Ligand 2	D	33 ^c	55/1
Ligand 4	D	39 ^c	39/1

^a All reactions gave 100% conversion of methyl acrylate. ^b Yield determined relative to internal standard. ^c Isolated yield of pure aldehyde. ^d Reaction conditions: (A) S/C 1000, 50 bar, 40 °C, 70 h; (B) S/C 1000, 50 bar, 50 °C, 20 h; (C) S/C 10000, 50 bar, 50 °C, 20 hr; D) S/C 10000, 75 bar, 75 °C, 5 h.

extremely low, even with an alternative phosphine catalyst. This was due to significant polymerisation and aldol condensation occurring which was clearly evident by the viscous reaction mixture observed upon opening of the autoclave.

Despite the ultimate failure to develop a practical process under solvent-free conditions, these reactions demonstrated that elevated temperature and pressure resulted in higher turnover. Applying these higher temperature and pressure (75–80 bar, 75 °C) conditions to hydroformylation reactions in solvent resulted in a much higher rate with a substrate to catalyst loading of 10 000. The rate is further enhanced by increasing the Rh/L ratio to 1/10 and reducing the volume of solvent by a factor of 2. It was found that under these optimal conditions, the caged ligand proved the best choice with almost twice the turnover frequency of the next best ligand (Table 3). The choice of solvent was found to be crucial for the reaction workup. Distillation was required for purification as the aldehyde was found to degrade on silica, even when just a plug of silica was used to remove the catalyst. For the reactions performed in toluene, distillation proved problematic as the aldehyde formed an azeotrope with the toluene and the pure product could not be obtained, even with a fractionation column. It was therefore reluctantly concluded that a very low boiling solvent was required. Although complete consumption

Table 3 Optimisation of hydroformylation conditions^a

Solvent	Ligand ^b	Time/min	Yield ^c	TOF/h ^{-1d}	Isolated yield ^e	B/L
Toluene	PPh ₃	300	44	880		77/1
Toluene	Ligand 3	300	36	720		>99/1
Toluene	Ligand 2	300	30	600		82/1
Toluene	Ligand 4	300	49	980		>99/1
Toluene	MeCgPPh	300	85	1700		96/1
THF	MeCgPPh	300	36	720		3/1
Et ₂ O	MeCgPPh	300	55	1100		71/1
Acetone	MeCgPPh	300	81	1620	39	>99/1
DCM	MeCgPPh	300	88	1760	75	>99/1
DCM ^f	MeCgPPh	130	92	4250	85	>99/1
Pentane ^f	MeCgPPh	240	92	2200	88	>99/1

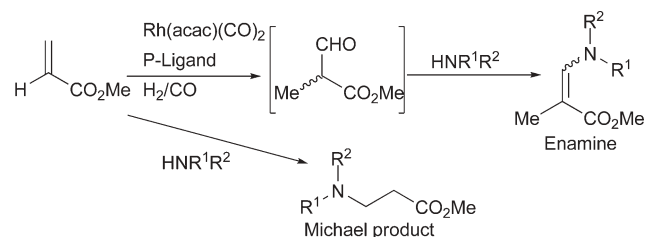
^a Reaction conditions: Rh(acac)(CO)₂ (0.01%), P-Ligand (1.0%), solvent (10 ml per mg Rh), 75 bar, 75 °C. ^b Ligands are tris-(3,5-bistrifluoromethyl)phenylphosphine **2**, tris-(2,4-di-*tert*-butyl) phenylphosphite, **3**, tris(2-benzofuryl)phosphine, **4**. ^c Yield to branched aldehyde determined by NMR relative to an internal standard. ^d Average TOF over complete reaction based on moles of product/total time in h mol⁻¹ of catalyst. Error is estimated at <50 h⁻¹. ^e Isolated yield of pure aldehyde after distillation. ^f Reaction carried out under 80 bar syngas.

of methyl acrylate was achieved in most of the common low boiling solvents, the degree of polymerisation and aldol condensation side products was affected by solvent choice as demonstrated by the conversion to product. The highest turnover frequencies were observed when using the environmentally unacceptable solvent, dichloromethane: 92% conversion was achieved in only 130 min. This overall TOF of 4250 mol h⁻¹ is to the best of our knowledge, the highest overall rate for the hydroformylation of acrylates.¹⁵ Although not ideal, we were pleased to find that pentane, a more environmentally and industrially friendly solvent than CH₂Cl₂ gave the highest isolated yield (88%) of pure branched aldehyde, and is the procedure recommended for synthetic purposes. The cage phosphine catalysts are very robust and it is noted here that the distillation residue could be re-used with similar yield in a further hydroformylation reaction.

A hot topic in green synthetic chemistry is the development of one-pot domino reactions that can save on solvent use and purification. A few years ago, Alper and co-workers reported the first examples of a hydroaminovinyl reaction.¹⁶ In this study only vinyl sulfones and a vinylphosphonate were used as substrates. We were therefore intrigued to discover whether hydroformylation of methyl acrylate in the presence of primary and secondary amines could be directed towards hydroformylation–enamine formation (hydroaminovinyl reaction), rather than the expected Michael addition products (Scheme 2).

When highly nucleophilic amines such as morpholine and benzylamine were introduced into the reaction mixture it was found that the competing Michael addition of the amine to methyl acrylate occurred at a faster rate to the hydroformylation reaction when triphenylphosphine was used (Table 4). The use of the caged phosphine resulted in enamine production being favoured although conversion remained low. To avoid the possibility of Michael addition occurring, less nucleophilic aromatic amines were tested. Again, Rh/PPh₃ showed little reaction whereas the caged phosphine catalyst gave complete conversion to the enamine which could be isolated in excellent yield and, if desired the *E/Z* isomers separated by column chromatography.

As hydroformylation in solvent-free conditions showed promise, being let down by polymerisation and aldol condensation of the product, it was decided to attempt hydroaminovinyl reactions without solvent. The presence of the amine would convert the aldehyde to the enamine before any aldol reactions could occur and temporarily act as a solvent for hydroformylation prior to its use as a reagent for enamine synthesis. In such reactions we decided to use the very



Scheme 2 Possible outcomes from regioselective hydroaminovinyl reactions.

Table 4 Hydroformylation of methyl acrylate in the presence of amines

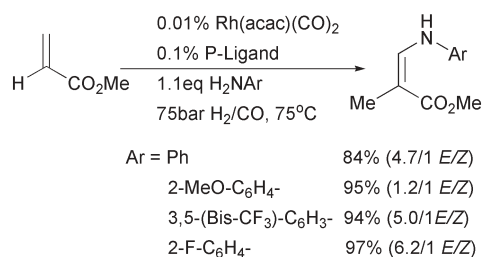
Amine	Ligand	Aldehyde (%)	Michael (%)	Enamine (%)	<i>Z/E</i>
	PPh ₃	0	82	0	N.D.
	MeCgPPh	0	39	61	16/84
	PPh ₃	0	100	0	N.D.
	MeCgPPh	0	83	17	N.D.
	PPh ₃	30	41	29	N.D.
	MeCgPPh	0	20	80	0/100
	MeCgPPh	30	20	50	0/100
	MeCgPPh	5	56	39	0/100
	PPh ₃	73	0	18	N.D.
	MeCgPPh	0	0	100 ^b	71/29
	PPh ₃	81	0	7	N.D.
	MeCgPPh	0	0	100 ^c	57/43
	MeCgPPh	50	0	50	82/18
	MeCgPPh	42	0	58	11/89

^a Product ratios determined by NMR. Conversion to products shown was ~100% in all cases. ^b 98% isolated yield (77% *Z*, 20% *E*).

^c 93% isolated yield (59% *Z*, 34% *E*); N.D. = Not determined

^d Reaction conditions: Rh(acac)(CO)₂ (0.2%), P-Ligand (1.0%), amine (1.1 eq.), toluene (1.0 ml per mg Rh), H₂/CO (1 : 1) (60 bar), room temperature, 24 h.

low catalyst loading at 75 bar syngas at 75 °C that favoured the neat hydroformylation reaction. The aniline derivatives were tested as they had already shown that Michael addition did not occur in any case and at higher temperature, all



Scheme 3 Hydroaminovinylations reactions.

aldehydes would be expected to further react to form the enamines. In a reaction mixture consisting of aldehyde with just 1.1 eq. of amine and S/C 10 000 catalyst, all reactions went to completion in 5 h. A simple acidic workup to remove excess amine followed by filtration through a short plug of silica to remove the catalyst yielded the enamine as an *E/Z* mix of isomers (Scheme 3). An interesting observation is that the *E/Z* ratio favours the *E* isomer in the neat reactions whereas the reverse was true for most of the reactions conducted in solvent.

Conclusions

Methyl acrylate can be a problematic substrate to hydroformylate with simultaneous high chemo- and regioselectivity and high turnover numbers. Although reports of methyl acrylate hydroformylation have been previously published, some with excellent turnover frequencies and selectivity, no definitive practical method has been devised. In this paper we demonstrated that not only does the phosphadamantane ligand modified rhodium catalyst greatly enhance the rate of reaction, the choice of conditions and solvent allow for simple isolation of the aldehyde providing a practical route to the product.

We have also demonstrated that such reactions can be performed in the presence of amines to produce enamines in high yield creating functionalised organic building blocks from a simple substrate in one easy step with only water as an essential by-product. Remarkably, these latter domino reactions work particularly well in solvent-free conditions, giving higher (and reversed) *E/Z* ratios, excellent yield and catalytic turnover. The procedures described here should be suitable for technical applications and provide the synthetic community with the greenest simplest methods to prepare the products described.

Experimental

General

All chemicals and solvents were obtained through commercial sources and used as supplied. Gases were obtained through BOC. Solvents were removed by rotary evaporation on a Heidolph labrota 4000. Flash column chromatography was performed using Davsil silica gel 35–70 u 60A (Fluorochem). NMR spectra were recorded on Bruker Avance 300 instruments. Proton signal multiplicities are given as s (singlet), d (doublet), t (triplet), q (quartet), m (multiplet) or multiples thereof. Infrared spectra were recorded on a Perkin Elmer Spectrum GX FT-IR system. Liquids were analysed as films, solids were analysed as KBr discs or nujol mull. Mass spectra were recorded on Waters Micromass LCT fitted with

lockspray for accurate mass (ESI). Hydroformylation and hydroaminovinylations experiments were carried out in glass lined stainless steel autoclaves, heated in oil baths and stirred magnetically. The synthesis of the caged phosphine **1** has been described previously.¹⁷

Typical optimised procedure for hydroformylation of methyl acrylate

To Rh(acac)(CO)₂ (2.0 mg (0.0078 mmol)) and cage phosphine **1** (23.0 mg (0.078 mmol)) was added pentane (20 ml) followed by methyl acrylate (6.69 g, 7.0 ml, 77.8 mmol). The mixture was transferred to an autoclave. The autoclave was filled and vented three times with syngas (1 : 1 H₂/CO) before filling to 80 bar and stirring at 75 °C for 2 h. The autoclave was cooled to room temperature before releasing the gas and opening. The pentane was removed by rotary evaporation and the product, which exists as both aldehyde and enol tautomers, distilled under vacuum condensing into a cooled flask to give 7.98 g (88%) of clear oil. (Bp below room temp. at 1 mm Hg, lit. 66–69 °C at 40 mm Hg.¹⁸)

Aldehyde. δ_{H} (300 MHz, CDCl₃) 1.41 (3H, d J = 7.2 Hz, CH₃), 3.44 (1H, dq J = 1.5 and 7.2 Hz, CH), 3.83 (3H, s, CO₂CH₃), 9.82 ppm (1H, d J = 1.3 Hz, CHO); δ_{C} (75 MHz, CDCl₃) 10.2 (CH₃), 51.3 (CH), 51.5 (CO₂CH₃), 170.2 (CO₂CH₃), 197.3 ppm (CHO).

Enol. δ_{H} (300 MHz, CDCl₃) 1.74 (3H, d J = 1.0 Hz, CH₃), 3.83 (3H, s, CH₃), 7.05 (1H, dq J = 1.0 and 12.5 Hz, CHOH), 11.32 ppm (1H, d J = 12.5 Hz, CHOH); δ_{C} (75 MHz, CDCl₃) 12.4 (CH₃), 52.5 (CO₂CH₃), 105.3 (C), 160.1 (CHOH), 172.9 ppm (CO₂CH₃); m/z (ES⁺) 117 (M + H)⁺; ν_{max} (film) 1674, 1724, 1740, 3433 cm⁻¹.

General procedure for solvent free hydroaminovinylations

To Rh(acac)(CO)₂ (1.0 mg, 0.0038 mmol) and caged phosphine **1** (11.2 mg, 0.038 mmol) was added methyl acrylate (3.35 g, 3.50 ml, 38.9 mmol) followed by amine (42.8 mmol, 1.1 eq.). The mixture was stirred under 75 bar syngas (1 : 1 H₂/CO) at 75 °C for 5 h. The mixture was dissolved in the minimum volume of diethyl ether and washed with 1 M HCl, dried over MgSO₄ and filtered through a short plug of silica before concentrating.

Hydroformylation of methyl acrylate in aniline

The general procedure gave an off-white solid (6.29 g, 84%). Mp (recryst. from hexane/EtOAc) 95–97 °C; δ_{H} (300 MHz, CDCl₃) 1.77 (2.12H, d J = 1.0 Hz, CH₃(*Z*)), 1.78 (0.88 Hz, d J = 1.3 Hz, CH₃(*E*)), 3.66 (0.88H, s, CO₂CH₃(*E*)), 3.68 (2.12H, s, CO₂CH₃(*Z*)), 6.16 (0.29H, d br. J = 13.1 Hz, NH(*E*)), 6.82–6.92 (3H, m, ArH (*E* and *Z*)), 7.08 (0.71H, dq J = 1.0 and 12.6 Hz, CHN(*Z*)) 7.18–7.24 (2H, m, ArH (*E* and *Z*)), 7.85 (0.29H, dq J = 1.0 and 13.3 Hz, CHN(*E*)), 9.69 ppm (0.71H, d br. J = 11.8 Hz, NH(*Z*)); δ_{C} (75 MHz, CDCl₃) 10.2, 16.2 (CH₃), 51.3, 51.7 (CO₂CH₃), 95.1, 99.6 (C=CH), 115.3, 122.1, 130.0 (ArC), 137.8, 141.2 (C=CH), 141.5 (N–ArC), 170.0, 171.2 ppm (CO₂CH₃); m/z (ES⁺) 214.0848 (M + Na)⁺

(C₁₁H₁₃NO₂Na requires 214.0844); ν_{\max} (KBr) 1602, 1636, 1672, 2954 and 3334 cm⁻¹.

Hydroformylation of methyl acrylate in *o*-anisidine

The general procedure gave a white solid (8.18 g, 95%). Mp 46–48 °C; δ_{H} (300 MHz, CDCl₃) (1.70H, d J = 1.0 Hz, CH₃(Z)), 1.80 (1.30H, d J = 1.0 Hz, CH₃(E)), 3.67 (1.30H, s, CO₂CH₃(E)), 3.70 (1.70H, s, CO₂CH₃(Z)), 3.82 (1.30H, s, OCH₃(E)), 3.83 (1.70H, s, OCH₃(Z)), 6.63 (0.43H, d br. J = 13.3 Hz, NH(E)) 6.75–7.05 (4H, m, ArH (E and Z)), 7.11 (0.57H, dq J = 0.5 and 12.8 Hz, CHN(Z)), 7.87 (0.43H, dd, J = 0.8 and 13.1 Hz, CHN(E)), 9.93 ppm (0.57H, d br. J = 12.0 Hz, NH(Z)); δ_{C} (75 MHz, CDCl₃): δ = 10.2, 16.5 (CH₃), 51.4, 51.6 (CO₂CH₃), 56.1, 56.2 (OCH₃), 95.5, 100.0 (C=CH), 131.0, 131.3 (MeO–ArC), 136.8, 140.2 (C=CH), 147.5, 148.0 (N–ArC), 170.0, 171.0 (CO₂CH₃), 110.1, 111.1, 111.9, 112.5, 121.4, 121.6, 121.8 ppm (CAr); m/z (ES⁺) 221.0949 (M + Na)⁺ (C₁₂H₁₅NO₃Na requires 244.0950; ν_{\max} (KBr) 1597, 1627, 1679, 2836, 2949 and 3317 cm⁻¹.

Hydroformylation of methyl acrylate in 3,5-bis(trifluoromethyl)aniline

The general procedure gave a white solid (11.90 g, 94%). Mp (recryst. from hexane/EtOAc) 128–130 °C; δ_{H} (300 MHz, CDCl₃) 1.78 (0.16H, s, CH₃(Z)), 1.91 (2.84H, s, CH₃(E)), 3.80 (3H, s, CO₂CH₃ (E and Z)), 6.62 (0.95H, d br. J = 12.8 Hz, NH(E)), 7.14 (0.05H, dq J = 1.3 and 12.0 Hz, CHN(Z)), 7.37 (2H, s, ArH (E and Z)), 7.45 (1H, s, ArH (E and Z)), 7.87(0.95H, dq J = 1.0 and 12.8 Hz, CHN(E)), 10.13 ppm (0.05H, d br. J = 12.5 Hz, NH(Z)); δ_{C} (75 MHz, CDCl₃) 9.9, 15.8 (CH₃), 51.3, 51.6 (CO₂CH₃), 103.2 (C=CH), 114.2 (d J = 2.9 Hz, *p*-ArCH), 114.7 (sept J = 3.8 Hz, *m*-ArCH), 123.0 (q J = 272.9, CF₃), 133.1 (q J = 33.4 Hz, F₃C–ArC), 135.2, 138.3 (C=O), 142.5 (N–CAr), 169.0 ppm (CO₂CH₃); δ_{F} (282 MHz, CDCl₃) –63.7 ppm; m/z (ES⁻) 326.0614 (M -H)⁻ (C₁₃H₁₁NO₂F₆ requires 326.0616); ν_{\max} (KBr) 1617, 1656, 1681, 2950 and 3347 cm⁻¹.

Hydroformylation of methyl acrylate in 2-fluoroaniline

The general procedure gave a yellow oil (7.84 g, 94%). δ_{H} (300 MHz, CDCl₃) 1.87 (0.42H, d J = 1.0 Hz, CH₃(Z)), 1.88 (2.58H, d J = 1.3 Hz, CH₃(E)), 3.77 (2.58H, s, CO₂CH₃(E)), 3.79 (0.42H, s, CO₂CH₃(Z)), 6.27 (0.86H, d br. J = 12.0 Hz, NH(E)), 6.85–7.20 (4.14H, m, ArH (E and Z) and CHN(Z)), 7.89 (0.86H, dt J = 1.3 and 13.3 Hz, CHN(E)), 9.90 ppm (0.14H, d br. J = 12.5 Hz, NH(Z)); δ_{C} (75 MHz, CDCl₃) 9.7, 15.9 (CH₃), 51.0, 51.3 (CO₂CH₃), 96.6, 101.2 (C=CH), 113.6, 114.2 (d J = 1.4 Hz, 5-CAr), 115.4, 115.7 (d J = 18.7 Hz, 3-CAr), 121.2, 121.5 (d J = 7.3 Hz, 4-CAr), 124.6, 124.9 (d J = 3.6 Hz, 6-CAr), 129.7 (d J = 10.5, N–ArC), 135.9, 139.4 (CHN), 151.6 (d J = 241.4 Hz, F–CAr), 169.2, 170.5 ppm (CO₂CH₃); δ_{F} (282 MHz, CDCl₃) –133.5, –135.5 ppm; m/z (ES⁺) 232.0753 (M + Na)⁺ (C₁₁H₁₂NO₂NaF requires 232.0753); ν_{\max} (film) 1516, 1651, 1688, 2958 and 3340 cm⁻¹.

Acknowledgements

The authors would like to thank the Leverhulme trust for financial support and the EPSRC for an equipment grant.

References

- (a) F. Ungvary, *Coord. Chem. Rev.*, 2005, **249**, 2946; (b) M. L. Clarke, *Curr. Org. Chem.*, 2005, **9**, 701; (c) M. Dieguez, O. Pamies and C. Claver, *Tetrahedron: Asymmetry*, 2004, **15**, 2113; (d) B. Breit, *Synthesis*, 2001, 1.
- (a) S. Breeden, D. J. Cole-Hamilton, D. F. Foster, G. J. Schwartz and M. Wills, *Angew. Chem., Int. Ed.*, 2000, **39**, 4106; (b) C. J. Cobley, K. Gardner, J. Klosin, C. Praquin, C. Hill, G. T. Whiteker and A. Zanotti-Gerosa, *J. Org. Chem.*, 2004, **69**, 4031; (c) M. M. H. Lambers-Verstappen and J. G. deVries, *Adv. Synth. Catal.*, 2003, **345**, 478.
- (a) E. Drent and W. W. Jager (Shell), *GB Pat.*, 2282137, 1995; (b) K. N. Bhatt and S. B. Halligudi, *J. Mol. Catal.*, 1994, **91**, 187.
- (a) S. Gladiali and L. Pinna, *Tetrahedron: Asymmetry*, 1991, **2**, 623; (b) K. Nozaki, N. Sakai, T. Nanno, T. Higashijima, S. Mano, T. Horuichi and H. Takaya, *J. Am. Chem. Soc.*, 1997, **119**, 4413.
- (a) C. K. Brown and G. Wilkinson, *J. Chem. Soc. A*, 1970, **17**, 2753; (b) Y. L. Hu, W. P. Chen, A. M. B. Osuna, J. A. Iggo and J. L. Xiao, *Chem. Commun.*, 2002, 788; (c) G. Fremy, Y. Castanet, J.-F. Carpentier, E. Monflier and A. Mortreux, *Angew. Chem., Int. Ed. Engl.*, 1995, **34**, 1474; (d) G. Fremy, Y. Castanet, R. Grzybek, E. Monflier, A. Mortreux, A. M. Trzeciak and J. J. Ziolkowski, *J. Organomet. Chem.*, 1995, **505**, 11; (e) W. Chen, L. Xu, Y. Hu, A. M. B. Osuna and J. Xiao, *Tetrahedron*, 2002, **58**, 3889; (f) C. W. Lee and H. Alper, *J. Org. Chem.*, 1995, **60**, 499; (g) Y. Hu, W. Chen, A. M. B. Osuna, A. M. Stuart, E. G. Hope and J. Xiao, *Chem. Commun.*, 2001, 725; (h) I. Amer and H. Alper, *J. Am. Chem. Soc.*, 1990, **112**, 3674; (i) C. G. Arena, F. Nicolo, D. Drommi, G. Bruno and F. Faraone, *J. Chem. Soc., Chem. Commun.*, 1994, 2251.
- (a) A. Michael, *Ber. Dtsch. Chem. Ges.*, 1905, **38**, 2087; (b) A. Harkins and P. Johnson, *J. Am. Chem. Soc.*, 1929, **51**, 1241; (c) F. de Sarlo, *Tetrahedron*, 1966, **22**, 2989; (d) A. Gambacorta, M. E. Farah and D. Tofani, *Tetrahedron*, 1999, **43**, 12615.
- D. Seebach, M. F. Zueger, F. Giovannini, B. Sonnleitner and A. Fiechter, *Angew. Chem., Int. Ed. Engl.*, 1984, **23**, 151; D. Seebach, M. F. Zueger, F. Giovannini, B. Sonnleitner and A. Fiechter, *Angew. Chem.*, 1984, **96**, 155.
- K. Schwirten, H. W. Schneider and R. Kummer, (BASF AG), *DE-B Pat.*, 2643205; K. Schwirten, H. W. Schneider and R. Kummer, *Chem. Abs.*, 1978, **89**, 005946.
- Recent review on β -amino acids: M. Liu and M. P. Sibi, *Tetrahedron*, 2002, **58**, 7991.
- A. M. Trzeciak and J. J. Ziolkowski, *J. Mol. Catal.*, 1987, **43**, 15.
- D. Niebecker and R. Reau, *Angew. Chem., Int. Ed. Engl.*, 1989, **28**, 500; D. Niebecker and R. Reau, *Angew. Chem.*, 1989, **101**, 479.
- (a) M. L. Clarke and G. J. Roff, *Chem.-Eur. J.*, 2006, **12**, 7978; (b) Using other phosphorous ligands gives lower selectivity: M. L. Clarke, *Tetrahedron Lett.*, 2004, **45**, 4043.
- M. L. Clarke, D. Ellis, K. L. Mason, A. G. Orpen, P. G. Pringle, R. L. Wingad, D. A. Zaher and R. T. Baker, *Dalton Trans.*, 2005, 1294.
- C. Santelli-Rouvier, C. Coin, L. Toupet and M. Santelli, *J. Organomet. Chem.*, 1995, **495**, 91; Other ligands with beta-oxygen substituents displayed very low hydroformylation activity: R. A. Baber, M. L. Clarke, A. G. Orpen and D. A. Ratcliffe, *J. Organomet. Chem.*, 2003, **667**, 112.
- Highest overall hydroformylation rate of methyl acrylate to date is 2196 h⁻¹, see ref. 5b. Highest initial rate of acrylate hydroformylation to date is 4300 h⁻¹, see ref. 5c.
- Y.-S. Lin, B. E. Ali and H. Alper, *J. Am. Chem. Soc.*, 2001, **123**, 7719; Beller and co-workers have studied a wider range of alkenes, but to the best of our knowledge, methyl acrylate hydroaminovinylation has never been reported. M. Ahmed, A. Majeedseayad, R. Jackstell and M. Beller, *Angew. Chem., Int. Ed.*, 2003, **42**, 5615; For a review on tandem hydroformylation reactions, see: P. Eilbracht, L. Bärfacker, C. Buss, C. Hollman, B. E. Kitsos-Rzychon, C. L. Kraneman, T. Rische, R. Roggenbuck and A. Schmidt, *Chem. Rev.*, 1999, **99**, 3329.
- R. A. Baber, M. L. Clarke, K. Heslop, A. Marr, A. G. Orpen, P. G. Pringle, A. M. Ward and D. A. Zambrano-Williams, *Dalton Trans.*, 2005, 1079.
- F. Kido, Y. Noda and A. Yoshikoshi, *Tetrahedron*, 1987, **43**, 5467.

The synthesis of *o*-cyclohexylphenol in supercritical carbon dioxide: towards a continuous two-step reaction

Rodrigo Amandi,^a Katherine Scovell,^a Peter Licence,^a Tobias J. Lotz^b and Martyn Poliakoff^{*a}

Received 2nd January 2007, Accepted 28th February 2007

First published as an Advance Article on the web 20th March 2007

DOI: 10.1039/b618727g

The use of supercritical carbon dioxide, scCO₂, as an environmentally friendly reaction medium for the continuous synthesis of the fine chemical *o*-cyclohexylphenol has been investigated. The alkylation of phenol was carried out using a solid acid catalyst, γ -Al₂O₃, using both cyclohexene and cyclohexanol as alkylating agents. Though cheaper, cyclohexanol gave poorer results because of the water formed in the reaction inhibiting the catalyst performance. The possibility of performing the reaction as a two-step process was then investigated. The dehydration of cyclohexanol over the same catalyst was found to be quantitative. Clearly, the water by-product must be eliminated before the alkylation step and, although this was found to be difficult to achieve on a small scale, the process looks promising as a two-step reaction.

Introduction

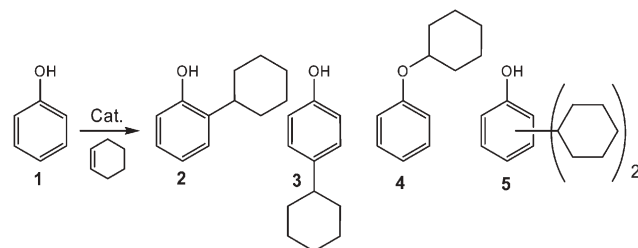
The alkylation of aromatic species, in particular phenol, has been widely investigated over the last few decades.^{1–3} The use of cyclic hydrocarbons as alkylating agents has also been the object of numerous studies.^{4,5} In this way, the acid catalysed alkylation of phenol with cyclohexene or cyclohexanol to form the corresponding alkylated species (Scheme 1) has been investigated. Thus, examples of the homogeneously,^{6,7} and heterogeneously^{5,8–13} catalysed alkylation of phenol to primarily form **2** and **3** can be readily found in the literature.

The alkylated products, **2** and **3**, are used extensively in industry for the manufacture of dyes, resins and biocides.^{5,12} In addition, they can be used as precursors for the synthesis of phenylphenols. *o*-Phenylphenol (*o*-PP) is an important product in the fine chemical industry and is employed widely as a dye stuff, antiseptic, surface activator and thermal stabiliser.^{12,14} In general, *o*-PP is manufactured by a two step process from cyclohexanone, which is firstly condensed in the presence of an

acid catalyst to form a dimer (2-(1-cyclohexenyl) cyclohexanone) and then dehydrogenated to *o*-PP.¹²

The use of supercritical fluids (SCFs), in particular supercritical carbon dioxide (scCO₂), has been described^{15–17} as a replacement for conventional organic solvents in alkylation reactions, in conjunction with heterogeneous catalysts, as an alternative route towards “greener” chemical processes. In this context, scCO₂ could offer significant advantages, including an enhancement of mass and heat transport,^{18,19} the possibility of carrying out continuous fixed-bed reactions, easier separation of the products from the reaction stream¹⁷ and an increase in the catalyst lifetime.^{20,21}

The use of scCO₂ in continuous flow processes for the synthesis of phenol-derived fine chemicals has been investigated previously. Thus, Amandi *et al.*²² investigated the synthesis of the fine chemical thymol in scCO₂ using *iso*-propanol and *m*-cresol as the starting materials and γ -Al₂O₃ as a solid acid catalyst. The authors reported that *ortho*-alkylation was achieved with high selectivity but that the water generated as a reaction by-product deactivated the catalyst. This problem could potentially be overcome by using the corresponding olefin as the alkylating agent. This opens up the interesting possibility of a two-step alkylation of phenol using the same alumina catalyst for both steps, Scheme 2. Here we investigate carrying out this alkylation in practice.



Scheme 1 Synthesis of *o*-cyclohexylphenol (**2**), *p*-cyclohexylphenol (**3**), cyclohexylphenylether (**4**) and di-cyclohexyl-phenol derivatives (**5**), from phenol (**1**) using cyclohexanol or cyclohexene as an alkylating agent, in the presence of an acid catalyst.

^aSchool of Chemistry, University of Nottingham, University Park, Nottingham, UK NG7 2RD.

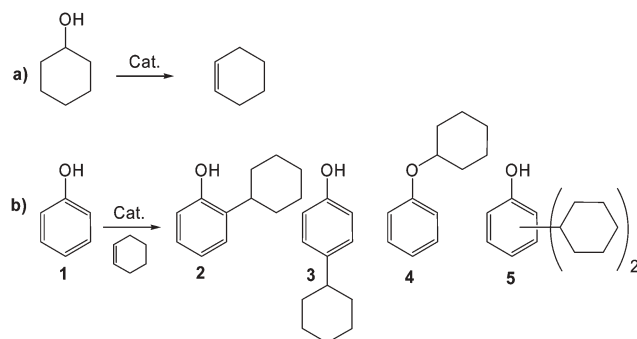
E-mail: Martyn.poliakoff@nottingham.ac.uk

^bSI Group-Switzerland GmbH, Kästeliweg 7, Postfach, Pratteln 1, CH-4133, Switzerland

Results and discussion

Alkylation of phenol with cyclohexanol in scCO₂

The synthesis of **2** was initially investigated by reacting phenol with cyclohexanol (CyOH) over γ -Al₂O₃ in scCO₂. Table 1 summarizes the effect of two reaction temperatures 275 and 300 °C. 275 °C has been previously reported²² as an optimum temperature for alkylation reactions when employing γ -Al₂O₃ as the solid acid catalyst. At both temperatures, the conversion of CyOH was almost quantitative. Cyclohexene (CyHex) and **2** were the major components detected in the reaction product mixture. Formation of CyHex suggests that the reaction begins



Scheme 2 Two step synthesis of **2** in scCO_2 using $\gamma\text{-Al}_2\text{O}_3$ as a catalyst. (a) Dehydration of cyclohexanol to cyclohexene followed by the elimination of water; (b) alkylation of phenol with cyclohexene.

with the dehydration of CyOH to form CyHex, followed by the subsequent reaction of the CyHex with **1**. Formation of **3**, **4** and **5** was observed, as well as other minor reaction by-products, including dicyclohexylether and various unidentified species.

Formation of such by-products increased at 300 °C, with a corresponding decrease in the overall selectivity for **2**. The selective formation of ethers from alcohols over solid acid catalysts and with scCO_2 as the reaction medium has already been described elsewhere.^{23,24}

Before proceeding further, it is important to demonstrate that scCO_2 performs a useful role in the alkylation of phenol **1** with cyclohexanol over $\gamma\text{-Al}_2\text{O}_3$. Therefore, the reaction was carried out in the absence of scCO_2 at similar flow rates of

organic substrate. Table 2 shows that 100% conversion of starting material was still achieved but the yield and selectivity for **2** were very low when compared to reactions where scCO_2 was employed as the reaction medium.

Thus, it appears that the use of scCO_2 in our reaction gives a clear advantage in terms of increased yield and selectivity for product **2**. The effect of the concentration of organic reactants in scCO_2 was then investigated for the alkylation of **1** with CyOH, Table 3.

Increasing the proportion of organic reactants by increasing the flow rate of the organic feed will reduce the residence time in the reactor. Thus, an increase to 40% w/w, resulted in a decrease in the conversion of the CyOH (from 91% to 81%). A change in residence time may account for part of the substantial decrease in the yield of **2**, but this decrease is also the result of increased volumes of water produced in the 40% experiment (see below). The amount of residual CyHex at 40% w/w was about three times higher than when the reaction was performed at 10% w/w of organic substrate.

By contrast, a decrease in the amount of organic within scCO_2 to 7.5% w/w did not affect the reaction outcome significantly, which suggests that the reaction had reached equilibrium. These observations are consistent with the dehydration of CyOH occurring first and the CyHex then reacting with phenol to form **2**, **3** and **5**.

Alkylation of phenol with cyclohexene in scCO_2

The synthesis of **2** was next attempted by reacting **1** with CyHex over $\gamma\text{-Al}_2\text{O}_3$ at various concentrations of organic

Table 1 Reaction of CyOH with **1** over $\gamma\text{-Al}_2\text{O}_3$ in scCO_2 at 275 and 300 °C^a

			% Yield					
	% Conv. CyOH	CyHex	2	3	4	5	Other by-products	% Selectivity for 2 ^b
275 °C	94.2	26.7	59.2	1.2	0.6	5.8	0.7	62.9
300 °C	98.4	22.8	53.5	5.6	0.5	5.0	11.0	54.4

^a Pressure 100 bar; 1 : 0.8 molar ratio (**1** : CyOH), a concentration of organic of 10% w/w in scCO₂, flow rate of CO₂ 0.65 l min⁻¹ and reactor volume 10 ml. ^b The selectivity for **2** was calculated by dividing the number of moles of **2** generated by the sum of the number of moles of CyHex, **2**, **3**, **4**, **5** and other by-products formed in the reaction.

^a Pressure 100 bar; **1** : 0.8 molar ratio (**1** : CyOH), a concentration of organic of 10% w/w in scCO_2 , flow rate of CO_2 0.65 l min⁻¹ and reactor volume 10 ml. ^b The selectivity for **2** was calculated by dividing the number of moles of **2** generated by the sum of the number of moles of CyHex, **2**, **3**, **4**, **5** and other by-products formed in the reaction.

Table 2 Alkylation of **1** with CyOH over $\gamma\text{-Al}_2\text{O}_3$ in the absence of scCO_2 ^a

SM/ml min ⁻¹ ^b	% Conv. CyOH	% Yield					Other by-products	% Selectivity for 2 ^c
		CyHex	2	3	4	5		
0.12 ^d	100	60.3	26.4	6.3	0.4	2.5	4.1	26.4
0.06 ^d	100	62.7	26.1	7.0	0.3	2.3	1.6	26.1

^a 275 °C. ^b SM (starting mixture) **1** : 0.8 molar ratio (**1** : CyOH). ^c See Table 1 for explanation. ^d Same volume of SM pumped per unit of time as if the reaction were carried out at 10% w/w of organic substrate within scCO_2 .

Table 3 Effect of % w/w of organic substrate within scCO_2 for the alkylation of **1** with CyOH using $\gamma\text{-Al}_2\text{O}_3$ as acid catalyst^a

% w/w	% Conv. CyOH	% Yield					Other by-products	% Selectivity for 2
		CyHex	2	3	4	5		
7.5	91.1	24.5	58.2	1.3	0.7	5.3	1.1	66.4
10	94.2	26.7	59.2	1.2	0.6	5.8	0.7	62.9
40	80.6	67.1	10.0	0.5	0.2	2.2	0.6	12.5

^a Pressure 100 bar, temperature 275 °C, **1** : 0.8 molar ratio (**1** : CyOH), flow rate of CO_2 0.65 l min⁻¹ and reactor volume 10 ml.

Table 4 Varying the % w/w of organic reactants within scCO_2 for the alkylation of **1** with CyHex over $\gamma\text{-Al}_2\text{O}_3$ ^a

% w/w	% Conv. CyHex	% Yield					Other by-products	% Selectivity for 2
		2	3	4	5			
10	88.1	75.2	3.4	0.3	7.1	2.1		93.1
40	22.4	20.1	0.4	0.5	1.1	0.3		91.2

^a Pressure 100 bar, temperature 275 °C, 1 : 0.8 molar ratio (**1** : CyHex), flow rate of CO_2 0.65 l min⁻¹ and reactor volume 10 ml.

Table 5 Effect of adding water to the reaction mixture for the alkylation of **1** with CyHex over $\gamma\text{-Al}_2\text{O}_3$ in scCO_2 ^a

% w/w added H ₂ O	% Conv. CyHex	% Yield					Other by-products	% Selectivity for 2
		2	3	4	5			
0	88.1	75.2	3.4	0.3	7.1	2.1		93.1
10	65.0	55.3	1.9	1.1	5.1	1.6		84.7
20	45.4	37.5	1.7	0.9	4.3	1.0		80.2

^a Pressure 100 bar, temperature 275 °C, 1 : 0.8 molar ratio (**1** : CyHex), a concentration of 10% w/w in scCO_2 , flow rate of CO_2 0.65 l min⁻¹ and reactor volume 10 ml.

substrate in scCO_2 , as shown in Table 4. At concentrations of 10% w/w, both the yield and selectivity for **2** were high, reaching values of 75% and 93% respectively. At higher concentrations, the results with CyHex were quite different from those with CyOH because the selectivity remained very high although the conversion dropped. Although the ultimate catalyst lifetime was not measured, these experiments were repeated using the same batch of catalyst, and the same high results were obtained even after several experiments.

A possible reason for the different results obtained when running the reaction using CyOH and CyHex is that the water formed in the dehydration of CyOH deactivates the catalyst towards the alkylation step. With this in mind, the alkylation with CyHex was repeated with small amounts of water being deliberately added to the reaction mixture, Table 5.

From Table 5, it can be seen that the addition of water to the reaction mixture has a significant effect on the performance of the catalyst; the yield of products decreases as increasing amounts of water are added. Furthermore, when the catalyst employed to conduct these experiments was used in a further alkylation of **1** with CyHex in scCO_2 *without water*, its catalytic properties were never restored, even after several hours of reaction. This observation suggests that scCO_2 cannot efficiently remove the water generated as a by-product in the alkylation of **1** with CyOH, from the catalyst surface, hence the decrease in the overall amount of products formed at high organic concentration (see Table 3). Thus, the elimination of water from the reaction stream seems to be crucial in developing a process to synthesise **2** in high yields.

Two step reaction in scCO_2 ; dehydration followed by the alkylation of phenol

The results obtained from the alkylation with CyHex were promising. However, CyHex is more expensive than CyOH. It would therefore be commercially advantageous to use CyOH rather than CyHex, particularly if the alumina catalyst, which was used to dehydrate CyOH to form CyHex, could then be used for the alkylation reaction, see Scheme 2. The dehydration was investigated at 275 °C, 150 bar and various concentrations of CyOH in scCO_2 , Table 6.

Table 6 Effect of % w/w of CyOH in scCO_2 on the yield of CyHex

% w/w	% Conv. CyOH	% Selectivity for CyHex
7.6	100	100
17	99.6	100
29	91.0	100

^a Pressure 100 bar, temperature 275 °C, flow rate of CO_2 0.65 l min⁻¹ and reactor volume 10 ml.

It can be seen from Table 6 that the conversion of CyOH was quantitative at a concentration of 7.6% w/w and, unlike the alkylation reaction (Table 3), remained high even at concentrations of 17 and 29% w/w, giving conversions of 99.6% and 91.0%, respectively. The selectivity for CyHex was very high and no other product was detectable by GC. As in the alkylation reaction, the catalyst remained active for several runs. The CyHex synthesised in this fashion was dried using a conventional moisture trap and **1** was added. The resulting mixture was employed as the starting material for further experiments to check the “quality” of the CyHex produced. Experiments revealed that the *in situ* generated CyHex from the dehydration of CyOH over $\gamma\text{-Al}_2\text{O}_3$ in scCO_2 gave comparable yields to those attained when using commercially available CyHex. There appears to be no evidence in any of our experiments for direct alkylation by CyOH without formation of CyHex as an intermediate.

Conclusions

In this paper, the alkylation of phenol has been carried out using cyclohexene over $\gamma\text{-Al}_2\text{O}_3$ giving high conversion and selectivity towards **2**. When the alkylation was carried out using cyclohexanol the selectivity dropped, possibly due to water, formed as a by-product in the reaction, deactivating the catalyst towards the alkylation step. The addition of H_2O to the reaction mixture of the alkylation of phenol with CyHex showed a significant decrease of conversion and selectivity towards product **2**, confirming that H_2O is indeed deactivating the catalyst. The reactions carried out in the presence of scCO_2 gave significantly better yields and selectivities than the reaction without CO_2 , thus suggesting that scCO_2 plays a positive role in the reaction.

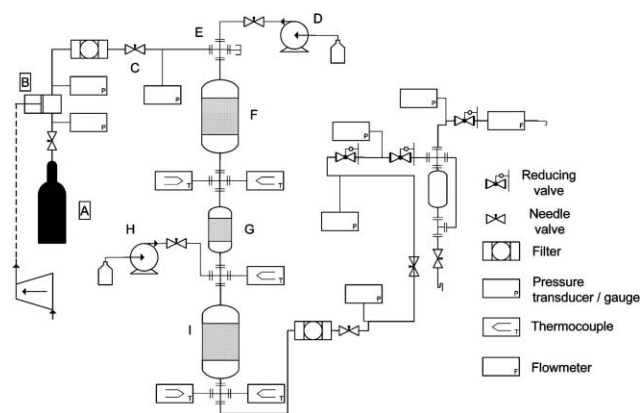


Fig. 1 Schematic of the supercritical fluid two-step continuous flow apparatus used in the synthesis of *o*-CHP (for labelling see text).

Recently, we reported a successful two-stage reaction in scCO_2 in which a ketone was hydrogenated over a Pd catalyst in the first stage and the resulting alcohol was then used as one reactant in an enantioselective enzymatic transesterification in the second stage.²⁵ Even without optimisation, the reaction worked well because neither H_2 nor unreacted ketone interfered with the transesterification. The alkylation of phenol by CyOH is different because the H_2O generated in the conversion of CyOH to CyHex needs to be removed before the alkylation, or the H_2O will deactivate the catalyst.

The value of a two stage reaction lies in the absence of any depressurisation between the stages, which substantially reduces the energy requirement compared to two separate supercritical reactions. This means that the H_2O must be removed without significant depressurisation, unlike the reaction above where we depressurised, isolated and dried the CyHex off-line. CyHex and H_2O are essentially immiscible at ambient temperature. Therefore in principle, the H_2O should be best removed by physical separation of the organic and aqueous phases. However, such separation is difficult to engineer on a scale as small as that of our reactor.

We did explore the possibility of using a desiccant, held in a dummy reactor, between the dehydration and alkylation reactors (see Fig. 1 and Experimental section). In practice this arrangement did not work; the desiccant was rapidly heated by the hot stream emerging from the reactor, with a corresponding reduction in its water-absorbing capacity. Indeed, we found little difference in the product distribution obtained with no desiccant, silica gel, CaCO_3 , or 4A-Z8 and 13X-Z8 molecular sieves (typically 100% conversion CyOH, 45.8% CyHex, 44.1% **2** and 10.1% other by-products with an overall selectivity towards **2** of 44.1%). Thus, although any demonstration of a continuous two stage reaction will need to be carried out on a larger scale than is conveniently used in our laboratory, we have demonstrated the feasibility of the underlying chemistry.

Experimental

The samples collected were analysed using a Shimadzu GC-17a fitted with AOC 20i autosampler, and a RTX-5 column (30 m length, 0.52 mm ID and 0.25 μm film thickness); carrier gas He

and an FID detector. Qualitative and quantitative analyses were carried out using commercially available standards.

Two different reaction systems were employed to conduct the experiments reported here: all of the single stage experiments were carried out in a system which has been described elsewhere.²² Fig. 1 shows the schematic diagram of the supercritical continuous flow apparatus used to carry out two stage reactions in scCO_2 : dehydration of CyOH followed by the alkylation of phenol.

The CO_2 is stored in a high pressure cylinder situated next to the apparatus (A) and is compressed above the desired reaction pressure using a refrigerated reciprocating pump (B) NWA PM101. The pressure regulator (C) controls the system pressure. CyOH was injected into the system using a standard Gilson 305 HPLC pump (D). The organic substrate and the scCO_2 were mixed using a static mixer (E) consisting of an unheated Swagelok crosspiece filled with glass beads. The mixture entered the first reactor (F), where the catalyst was loaded and held inside by a frit piece situated at the bottom of the reactor. The desiccant material employed unsuccessfully to trap generated water was placed in the dummy reactor (G). HPLC pump (H), Gilson 305, pumped a mixture of phenol/cyclohexane, which was then mixed with the product stream from (G) in a static mixer. The alkylation occurred in the second reactor (I). Thermocouples inside the catalyst and desiccant bed, heating blocks and in the product stream were used to monitor the reaction temperature.

The pressure was decreased step-wise and the products separated from the fluid in the expansion unit. The flow rate of the exhausted gases was measured by a flowmeter fitted in the vent line. The flow rate of the exhausted gases was set to 0.65 l min^{-1} of CO_2 at 1 bar and 20 $^\circ\text{C}$ which corresponds to 1.06 g min^{-1} .

$\gamma\text{-Al}_2\text{O}_3$,²² was used as “supplied”. Before pumping the organic substrate into the flow apparatus, the catalyst was dried *in situ* by flowing scCO_2 at the reaction temperature for 1 h. The reactors used in the experiments (see below), were filled with catalyst. This equates to approximately 7.5 g of catalyst used in each run. Cyclohexanol, cyclohexene and phenol (Aldrich) were used as supplied.

The reactors used in our experiments consisted of 12 mm (OD) 316-stainless steel tubing with an internal volume of 10 ml ((F) and (I)) and 5 ml (G).

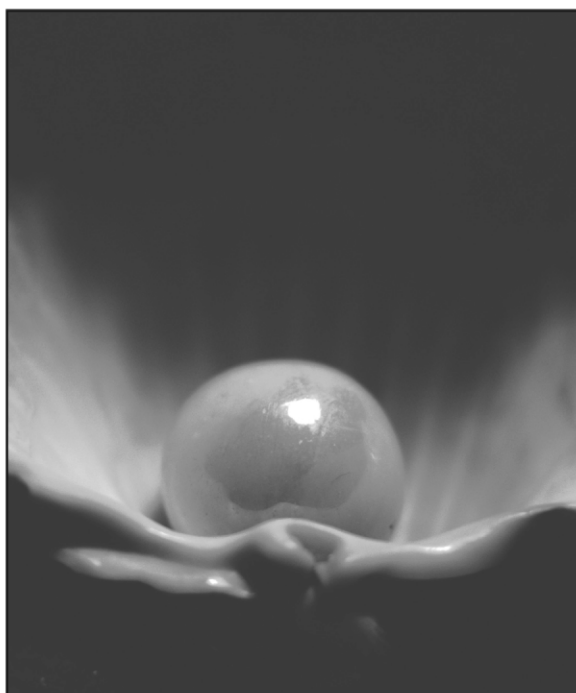
Acknowledgements

We thank the SI Group Switzerland GmbH, EPSRC, EU FP5 project “CPFCO2” and the Marie Curie Programme for funding, and M. Dellar, M. Guyler, R. Wilson and P. Fields for technical support at the University of Nottingham.

References

- 1 K. G. Chandra and M. M. Sharma, *Catal. Lett.*, 1993, **19**, 309.
- 2 C. W. Hu, Y. F. Zhang, L. Xu and G. Peng, *Appl. Catal., A*, 1999, **177**, 237.
- 3 S. Sato, R. Takahashi, T. Sodesawa, K. Matsumoto and Y. Kamimura, *J. Catal.*, 1999, **184**, 180.
- 4 P. H. J. Espeel, K. A. Vercruysse, M. Debaerdemaker and P. A. Jacobs, in *Zeolites and Related Microporous Materials; State of the Art 1994*, Elsevier, Amsterdam, Netherlands, 1994, vol. 84.

- 5 G. D. Yadav and P. Kumar, *Appl. Catal., A*, 2005, **286**, 61.
- 6 M. Seino, S. Okazaki and T. Saito, *Bull. Jpn. Pet. Inst.*, 1976, 18.
- 7 M. V. Postnova, S. G. Koshel, N. V. Lebedeva, E. A. Kuznetsova and G. N. Koshel, *Russ. J. Org. Chem.*, 2003, **39**, 1415.
- 8 R. Anand, T. Daniel, R. J. Lahoti, K. V. Srinivasan and B. S. Rao, *Catal. Lett.*, 2002, **81**, 241.
- 9 R. Anand, K. U. Gore and B. S. Rao, *Catal. Lett.*, 2002, **81**, 33.
- 10 S. Velu and C. S. Swamy, *Res. Chem. Intermed.*, 2000, **26**, 295.
- 11 A. Chakrabarti and M. M. Sharma, *React. Polym.*, 1992, **17**, 331.
- 12 G. J. Lee, J. M. Garces, D. A. Hucul, T. L. Young and K. A. Burdett, *US Pat.* 5583268, 1996.
- 13 P. P. Yang, Z. L. Wang, J. F. Yu, Q. S. Liu and T. G. Wu, *React. Kinet. Catal. Lett.*, 2004, **83**, 129.
- 14 C. Cai and C. X. Lu, *Chem. Innovation*, 2001, **31**, 37.
- 15 E. J. Beckman, *J. Supercrit. Fluids*, 2004, **28**, 121.
- 16 S. van den Hark, M. Härröd and P. Møller, *J. Am. Oil Chem. Soc.*, 1999, **76**, 1363.
- 17 P. Licence, J. Ke, M. Sokolova, S. K. Ross and M. Poliakoff, *Green Chem.*, 2003, **5**, 99.
- 18 A. Baiker, *Chem. Rev.*, 1999, **99**, 453.
- 19 P. G. Jessop and W. Leitner, *Chemical Synthesis Using Supercritical Fluids*, Wiley-VCH, Weinheim, Germany, 1999.
- 20 B. Subramaniam, *Appl. Catal., A*, 2001, **212**, 199.
- 21 B. Subramaniam, C. J. Lyon and V. Arunajatesan, *Appl. Catal., B*, 2002, **37**, 279.
- 22 R. Amandi, J. R. Hyde, S. K. Ross, T. J. Lotz and M. Poliakoff, *Green Chem.*, 2005, **7**, 288.
- 23 B. Walsh, J. R. Hyde, P. Licence and M. Poliakoff, *Green Chem.*, 2005, **7**, 456.
- 24 W. K. Gray, F. R. Smail, M. G. Hitzler, S. K. Ross and M. Poliakoff, *J. Am. Chem. Soc.*, 1999, **121**, 10711.
- 25 H. R. Hobbs, B. Kondor, P. Stephenson, R. A. Sheldon, N. R. Thomas and M. Poliakoff, *Green Chem.*, 2006, **8**, 816.



Looking for that **special**
research paper from applied
and technological aspects of the
chemical sciences?

TRY this free news service:

Chemical Technology

- highlights of newsworthy and significant advances in chemical technology from across RSC journals
- free online access
- updated daily
- free access to the original research paper from every online article
- also available as a free print supplement in selected RSC journals.*

*A separately issued print subscription is also available.

Registered Charity Number: 207890

RSCPublishing

www.rsc.org/chemicaltechnology

22030683

Direct synthesis of H_2O_2 from O_2 and H_2 over precious metal loaded TS-1 in CO_2

Qunlai Chen and Eric J. Beckman*

Received 2nd January 2007, Accepted 1st March 2007

First published as an Advance Article on the web 21st March 2007

DOI: 10.1039/b618934b

H_2O_2 was synthesized directly from O_2 and H_2 over precious metal loaded titanium silicalite (TS-1) in compressed CO_2 and yields were measured by immediately reacting the *in situ* generated H_2O_2 with an “indicator”—pyridine. Experimental results proved that H_2O_2 could be effectively synthesized from O_2 and H_2 in compressed CO_2 . The effects of the following factors on H_2 conversion, H_2O_2 selectivity and yield were examined: O_2/H_2 molar ratio, H_2 concentration, catalyst mass, Pd content in the catalyst and the addition of Pt to the catalyst. Under the optimal reaction conditions, H_2O_2 yield reached 31.7% with an H_2O_2 selectivity of 56.1%.

Introduction

Hydrogen peroxide (H_2O_2) is an important green oxidant because it contains a high fraction of active oxygen and generates water as its only by-product. Although the current major applications of H_2O_2 are in non-selective oxidation reactions (pulp and paper bleaching *etc.*), using it as a selective oxidant to conduct green oxidations is becoming more attractive to both academia and industry.^{1,2} In 2005, global annual H_2O_2 capacity reached 3.53 million metric tons (as 100% H_2O_2).³ Industrially, H_2O_2 is produced by the anthraquinone auto-oxidation (AO) process. Here, 2-alkyl anthraquinone (AQ) is dissolved in a mixture of organic solvents to form the “working solution” and then hydrogenated over a precious metal catalyst to form 2-alkyl anthrahydroquinone (AQH₂). AQH₂ is then oxidized by compressed air to generate H_2O_2 and regenerate AQ. This AO process is successfully used to produce most of the world’s H_2O_2 because it prevents direct contact between O_2 and H_2 and can be operated continuously under mild reaction conditions.⁴ However, this process is far from green in view of the 12 principles of green chemistry.⁵ First, it generates several wastes from the sequential hydrogenation and oxidation of AQ, the unintended oxidation of organic solvents, and the phase behavior in each reactor.⁴ These will inevitably cause the loss of AQ and solvent and, more seriously, the contamination of H_2O_2 . Therefore, makeup AQ and solvents must be added to the system periodically, and the crude H_2O_2 has to be purified and concentrated prior to its commercial use. This purification and concentration process consumes large amounts of steam⁶ in order to almost completely evaporate the crude H_2O_2 solution. The lost AQ and solvents will eventually go to waste streams, including waste water and tail gas (from the oxidation step in the AO process). The waste water needs to be treated to decompose AQ (and its derivatives) and solvents (and their derivatives) prior to its discharge; the organic solvents

contained in tail gas have to be recovered by an adsorption method before its release.⁷ Finally, this AO process is not as efficient as desired because of the limited solubility of AQ in the solvents, controlled hydrogenation conversion (<70% in order to minimize the side-reactions), and low H_2O_2 concentration in the working solution (usually <1.5%). Substantial extraction equipment has to be used and large amounts of working solution must be circulated in order to obtain a commercially viable H_2O_2 solution (30% or greater). Because of the complexity of the AO process, the current H_2O_2 price is high enough such that many oxidation reactions can not be carried out economically, even though the reactions themselves are attractive (such as that given by Sato *et al.*,⁸ using 30% H_2O_2 to oxidize cyclohexene for the green synthesis of adipic acid).

Direct synthesis of H_2O_2 from O_2 and H_2 is an attractive green technology to replace the current AO process since it is the most atom-efficient method by which H_2O_2 can be synthesized. Direct synthesis could greatly simplify the process, dramatically cut the production cost and generate almost no waste. In 1914, Henkel and Weber⁹ were awarded probably the first patent on direct synthesis of H_2O_2 from O_2 and H_2 over a precious metal catalyst. However, little progress was made following 1914 because of safety issues, and it was almost completely ignored after the AO process was commercialized in the 1950s. There was renewed interest in direct synthesis after 1980 driven by the strong demand for H_2O_2 ,¹⁰ especially in recent years.^{11–16} The reaction systems used can be homogeneous but are usually heterogeneous. The homogeneous reaction system was reported by Hancu *et al.*¹² using CO_2 as the solvent and a CO_2 -soluble palladium complex as the catalyst to synthesize H_2O_2 from O_2 and H_2 . Because the mass transfer resistance was completely eliminated in this homogeneous system, the H_2O_2 yield reached as high as 38%. However, the synthesis of the CO_2 -soluble palladium catalyst was tedious and expensive. Many researchers have used gas–liquid–solid three-phase heterogeneous reaction systems to conduct direct synthesis of H_2O_2 from O_2 and H_2 . Palladium and/or platinum loaded carbon, Al_2O_3 , SiO_2 and TiO_2 were typically used as the catalysts. Recently, nano-sized gold was

Department of Chemical & Petroleum Engineering, University of Pittsburgh, Pittsburgh, PA, 15261, USA.
E-mail: beckman@engr.pitt.edu; Fax: +1-412-624-7820;
Tel: +1-412-624-4828

found to exhibit high activity in catalyzing the direct synthesis of H_2O_2 , especially when it was used together with palladium.^{15,17–20} The solvents used were methanol, water or their mixtures. Under the same reaction conditions, using methanol or a mixture of methanol and water as the solvent gave higher H_2O_2 yield than in water alone because of a higher mass transfer rate^{21,22} due to more favorable gas solubility²³ and surface tension in methanol. Even adding small amounts of methanol could lead to higher H_2O_2 yield²⁴ possibly because of the significant increase in gas holdup and decrease in gas bubble size.^{25,26} Mineral acid (HCl , H_2SO_4 or H_3PO_4) and bromide were widely used as promoters. Since the O_2/H_2 mixture is explosive over a broad concentration range (4–95.2% H_2 in O_2 at 1 bar and 20 °C), the O_2/H_2 molar ratios used were usually high enough to avoid operating in the explosive range. For lower O_2/H_2 molar ratio, an inert gas was used to dilute the O_2/H_2 mixture. Mild reaction temperatures were used by most researchers in order to minimize H_2O_2 decomposition. The operating pressures ranged from ambient to ~200 bar; generally speaking, higher pressure resulted in higher H_2O_2 yield under the same reaction conditions because the increase in operating pressure increased the mass transfer rate.²⁶

The latest progress in direct synthesis was recently reported by Degussa/Headwaters:²⁷ a pilot plant was reported to be undergoing testing and the process could be commercialized soon. The companies disclosed that methanol was used as the solvent in this new process; safety issues could still exist since methanol is a flammable and volatile organic solvent, and furthermore methanol will likely be oxidized during the synthetic process, forming formaldehyde and other by-products.^{28,29} The product obtained in this direct synthetic process was dilute H_2O_2 in methanol; concentration and separation processes are required in order to obtain a commercially viable aqueous H_2O_2 solution. Therefore, this new process was not intended to replace the current AO process; it was rather to be used as an *in situ* H_2O_2 source to be integrated with a new propylene oxide production process.

CO_2 could be used to replace methanol as the solvent for *in situ* generation of H_2O_2 from O_2 and H_2 . A CO_2 -based system has the following advantages.³⁰ (1) As mentioned before, the mixture of O_2 and H_2 is explosive over a broad concentration range. Recently, Pande and Tonheim³¹ pointed out that the non-explosive limit for a gas mixture of H_2 and O_2 in CO_2 is significantly higher than that in N_2 . (2) Since O_2 and H_2 are each miscible with CO_2 above 31 °C, the gas–liquid–solid three-phase reaction system is simplified to a fluid–solid two-phase system. This will dramatically reduce, or could even eliminate, mass transfer resistance. (3) CO_2 can react with water present in the reaction system forming carbonic acid, favoring the stabilization of direct synthesized H_2O_2 . (4) CO_2 is non-flammable (a significant safety advantage over conventional organic solvents), naturally abundant, easy to obtain and less toxic than many other organic solvents [the threshold limit value (TLV) of CO_2 is 5000 ppm, while the values for acetone, methanol and benzene are 750 ppm, 200 ppm and 0.5 ppm, respectively]. Therefore, it is expected that the direct synthesis of H_2O_2 from O_2 and H_2 in compressed CO_2 could be carried out more effectively than that in the conventional solvents.

However, some contradictory conclusions have been reported in the literature. Beckman⁴ and Danciu *et al.*³² had previously reported that propylene oxide (PO) could be effectively generated from the oxidation of propylene by *in situ* generated H_2O_2 from O_2 and H_2 using Pd/TS-1 as the catalyst and CO_2 as the solvent. However, Landon *et al.*¹⁵ found that the generation of H_2O_2 in CO_2 was not as effective as that in conventional solvents. Until now, there has not been a reliable method available to measure the amount of *in situ* generated H_2O_2 in CO_2 since: (1) it is difficult to accurately take H_2O_2 samples from a high pressure reactor filled with CO_2 ; (2) the precious metal loaded catalyst used for synthesizing H_2O_2 can also catalyze the decomposition of generated H_2O_2 , as was observed by Landon *et al.*¹⁵ Therefore, simply releasing the reaction pressure and then taking samples for titration after reaction is not likely to be the best method to accurately measure the amount of *in situ* generated H_2O_2 in compressed CO_2 .

In this paper, the amount of *in situ* generated H_2O_2 in CO_2 was measured by reacting it immediately with an “indicator” compound. Through the quantification of the conversion of this “indicator” compound, the amount of *in situ* generated H_2O_2 was calculated. Further, the selectivity of H_2 conversion to H_2O_2 was measured *via* a gas chromatograph. Experimental results showed that H_2O_2 could be effectively synthesized from O_2 and H_2 in CO_2 with precious metal loaded titanium silicate (TS-1) as the catalyst.

Results and discussion

Selection of “indicator” compound

An “indicator” compound was used to measure the amount of *in situ* generated H_2O_2 in compressed CO_2 without the need to titrate samples. This “indicator” had to meet the following criteria. (1) It should be easily oxidized by H_2O_2 under mild reaction conditions with TS-1 as the catalyst. One problem associated with using H_2O_2 as a selective oxidant in carrying out green oxidation is the presence of water in H_2O_2 solution, since water can usually cause the deactivation of many catalysts, especially those used in organic oxidations. The discovery of TS-1 removed this obstacle because the hydrophobic nature of TS-1’s micro-pores favors the diffusion of organic substrates to the active site and protects the active site from deactivation by water.¹ This makes TS-1 one of the most studied catalysts in carrying out green oxidation reactions with H_2O_2 . Therefore, proving that precious metal loaded TS-1 is an effective catalyst in direct synthesis of H_2O_2 has special meaning in future applications. (2) The indicator should not be oxidized by oxygen alone or hydrogenated; this is obvious since the mixture of O_2 and H_2 is used for direct synthesis of H_2O_2 . (3) The selectivity to its oxide should be high at reasonable H_2O_2 concentration, because the formation of more than one product will make the measurement complicated. (4) The “indicator” should be converted to its oxide proportional to the amount of H_2O_2 added. (5) The “indicator” and its oxide should both be soluble in CO_2 . This proposed “indicator” compound can be selected from a list of various alcohols, tertiary amines and sulfides.¹ Ultimately,

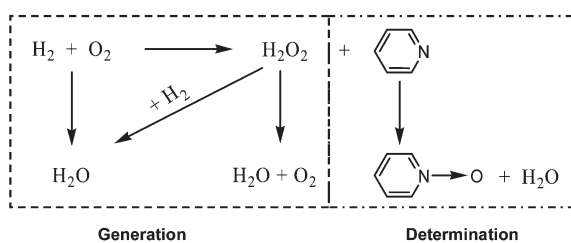


Fig. 1 Reactions involved in the direct synthesis of H_2O_2 and its determination.

pyridine was selected as the “indicator” according to above mentioned criteria.

The reactions involved in the direct synthesis of H_2O_2 from O_2 and H_2 and its determination by using pyridine as the “indicator” are given in Fig. 1. The oxidation of pyridine by H_2O_2 is fast, as shown by Prasad *et al.*³³ In this study, the direct synthesis of H_2O_2 was carried out for 5 h at 60 °C in compressed CO_2 with pyridine as the “indicator”. Gas chromatographic (GC) analysis during control experiments using aqueous H_2O_2 under these conditions showed only two peaks: one for pyridine *N*-oxide, and another for un-reacted pyridine. Further control experiments also showed that pyridine was not oxidized by O_2 alone over TS-1 or Pd/TS-1, or by the mixture of O_2 and H_2 with or without TS-1 as the catalyst.

Direct synthesis of H_2O_2 from O_2 and H_2 in CO_2

The direct synthesis of H_2O_2 was conducted using a mixture of O_2 and H_2 as the starting reactants over precious metal loaded TS-1 with pyridine as the “indicator” in compressed CO_2 . The amount of *in situ* generated H_2O_2 from O_2 and H_2 could be calculated according to the obtained pyridine *N*-oxide yields by applying the stoichiometric relationship between the *in situ* generated H_2O_2 and pyridine *N*-oxide shown in Fig. 1. Here, precious metal loaded TS-1 is a bifunctional catalyst: the precious metal functioned as the catalyst for direct synthesis of H_2O_2 from O_2 and H_2 , while TS-1 functioned as the catalyst for the oxidation of pyridine by *in situ* generated H_2O_2 .

The O_2/H_2 molar ratio should have a significant effect on the direct synthesis of H_2O_2 , although literature results in conventional solvents showed differing conclusions. Chinta and Lunsford³⁴ concluded that the selectivity for H_2O_2 decreased with the increase of the O_2/H_2 molar ratio, and Hwang *et al.*³⁵ found that a feed ratio of $\text{O}_2 : \text{H}_2 = 1 : 1$ led to the optimal H_2O_2 production. By contrast, Dalton and Skinner³⁶ stated that, in order to improve the direct synthesis of H_2O_2 from O_2 and H_2 in an acidic medium containing an oxygenated or nitrogenous organic compound, the O_2/H_2 molar ratio should be higher than 3.4. Here we also examined the effect of O_2/H_2 molar ratio on the direct synthesis of H_2O_2 in CO_2 and the results are given in Fig. 2. It reveals that H_2 conversion, H_2O_2 selectivity and H_2O_2 yield (see their definitions in Experimental section) all decreased with an increase of O_2/H_2 molar ratio. The optimal H_2 conversion, H_2O_2 selectivity and H_2O_2 yield were obtained at an O_2/H_2 molar ratio of 1. Although the reason behind this phenomenon is not clear, the results in this study coincide with those of

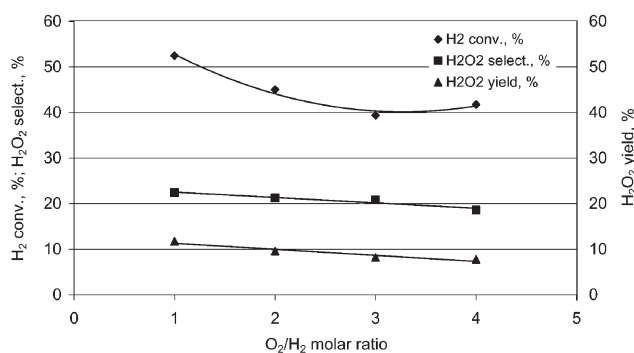


Fig. 2 Effect of O_2/H_2 molar ratio on the direct synthesis of H_2O_2 in CO_2 . Experimental conditions: $\text{H}_2 = 6.2$ mmol, indicator = 6.2 mmol, water = 27.8 mmol, 0.35% Pd/TS-1 = 0.05 g; $P = 125$ bar, $T = 60$ °C, reaction time = 5 h.

Chinta and Lunsford³⁴ and Hwang *et al.*³⁵ In the rest of this study, the O_2/H_2 molar ratio was kept at 1 in order to maximize the formation of H_2O_2 in CO_2 .

The effect of H_2 concentration on direct synthesis of H_2O_2 has not been well explored in the literature. The results shown in Fig. 3 disclose the effect of H_2 concentration (defined as the amount of H_2 added to the reactor over the net volume of the reactor, mM) on H_2 conversion, H_2O_2 selectivity and H_2O_2 yield at constant O_2/H_2 ratio. It is concluded that with the increase of H_2 concentration in the reactor, H_2 conversion, H_2O_2 selectivity and H_2O_2 yield all increased until H_2 concentration reached 500 mM. When H_2 concentration was increased from 250 mM to 500 mM, H_2 conversion only increased about 20% (from 52.5% to 62.6%), while H_2O_2 selectivity almost doubled (from 22.4% to 39.3%). This in turn resulted in the increase of H_2O_2 yield from 11.8% to 24.6%. Fig. 3 also shows that when the H_2 concentration was below 500 mM, the relationship between H_2O_2 yield and H_2 concentration was linear, implying that the reaction rate for the direct synthesis of H_2O_2 from O_2 and H_2 in CO_2 was first order with respect to H_2 concentration. Further increase to H_2 concentration led to a decrease in H_2O_2 selectivity at similar H_2 conversions. The possible reason is that, at higher H_2 concentration, the existence of significant amounts of H_2 favored the hydrogenation of H_2O_2 (as shown in Fig. 1) over

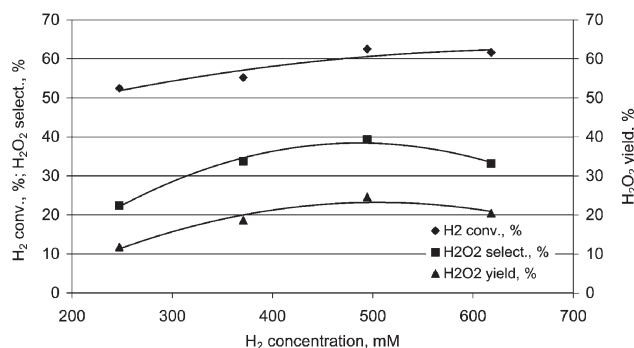


Fig. 3 Effect of H_2 concentration on the direct synthesis of H_2O_2 in CO_2 . Experimental conditions: $\text{O}_2/\text{H}_2 = 1$, indicator = 6.2 mmol, water = 27.8 mmol, 0.35% Pd/TS-1 = 0.05 g; $P = 125$ bar, $T = 60$ °C, reaction time = 5 h.

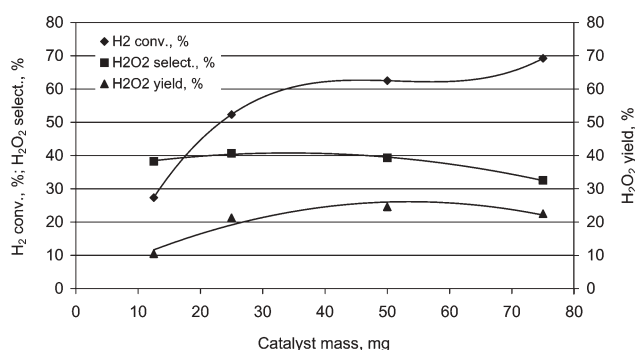


Fig. 4 Effect of catalyst mass on the direct synthesis of H₂O₂ in CO₂. Experimental conditions: H₂ = 12.4 mmol, O₂/H₂ = 1, indicator = 6.2 mmol, water = 27.8 mmol, 0.35 %Pd/TS-1; *P* = 125 bar, *T* = 60 °C, reaction time = 5 h.

the Pd/TS-1 catalyst. Therefore, part of the *in situ* generated H₂O₂ could be hydrogenated before it can react with the “indicator”.

The influence of catalyst mass on the formation of H₂O₂ is given in Fig. 4. H₂ conversion increased with the increase of catalyst mass, especially at the lower catalyst mass ranges, while H₂O₂ selectivity initially increased with the increase of catalyst mass and then steadily decreased. The combination of these effects resulted in an initial increase and then a plateau in H₂O₂ yield. This could be attributed to the occurrence of the hydrogenation of *in situ* generated H₂O₂ at higher catalyst concentration, which, in turn, led to the increase in H₂ conversion, the decrease in H₂O₂ selectivity and almost no change in H₂O₂ yield. When conducting direct synthesis of H₂O₂ using a palladium catalyst in an aqueous medium, Izumi *et al.*³⁷ also observed a similar phenomenon: the formation of H₂O₂ increased initially with the increase of catalyst concentration and then reached a plateau with the further increase in the catalyst concentration.

A survey of the literature showed that high palladium ($\geq 1\%$ Pd) contents were preferred by many researchers^{11,14–16,18} in carrying out direct synthesis of H₂O₂ from O₂ and H₂. Few investigators³⁵ examined the direct synthesis by using lower Pd content catalysts ($\leq 1\%$ Pd). From an economic viewpoint, for a similar H₂O₂ yield, the lower the Pd content in the catalyst, the more competitive the catalyst will be. In this study, a series of catalysts with Pd contents ranging from 0.2–1.0% were used to conduct direct synthesis of H₂O₂ in CO₂, and the results are given in Fig. 5. With the increase of Pd content in the catalyst, H₂ conversion increased while H₂O₂ selectivity decreased steadily. The combination of these changes led to almost no change in H₂O₂ yield until the Pd content reached 0.6%. Further increasing Pd content in the catalyst resulted in a decrease in H₂O₂ yield. In order to explore the reason behind this phenomenon, H₂O₂ decomposition experiments were conducted using catalysts with different Pd contents; the results are shown in Fig. 6. We should point out that higher pyridine *N*-oxide yields in Fig. 6 mean that less H₂O₂ was decomposed by the catalyst. By comparing with TS-1 alone, we found that Pd on TS-1 can cause significant decomposition of H₂O₂. The amounts of H₂O₂ decomposed by Pd/TS-1 increased with the increase in Pd contents in the catalysts. 1.0%

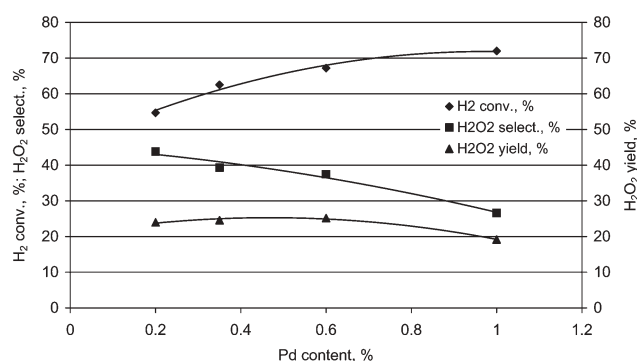


Fig. 5 Effect of Pd content on the direct synthesis of H₂O₂ in CO₂. Experimental conditions: H₂ = 12.4 mmol, O₂/H₂ = 1, indicator = 6.2 mmol, water = 27.8 mmol, Pd/TS-1 = 0.05 g; *P* = 125 bar, *T* = 60 °C, reaction time = 5 h.

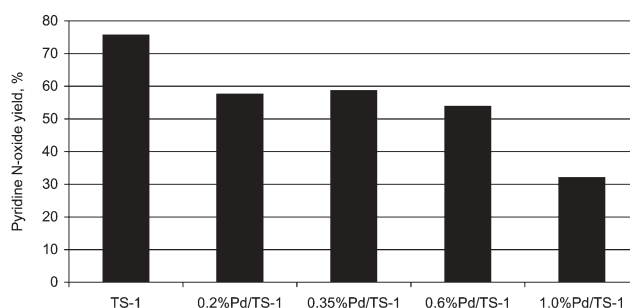


Fig. 6 Experimental results for the decomposition of H₂O₂ by different catalysts. Experimental conditions: H₂O₂/indicator = 1, indicator = 12.4 mmol, catalyst = 0.1 g; *P* = 1 bar, *T* = 60 °C, reaction time = 5 h.

Pd/TS-1 could decompose about 50% of H₂O₂ under the given experimental conditions. Therefore, the decrease in H₂O₂ yield when using the higher Pd loaded catalyst was likely because the higher Pd loaded catalyst could cause the partial decomposition of *in situ* generated H₂O₂ before it could react with the “indicator”. Finally, the lower selectivities observed upon raising Pd content could be due to hydrogenation of H₂O₂ as well.

Platinum (Pt) has the ability to promote the direct synthesis of H₂O₂ from O₂ and H₂ over Pd catalysts, the optimal amount of Pt is typically about one tenth that of Pd.^{11,38,39} In this study, the influence of adding Pt (Pt/Pd = 0.1 by weight) to Pd/TS-1 catalysts was investigated, the results, given in Fig. 7, supported the previous literature conclusions. It can be seen from Fig. 7 that the addition of Pt to the Pd/TS-1 catalyst had significant influence on direct synthesis of H₂O₂ in compressed CO₂, especially when Pd content was less than 0.6%. This influence was mainly on H₂O₂ selectivity, while for H₂ conversion, it was minor. The combination of these effects led to an increase in H₂O₂ yield. For example, adding 0.02% Pt to 0.2% Pd/TS-1 could increase H₂O₂ selectivity from 43.8% to 56.1% with almost no change in H₂ conversion, which, in turn, resulted in the increase in H₂O₂ yield from 23.9% to 31.7%. As pointed out by Meiers *et al.*,⁴⁰ during the preparation of Pd/TS-1, the interaction of the Pd precursor, [Pd(NH₃)₄]²⁺, with TS-1 (support) created a new Pd species, Pd(II), with a

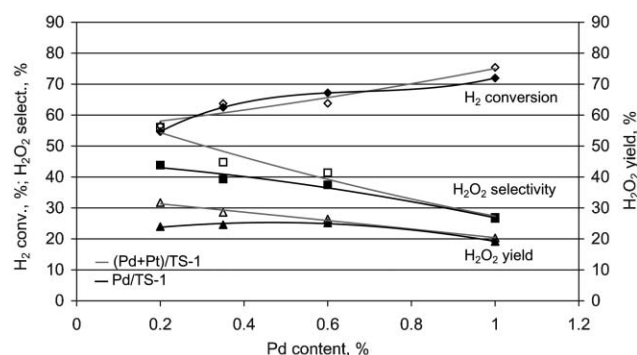


Fig. 7 Effect of adding Pt to the Pd/TS-1 catalysts in direct synthesis of H_2O_2 . Experimental conditions: $\text{H}_2 = 12.4$ mmol, $\text{O}_2/\text{H}_2 = 1$, indicator = 6.2 mmol, water = 27.8 mmol, catalyst = 0.05 g; $P = 125$ bar, $T = 60$ °C, reaction time = 5 h.

binding energy in the range of 337.2–337.8 eV. This new Pd species was neither Pd^0 (binding energy in the range of 335.3–335.5 eV) nor PdO (binding energy: 336.1–336.2 eV), and it played an important role in epoxidation of propylene by the mixture of O_2 and H_2 (via the *in situ* generation of H_2O_2). Adding small amounts of Pt to Pd/TS-1 could dramatically increase the fraction of Pd(II) sites, thus, leading to an increase in H_2O_2 yield. However, one should be aware that the addition of Pt to Pd/TS-1 affects not only the Pd oxidation state but also particle features. A further increase in Pt content could only slightly increase the fraction of Pd(II), but significantly changed the surface morphology of the Pd aggregates from primarily needle-shaped to a mixture of needle-shaped crystallites and the undesirable spherical crystallites.⁴⁰

Interaction between H_2O_2 and TS-1

Upon contact between H_2O_2 (pre-formed or *in situ* generated) and TS-1, two reactions occur simultaneously. The first reaction, as disclosed by Antcliff *et al.*,⁴¹ could be called “self-degradation” of H_2O_2 catalyzed by TS-1 to generate HOO^\bullet , with subsequent deprotonation to form superoxide (O_2^- or OO^\bullet) radicals. Some of these radicals could eventually form O_2 , especially when TS-1 is loaded with a metal. The second reaction (and also the dominant one) is the formation of Ti-peroxo species—which are active in oxidation reactions. However, Bonino *et al.*⁴² observed that a small fraction (about 10%) of peroxo species (characterized by a cream color) appeared to be poorly reactive toward organic substrates. This implies that, in any oxidation reaction involving H_2O_2 and TS-1, part of the consumed H_2O_2 will not play any role in catalytic oxidation reactions owing to degradation over TS-1.

We conducted a series of experiments using different amounts of pre-formed 30% aqueous H_2O_2 solution in compressed CO_2 to oxidize the “indicator” under the reaction conditions given in Table 1. The relationship between H_2O_2 /pyridine molar ratios and the pyridine *N*-oxide yields is shown in Fig. 8. It is clear from these data that in the case of pre-formed H_2O_2 , only about 70% of the consumed H_2O_2 reacted with the “indicator” to generate pyridine *N*-oxide in compressed CO_2 . It should be pointed out that there might be a difference in pyridine *N*-oxide yield found using pre-formed

Table 1 Experimental conditions in determining the calibration curve in CO_2 ^a

$\text{H}_2\text{O}_2/\text{mmol}$	0.29	0.49	0.97	1.55	3.11	6.21	8.73
$\text{H}_2\text{O}_2/\text{pyridine (mol/mol)}$	0.047	0.079	0.16	0.25	0.50	1.01	1.41
Water ^b /ml	0.47	0.45	0.40	0.34	0.18	—	—

^a Indicator = 6.2 mmol, TS-1 = 0.05 g; $P = 125$ bar, $T = 60$ °C, reaction time = 5 h. ^b Water was used to compensate the total volume of liquid reactants if it was less than 1.0 ml.

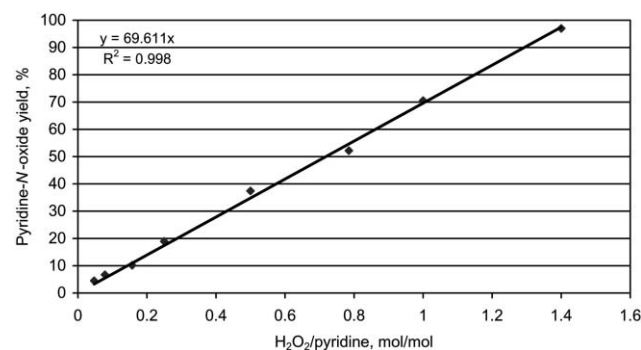


Fig. 8 Calibration curve for the measurement of H_2O_2 in CO_2 . Indicator = 6.2 mmol, TS-1 = 0.05 g; $P = 125$ bar, $T = 60$ °C, reaction time = 5 h.

H_2O_2 versus using *in situ* generated H_2O_2 . By adding small aliquots (10–20 μL) of pre-formed H_2O_2 every 5 minutes into the reactor, one could possibly mimic the *in situ* generation of H_2O_2 from O_2 and H_2 . The result at ambient pressure and 60 °C showed that the difference in pyridine *N*-oxide yield between adding pre-formed H_2O_2 at the beginning and adding it aliquot by aliquot was within 10%. Therefore, we might say that the H_2O_2 yield obtained in this study during reactions in CO_2 was the minimum amount of *in situ* generated H_2O_2 , while the H_2O_2 selectivity was the minimum selectivity toward the direct synthesis of H_2O_2 from O_2 and H_2 in compressed CO_2 . In comparison, we recalculated the H_2O_2 selectivity and yield by using the calibration curve given in Fig. 8. The results are listed in Table 2. Naturally, at the same H_2 conversion, H_2O_2 selectivity and yield calculated using the calibration curve were each higher than those obtained before—these results might represent an upper bound to these values.

Table 2 The comparison of experimental results with and without the consideration of the calibration curve^a

Catalyst	H_2 conversion (%)	H_2O_2 selectivity (%)		H_2O_2 yield (%)	
		A ^b	B ^b	A ^b	B ^b
0.2% Pd/TS-1	54.7	43.8	62.9	24.0	34.4
0.35% Pd/TS-1	62.5	39.3	56.4	24.6	35.3
0.6% Pd/TS-1	67.2	37.5	53.8	25.2	36.1
1.0% Pd/TS-1	72.0	26.6	38.2	19.2	27.5
(0.2% Pd + 0.02% Pt)/TS-1	56.5	56.1	80.4	31.7	45.5
(0.35% Pd + 0.035% Pt)/TS-1	63.7	44.8	64.3	28.5	41.0
(0.6% Pd + 0.06% Pt)/TS-1	63.8	41.4	59.4	26.4	37.8
(1.0% Pd + 0.1% Pt)/TS-1	75.4	26.9	38.7	20.3	29.1

^a Experimental conditions: $\text{H}_2 = 12.4$ mmol, $\text{O}_2/\text{H}_2 = 1$, indicator = 6.2 mmol, water = 27.8 mmol, catalyst = 0.05 g; $P = 125$ bar, $T = 60$ °C, reaction time = 5 h. ^b A is the results without considering degradation of H_2O_2 on TS-1 and the calibration curve; B is the results with the consideration of calibration curve.

Experimental

Chemicals and catalysts

The purities of O₂, H₂ and CO₂ (from Penn Oxygen, Jeannette, PA, USA) used in this study were all above 99.9%. Pyridine (99+%, Aldrich), pyridine *N*-oxide (95%, Aldrich), H₂O₂ (30%, J. T. Baker), methanol (99.9%, Fisher), [Pd(NH₃)₄](NO₃)₂ (10% (wt) solution in water, Aldrich) and Pt(NH₃)₄Cl₂·H₂O (98%, Aldrich) were all used as received without further purification.

TS-1 and 0.35%Pd/TS-1 were from Lyondell Chemical Company. The methods for preparing 0.2% Pd/TS-1, (0.2% Pd + 0.02% Pt)/TS-1, (0.35% Pd + 0.035% Pt)/TS-1, 0.6% Pd/TS-1, (0.6% Pd + 0.06 %Pt)/TS-1, 1.0% Pd/TS-1 and (1.0% Pd + 0.1% Pt)/TS-1 catalysts were similar to that given by Hancu *et al.*⁴³ The procedures of this method were described in the following, with the preparation of (1.0%Pd + 0.1%Pt)/TS-1 as an example: 3.0 g of TS-1 and 12 ml of deionized water were added to a glass flask and then heated to 80 °C under continuous stirring. To this solution, 0.82 ml of 10% (wt) [Pd(NH₃)₄](NO₃)₂ solution and 0.26 ml of 2% (wt) Pt(NH₃)₄Cl₂ solution were added. This mixture was kept stirring for 24 h and then cooled to room temperature. The solid was recovered by filtering and washing 3 times with deionized water and then dried at 80 °C overnight. It was then calcined in air at 150 °C for 4 h and reduced by H₂ at room temperature for 4 h.

General procedures for direct synthesis of H₂O₂ in CO₂

Direct synthesis of H₂O₂ from O₂ and H₂ in compressed CO₂ was conducted in a 30 ml stainless steel reactor manufactured by the University of Pittsburgh. A cylindrical glass liner was used to prevent the decomposition of H₂O₂ by the metal wall. The net reactor volume was therefore reduced to 25 ml. Initially, the reactor and the glass liner were both passivated with 35% HNO₃ for 4 h and 30% H₂O₂ for 10 h; after each experiment, they were also passivated by 30% H₂O₂ for 4 h. In a typical experiment, 0.5 ml of “indicator” compound (pyridine), 0.5 ml water and 0.05 g of catalyst were loaded in to the reactor. A magnetic stirring bar was placed inside the reactor in order to keep the reactants mixing well. The reactor was first charged with known amount of O₂/CO₂, followed by CO₂, and then known amount of H₂. The reaction pressure was finally adjusted to 125 bar by adding more CO₂. The reaction temperature was controlled at 60 °C by a stirrer/hotplate. The direct synthesis of H₂O₂ was allowed to run for 5 h, and the amount of un-reacted H₂ in the reactor was analyzed by using an online HP 5890A gas chromatograph (GC) equipped with a TCD detector and a HayeSep D packed column (20ft × 1/8”) and controlled by a HP ChemStation. The reactor was then ice-cooled to 0–5 °C and the gas mixture inside the reactor was vented into a certain amount of methanol. This methanol solution was used to extract pyridine *N*-oxide and un-reacted pyridine from the reactor and analyzed by another 5890A GC equipped with a FID detector and a DB-1 capillary column (30 m × 0.253 mm × 0.50 μm) to determine the quantities of pyridine *N*-oxide and pyridine. A proportional relief valve was installed for safety.

H₂ conversion, H₂O₂ selectivity and H₂O₂ yield were defined by the following equations.

H₂ conversion (%) =

$$\frac{\text{the amount of H}_2 \text{ consumed during reaction (mmol)}}{\text{the amount of H}_2 \text{ added to the reactor (mmol)}} \times 100$$

H₂O₂ selectivity (%) =

$$\frac{\text{the amount of } in \text{ situ generated H}_2\text{O}_2 \text{ (mmol)}}{\text{the amount of H}_2 \text{ consumed during reaction (mmol)}} \times 100$$

H₂O₂ yield (%) =

$$\frac{\text{the amount of } in \text{ situ generated H}_2\text{O}_2 \text{ (mmol)}}{\text{the amount of H}_2 \text{ added to the reactor (mmol)}} \times 100$$

The experiments for obtaining calibration curve were similar to the direct synthesis of H₂O₂ except that the reactants were 0.5 ml of “indicator” compound (pyridine), a certain amount of 30% H₂O₂ and 0.05 g TS-1. If the total volume of reactants was less than 1.0 ml, water was added to compensate the rest volume. The reaction pressure was adjusted to 125 bar by using only compressed CO₂. The yield of pyridine *N*-oxide was also analyzed by the GC.

General procedures for the decomposition of H₂O₂

The experiments for the decomposition of H₂O₂ were conducted at ambient pressure in a 50 ml glass flask. The flask was placed in an oil bath in order to keep temperature at 60 °C during the experiment. 0.1 g of catalyst and 12.4 mmol of “indicator” compound (pyridine) were placed into this flask. 12.4 mmol of 30% H₂O₂ was then added to the above mixture and the reactor was kept stirring for 5 h. During the decomposition experiment, the flask was connected to a condenser to prevent the reactants from evaporating. After reaction, methanol was used to extract product and reactant. This methanol was analyzed by 5890A GC to determine the yield of pyridine *N*-oxide.

Conclusion

Based on the criteria given in this study, pyridine was selected as an “indicator” compound to react quickly with H₂O₂ synthesized from O₂ and H₂ in compressed CO₂ over precious metal loaded TS-1.

The experimental results in this study showed that H₂O₂ could be effectively synthesized from O₂ and H₂ in compressed CO₂. H₂ conversion, H₂O₂ selectivity and H₂O₂ yield all decreased with an increase in O₂/H₂ molar ratio. The optimal O₂/H₂ molar ratio was 1 in the range of this study. An increase in H₂ concentration led to an increase in H₂ conversion, H₂O₂ selectivity and yield. H₂O₂ yield was linearly proportional to H₂ concentration below 500 mM of H₂, implying that direct synthesis of H₂O₂ from O₂ and H₂ in compressed CO₂ was first order with respect to H₂ concentration. H₂ conversion increased, while H₂O₂ selectivity decreased, with the increase of catalyst mass, these in turn resulted in almost no change in H₂O₂ yield in a broad range of catalyst mass. Experimental results also proved that H₂ conversion increased with an increase of Pd content in Pd/TS-1 catalyst, while H₂O₂

selectivity decreased. The combination of these effects led to the almost no change in H_2O_2 yield versus Pd content from 0.2–0.6%. The addition of Pt to the Pd/TS-1 catalysts has a significant positive influence on H_2O_2 selectivity, while its effect on H_2 conversion is minor.

Since the support, TS-1, used in this study is an excellent catalyst for using H_2O_2 to conduct green oxidations, the direct synthesis of H_2O_2 from O_2 and H_2 in CO_2 with precious metal loaded TS-1 as the catalysts could be used as an *in situ* H_2O_2 source in carrying out selective oxidation. From our work with pyridine, it appears that the formation of the H_2O_2 would be the limiting step in simple oxidations. If the reaction of O_2 and H_2 in CO_2 was desired for generation of H_2O_2 as the final product, one should design the system such that the H_2O_2 is quickly removed from the vicinity of the Pd/Pt catalyst (to minimize degradation). It is likely in such a case that a different support for the metals would be employed.

Acknowledgements

The authors gratefully acknowledge US Environmental Protection Agency (EPA) for its grant RD83153301-01.

References

- 1 C. W. Jones, *Applications of Hydrogen Peroxide and Derivatives*, ed. J. H. Clark, The Royal Society of Chemistry, Cambridge, 1999.
- 2 R. Noyori, M. Aoki and K. Sato, *Chem. Commun.*, 2003, 1977–1986.
- 3 *Chem. Week*, 2005, **167**, 27, p. 36.
- 4 E. J. Beckman, *Green Chem.*, 2003, **5**, 332–336.
- 5 P. T. Anastas and J. C. Warner, *Green Chemistry: Theory and Practice*, Oxford University Press, Oxford, 1998.
- 6 A. P. Gelbein, *Chemtech*, 1998, **28**(12), 1–2.
- 7 Q. Chen, *J. Clean. Prod.*, 2006, **14**, 708–712.
- 8 K. Sato, M. Aoki and R. Noyori, *Science*, 1998, **281**, 1646–1647.
- 9 H. HenkelW. Weber, *US Pat.*, 1 108 752, 1914.
- 10 T. H. Hess, in *Kirk-Othmer Encyclopedia of Chemical Technology*, ed. I. Kroschwitz and M. Howe-Grant, John Wiley & Sons, New York, 4th edn, 1995, **13**, 961–995.
- 11 R. Meiers and W. F. Holderich, *Catal. Lett.*, 1999, **59**, 161–163.
- 12 D. Hancu and E. J. Beckman, *Green Chem.*, 2001, **3**, 80–86.
- 13 D. P. Dissanayake and J. H. Lunsford, *J. Catal.*, 2002, **206**, 173–176.
- 14 R. Burch and P. R. Ellis, *Appl. Catal., B*, 2003, **42**, 203–211.
- 15 P. Landon, P. J. Collier, A. F. Carley, D. Chadwick, A. J. Papworth, A. Burrows, C. J. Kiely and G. J. Hutchings, *Phys. Chem. Chem. Phys.*, 2003, **5**, 1917–1923.
- 16 Y.-F. Han and J. H. Lunsford, *J. Catal.*, 2005, **230**, 313–316.
- 17 T. Haas, G. Stochiol and J. Rollmann, *US Pat.*, 7 005 528, 2006.
- 18 J. K. Edwards, B. E. Solsona, P. Landon, A. F. Carley, A. Herzing, C. J. Kiely and G. J. Hutchings, *J. Catal.*, 2005, **236**, 69–79.
- 19 G. Li, J. Edwards, A. F. Carley and G. J. Hutchings, *Catal. Today*, 2006, **114**, 369–371.
- 20 B. E. Solsona, J. K. Edwards, P. Landon, A. F. Carley, A. Herzing, C. J. Kiely and G. J. Hutchings, *Chem. Mater.*, 2006, **18**, 2689–2695.
- 21 P. A. Ramachandran and R. V. Chaudhari, *Three-Phase Catalytic Reactors*, ed. R. Hughes, Gordon and Breach Science Publishers, New York, 1983.
- 22 K. Akita and F. Yoshida, *Ind. Eng. Chem. Proc. Des. Dev.*, 1974, **13**, 84–91.
- 23 V. V. Krishnan, A. G. Dokoutchaev and M. E. Thompson, *J. Catal.*, 2000, **196**, 366–374.
- 24 M. Rueter, B. Zhou and S. Parasher, *US Pat. Appl.* 2005025697, 2005.
- 25 B. G. Kelkar, S. P. Godbole, M. F. Honath, Y. T. Shah, N. L. Carr and W. D. Deckwer, *AIChE J.*, 1983, **29**, 361–369.
- 26 L.-S. Fan, *Gas-Liquid-Solid Fluidization Engineering*, Butterworth-Heinemann, Boston, 1989.
- 27 www.tigrp.com/data/upfiles/news/Degussa.pdf.
- 28 M. G. Clerici, G. Bellussi and U. Romano, *J. Catal.*, 1991, **129**, 159–167.
- 29 G. Jenzer, T. Mallat, M. Maciejewski, F. Eigenmann and A. Baiker, *Appl. Catal., A*, 2001, **208**, 125–133.
- 30 E. J. Beckman, *J. Supercrit. Fluids*, 2004, **28**, 121–191.
- 31 J. O. Pande and J. Tonheim, *Process Saf. Prog.*, 2001, **20**, 37–39.
- 32 T. Danciu, E. J. Beckman, D. Hancu, R. N. Cochran, R. Grey, D. M. Hajnik and J. Jewson, *Angew. Chem., Int. Ed.*, 2003, **42**, 1140–1142.
- 33 M. R. Prasad, G. Kamalakara, G. Madhavi, S. J. Kulkarni and K. V. Raghavan, *J. Mol. Catal. A: Chem.*, 2002, **186**, 109–120.
- 34 S. Chinta and J. H. Lunsford, *J. Catal.*, 2004, **225**, 249–255.
- 35 J. S. Hwang, C. W. Lee, D. H. Ahn, H. S. Chai and S. E. Park, *Res. Chem. Intermed.*, 2002, **28**, 527–535.
- 36 A. I. Dalton, Jr. and R. W. Skinner, *US Pat.*, 4 336 239, 1982.
- 37 Y. Izumi, H. Miyazaki and S. Kawahara, *US Pat.*, 4 009 252, 1977.
- 38 G. Paparatto, R. D'Aloisio, G. De Alberti and R. Buzzoni, *Eur. Pat.*, 1 160 196, 2001.
- 39 L. W. Gosser and J. A. T. Schwartz, *US Pat.*, 4 832 938, 1989.
- 40 R. Meiers, U. Dingerdissen and W. F. Holderich, *J. Catal.*, 1998, **176**, 376–386.
- 41 K. L. Antcliff, D. M. Murphy, E. Griffiths and E. Giamello, *Phys. Chem. Chem. Phys.*, 2003, **5**, 4306–4316.
- 42 F. Bonino, A. Damin, G. Ricchiardi, M. Ricci, G. Spano, R. D'Aloisio, A. Zecchina, C. Lamberti, C. Prestipino and S. Bordiga, *J. Phys. Chem. B*, 2004, **108**, 3573–3583.
- 43 D. Hancu, E. J. Beckman and T. Danciu, *US Pat.*, 6 710 192, 2004.

The large scale synthesis of pure imidazolium and pyrrolidinium ionic liquids

Anthony K. Burrell, Rico E. Del Sesto, Sheila N. Baker, T. Mark McClesky and Gary A. Baker

Green Chem., 2007, **9**, 449–454, (DOI: 10.1039/b615950h)

The caption for Fig. 3 should read: Fluorescence spectra of 1-butyl-3-methylimidazolium tetrafluoroborate, commercial samples (A and B) and a sample prepared in our laboratory (C).

The text related to Fig. 3 should also read: 1-butyl-3-methylimidazolium tetrafluoroborate.

The Royal Society of Chemistry apologises for these errors and any consequent inconvenience to authors and readers.

Additions and corrections can be viewed online by accessing the original article to which they apply.

Fast tracked communications

Lab on a Chip offers a **quick** and **highly cited** vessel for your research

A simple pneumatic setup for driving microfluidics

Thomas Braschler, Lynda Metref, Ronit Zvitov–Marabi, Harald van Lintel, Nicolas Demierre, Joël Theytaz and Philippe Renaud, *Lab Chip*, 2007, **7**

DOI: 10.1039/b617673a

A class of low voltage, elastomer–metal ‘wet’ actuators for use in high-density microfluidics

Tushar Bansal, Meng-Ping Chang and Michel M. Maharbiz, *Lab Chip*, 2007, **7**

DOI: 10.1039/b614419e

Accelerated synthesis of titanium oxide nanostructures using microfluidic chips

Ben F. Cottam, Siva Krishnadasan, Andrew J. deMello, John C. deMello and Milo S. P. Shaffer, *Lab Chip*, 2007, **7**

DOI: 10.1039/b616068a

Solvent resistant microfluidic DNA synthesizer

Yanyi Huang, Piero Castrataro ‡, Cheng-Chung Lee ‡ and Stephen R. Quake, *Lab Chip*, 2007, **7**

DOI: 10.1039/b613923j

Lab on a Chip is the leading journal on miniaturisation at the micro- and nano-scale. Highly cited and known for its quality research, *Lab on a Chip* has a healthy impact factor of over 5 to compliment the consistently growing publication that it is. Communications are given the highest priority throughout the publication process, and with submission rates increasing steadily, *Lab on a Chip's* ability to host the most up to date research is becoming fast known throughout the research community.



Submit your next communication to *Lab on a Chip* at www.rsc.org/ReSource

01060701

RSC Publishing

www.rsc.org/loc

Registered Charity Number 207890

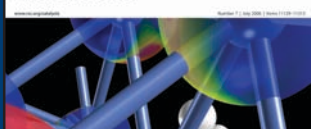
Specialised searching



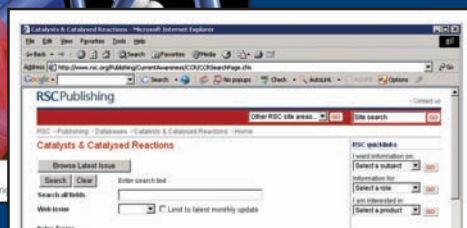
The graphical abstracting services at the RSC are an indispensable tool to help you search the literature. Focussing on specific areas of research they review key primary journals for novel and interesting chemistry.

requires specialised tools

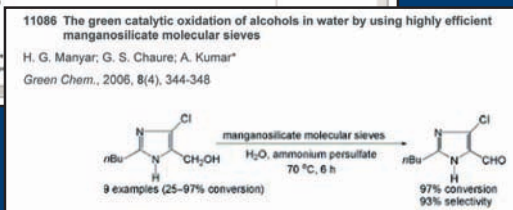
Catalysts & Catalysed Reactions



Catalysts and Catalysed Reactions covers all areas of catalysis research, with particular emphasis on chiral catalysts, polymerisation catalysts, enzymatic catalysts and clean catalytic methods.



The online database has excellent functionality. Search by: authors, products, reactants and catalysts, catalyst type and reaction type.



With Catalysts and Catalysed Reactions you can find exactly what you need. Search results include diagrams of reaction schemes. Also available as a print bulletin.

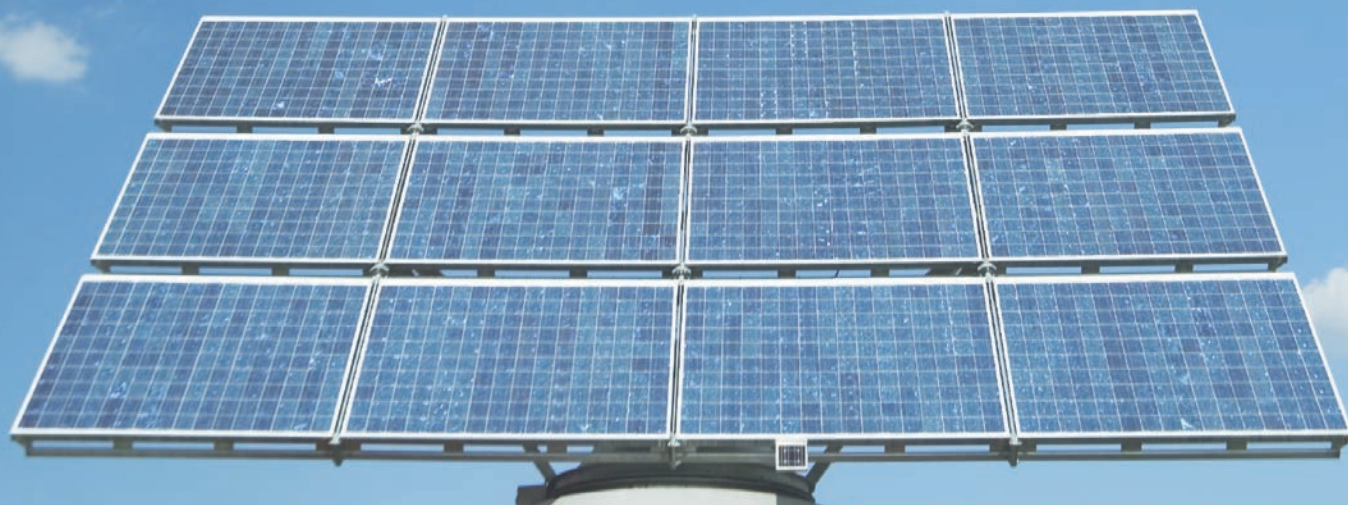
Alternative Fuel Technologies

A series of PCCP special issues guest edited by Joachim Maier (MPI Stuttgart), Dirk Guldi (Universität Erlangen-Nürnberg), and Adriano Zecchina (University of Torino)

Following on from the highly successful nano-themed issues, PCCP presents a series of themed issues on Alternative Fuel Technologies. Published in selected printed issues of PCCP in spring 2007 and collected online on a dedicated website, these issues feature the very latest research including:

- ▶ fuel cells
- ▶ electrochemical energy conversion
- ▶ supercapacitors and molecular materials
- ▶ hydrogen storage
- ▶ solar energy conversion
- ▶ biohydrogen

Sign up for RSS alerts to have the latest articles delivered directly to your desktop



RSCPublishing

www.rsc.org/pccp/altfuel

Registered Charity Number 207890